UNIVERSITY
OF TASMANIA

THE DEVELOPMENT OF RESIN SORBENTS SELECTIVE FOR GOLD IN AMMONIACAL THIOSULFATE LEACH LIQUORS

by

Andrew Clifton Grosse, B.Sc. (Hons.), M.Sc.

This thesis submitted in fulfilment of the requirements for the degree of Doctor of Philosophy at the University of Tasmania.

School of Chemistry,

University of Tasmania,

September 2006.

DECLARATION

To the best of my knowledge, this thesis contains no copy or paraphrase of any material previously published or written except where due reference is made.

Andrew C. Grosse

Authority of Access

This work is to be held confidential for 12 months from the date of publication.

After this time, the contents may be made available for loan or copying

in accordance with the *Copyright Act 1968*.

List of publications arising from this work

1. Grosse, A.C., Dicinoski, G.W., Shaw, M.J., Haddad, P.R., "Leaching and recovery of gold using ammoniacal thiosulfate leach liquors (a review)". *Hydrometallurgy*, **69**: p. 1-21; 2003.

Statement of Authorship

I have incorporated a modified version of the published paper referenced below [1] into Chapter 1 of my PhD thesis "The Development of Resin Sorbents Selective for Gold in Ammoniacal Thiosulfate Leach Liquors". This work was co-authored with Dr. Matthew Shaw, Dr. Greg Dicinoski, Prof. Paul Haddad, with the great majority of the text and figures prepared by myself. The remaining contribution of the other authors was in the revision and proofreading of the final paper.

1. Grosse, A.C., Dicinoski, G.W., Shaw, M.J. & Haddad, P.R.; "Leaching and recovery of gold using ammoniacal thiosulfate leach liquors (a review)". *Hydrometallurgy*, **69**: p. 1-21; 2003.

Approximate proportionate breakdown of authorship:

Andrew Grosse	94%	Dr. Matthew Shaw	2%
Dr. Greg Dicinoski	2%	Prof. Paul Haddad	2%

Signed:

Andrew C. Grosse .....

Dr. Matthew J. Shaw .....

Dr. Greg W. Dicinoski .....

Prof. Paul R. Haddad .....

Date: 5th September, 2006

Acknowledgements

I would like to thank the following individuals and organisations, and acknowledge their contribution to this enterprise. I am particularly grateful for assistance from the postgraduate students, academic and general staff at the School of Chemistry. The following people deserve special mention:

Dr. Greg Dicinoski	Dr. David Graham	Prof. Paul Haddad
Dr. John Madden	Dr. John O'Reilly	Dr. Matthew Shaw
A/Prof. Brian Yates	and the late Mr. Martin Hitchman.	

Thanks is also extended to all staff of the Central Science Laboratory, UTAS, and the following individuals in particular:

Mr. Mike Brandon	(Glassware)	Mr. John Davis
Dr. Noel Davies	(Mass Spectra)	Mr. Peter Dove
Dr. Evan Peacock	(CP-MAS ^{13}C-NMR Spectra)	Dr. Ashley Townsend
Dr. Graham Rowbottom	(Elemental Analysis)	Mr. Paul Waller

Assistance from the following individuals is also gratefully acknowledged:

Dr. Mike Johnson (Analytical Services Tasmania)

Dr. Phil Robinson (School of Earth Science, UTAS)

Dr. Peter Traill (School of Pharmacy, UTAS)

Mr. Chris Brown and Mr. Peter Hutchinson (Osleach)

A/Prof. George Heard (UNCA, NC, USA)

Prof. Jannie van Deventer (Melbourne Uni)

Dr. Matthew Jeffrey (Monash)
Dr. Paul Breuer (Monash)
Mr. Chris Fleming (Barrick Gold)
Dr. Marthie Kotze (Mintek)
Dr. Murdoch MacKenzie (Cognis)
Prof. Alan White (UWA)
Dr. Eric Chan (UWA)
Prof. Mike Nicol (Murdoch)
Dr. Glen O'Malley (Murdoch)

I am grateful to the University of Tasmania for providing an Australian Postgraduate Award scholarship. I would also like to thank Dionex Inc. (Sunnyvale, CA, USA) for the provision of the IC apparatus.

Finally, a very special thanks is extended to my wife Melysa, my children (Beowulf and Djatalysianne), my parents, and all my friends and colleagues over the past six years. This work is dedicated to the memory of my late psychotic cat, Xiombarg.

--

Andrew Grosse, September 2006

ABSTRACT

A set of 48 novel ion-exchange (IEX) resins bearing a range of amine and quaternary ammonium moieties were prepared on a polystyrene-divinylbenzene substrate. These were tested in Bottle-Roll (B/R) tests using a simulated ammoniacal thiosulfate leach solution. The relative gold sorption capacities of these resins were compared and assessed in terms of common structural features, with a view to developing a gold-selective resin for use with thiosulfate leachates. Elution of the gold-loaded resins was also examined, and a shortlist of promising structural features was derived from the combined results.

A common reaction scheme was employed for most preparations, via treatment of the exhaustively chloromethylated resin substrate with excess amine in dimethylformamide. The subsequent functionalised resins were characterised using infra-red spectroscopy, solid state ^{13}C-NMR spectroscopy, ion-exchange testing and elemental analysis. The weak-base resins prepared in this manner were then exhaustively alkylated with either benzyl chloride or iodomethane, to provide a range of structurally related moieties. These included alkylated derivatives of ethanolamine, diethanolamine, piperidine, morpholine, piperazine, imidazole, and tetramethyl-1,2-diaminoethane.

The resin moieties were examined by computational techniques to determine approximate pK_a values, and by ^{13}C-NMR spectroscopy. Minimum-energy structural conformations were obtained using molecular modelling (*MM+* parameters). The gold and copper thiosulfate complexes, along with the thiosulfate, trithionate and tetrathionate anions were modelled using *ab-initio* density functional theory (DFT).

The performance of the resins was compared in B/R tests using an artificial leach liquor (pH ~10.2) containing gold (20 ppm), copper (200 ppm), ammonia

(1.3 M) and thiosulfate (0.1 M). Gold sorption by the resin was followed by periodic sampling of the liquor and AAS analysis, over a 24 hour period. Relative gold affinity for each resin was assessed using the ratio of maximum gold sorption to IEX capacity (ie. $[Au]_R/C_M$), with values ranging up to 16.2 mmol Au per mol of IEX sites (resin BIM1; *N'*-benzylimidazole).

Comparison between the various methyl and benzyl- derivatives showed that gold loading was relatively insensitive to the steric bulk of the functional group. However, gold affinity was apparently enhanced by 2-hydroxyethyl and imidazolium moieties. A set of promising moieties (piperidineethanol, quinuclidine, TMEDA, and methyl derivatives of diethanolamine, imidazole, morpholine and piperazine) had similar $[Au]_R/C_M$ values to the commercial IEX resins Dowex-1, IRA-410 and Amberlite A26 (~10 mmol/mol). These resins were examined in controlled B/R tests spiked with 10 ppm trithionate, with the trithionate and tetrathionate concentrations followed by ion chromatography (IC). The novel resins loaded more slowly and were more perturbed by the presence of an initial 10 ppm trithionate, while the commercial resins were more rapidly fouled by trithionate.

The quinuclidine resin was subjected to four cycles of B/R gold loading and elution. The resin retained 89% of the initial gold sorption capacity, and 99% of the adsorbed gold was eluted with a modified nitrate eluent.

Table of Contents

List of Figures

List of Tables

1. Introduction

Worked metals have been a signpost of civilisation longer than recorded history. It is likely that gold was the very first metal used by man [1]. The only useful metals to be found in the pure state were gold, silver, copper and lead, and most such deposits have long ago been exploited and exhausted. The development of tool metal industries has mirrored this process and many easily exploited mineral resources have also been depleted. In the absence of easily exploited deposits of native metals, the only viable process to obtain a pure base metal was to smelt a mineral ore. New technologies were developed in the nascent science of pyrometallurgy, in which the physical properties of the target metals (such as melting point) were exploited to achieve their separation from a mineral matrix. A plethora of secondary processes was subsequently developed, utilising physical properties of the target minerals to effect their separation and concentration (e.g. calcining, flotation).

In order to treat the more difficult ores, obtain new materials, and to improve the efficiency of the metal refining industry, aqueous treatment processes were investigated and implemented. The treatment or processing of ores by dissolution of the embedded metals in aqueous solution is known as the art of *Hydrometallurgy*. The older smelting processes often released significant amounts of toxic metals (arsenic, lead, and mercury) and many other by-products (such as sulfurous gases) that resulted in detrimental effects on local communities and their environments. The implementation of modern hydrometallurgical processes can result in a reduction of the environmental impact of mining and mineral refining operations. In particular, the recovery of gold from its ores is conducted principally by hydrometallurgical processes [2].

In a hydrometallurgical extraction process, the ore is extensively mixed with an aqueous solution of reagents which then dissolve ('leach') the embedded metals or metal complexes. The reagent or reagents ('lixiviants') in the leach solution ('liquor') are chosen for their ability to form a stable water-soluble complex with the metal of interest. An oxidant is often also present to oxidise native metals into soluble ions, and/or to decompose the matrix in which it is embedded. In this way, an entirely new set of properties becomes available: in addition to the bulk properties of the mineral and the physical properties of the metal, the chemical and electrical properties of the metal may now be exploited to effect separation. The efficacy of the leaching process is dependent upon the particle size and mineral disposition of the ore, the temperature, the concentration and type of reagents in the leach liquor, and the time allowed for leaching. In many processes, optimal conditions must be found by trial and error due to the varying nature of the mineral ore upon which it operates.

However, coaxing the metal into solution is only half the problem. The metal-bearing solution must then be treated in a way that permits a majority of the desired metal to be subsequently recovered from solution, preferably in a form that is more concentrated than the original ore. Alternatively, hydrometallurgical processing of an ore may be conducted to remove a problematic contaminant which devalues the product or complicates later processing; that is, to purify (upgrade) the metal product. Highly value-added metal product(s) can be obtained if the various components can be separately removed from the solution.

Recovery of metal ions from aqueous solutions can be achieved by simple chemical processes such as precipitation, or by electrochemical means such as electrowinning. These techniques are relatively crude and are inclined to contaminate the product with other metals from the leach solution. Another type of recovery process that has been applied for over a century is the use of conventional

mineral adsorbents. Some dissolved ions have a strong affinity with certain mineral phases, such as clays, zeolites or activated carbon, which can be contacted with leach solutions and then physically removed along with the adsorbed metals. A second hydrometallurgical step may then be applied to strip the adsorbent and yield a concentrate of the desired metal, and the adsorbent can then be returned to the leach liquor for further adsorption cycles.

With the rise and development of the modern polymer industry, a new prospect has arisen for hydrometallurgical processing: Ion Exchange (IEX) Resins. These are porous polymeric substrates whose surfaces bear abundant functional groups of a known type (Figure 1.1). When in contact with a leach liquor, the soluble ions will associate with the IEX groups of a resin with differing affinities, depending on factors such as charge, size, and polarisability. The particles of resin, which are generally more durable than their mineral forebears, can be readily removed from the liquor, and with them the associated ions – which can then be removed in a subsequent step to yield a concentrate.

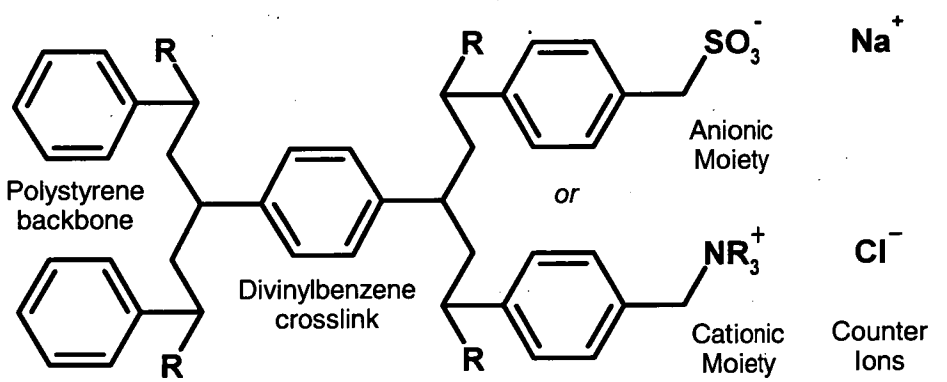

Figure 1.1 General Structure of a Polystyrene-based Ion Exchange Resin

Ion exchange adsorbents have had some success in the remediation of heavy-metal contaminated toxic waste (eg. mine tailings, industrial effluent, sewage) [3].

This is often achieved by the scavenging of stray transition metals from acidic solutions by cation-exchange resins. Ion exchange resins also have the advantage over mineral adsorbents in that they may be custom-made for a particular application. That is, the functional group(s) may be engineered to be highly selective for a given ion and to exclude unwanted ions. This discriminative aspect, known as selectivity, is the most significant advantage of IEX resins over their predecessors.

It is the aim of this project to develop novel IEX resins that will selectively scavenge gold from ammoniacal thiosulfate leach liquors. In order to address this issue, a review of the present hydrometallurgical techniques for the recovery of gold is in order.

1.1 Gold Hydrometallurgy

One of the driving forces behind the development of hydrometallurgical processes has been the precious metal industry. The processing of relatively low-grade ores has been made economically viable due to the high price commanded by gold, platinum, and a number of other metals. This has, in turn, generated interest in improving the efficiency of the process steps where possible, such as minimising reagent consumption and improving the recovery of precious metals. For example, gold was initially recovered from cyanide leach solutions by a rather crude process known as 'cementation'. It was later found that gold could be recovered from cyanide leach liquors more efficiently by the use of carbon adsorbents, and later by highly selective polymeric ion-exchange resins. This achievement rests at the summit of over a century of hydrometallurgical development, having surpassed all the previous technologies for the processing of low-grade gold ores.

However, the current use of cyanidation techniques to leach gold from its various ores is undesirable from an environmental perspective. In recent years,

cyanide leaching has been banned in many regions due to environmental concerns. For example, the town of Esquel in Argentina, close to the proposed Meridian Gold project site, has banned cyanide within its limits [4]. Such prohibitions are due predominantly to the acute toxicity of cyanide, effectively demonstrated by the globally publicised Baia Mare tailings dam breach and subsequent pollution of the Tisza river in Romania. Numerous other incidents in recent years have contributed to the negative public perception of cyanide, including a spill near the Granites gold mine in the Northern Territory in February 2002 which caused a significant kill of local wildlife [4]. Pressure from environmental lobby groups has recently driven the Australian Federal government to declare its commitment to the International Cyanide Management Code, which comprises a set of guidelines intended to minimise industrial cyanide accidents [5].

In addition, problems can occur when leaching gold from complex ores, such as those containing copper or carbonaceous material [2], resulting in poor recoveries of gold unless multi-step extraction and/or elution steps are incorporated into the process. Reserves of such refractory ores are increasing as the more profitable ores become exhausted, giving incentive for the development of new hydrometallurgical processes [6]. The use of alternative lixiviants for gold extraction has been investigated for some time, and has been discussed in numerous reviews [6-13]. A suitable replacement for cyanide may be the use of thiosulfate in the presence of ammonia and copper(II). The advantages of using this approach include a far lower possibility of an adverse environmental impact, a more cost-effective operation due to the fact that thiosulfate is substantially less expensive than cyanide, and thiosulfate facilitates the leaching of complex materials including manganiferous ores through matrix degradation. In addition, the thiosulfate anion is a more effective lixiviant for preg-robbing and high-copper ores through heap-leaching than

cyanide [14-17]. However, there are presently certain problems associated with using thiosulfate to leach gold and no suitably robust leaching regime exists. Moreover, the actual leaching mechanism is still not fully understood, due predominantly to the ease with which thiosulfate undergoes disproportionation or oxidation in aqueous solutions, forming various other sulfur species including sulfide, sulfite, sulfate, di-, tri- and higher polythionates as a function of pH and Eh [18-21]. Furthermore, the metallo-thiosulfate complexes themselves are readily susceptible to decomposition to produce metallic sulfides or other species [22]. Nevertheless, the potential benefits of using thiosulfate as a lixiviant for gold have generated significant interest worldwide. A recent comprehensive review of leaching gold ores using the thiosulfate anion has been prepared by Aylmore and Muir [23].

In this chapter, cyanide and thiosulfate leaching processes will be compared, after which the chemistry involved in using thiosulfates to extract gold from its ores will be outlined. A detailed evaluation of available ion exchange resin materials will then be presented, together with a comparison of these materials with other techniques for extracting gold from thiosulfate leach liquors, including adsorption onto activated carbon, solvent extraction and electrowinning.

This summary serves to frame the objectives of this project, and illustrate the difficulties inherent in the development of a new hydrometallurgical process. This project focuses on the use of polymeric resins to selectively extract gold from ammoniacal thiosulfate leach solutions, in a fashion analogous to the current treatment of cyanide liquors (Section 1.5). These resins are likely to be the key to high yield extractions of gold from interfering species present in leach liquors, such as other metal complexes (in particular those containing copper) and thiosulfate decomposition products, especially trithionate. This will be pursued through the synthesis and evaluation of the behaviour of a range of functionalised polymer

resins. Appropriate testing of the resin products requires selection of appropriate and consistent experimental conditions, such as the composition of the leach liquor, which must be reasonably representative of current industrial practice. These conditions, along with a more refined version of the principal project objectives, and problems to be overcome, will be summarised at the end of this chapter.

1.2 *A Comparison of Cyanide and Thiosulfate Leaching Regimes*

It has long been observed that silver and gold will dissolve in oxidising solutions containing thiosulfate ions [24-25]. This reaction was first utilised in the silver mining industry as the Patera process for the recovery of silver from very high-grade ores [26]. The modern addition of ammonia to these solutions has improved gold dissolution through the formation and catalytic leaching activity of the copper(II) tetrammine complex, and by hindering the solubility of some refractory metals, thereby reducing the consumption of thiosulfate. It now appears that the leaching of gold-bearing ores with ammoniacal thiosulfate solutions can accomplish the recovery of a major portion of the refractory gold from a range of ores [21, 27-30]. In comparison with conventional cyanide processing, the thiosulfate process often has the advantages of greater efficiency and versatility, coupled with a significantly lower environmental impact [10, 31]. Thiosulfate liquors are less prone to fouling by unwanted metal ions, and hence can be applied to a wide array of refractory ores. The common thiosulfate salts (Na^+, K^+, Ca^{2+} and NH_4^+) are biodegradable and are regarded as non-hazardous by Worksafe Australia [32]. These thiosulfate salts are 'Generally Recognised As Safe' (GRAS) in the USA, and are not considered dangerous substances by European standards [15, 33-34]. In addition, conventional treatment of refractory ores often involves the costly step of roasting the ore prior to leaching, often resulting in the consequent environmentally contentious release of

sulfurous gases. Roasting of some ores could be minimised by use of the thiosulfate process, due to the partial dissolution of the matrix by the lixiviant, a lack of preg-robbing behaviour, and the advent of bio-oxidation. In this context, it is arguable that the thiosulfate process represents a significant advance in precious metal recovery techniques.

A disadvantage of thiosulfate leaching is the presence of ammonia, which has significant toxicity to aquatic organisms. This volatile and noxious reagent can readily escape from open leaching vessels and contaminate the surroundings, necessitating containment of the leach liquors. Ammoniacal waste needs to be remediated to avoid adverse environmental impact. In an efficient system, it may be possible for the ammonia to be recovered from tailings by distillation, and recycled into fresh leach liquor.

Conventional processing of low-grade gold ore is generally conducted by leaching finely divided ore in a basic solution of alkali metal cyanide. Zerovalent metals are oxidised from the metallic state to soluble M^{X+} ions by dissolved oxygen, and these metal ions are then strongly complexed by cyanide ligands (Eqn. 1.1) [35]. This equation represents the collective sum of a more complex series of reactions in which lead is an active participant. It is has been known for some time that the oxidation of metallic gold in cyanide solutions is strongly catalysed by trace amounts of lead in the liquor [2, 36].

$$4Au^0 + O_2 + 8CN^- + 2H_2O \rightarrow 4[Au(CN)_2]^- + 4OH^- \qquad (1.1)$$

Lixiviation of undesirable base metals, such as copper and iron, reduces the efficiency of the process by consuming additional reagents, and necessitates further processing to remove these contaminants [37-40]. There are numerous complex ores

from which gold cannot be efficiently recovered by cyanidation technology. These complex ores are often termed "refractory", implying a problematic mineral structure resistant to leaching, which often includes one or more of the following types [6]:

- Pyrite Ore – Finely divided gold embedded in a sulfide matrix.
- Cuprous Ore - Copper is abundant in the mineral matrix.
- Base Metal Ores – Lead or zinc sulfides encapsulate the gold.
- Manganous Ore - High levels of manganese are present.
- Telluride Ore – Gold is associated with tellurium in the ore.
- Carbonaceous Ore – Fine organic 'preg-robbing' carbon contaminates the ore.

In most of the above cases, cyanidation is unable to lixiviate significant quantities of desirable metals without consuming excessive, and typically uneconomical, quantities of reagents [17, 41-43]. This may also result in significant contamination of the leach liquor with undesirable solubilised metals. Alternatively, in the case of organic carbon, the gold cyanide complex is adsorbed onto fine particles of native carbon. This gold is then lost to the tailings, hence this organic carbon robs the pregnant leach liquor of solubilised gold (ie. 'preg-robbing').

Ammoniacal thiosulfate leaching is less sensitive than cyanidation to contamination by unwanted cations [24]. The presence of abundant ammonia has the effect of hindering the dissolution of undesirable ions such as silicates and carbonates [44]. Similarly, a number of metals and minerals, such as CaO, Fe_2O_3, and MnO_2, are converted into insoluble hydroxides by ammonium hydroxide at pH > 9.5 [45]. Importantly, it is also reported that the aurothiosulfate complex is not significantly adsorbed onto native carbon, thus reducing losses due to preg-robbing [46-48].

It has also been claimed that ammoniacal thiosulfate leaching beneficiates auriferous sulfide ores via corrosion of chalcopyrite, pyrrhotite, arsenopyrite, and to a lesser degree, pyrite [49-50]. Whilst it is clear that some copper sulfide minerals may be lixiviated [24], a number of studies have concluded that the dissolution of pyrite ores does not take place in thiosulfate liquors [23, 51]. Ammoniacal thiosulfate lixiviant can leach finely ground sulfide ores more efficiently by maximising contact with the smaller grains of embedded gold. Cyanide leaching cannot exploit this principle, as the sulfide minerals are cyanicides.

1.3. Species Present in Thiosulfate Leach Liquors

1.3.1 Metal Complexes

Thiosulfate is a divalent type 'A' soft ligand, which tends to form more stable complexes with low-spin d^8 {Pd^{II}, Pt^{II}, Au^{III}} and d^{10} {Cu^{I}, Ag^{I}, Au^{I}, Hg^{II}} metal ions [52-53]. Commonly, the thiosulfate ion acts as a unidentate ligand via the terminal sulfur atom, establishing strong σ-bonds with a metal ion which are stabilised by *pπ-dπ* back-bonding. Thiosulfate ligands may also act in a bridging role via the terminal sulfur atom or as a bidentate ligand through a sulfur and an oxygen atom, usually resulting in an insoluble complex (see Figure 1.2) [52, 54-56].

In a thiosulfate leach liquor, the formation of gold and silver thiosulfate complexes proceeds via the catalytic oxidation of the zerovalent metal by a suitable soluble metal complex, which is typically the copper(II) tetra-ammine complex acting as the primary oxidant [57-60]. The reduction of the copper(II) ammine complex is believed to transfer two ammonia ligands, allowing the kinetically favoured diaminoaurate(I) complex to form [61-62]. This exchanges ligands with the free thiosulfate ions to form the more thermodynamically stable aurothiosulfate complex [63-65].

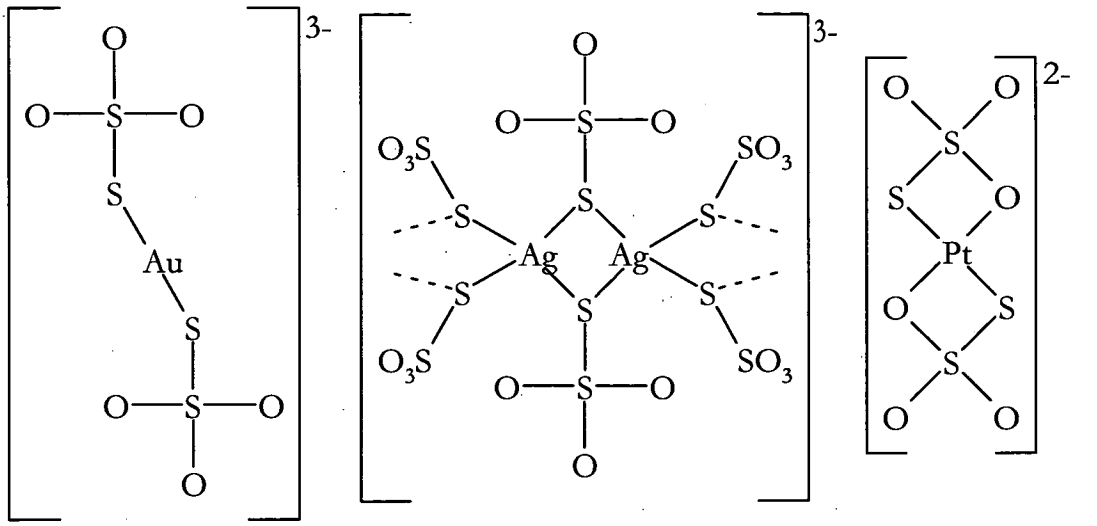

Gold(I) complex unidentate thiosulfate

Silver(I) complex bridging thiosulfate

Platinum(II) complex bidentate thiosulfate

Figure 1.2 Structure of Thiosulfate Complexes [52, 54-56]

There is some contention as to the role of the gold ammine complex, which has not been positively identified in ammoniacal thiosulfate leach liquors. Logarithmic values of 13-26 have been reported for the stability constant of this complex [66]. Some treat this step as a surface phenomenon which catalyses the formation of the thiosulfate complex. Thermodynamic calculations using two different values reported for the free energy of formation of the thiosulfate ion lead to divergent results. This causes a change of 26.8 kJ/mol in the free energy of the equilibrium reaction between $[Au(S_2O_3)_2]^{3-}$ and $[Au(NH_3)_2]^+$, making the formation of the diammineaurate complex far less energetically feasible and hence is unlikely to be present in leach solutions [67].

At the same time, the reaction between dissolved oxygen and the copper(I) thiosulfate complex regenerates the copper(II) tetrammine complex. The activation energy required to lixiviate metallic gold in the presence of ammonia (pH 10), excess thiosulfate and Cu(II) is 15.54 kJ/mol [68]. The activation energy rises to

27.99 kJ/mol in the absence of Cu(II) and ammonia, demonstrating the catalytic effects of Cu(II). The reactions that describe the leaching behaviour of gold in the ammoniacal thiosulfate system are shown below (Eqns. 1.2 – 1.5) [13-14, 27, 64, 69-72]:

$$Au^0 + [Cu(NH_3)_4]^{2+} + 3S_2O_3^{2-} \rightarrow [Au(NH_3)_2]^+ + [Cu(S_2O_3)_3]^{5-} + 2NH_3 \quad (1.2)$$

$$[Au(NH_3)_2]^+ + 2S_2O_3^{2-} \rightarrow [Au(S_2O_3)_2]^{3-} + 2NH_3 \quad (1.3)$$

$$4[Cu(S_2O_3)_3]^{5-} + 16NH_3 + O_2 + 2H_2O \rightarrow 4[Cu(NH_3)_4]^{2+} + 12S_2O_3^{2-} + 4OH^- \quad (1.4)$$

$$\underline{\textit{Net Reaction}}: \; 4Au^0 + 8S_2O_3^{2-} + O_2 + 2H_2O \rightarrow 4[Au(S_2O_3)_2]^{3-} + 4OH^- \quad (1.5)$$

In ammoniacal thiosulfate liquors, metal ions can form a range of complexes with ammonia, thiosulfate and hydroxide ions. If metal hydroxides are formed, they are generally sparingly soluble, or insoluble (and precipitate). Copper(I) is often reported only as $[Cu(S_2O_3)_3]^{5-}$, yet at concentrations of thiosulfate below 0.05 M, the primary complex is expected to be $[Cu(S_2O_3)_2]^{3-}$ [21, 73-74]. In strongly ammoniacal liquors with low oxidation potential, the readily oxidised ammine complex, $[Cu(NH_3)_2]^+$, may also be present. Copper(II) is almost exclusively found as $[Cu(NH_3)_4]^{2+}$, although it is suggested that the triammine complex $[Cu(NH_3)_3]^{2+}$ may be the primary oxidising species [75-76]. There appears to be a maximum solubility of copper, in that approximately one gram of copper will be soluble for every 1% $(NH_4)_2S_2O_3$ (w/w) present in the leach solution [77]. Under unfavourable conditions, precipitation of $Cu_2S_2O_3$ or mixed cuprous-ammonium thiosulfate salts may occur [61, 78].

Soluble thiosulfate complexes are also known for a number of heavy metals, with their stepwise stability constants (β_n) and coordination numbers illustrated in Figure 1.3 [13, 22, 52, 54, 79-90]. Apart from the formation of anionic thiosulfate

complexes, some metal cations are expected to form cationic ammine complexes, as detailed in Figure 1.4 [85]. Several copper and palladium complexes bearing both ammine and thiosulfate ligands are also known, although their stability constants and solubility remain unknown [89].

Comparison of the stability constants in Figures 1.3 and 1.4 reveals that many important metals will form thiosulfate complexes in preference to their corresponding ammine complexes. A useful method of studying the distribution of the various metal complexes in the reaction mixture is to construct a *Pourbaix diagram*, ie. a chart of solution potential (Eh) versus hydrogen ion concentration (pH) [91]. These diagrams use a set of calculated or experimentally determined electrochemical reaction potentials to plot domains of complex stability, and can be useful in determining the abundance and distribution of various ions. The reliability of the resulting figures depends upon the accuracy of both the input (*standard reaction potentials*) and the knowledge of the solution components, which decide the set of electrochemical half-cell reactions to be considered.

Numerous papers have reported Eh-pH plots for aqueous systems containing copper, silver and/or gold in the presence of ammonia and/or thiosulfate [17, 21-24, 28, 58, 61, 66-67, 88, 92-96]. The behaviour of the metals cadmium, cobalt, chromium, nickel, lead, zinc, aluminium, platinum and palladium in these liquors has also been examined by Eh-pH diagrams [28, 97-98]. The borders of such diagrams are strongly dependent on the concentrations of the reagents, which vary widely in the reported studies [Table 1.1]. As such, a comprehensive analysis of the disposition of the soluble metals will not be given. Generally, thiosulfate complexes are expected to predominate for gold(I), silver(I), mercury(II) and lead(II), whereas the metal ions cobalt (II), copper(I), zinc(II) and cadmium(II) should be found as an equilibrium mixture of thiosulfate and ammine complexes. The remaining soluble transition

metal ions (such as chromium(III), cobalt(III), and nickel(II)) are expected to occur primarily as ammine complexes. The ligands of the aurothiosulfate complex are believed to be quite labile, as near-stoichiometric quantities of cyanide added to a thiosulfate liquor were found to rapidly form the corresponding aurocyanide complex [70, 99]. This is especially significant when the rapid reaction between cyanide and thiosulfate ions is taken into account (Eqn. 1.9).

The complexes $[Pd(S_2O_3)_4]^{6-}$ and $[Pt(S_2O_3)_4]^{6-}$ have aqueous solubilities above 10 ppb at pH 7 and 25°C, and quite low oxidation potentials ($-E^0$) of 0.116 mV and 0.170 mV respectively [97, 100]. However, they are thermodynamically unstable, and slowly decompose into insoluble S-bridged oligomers similar to the silver complex in Figure 1.2 [101]. Metals in higher oxidation states such as Au(III) and Fe(III) are readily reduced by thiosulfate ions, and hence are not significant in leach liquors. Other anions from the leach liquor or the mineral matrix, such as chloride, hydroxide or sulfate may also participate in metal ion solvation. Stable, soluble complexes bearing a mixture of ligands may be present, similar to the copper salts $[Cu(CN)_X(NH_3)_Y]^{(1-X)}$ found in ammoniacal cyanide leach liquors [102]. However, relevant mixed ligand thiosulfate complexes have not been reported in the literature.

Ref #	Year	Ore Type	$[S_2O_3^{2-}]$	Cation	[Cu]	Anion	$[NH_3]$	$[NH_4^+]$	Ion	pH	$[SO_3^{2-}]$	Cation	Temp (C)	$[O_2]$	Au%	Time (h)	NOTES
[71]	1972	Complex Sulfide (Kuroko)	0.5	Na	0.04	SO_4	0.5						65	1 atm			
[27]	1978	Cu and Sulfide Ores	0.4 - 0.8	NH_4	2 - 6 g/L		8:1 A/M^+			9.5 - 10			25 - 50		94.4	1	
[103]	1979	Chalcopyrite Concentrates	0.34 - 0.67	NH_4	3 - 5 g/L					10			38 - 60	N_2 sparging	88 - 95	3 - 5	
[31]	1981	Refractory (Mn)	12 - 25%	NH_4	1 - 4 g/L	SO_4	(pH > 8)$^{\propto}$			> 8	0.1 - 4 %	NH_4	50 - 60		86.7		
[104]	1983	Refractory (Mn, Cu, As, Sb, Te, Se)	12 - 25%	NH_4	1 - 4 g/L	SO_4	(pH > 8)$^{\propto}$			> 8	0.1 - 4 %	NH_4	40 - 60		86.7		
[45]	1987	La Colorada Sur Tails	60 g/L	Cu/NH_4	3.4 g/L	S_2O_3		7 g/L	SO_3	10	7 g/L	NH_4	20 - 60		94	2.5	
[21]	1988	Oro Blanco Rhyolite (Mn)	0.22	NH_4	0.015	SO_4	0.07			9.5 - 10			50		90	1	
[105]	1989	Carbonaceous (Pink Ore)	0.71	NH_4	(native)$^{\theta}$		3			10.5	0.1 - 0.22	NH_4	35	103 kPa	73	1	
[106]	1991	High Cu Sulfide	1	Na	1 g/L	SO_4	2	0.1 - 0.4	SO_4		0.1	Na	40 - 50		95.6	37623	
[94]	1992	Sulfide Concentrate (< 200 mesh)	0.2	NH_4	3.0 g/L		3	1 - 1.6	SO_4	10.2			60	1.0 L/min (air)$^{\ni}$	97	2	
[15]	1992	Oxidised Ore (Nevada)	0.2	Na	1.0 mM	SO_4	0.09			10.35	6.25 mM	Na	ambient		83	48	
[64]	1992	Cu Sulfide Concentrate (Rushan)	1		0.1		1			10			20		95		
[107]	1992	Sulfide Au Concentrate	0.2 - 0.3		3 g/L		2 – 4	1.4 - 2.2	SO_4	10 - 10.5			60		> 95	2	
[49]	1993	Sulfide Concentrate (< 300 mesh)	0.7	NH_4	4 g/L		1	0.4 - 2.0	SO_4				20 - 60	0.7 L/min (air)$^{\ni}$	96.3	14	
[25]	1993	Fine Copper Ore	0.5	NH_4	10 - 100 mM	SO_4	0.25			10.1			25		81.8	6	
[68]	1993	Cuprous Ore	4 - 15%		0.02		0.5			7 - 10.8			50			4	
[108]	1994	Bio-oxidised C/S (Gold Quarry)	0.05 - 0.2	Na/NH_4	1.0 mM	SO_4	0.1			9.2 - 10			ambient		64.7	72	Heap Leach
[44]	1995	Cretaceous Arc (Dominican)	2	Na	0.1	SO_4	4			8.5 - 10.5			25 - 60		80	3	
[70]	1996	Oxidised C/S (Carlin)	0.025 - 0.1	NH_4	50 - 100 ppm	SO_4	> 7 mM			7 - 8.7	1 - 100 mM	Na	40 - 55		81.2	4	
[109]	1996	Oxidised Pyrite Concentrate	~ 0.5		4 g/L	SO_4	0.3 - 0.6						ambient		91.2	2	
[110]	1996	Bio-oxidised Pyrite (Zlata)	0.13	NH_4	0.5 g/L		(pH 10)$^{\propto}$			9.5 - 10	0.5 g/L		20		84.2	288	Column Leach
[111]	1996	Cu Sulfide	0.4	Na/NH_4	1.9 g/L		0.2			11			ambient		90	24	
[16]	1997	Bio-oxidised C/S (Carlin)	0.1	NH_4	0.5 mM		0.1			9			ambient		66	2784	Heap Leach
[17]	1997	Low Grade C/S (Carlin)	0.1	NH_4	0.5 mM		0.1						ambient			~6 months	Heap Leach
[59]	1998	Autoclaved C/S	0.01 - 0.1	NH_4	10 - 100 ppm	SO_4	> 7 mM			7 - 8.7	1 - 100 mM	Na	45 - 55		85	1	Resin-In-Leach
[112]	1998	Refractory Cu Sulfide	0.5	NH_4			6			10.2			ambient		95 - 97	24	
[113]	1999	Pyrite/Chalcopyrite (Canadian)	0.3	NH_4	0.05	SO_4	6			10.2			ambient		72	1200	Heap Leach
[13]	2000	Refractory C/S Ore	0.05	NH_4	0.03		0.1			7.5 - 8			40 - 60		81 - 92	8	
[114]	2000	Limonitic Barite	2		6.4 g/L		4						25		80		
[96]	2001	Blended Calcined Ores	0.05							8 - 9.5	1 mM		25 - 35			24	
[51]	2001	Autoclaved C/S (Goldstrike)	0.4	Na	4.0 g/L	SO_4	1.87				5.0 g/L	Na	ambient		90 - 100	7	Column Leach
[115]	2001	Sulfide Concentrate	0.2	NH_4	0.08	SO_4	3	1	SO_4	10.2			50	1.0 L/min (air)$^{\ni}$	> 95	3	
[115]	2001	Copper Concentrate	0.7	NH_4	2.0 g/L	SO_4	2	0.2 - 0.4	SO_4	10.2			50	1.0 L/min (air)$^{\ni}$	95.9	1.5	
[24]	2001	Au-Cu Sulfide Concentrate	0.8	Na	0.05	SO_4	4			10.2			ambient		96	96	
[116]	2001	Sulfide Ore (Nevada)	0.1	Na	0		0			9			60	100 psi	81	6	
[117]	2002	Silicate Ore (Hishikari)	0.3	NH_4	30 mM	SO_4	1			9.5			ambient				
[30]	2002	Sulfide Concentrate (Chile)	0.3	NH_4	50 mM	SO_4	> 0.2			10			25		94	15	
[118]	2002	Preg-Robbing Ores (Goldstrike)	0.05	NH_4	0.5 mM	SO_4	0.1			7.5 - 8			40 - 60		86.7	8	
[28]	2002	Fine Silicate Ore	0.05	NH_4	0.1 mM	SO_4	0.5			9.5			ambient		94	12	
[29]	2002	Fine Cu-Pb-Zn Concentrate	0.5	NH_4	10 g/L	SO_4	0			6 - 7			70		99	1	

Table 1.1 Historical Development of Ammoniacal Thiosulfate Leaching

All concentrations in mol/L except where specified otherwise; A/M^+: Ratio of NH_3 to Metals; $\propto$: Ammonia added to achieve stated pH; θ : the only copper source was the leached ore;

Au%: Percentage of embedded gold dissolved in solution; $\ni$: Solution sparged with air; g/L: grams per Litre; ppm: parts per million (mg/L); psi: pounds per square inch; kPa: kiloPascals.

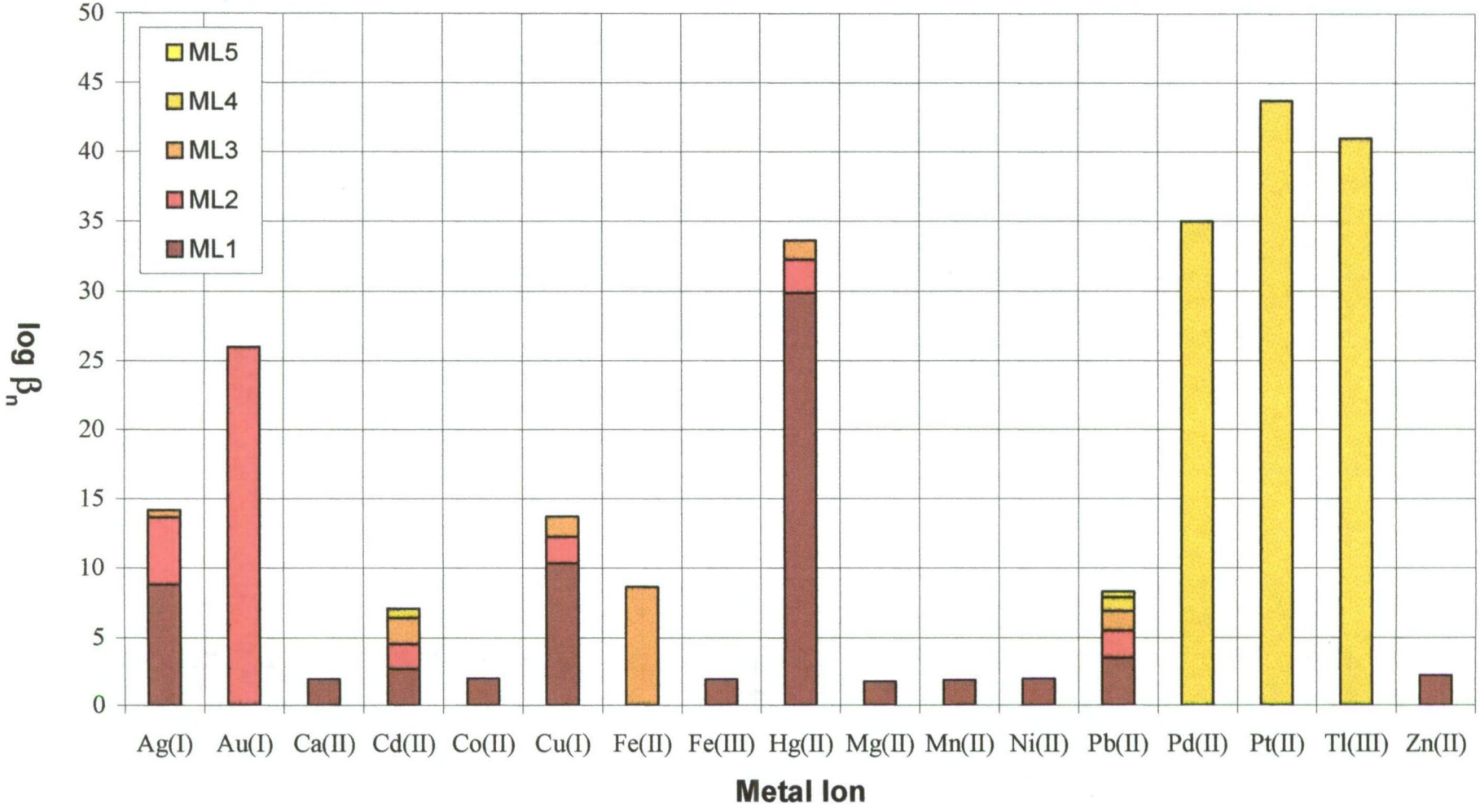

Figure 1.3 Stepwise Stability Constants for Thiosulfate Complexes [13, 22, 52, 54, 79-90]

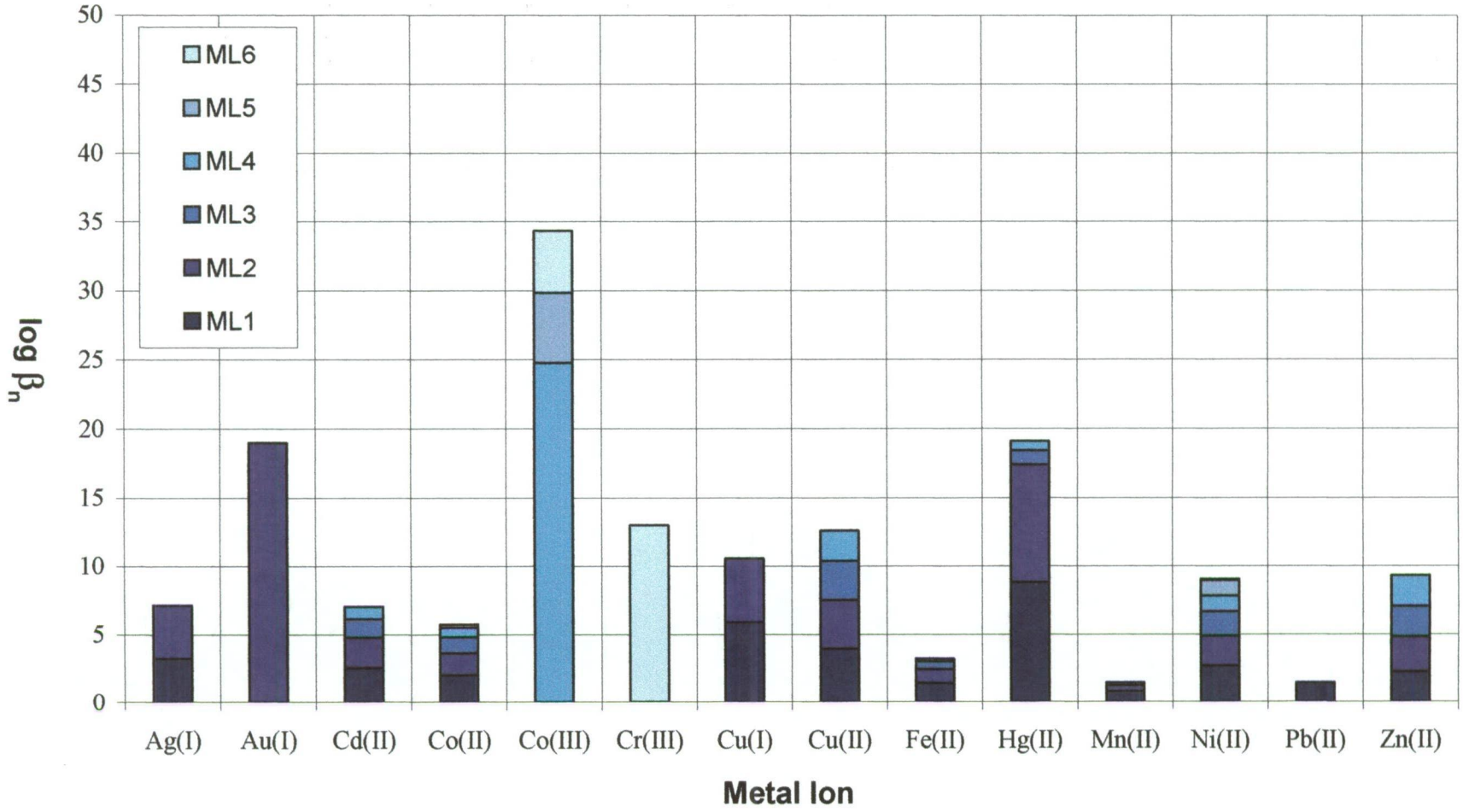

Figure 1.4 Stepwise Stability Constants for Ammine Complexes [85]

1.3.2 Sulfur-Oxygen Anions

The sulfoxy anions initially present in an ammoniacal thiosulfate leach liquor are thiosulfate, plus some sulfate and perhaps sulfide from mineral sources. However, thiosulfate is metastable, which means it may be readily oxidised or reduced according to the initial solution potential. Depending on the aqueous environment, thiosulfate can break down into sulfite, sulfate, tri-, tetra-, penta-thionate and higher polythionates ($S_xO_y^{2-}$), sulfide and/or polysulfides (S_x^{2-}). An important factor in thiosulfate stability is the pH of the solution, since thiosulfate rapidly decomposes in acidic media [58]. Certain metal ions and reagents also cause the breakdown of thiosulfate, as shown below (Eqns. 1.6 – 1.12) [13, 44, 63, 72, 86, 90, 119]. Note that the anions trithionate ($S_3O_6^{2-}$) and tetrathionate ($S_4O_6^{2-}$), which are not known to have any lixiviating activity [23], can interfere with resin-based recovery methods by displacing metal complexes from ion-exchange sites [13, 96]. Sulfide complexes are generally insoluble in water, although the polysulfides (S_x^{2-}) may have some ability to leach metal ores [120-122]. It is possible that the activity of polysulfide systems may derive from the rapid oxidation of sulfides into thiosulfate, which then complexes the gold. Leaching of gold ores using a sulfite lixiviant has also been patented [123], although thiosulfate ions may also play a role in that system.

$$4S_2O_3^{2-} + 4H^+ + O_2 \rightarrow 2S_4O_6^{2-} + 2H_2O \quad (1.6)$$

$$S_2O_3^{2-} + 2H^+ \rightarrow S^0_{(ppt)} + SO_{2(gas)} + H_2O \quad (1.7)$$

$$S_2O_3^{2-} + CN^- + \tfrac{1}{2}O_2 \rightarrow SCN^- + SO_4^{2-} \quad (1.8)$$

$$2[Fe(S_2O_3)]^+ \rightarrow 2Fe^{2+} + S_4O_6^{2-} \quad (1.9)$$

$$S_2O_3^{2-} + Cu^{2+} + 2OH^- \rightarrow SO_4^{2-} + H_2O + CuS_{(ppt)} \quad (1.10)$$

$$2Cu^{2+} + 2S_2O_3^{2-} \rightarrow 2Cu^+ + S_4O_6^{2-} \quad (1.11)$$

In addition to the above reactions, thiosulfate is also consumed by peroxides, phosphines, polysulfides, permanganates, chromates, the halogens (chlorine, bromine and iodine), and their oxyanions. In addition, certain species of fungi, microfauna and microflora can digest thiosulfate ions, albeit quite slowly [72].

Although the thiosulfate ligand is also significantly less stable than cyanide in similar conditions, which limits leaching times and increases reagent consumption, this native instability of thiosulfate becomes an asset when environmental considerations are taken into account. The ligand itself is of very low toxicity, with its common salts being regarded as non-hazardous, while many of its soluble metal complexes break down to relatively harmless materials such as sulfates, insoluble sulfides and oxides, which present a significantly lesser threat to the environment than cyanides [15, 32-33].

The degradation of thiosulfate ions may be caused, or catalysed, by the presence of certain metal ions. Iron(III) accelerates the decomposition of thiosulfate by intramolecular electron transfer. The deep purple $[Fe(S_2O_3)]^+$ complex is formed, and decomposition occurs via reduction of the metal and concomitant oxidation and dimerisation of the ligand to form the tetrathionate ion (Eqn. 1.9) [45, 90, 124]. Similarly, the salts of arsenic, antimony and tin catalyse the formation of pentathionate from thiosulfates, while metallic copper, zinc, and aluminium result in the formation of sulfides [33, 72]. Both mercury and silver tend to form nearly insoluble sulfides, although complexation in excess thiosulfate tends to minimise this precipitation [33].

Thiosulfate leaching is accelerated by light [77], although this also encourages the consumption of thiosulfate ions in reactions with semiconductor minerals such as TiO_2 and Fe_2O_3. Many iron minerals, such as pyrite and haematite will catalyse the oxidative degradation of thiosulfate ions into tetrathionate [22, 72]. However, the side-

reactions and decomposition processes of many metal thiosulfate complexes are not well characterised. In any case, when leaching minerals it is essential to allow for the natural degradation of thiosulfates via ubiquitous O_2, H_3O^+, trace Fe^{3+}, and other oxidants. One important example is copper(II) (see Eqn. 1.11), which also contributes to the essential gold oxidation step (Eqn. 1.2). The gradual but inevitable loss of thiosulfate from leaching solutions necessitates relatively speedy leaching and handling operations to optimise gold leaching and minimise precipitation.

It has been proposed that the ammoniacal liquor used in a thiosulfate leaching regime may be substantially recycled in the leach process after precious metal recovery [17, 44, 104]. The recyclability of the liquor strongly depends on the precious metal recovery technique employed, which may cause significant degradation of the liquor by oxidation, reduction, or contamination [17, 22, 75, 125]. Ammonia could be stripped from exhausted liquor (tailings) by exploiting its significant volatility [70]. By-products and tailings from thiosulfate processing should consist primarily of low toxicity metal hydroxides, oxides, sulfates, polythionates, polysulfides and/or insoluble sulfides, although pilot studies to date have not directly addressed waste management.

There are many reversible reactions in which thiosulfate is either consumed or generated. Some provide important contributions to thiosulfate leaching by recycling various breakdown products and regenerating thiosulfate ions. These equilibria are summarised below (Eqns. 1.12 – 1.30 below) where each has been formulated with thiosulfate as the product [13, 21, 33, 45, 72, 76, 106, 126-128]. This summary contains those reactions considered relevant in the literature surveyed, but may not encompass the whole of aqueous thiosulfate equilibria.

$$SO_3^{2-} + 2OH^- + S_4O_6^{2-} \leftrightarrow 2S_2O_3^{2-} + SO_4^{2-} + H_2O \quad (1.12)$$

$$3SO_3^{2-} + 2S^{2-} + 3H_2O \leftrightarrow 2S_2O_3^{2-} + 6OH^- + S^0 \quad (1.13)$$

$$SO_3^{2-} + S_5O_6^{2-} \leftrightarrow S_2O_3^{2-} + S_4O_6^{2-} \quad (1.14)$$

$$SO_3^{2-} + S_4O_6^{2-} \leftrightarrow S_2O_3^{2-} + S_3O_6^{2-} \quad (1.15)$$

$$2S_5O_6^{2-} + 6OH^- \leftrightarrow 5S_2O_3^{2-} + 3H_2O \quad (1.16)$$

$$4S_4O_6^{2-} + 6OH^- \leftrightarrow 5S_2O_3^{2-} + 2S_3O_6^{2-} + 3H_2O \quad (1.17)$$

$$2S_3O_6^{2-} + 6OH^- \leftrightarrow S_2O_3^{2-} + 4SO_3^{2-} + 3H_2O \quad (1.18)$$

$$S_4O_6^{2-} + H_2S \leftrightarrow 2S_2O_3^{2-} + S^0 + 2H^+ \quad (1.19)$$

$$2S_2O_4^{2-} \leftrightarrow S_2O_3^{2-} + S_2O_5^{2-} \quad (1.20)$$

$$2S^{2-} + 4SO_4^{2-} + 8H^+ + 8e^- \leftrightarrow 3S_2O_3^{2-} + 6OH^- + H_2O \quad (1.21)$$

$$2S^{2-} + 2SO_2 + 2HSO_3^- \leftrightarrow 3S_2O_3^{2-} + H_2O \quad (1.22)$$

$$2S^{2-} + 3SO_2 + SO_3^{2-} \leftrightarrow 3S_2O_3^{2-} \quad (1.23)$$

$$2HS^- + 4HSO_3^- \leftrightarrow 3S_2O_3^{2-} + 3H_2O \quad (1.24)$$

$$S_6O_6^{2-} + 3SO_3^{2-} \leftrightarrow 3S_2O_3^{2-} + S_3O_6^{2-} \quad (1.25)$$

$$S^0 + SO_3^{2-} \leftrightarrow S_2O_3^{2-} \quad (1.26)$$

$$S_{(X)}^{2-} + SO_3^{2-} \leftrightarrow S_2O_3^{2-} + S_{(X-1)}^{2-} \quad (1.27)$$

$$S_{x+1}O_6^{2-} + SO_3^{2-} \leftrightarrow S_xO_6^{2-} + S_2O_3^{2-} \quad (1.28)$$

$$S_xO_6^{2-} + S^{2-} \leftrightarrow (x-3)S + 2S_2O_3^{2-} \qquad \{x = 3\text{-}6\} \quad (1.29)$$

$$4S_4O_6^{2-} + 2S^{2-} + 3H_2O \rightarrow 9S_2O_3^{2-} + 6H^+ \quad (1.30)$$

Thiosulfate is ultimately transformed either directly or via intermediates into sulfide and/or sulfate. Apart from sulfide and sulfate, the breakdown products of thiosulfate are not known to form particularly stable complexes with most metal ions of interest [23, 85]. Metal sulfide complexes are generally sparingly soluble, while sulfate has negligible chelating ability. Sulfamate ions ($H_2NSO_3^-$) are also produced

in ammoniacal thiosulfate leach liquors (Eqn. 1.36), but their compounds are of little importance in this system.

Kerley has augmented the leaching system by adding sulfite, with the twofold aims of regenerating some decomposed thiosulfate (Eqns. 1.23 & 1.28) and lixiviating refractory manganese dioxide (Eqn. 1.35) [31, 104]. The addition of sulfite to the lixiviant has also been investigated by other researchers for similar reasons [15, 77-78, 99, 105, 110, 129]. The benefits of this treatment are questionable, as sulfite is readily oxidised by the abundant Cu(II), producing Cu(I), sulfate and dithionate ions [23]. Augmentation of the system with excess sulfate has also been examined, with a view to enhancing thiosulfate stability [49, 105-106]. The 8-electron reaction describing the reduction of sulfate is unlikely to be significant (Eqn. 1.21).

A related thiosulfate leaching regime has been developed in China, denoted the Lime-Sulfur Synthetic Solution (LSSS) [130-132]. The leach liquor may be prepared by combining calcium hydroxide, sodium sulfite, sulfur, and unspecified oxidants in water at elevated temperature to produce a liquor rich in thiosulfate and other sulfur-oxygen anions. Portions of this mother liquor were then diluted into leach slurries, sometimes in combination with ammonia and/or copper salts, and have been successful in lixiviating gold and silver from a number of ores. A similar scheme has been patented by Freeport-McMoRan, wherein gold is lixiviated by the action of sulfur dioxide and oxygen on a sulfide-rich ore slurry [123]. It is clear that this treatment should produce a significant concentration of thiosulfate ions (Eqns. 1.13, 1.22 - 1.24, 1.32), although the authors imply that gold is dissolved as hydrosulfite or sulfite complexes. Thiosulfate ions are likely to play a significant role in these systems, although polysulfide and sulfite ions may also contribute to the leaching ability of the liquor.

A number of authors report the in-situ synthesis of thiosulfate ions from sulfoxy compounds or ions during carefully controlled oxidative leaching [27, 61, 104, 116, 133]. As a by-product of the destruction of a sulfide matrix, the oxidation of native sulfur or sulfides may be the cheapest source of lixiviant generation (Eqns. 1.26 - 1.27 & 1.31 - 1. 34) [27, 33, 61, 133]. The reaction mechanism(s) that permit this transformation appear to involve the attack on elemental sulfur by transitory polysulfide species (ie. NaS_xH in Eqn. 1.34) [33, 133]. The sulfur dioxide produced in an ore roasting step may also be used to generate thiosulfate lixiviant [23-24]. Recovering harmful sulfurous matter in this fashion also has the advantage of minimising the environmental impact of the operation. However, recycling and/or in-situ generation of thiosulfate has yet to be implemented at a significant scale.

$$4S_{(x+1)} + 6OH^- \rightarrow S_2O_3^{2-} + 2S_x^{2-} + 3H_2O \quad (1.31)$$

$$2NH_3 + SO_2 + S^0 + H_2O \leftrightarrow (NH_4)_2S_2O_3 \quad (1.32)$$

$$2(NH_4)_2S + 2SO_2 + O_2 \rightarrow 2(NH_4)_2S_2O_3 \quad (1.33)$$

$$S_8 + 8NaOH \rightarrow 2(Na_2S_2O_3) + 2NaS_xH + H_2O \quad (1.34)$$

$$MnO_2 + 2[(NH_4)_2SO_3] + 2H_2O \rightarrow MnS_2O_6 + 4NH_4OH \quad (1.35)$$

$$HSO_4^- + NH_4^+ \rightarrow HSO_3NH_2 + H_2O \quad (1.36)$$

Recent modifications to the leaching regime show considerable promise in this regard [116]. Supra-atmospheric pressures of oxygen at pH < 9 displace copper as the primary gold oxidant, and hence ammonia and copper can be omitted entirely (Eqn. 1.5). The most critical step of this patented process involves treatment of the pregnant leach liquor with sulfide ions whilst controlling oxygen pressure, temperature and pH. Depending upon the conditions used, this treatment can either

selectively recycle a substantial portion of the polythionate byproducts (Eqns. 1.19, 1.27, 1.29 & 1.30), precipitate the gold from solution, or both.

1.4. Recovery of Gold from Thiosulfate Leach Liquors

The removal and recovery of gold from conventional cyanide leach liquors has been pursued using variations of the five techniques listed below:

- Precipitation
- Electrowinning
- Solvent Extraction
- Carbon Adsorption
- Resin Adsorption

Similarly, these same processes have also been applied to the recovery of gold from ammoniacal thiosulfate leach liquors, with varying degrees of success.

1.4.1 Precipitation

Precipitation of the majority of gold from a pregnant leach liquor can be achieved by adding a pulverised metal. Otherwise known as the Merrill-Crowe process, or cementation, the primary mechanism of this recovery technique is the redox reaction between the zerovalent base metal grains and the target noble metals [134]. The precipitant, carefully chosen for redox potential, stoichiometrically displaces the precious metals in solution (see Eqn. 1.37). The more common precipitants are copper and zinc, although iron or aluminium are sometimes employed [70, 112, 134].

$$2Au^{+} + M^{0}_{(solid)} \rightarrow 2Au^{0}_{(ppt)} + M^{2+} \qquad (1.37)$$

Metallic precipitants often have the deleterious effect of reducing thiosulfate ions whilst producing unwanted cations, thus complicating the recycling of the lixiviant. Copper is a reasonable choice, as solutions of copper ions in thiosulfate liquors may be recycled as leach liquor. Some contamination of the solid product often occurs, through either undissolved (excess) precipitant or by co-precipitation with other metal ions in solution, necessitating further purification. In one published article, the authors report that a 30-fold excess of zinc or aluminium powder was required to precipitate all the dissolved gold, whereas a 50-fold excess of copper could only recover 93% of the gold [117].

Precipitation by the addition of sulfide salts, or by chemical reduction with sodium borohydride, hydrogen or sulfur dioxide has also been investigated [77, 125, 135]. These techniques have not been highly favoured, as they tend to precipitate most metals from solution as well as hindering re-use of the leach liquor. Many of these drawbacks have been overcome in a recent patent by Placer-Dome [116], wherein a sulfide solution is used to selectively recycle polythionates and/or precipitate a major portion of the dissolved gold from solution. However, this development is limited to the treatment of leach liquors bearing low levels of ammonia and copper.

1.4.2 Electrowinning

The recovery of metal ions from solution by the application of direct current is known as electrowinning. Aurothiosulfate ions in the solution will migrate to the cathode and form a metallic deposit [44, 134, 140]. Electrowinning is especially problematic in the presence of a great excess of unwanted cations {ie. Cu(I) and Cu(II)}, as they may contaminate the metallic product. This results in a devalued product requiring further purification. Side reactions involving the oxidation or reduction of thiosulfate may also interfere [23]. This lowers the efficiency of electrowinning by increasing the energy input required to recover the desired metals from solution. Due to the abundant copper and thiosulfate ions in these liquors, electrowinning does not appear to be a viable option. However, a modified system can be applied to leach liquors with low levels of copper and ammonia, by adding sacrificial quantities (0.01 – 2 M) of sulfite [116]. The sulfite ions are reduced to sulfate at the anode, preventing fouling by elemental sulfur.

1.4.3 Solvent Extraction

In this technique, the leach liquor is contacted with a solution of extractant in a water-immiscible organic solvent. The gold complex is partitioned into the organic phase, whereas the other metals ideally remain in the aqueous phase. The organic phase may then be separated, stripped of gold, and returned to the extraction circuit. There have been a number of studies in which gold has been extracted from ammoniacal thiosulfate liquors by solvent extraction. Zhao *et al* report the application of a number of potential gold extraction reagents using varied diluents, such as benzene, kerosene, and 1- and 2-octanol. The extractants employed in these solvents were primary, secondary and tertiary alkylamines, tertiary amine oxides, phosphines, phosphine oxides, and phosphate esters [56, 61, 136-139]. Each of these

neutral reagents bore large alkyl groups to enhance solubility in the organic phase. The results of these studies are shown in Table 1.2.

Artificial thiosulfate liquors (0.8 M) were examined with and without ammonia. The presence of ammonia in the liquor was reported to improved extraction in several cases [56, 138]. The amines alone were effective extractants, with efficacy increasing in the order 1° > 2° > 3° alkylamines. Aromatic diluents or kerosene performed better than n-octanol and chloroform, apparently due to inductive electron-acceptor effects of the latter solvents on the amines [61, 137-138]. The organic phase was stripped of more than 96% of the extracted gold in 10 minutes using aqueous sodium hydroxide (pH>10) [138]. Phosphorus compounds performed better in the presence of the primary amine than alone, suggesting synergistic electron-donating effects [56, 137]. The performance of the amine extractants was significantly improved in the presence of a trialkylamine oxide (TRAO), which was also accounted for by electron-donating synergism [136, 138]. The addition of ammonia significantly enhanced selectivity of the organic phase for gold from an artificial solution containing copper, zinc, nickel, gold and silver [61, 139]. This was supported by the selective extraction of gold from a real leach liquor (0.8 M thiosulfate + 2 M ammonia) containing Au(I) (10.66 ppm), Ag(I) (5.59 ppm), and 0.11% soluble copper [139]. The authors have characterised the metal selectivity of the solvent extraction system by the 'Separation Factor' (α), an unquantified term. The results of these selectivity tests are summarised in Table 1.3.

Another approach, patented by Virnig *et al*, utilises a variety of N-alkylated guanidines in aliphatic or aromatic solvents [141-142]. Alternatively, the lixiviant can be a mixture of a quaternary ammonium compound and a weak acid, such as phenol. These mixtures were contacted with leach liquors containing thiosulfate (25 – 200 mM) and ammonia (> 50 mM) at pH 8 - 10. Although no process results were

reported, it was claimed that the organic phase could be stripped of gold by aqueous NaOH. Solid phase sorbents impregnated with the solvent phase were recommended to facilitate separation of the gold-loaded solvent.

	Au	Ag	Cu	Zn	Ni
Artificial Liquor (mmol/L)	0.20	0.24	14.98	0.20	0.21
Approximate Recovery %¤	95	32	< 2	12	< 2
Leach Liquor (ppm)	10.66	5.59	1100	-	-
Approximate Recovery %¤	95	15	< 1	-	-
Au Separation Factor (α)	-	15	1695	-	-

Table 1.3 Solvent Extraction of Metals from Thiosulfate Liquors [139]

Lixiviants: N_{1923} and TRAO; diluent: n-octane; phase ratio 1:1

¤ Conditions: 10 min. contact time at ambient temperature (20°C).

Solvent extraction has numerous constraints that limit the scope of possible industrial applications. Evaluation requires an analysis of the loss of the organic phase and extractive reagent by dissolution in the aqueous phase, through chemical degradation and by evaporation. In any case, the application of solvent extraction is limited to clarified liquors, free of particulate matter [134, 139-140]. To produce clarified liquor from a mineral pulp, additional plant equipment and processing time would be required, and these steps would result in considerable increases in capital costs and operating expenses.

%Gold Extraction	Extraction Reagent(s)	Concentrations (mol/L)	Effective Diluent(s)	$[S_2O_3^{2-}]$ (mol/L)	$[NH_3]$ (mol/L)	[Au] (mmol/L)	pH	Ref.
~ 92	1° - 3° amines	0.5	octane	0.2-0.8	0	0.24	< 8.0	[136]
95	TRPO + APE	25% v/v	octane/none	0.2-0.8	0-0.15	0.24	> 10.0	[56]
~ 96	N_{1923} + APE	0.5 + 0.2-0.6	kerosene/octane	0.8	0	0.24	< 8.0	[137]
~ 97	N_{1923} + TRAO	0.2-0.3 + 0.3-0.6	octane	0.8	0	0.24	< 7.5	[138]
~ 95	N_{1923} + TRAO	0.5 + 0.15	octane/kerosene	0.8	1.6	0.20	< 9.0	[139]

Table 1.2 Solvent Extraction of Gold from Thiosulfate Liquors

Conditions: Ambient Temperature (~20°C); 1:1 phase ratio; APE: alkylphosphorus esters

N_{1923}: primary amine with $C_{19\text{-}23}$ alkyl group; TRPO: trialkylphosphine oxide; TRAO: trialkylamine oxide

1.4.4 Carbon Adsorption

The capture of the dicyanoaurate complex $[Au(CN)_2]^-$ onto activated carbon has been the mainstay of gold hydrometallurgy for several decades. This technique has superseded precipitative and electrochemical techniques due to its high efficiency, relatively low costs and purity of product. A schematic diagram of a typical CIP plant is show in Figure 1.5. Porous granules of carbon are contacted with gold-bearing cyanide liquor, then recovered with the adsorbed gold. The adsorption step may take place in the presence of the mineral pulp (CIP: Carbon-In-Pulp), or may be conducted with the clarified liquor. The former technique is often preferred, as this tends to reduce capital costs. Clarification of liquors is not only expensive and time consuming, but higher recoveries of gold can be achieved using the scavenging behaviour of CIP techniques.

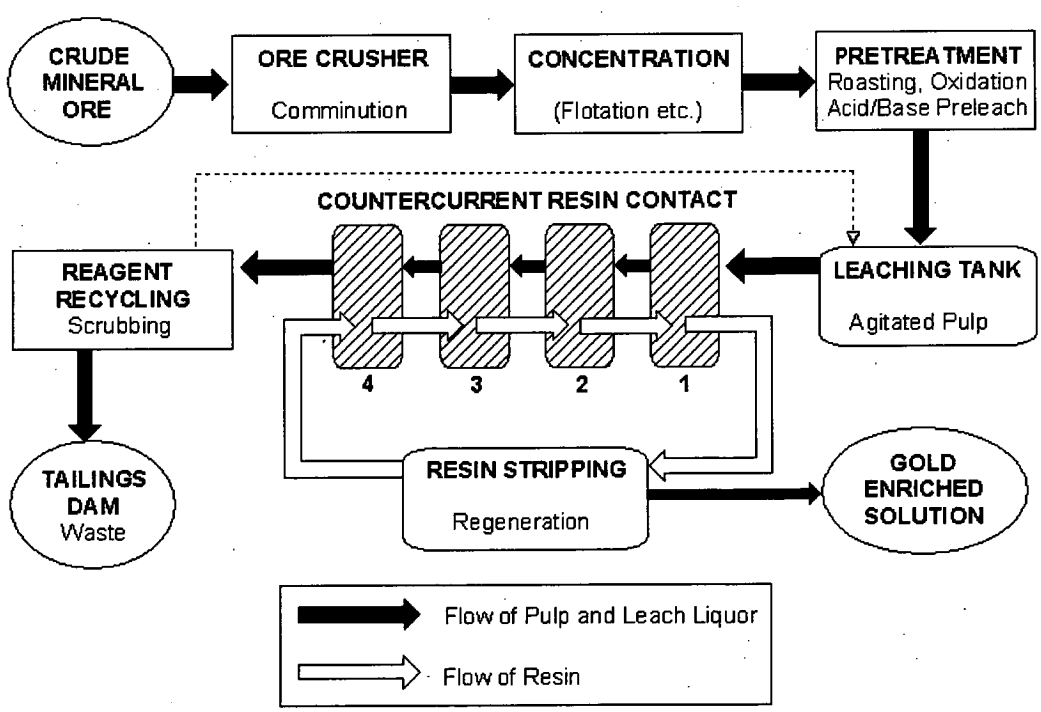

Figure 1.5 Generic Process Diagram for a RIP/CIP Plant

Once separated, the gold-bearing carbon is commonly eluted with a hot caustic cyanide solution, often under pressure. The stripped carbon is usually regenerated for re-use by washing with aqueous acid, then heated in an oven at 650°C for several hours under a non-oxidising atmosphere [6]. Gold in dilute thiosulfate liquors may be quantitatively converted into the more stable aurocyanide complex by adding a slight excess of cyanide ions [70, 99]. Although permitting the recovery of the gold onto carbon, this introduces cyanide complexes that can contaminate both the product and the effluent, thus defeating the environmental advantages of the thiosulfate process.

There appears to be some contention as to the affinity of the aurothiosulfate complex for carbon. Activated carbon achieved a 95% gold recovery after 6 hours contact at 25°C with a gold-bearing leach liquor (15.8 mg/L Au) derived from a Dominican ore via an ammoniacal thiosulfate lixiviant (2.0 M $Na_2S_2O_3$ + 4.0 M NH_3; pH 10.5) [44, 114]. Conversely, a 0.1 M solution of the aurothiosulfate complex in KOH (10^{-4} M; pH 9.7) was found to have little or no affinity for carbon at 25°C [46-47]. This discrepancy may be due to a loss of sensitivity to small changes in the surprisingly high gold concentration in the latter experiment. However, in other studies, many types of carbon adsorbents were contacted with ammoniacal thiosulfate leach liquor, and all were found to have a poor capacity for aurothiosulfate [48, 143]. Certainly, the $[Au(S_2O_3)_2]^{3-}$ complex has significantly less affinity for carbon than the $[Au(CN)_2]^-$ anion. It has not been established whether this effect is due to the larger size or charge of the thiosulfate complex, or to other factors. Techniques for elution of carbon-adsorbed aurothiosulfate have not yet been reported.

1.5 Resin Adsorption

The use of resin adsorbents for the recovery of precious metals is a relatively under-developed area of hydrometallurgy. The principal reason behind this is the abundance and efficacy of cheap activated carbon adsorbents. Although resins are extensively utilised in the CIS (Commonwealth of Independent States) for the recovery of gold from cyanide liquors [13], resin adsorbents are more expensive than carbon, and their application requires the installation of specialised apparatus [144]. The treatment may be RIL (Resin in Leach), wherein the adsorbent is added to the ore at the same time as the leaching reagents, or RIP (Resin in Pulp), in which the adsorbent is introduced after an initial leaching (induction) period. The operation of a typical RIP plant is illustrated in Figure 1.5, revealing a similar mode of operation to the CIP (and CIL) techniques, although there are some fundamental differences between the Carbon- and Resin-based processes.

Both carbon and ion exchange resins must be chemically stripped after separation from the leach pulp. However, in contrast to activated carbon which must be thermally regenerated (activated) rather than treated chemically, a careful choice of eluent can allow the resin elution and regeneration steps to occur simultaneously, and quite rapidly. Importantly, activated carbon is understood to adsorb the aurocyanide between optimally spaced uncharged graphitic layers of the matrix [51], whereas ion-exchange resins have abundant functional groups of like charge which concentrate solvated ions of opposite charge (counterions). Unlike carbon, the functional groups of a polymeric resin can be tailored for selectivity for a particular ion or complex by exploiting differences in charge or structure.

This advantage has been exploited by several groups in the preparation of resins that are highly selective for the aurocyanide complex in conventional and ammoniacal cyanide liquors [145-146]. These resins, Aurix and Minix, have been

optimised for gold recovery from cyanide solutions by altering properties such as functional group, capacity, active group spacing and geometry, matrix crosslinking and porosity. Aurix®, marketed by Henkel Australia, is reported to bear guanidine moieties, whereas Minix®, which is marketed by Mintek, South Africa, bears optimally distributed tributylammonium groups.

Resin performance can be characterised by the Selectivity Ratio (S_R):

$$S_R\{Au,M\} = [Au]_R / [M]_R$$

where M is a metal ion and $[M]_R$ is the molar concentration of M on the resin phase. This gives an indication of the preference of a functional group for gold over the competing metal, M., although it can strongly depend upon the initial concentrations used. Table 1.4 contains the Selectivity Ratios of gold over copper for a number of specialty resins, including the commercialised gold-selective resins Minix® and Aurix®. Elution of the adsorbed gold from Minix® resin can be achieved using thiourea (1.0 M) in aqueous H_2SO_4 (0.1 M) at 60°C, whereas gold can be eluted from Aurix® with aqueous NaOH (1.0 M). The stripped resins are then ready for re-use in the next cycle of gold adsorption. The improve selectivity of the novel cage-like moiety of Notren resin was attributed to increased steric hindrance [145].

A more complete characterisation of the affinity of a resin for one metal over another is given by the Selectivity Coefficient ($S_C\{Au\}$), which can take all metal ions into account:

$$S_C\{Au\} = \frac{[Au]_R}{[Au]_S} \cdot \prod_M \frac{[M]_S}{[M]_R}$$

where other terms are defined as before, and $[M]_S$ is the concentration of metal M in solution. Although less dependent upon initial conditions than S_R, this term is still depends upon which ions are used in the test solution. Moreover, it requires considerably more data to calculate.

ppm (g/t)	Au	Ag	Cu	Zn	Ni	Co	Fe	$S_{R\{Au,Cu\}}$
Initial	6.1	< 1	12	4.5	20	2.1	6.8	
Aurix[§]	10560	331	571	1942	5284	175	441	6.0
Initial	5.0	0.5	10.0	2.0	5.0	1.0	10.0	
Minix[¤]	36500	-	2300	9880	5600	-	292	5.1
Notren[¤]	39089	-	1000	575	1550	-	106	12.6
Carbon	25200	< 200	< 200	< 200	460	< 200	1500	40.6

Table 1.4 Performance of Gold Selective Resins in Cyanide Liquors [145, 146]

[§] 15 min/stage (7 stages); 28g resin/l. [¤] Selectivity Test; 250 ppm CN.

Leach liquors with a high thiosulfate concentration may function as an efficient eluent, desorbing some silver (and possibly gold) from anion-exchange resins and resulting in a poor recovery [10, 147]. An alternative that has been explored is to add cyanide ions to convert the aurothiosulfate complex to the more stable aurocyanide, and recover that on a resin [70, 99]. However, the recovery of silver from thiosulfate solutions using ion-exchange resins has been extensively investigated as a cost-saving measure in the photographic industry [148-151]. Analogous treatments for gold-bearing solutions are currently under development using similar techniques to those applied to silver recovery [48, 59, 70, 96, 112, 116, 152]. For this reason, approaches used for silver recovery are discussed further below.

1.5.1 Recovery of Silver using Resins

Silver is used extensively used in the developing and fixing of photographic films, a process which generates a thiosulfate effluent solution containing silver. This effluent often contains up to 50 ppm Ag(I) in ~0.01 M sodium thiosulfate, and may also contain additives such as the Fe(II)-EDTA complex to aid in the fixing process [148-150]. Silver must be removed from the effluent to meet environmental discharge requirements, and to reduce the processing expenses by recycling. There have been many attempts to recover silver from thiosulfate solutions by the use of ion-exchange processes. For example, the Russian strong-base resin AV-17 (Me_3N^+ groups on polystyrene gel matrix; 4.7 meq/g) in hydroxide form was used to adsorb 66% of the silver from a solution of $Na_3[Ag(S_2O_3)_2]$ (4.5 mM) at pH 5.0-5.5 [153]. The adsorbed silver was fully eluted from the resin (8.6 g dry mass) with aqueous $Na_2S_2O_3$ (600 mL x 3.4 M). However, when strong base resins were applied to more dilute solutions(ca. 0.23 mM Ag(I)), the silver thiosulfate complex decomposed within the resin to form insoluble Ag_2S [154-155]. It was proposed that a thiosulfate

ligand was lost from the adsorbed silver complex, and decomposition of the remaining $[Ag(S_2O_3)]^-$ was then catalysed by the active alkylammonium groups on the resin [154]. Although this silver could be recovered using strong acid as eluent, it was not considered economically viable given the quantity of reagents consumed by the precipitation and elution cycle. Ion exchanger-mediated decomposition of thiosulfate complexes has not been observed elsewhere.

The proprietary *AkwaKlame* system claims to have overcome pre-existing problems relating to the irreversible binding of silver to strong-base ion exchange resins [148]. It should be noted that these researchers provide no details of the properties of the resin used, nor any characteristics of the feed liquor or eluent. They believed that $[AgS_2O_3]^-$ was the main silver-bearing complex adsorbed, a claim supported by Marcus [156]. However, Mina has reported that the silver in photographic effluent is primarily found as the complex ion $[Ag(S_2O_3)_2]^{3-}$ [150]. Recovery of up to 98% of dissolved silver was achieved at pH 4 using the weak base resin IRA-68 (Rohm & Haas; 5.6 meq/g; 3°-alkylamine, pK_A 9.2). The low pH was used primarily to prevent fouling by the ferrous EDTA complex found in the liquor. It was found that the resin loaded more silver when the thiosulfate concentration in the liquor was low, indicating that free thiosulfate ligands compete significantly for ion-exchange sites. Ammonium thiosulfate (pH 6; 1-2 M) with some added sulfite was found to be the most efficacious eluent for removal of the loaded silver and regeneration of the resin [150, 157].

Three commercial resins have been examined for their ability to recover silver from ammoniacal thiosulfate solutions: IRA-400 (quaternary ammonium, gel matrix, 3.8 meq/g), IRA-68 (weak base, gel, 5.6 meq/g) and IRA-94 (weak base dimethylamine, macroreticular, 4.2 meq/g) (all resins from the Amberlite range, Rohm & Haas). Batches of resin (10 g) were stirred in artificial leach solutions

(500 mL) containing thiosulfate (0.2 – 0.9 M), copper (200 – 800 ppm), ammonia (0.3 – 1.8 M) and 20 ppm silver [147]. The efficiency of the resins was determined via their calculated selectivity coefficients, $S_C\{Ag, Cu\}$, which were found to be: 8.97 (IRA 400); 2.84 (IRA-68), and 4.46 (IRA-94). Under these conditions, copper and silver showed relatively poor affinities for the resins, and were slowly displaced by tetrathionate (and probably trithionate) ions.

The Ukranian-made ion-exchanger AM-2B (Atlantis; Me_2N & Me_3N^+ groups, 1.1 meq/mL), commonly applied to the recovery of $[Au(CN)_2]^-$ from cyanide liquors in the CIS, has also been examined as an adsorbent for silver from thiosulfate liquors [158]. Between 85-95% of the adsorbed silver was eluted with unspecified solutions of sodium thiosulfate, sodium sulfite, sodium chloride, or ammonium nitrate. Complete recovery of silver from model thiosulfate liquors has been reported, using Russian strong-base anion exchangers AV-17 and AM-p (macroporous; 4.2 meq/g) [151]. Elution was achieved using a thiosulfate solution (1-3 N), or by a 5% solution of thiourea in dilute sulfuric acid (see Table 1.5).

Commercial IEX resins IRA-67 (same as IRA-68) and IRA-458 (quaternary ammonium, 4.4 meq/g), both manufactured by Rohm & Haas, were used to recover silver (50 ppm) from weak thiosulfate liquors (5 - 10 mmol) at various pH values [149]. The weak base resin was only effective between pH 2 – 6, whereas the strong base resin adsorbed more than 90% Ag(I) at all pH values studied. The organic polymer Chitosan (poly(*d*-glucosamine)) was also examined for its capacity to adsorb silver from a variety of solutions, including thiosulfate liquors [149]. Unfortunately, the highest silver retention levels were obtained in acidic solution, and Chitosan was not competitive with commercial resins (see Table 1.5).

Resin Data	Functional Group Affixed to Polymer	$[S_2O_3^{2-}]$ (mmol/L)	pH	[Ag] (ppm)	%R	%E	Eluent(s) Tested (mol/L)	[Ref]
AV-17 (OH)	®-$N^+(CH_3)_3$	3400	5-5.5	130	66	94	$Na_2S_2O_3$ (3.4 M)	[154]
Wofatite P	'Organic Cationite'	2.8-3.5	-	76	-	-	NaOH, H_2SO_4, HNO_3 (5.6 M)	[155]
VDP-1 VDP-2 N-0, MVP-10 MVP-2, AV-16-G AV-17	pyridine α-picoline *[commercial]* benzyl α-picoline ®-$N^+(CH_3)_3$	-	-	216-10790	100	-	NaOH, H_2SO_4 or $Na_2S_2O_3$	[153]
AM-2B	'Strong Base'	-	-	-	-	95	$Na_2S_2O_3$, Na_2SO_3 NaCl or NH_4NO_3	[158]
AV-17, AM-p AN-221	®-$N^+(CH_3)_3$ 'Weak Base'	100-3000	-	100-1000	-	100	$Na_2S_2O_3$ (1-3 M) or thiourea in H_2SO_4	[151]
Dowex-1	®-$N^+(CH_3)_3$	10-4000	-	11	-	-	-	[156]
IRA-68	'Weak Base'	54-517	4-7	200¤	98	>90	$(NH_4)_2S_2O_3$ (1 M)	[150]
		-	4.2	100-150¤	98	-	$(NH_4)_2S_2O_3$ (0.81 M) + Na_2SO_3 (0.16 M)	[157]
IRA-67 IRA-458 GT-73 IRC-718 Chitosan	Polyamine ®-$N^+(R)_3$ Thiol ®-$N(CH_2COOH)_2$ Chitosan	5-10	2-10	50§	96	-	H_2SO_4	[149]

Table 1.5 Polymer Adsorbents for Silver from Thiosulfate Liquors

Temperature: 20-30°C; %R = gold adsorbed; %E = gold eluted; ¤: Solution contains < 500 mg/L Fe; §: Solution contains 10 mM SO_3^{2-}

1.5.2 Recovery of Gold using Resins

The earliest attempts to apply ion-exchange resins to the recovery of gold from ammoniacal thiosulfate solutions appear in the work of Atluri [147]. Ten gram batches of the commercial Amberlite resins IRA-400 (strong base), IRA-68 and IRA-94 (weak bases) were stirred in synthetic solutions (500 mL) containing thiosulfate (0.2 – 0.9 M), copper (200 – 800 ppm), ammonia (0.3 – 1.8 M) and 20 ppm gold. A drop in pH from 10.2 (initially) to 9.8 (60 minutes) was observed in these liquors. Unsurprisingly, the strong base resin was found to be the most effective at removing gold from solution. As before, these resins were characterised according to their selectivity coefficients, $S_C\{Au, Cu\}$, which were: 10.23 (IRA-400); 5.39 (IRA-68), and 9.84 (IRA-94). Elution of resins IRA-68 and IRA-400 in stirred batches of ammonium thiosulfate solution (500 mL; 0.9 - 2.7 M) was slow, with copper significantly co-eluting with silver - but not with gold.

The patent of Jay [159] utilised amine-functionalised ion-exchange resins embedded in a porous polyurethane matrix to adsorb gold from a range of gold-bearing thiosulfate solutions. Quaternary ammonium moieties were preferred, giving the best capacity and broadest effective pH range. The presence of a water-immiscible alcohol such as 1-octanol (ie. solvent impregnation) improved the loading characteristics of the resins. It was claimed that gold could be stripped from the adsorbent using unspecified solutions of sodium or ammonium thiocyanate, and more rapidly by augmenting the eluent with dimethylformamide, acidic thiourea, zinc cyanide or sodium benzoate. There is no evidence to support these latter claims, and insufficient data were provided to calculate the efficacy of gold recovery or the gold loading on the sorbents.

Mohansingh has examined the adsorption of gold from artificial thiosulfate liquors onto activated carbon and three commercial ion-exchange resins. In

summary, the best results were obtained using the strong base resin Amberlite IRA-400 at ambient temperature and a pH of 9 [143]. Elution was more problematic, with only 76% of the adsorbed gold eluted with the best performing eluent (5 M aqueous NaCl) over 24 hours. The resin selectivity for gold over copper was not examined.

The use of a weak-base ion exchange resin such as Amberlite IRA-743 (Rohm & Haas; weak base polyamine; 0.6 meq/mL) to recover gold from dilute thiosulfate leach liquors has been claimed by the Barrick Gold Corporation [70]. It was suggested that this might be followed by a similar recovery of the cationic cupric tetrammine complex. A subsequent patent by the same authors described the recovery of aurothiosulfate via a wide variety of strong base ion-exchange resins in RIP and RIL processes [59]. A single weak base resin, Amberlite A7 (Rohm & Haas, polyamine, 13.9 meq/g) was also reported to be applicable to this process. The preferred adsorbents for this patented process bear quaternary amine functional groups of Type I (trialkylammonium) or Type II (hydroxyalkylammonium), preferably affixed to macroporous beads. The preferred treatment regime consisted of 12 x 1 hour pulp contact stages, then multi-stage stripping as detailed below. The presence of the resin in the pulp was reported to minimise the degradation of the thiosulfate leach liquor. Relatively dilute leach liquors were used, containing 0.03 - 0.05 M thiosulfate, 0.5-1.6 mM Cu(II), and 7-100 mM NH_3, at pH values ranging from 7 to 9 [59, 152]. The resin(s) were contacted with the leach pulp in a Pachuca tank for up to 12 hours, then isolated by screening. Copper and gold were then eluted separately from the resin. The selective elution of copper was achieved using ammoniacal ammonium thiosulfate (ca. 100-200 g/L, 5-6 bed volumes) or oxygenated ammonia buffered by ammonium sulfate. The latter reagent was preferred, as it facilitated the recycling of the eluent as leach liquor [152]. Gold was

then stripped from the resin with a solution of ammonium, potassium, or calcium thiocyanate (ca. 100-200 g/L, 5-6 bed volumes).

Thiocyanate counter-ions on the resin are undesirable, as they are quite costly and toxic, and their presence would worsen the environmental impact of an installation [70]. Subsequent testing has revealed that the thiocyanate eluent may be substituted with cheaper and less toxic trithionate or tetrathionate eluents [152]. The polythionate eluents cause less deviation in pH levels, thus minimising osmotic shock and consequent resin attrition. After copper stripping, gold-loaded resins were eluted with up to 8 bed volumes of a solution of trithionate and/or tetrathionate (40 - 200 g/L; see Table 1.6). This eluent is prepared cheaply by controlled oxidation of thiosulfate. The resin was regenerated by flushing with a solution of sodium hydrogen sulfide (NaSH; ~2 g/L), recycling both tetrathionate and trithionate into thiosulfate ions (Eqns. 1.27 & 1.30). The various schemes for elution of the aurothiosulfate complex from strong base resins are illustrated in Figure 1.6.

An ammoniacal leach liquor bearing gold and copper was treated with the macroporous strong base resin A-500C (Purolite, quaternary ammonium, 1.15 meq/mL) using the above procedure [152], resulting in a discharge solution retaining very little gold and copper (see Table 1.6). Copper was stripped with 99.9% efficacy over 2 hours, using ammonium thiosulfate eluent (150 g/L, 4 bed volumes). The resin was then flushed for 4 hours at a rate of 2 bed volumes of polythionate liquor per hour (either ~200 g/L trithionate, or ~40 g/L trithionate with ~80 g/L tetrathionate). Both solutions resulted in >99% elution of the adsorbed gold.

Resin Data	Type	meq/g	Matrix	$[S_2O_3^{2-}]$	$[NH_3]$	pH	T°C	Sorption	[Au]§	[Cu]§	%Au	Eluent(s)	$S/R_{(Au,Cu)}$	Ref.
IRA-743	WB	1.0	-	0.03 M	7-100	7-9	-	12 hr	-	-	-	Cu: SO_4^{2-}, $S_2O_3^{2-}$, NH_3	-	[59]
Amberlite A7	WB	-	MP		mM							Au: SCN^-		[70]
Type I/II resins	SB	-	-											
A500C *(Purolite)*	R_4N^+	1.7	MP	0.05 M	0.1 M	8.0	60	6 x 1 hr	1.8	22	99.45	Au: SCN^-	0.034	[14]
A500C *(Purolite)*	R_4N^+	1.7	MP	-	-	6-8	20	4 hr	-	-	-	Au: $S_3O_6^{2-} + S_4O_6^{2-}$	0.038	[13]
AV-17-10P etc.	R_4N^+	-	-	0.5 M	0.5 M	5-	-	5 hr	9.5-	-	94.2	Au: thiourea + H_2SO_4	-	[48]
(see Table 1.7)						11			17.9					
AmberJet 4200	R_4N^+	3.7	Gel	0.05 M‡	0.8 M	8-	22	6 x 2 hr	8.9	8.7	>99.4	Au: SCN^-/NO_3^-	2.39	[160]
(Rohm & Haas)						9.5					4			
Aurix ® *(Henkel)*	Guan	-	-	25-200	0.05-	8.0-	-	-	-	-	-	Au: NaOH, CN^- and	-	[141]
				mM	0.1 M	10						sodium benzoate		
AmberJet 4200	R_4N^+	3.7	Gel	0.05 M	0.2 M	9.5	-	-	10	10	99	Cu: SO_4^{2-}, NH_3, O_2	-	[96]
Vitrokele 911 (R&H)	R_4N^+	1.7	MR									Au: NH_4NO_3 (2 M)		
IRA-400 *(R&H)*	R_4N^+	3.8	Gel	1.0 M	0.1 M	9-	20-	8 hr	9.27	31.8	94.7	Au: NaCl (5 M)	-	[143]
Dowex *(Dow)*	R_4N^+	-	-			12	60		9.12		75.98			
Eichrom	SA	-	-						9.31		9.23			

Table 1.6 Polymer Adsorbents for Gold from Ammoniacal Thiosulfate Liquors

§: reported in ppm; ‡: contains 1.0 mM sulfite; WB: weak base; SA: strong acid; Guan: guanidyl

R_4N^+: quaternary ammonium (strong base); Matrix: MP = macroporous; MR = macroreticular;

The principal drawback of this technique is the requirement for two separate elution stages, and in particular the additional handling time and reagents this demands. Processing time and related costs may be minimised by using an adsorbent that is highly selective for gold, thus eliminating the need for multi-stage stripping.

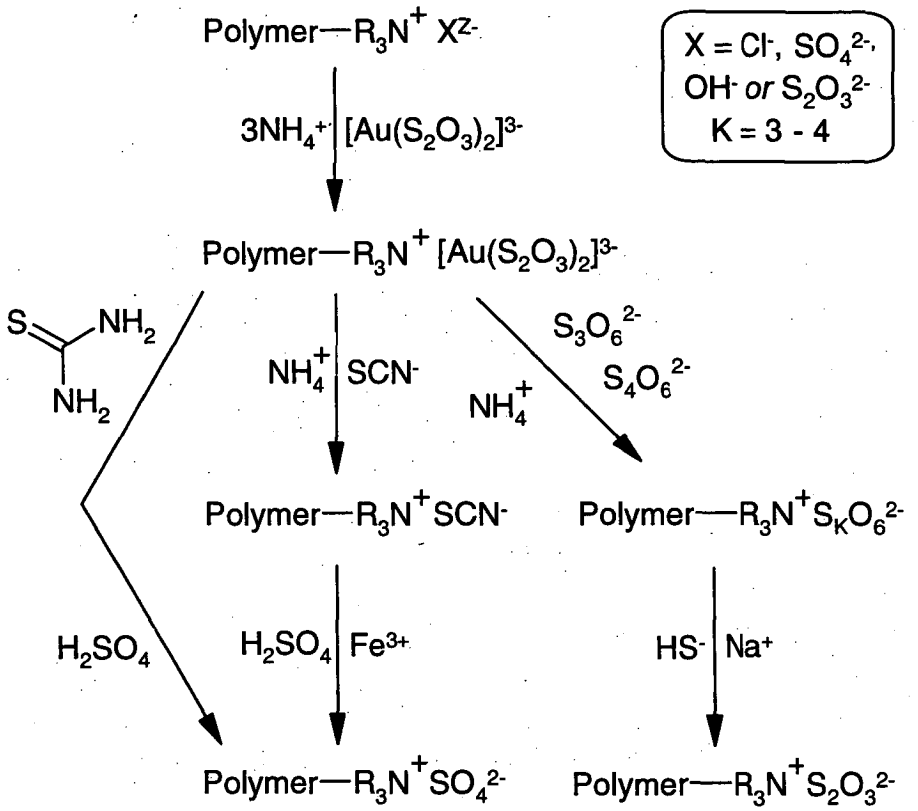

Figure 1.6 Elution of Aurothiosulfate from Anion Exchange Resins

A recent development of this process is the subject of a patent by Placer Dome Technical Services Ltd. [116]. Leaching is conducted at relatively low pH (< 9) in liquors substantially free of copper (< 15 ppm) and ammonia (< 0.05 M), with the role of oxidant fulfilled by high pressures of oxygen (4-500 psi). Under these conditions, dissolved anionic copper is minimised, and hence prevented from fouling adsorbents. The critical process of this development is the reduction of polythionates with sulfide (Eqn. 1.40). This procedure can regenerate thiosulfate from the

polythionate byproducts, and may also be used to precipitate the majority of gold as a sulfide (Eqn. 1.41). Alternatively, the gold may be recovered from this liquor by electrowinning, by solvent extraction, or by ion-exchange onto a resin. Importantly, this new process minimises the two environmentally hazardous components, namely copper and ammonia.

$$S_xO_6^{2-} + S^{2-} \rightarrow S_2O_3^{2-} \qquad (60°C / pH\ 7 / O_2\ atm.) \qquad (1.40)$$

$$[Au(S_2O_3)_2]^{3-} + SxO_62^{-} + S^{2-} \rightarrow S_2O_3^{2-} + Au_2S \qquad (22°C / pH\ 10 / N_2\ atm.) \qquad (1.41)$$

A series of novel Russian ion exchange polymers was examined for their capacity to adsorb gold (9.5 – 17.9 ppm) from clarified thiosulfate leach liquors. These were prepared by applying a solution containing equimolar amounts of sodium thiosulfate and ammonia (0.5 M each) to an oxidised arsenopyrite flotation concentrate containing high levels of arsenic (4.8%) and iron (7.1%) [48]. Consistently, more gold was adsorbed at the lower pH values (in the range 5 – 11) (see Table 1.6). The most efficient sorbent was the trimethylammonium (strong base) functionalised polymer AV-17-10P, which achieved a gold recovery of 94% at pH 6 and 85% at pH 11. Good gold recoveries were also observed at pH 6 using resins with both strong- and weak-base groups (polyfunctional resins), resins with weak-base groups, and with amphoteric phosphonic acid-pyridine copolymers (see Table 1.7). Elution of resins AV-17-10P and AP-100 (5.0 g each) was performed at ambient temperature, using thiourea in aqueous sulfuric acid (0.5 M each). After one hour, the eluent (120 mL) had removed 92.7% and 96.8% of the adsorbed gold, respectively.

Adsorbent Examined	**Functional group affixed to polymer**	**TEC meq/g**	**SBC meq/g**	**Au% recovery** pH 5.8 – 6.1	**Au% recovery** pH 10.8 – 11.0
AV-17-10P	®-$N^+(CH_3)_3$	4.4	4.1	94.2	85.4
AP-100	1° & 2°-amines + ®-N^+R_3	3.9	0.7	91.3	72.9
AP-2-12P	®-$(CH_3)_2N^+CH_2N(CH_3)_2$	3.7	1.1	90.4	65.8
AP-24-10P	®-$N(CH_2CH_2CH_2CH_3)_2$ & ®- $N^+(CH_3)_2Ph$	4.1	1.3	86.5	47.9
AN-85-10P	®-$NHCH_2CH_2NH_2$	6.2	-	86.5	51.0
AN-106-7P	®-$NH(CH_2)_2NH(CH_2)_2NH_2$	8.9	-	88.1	39.0
ANKF-5 *(No pores)*	®-$PO(ONa)_2$ + $\{N(CH_3)_2\}_n$ + poly(vinylpyridine)	U	-	87.5	54.2

Table 1.7 Recovery of gold by polymer sorbents (Kononova *et al*) [48]

Conditions: Ambient Temperature; 5 hrs contact time; 0.5 M NH_3; 0.5 M $Na_2S_2O_3^{2-}$; 9.5-17.9 ppm Au

TEC: Total Exchange Capacity; SBC: Strong Base Capacity; U: Unknown

The recovery of aurothiosulfate using a set of commercially available anion exchange resins has been studied by O'Malley and Nicol [96]. Equilibration of each resin with simple solutions of trisodium aurothiosulfate at pH 9.5 (22°C) yielded isothermal ion distributions (*isotherms*), which clearly demonstrated that strong-base resins were superior to weak base resins for this application. Moreover, they loaded efficiently even at very low solution concentrations of gold. The larger capacity of strong base resins should also make them more tolerant to low levels of competing anions. However, Minix, a strong base resin with excellent selectivity for aurocyanide, performed as poorly as the weak base/polyamine resins (at pH 8).

The best performing resin, Amberjet 4200 (Rohm & Haas, quaternary ammonium, 3.7 meq/g), was used successfully to scavenge gold from a thiosulfate leach pulp (see Table 1.6). It was noted that the copper concentration in the pulp rose as gold displaced it from the resin. Due to the gradual formation of the competing ions trithionate and tetrathionate in the liquor, the resin contact time must be minimised. A thiosulfate eluent rapidly displaced copper, and elution of the adsorbed gold could be achieved using an ammonium thiocyanate solution, or by using the patented Parker eluent (2 M aqueous NH_4NO_3) [96, 160]. The latter was preferred, as ferric sulfate was required to regenerate the resin after thiocyanate elution.

In addition to gold, the thiosulfate complexes of other metals such as lead, copper, zinc and silver are adsorbed onto strong base resins from ammoniacal thiosulfate leach liquors [96, 161]. This reduces the capacity of the resin to adsorb gold, and unless these can be separately stripped from the adsorbent, these metals will contaminate the final gold eluate. Advantageously, aurothiosulfate has been shown to displace the more rapidly adsorbed copper on a strong base resin [96]. The proposed affinity order for adsorption of thiosulfate complexes onto strong-base resins, based on mixed metal adsorption tests, was reported to be:

$$Au > Pb >> Ag > Cu >> Zn.$$

The main products of thiosulfate oxidation, namely trithionate and tetrathionate, can thermodynamically displace copper and gold thiosulfate complexes from strong base resins [96, 161]. Although kinetically slower to adsorb, the presence of these anions in leach liquors restricts the maximal gold recovery that can be achieved. This may become a major problem for the more aggressive leaching operations, where considerable thiosulfate is consumed during leaching and hence polythionates are abundant in the liquor. Tetrathionate, formed by the oxidation of thiosulfate by O_2, Fe(III), Cu(II) or H^+ (Eqns. 1.6 – 1.11), is short-lived in leaching conditions and is eventually transformed into trithionate. Fleming *et al* found that trithionate could only be eliminated from solution by adding sulfide (to form thiosulfate, Eqn. 1.27), which had the undesirable effect of precipitating gold sulfide [152]. Oxidation of thiosulfate must therefore be minimised in leaching, both to conserve the lixiviant and to ensure efficient gold recovery.

Henkel Australia have claimed a patent for the application of their guanidine functionalised polystyrene resin (*Aurix*®) to the recovery of gold from liquors containing thiosulfate (25 - 200 mM) and ammonia (> 50 mM) at pH 8 – 10 [141]. The high pK_a of guanidine (13.5) permits the protonated form of the resin to be present in such liquors, so they should behave similarly to quaternary ammonium resins. The proponents claim that gold can be stripped from the sorbent using aqueous NaOH (pH > 11), with the optional additives of NaCN and/or a carboxylic acid such as sodium benzoate to facilitate more efficient elution. No process examples or experimental details were provided with this claim.

1.6 Conclusions

Ammoniacal thiosulfate leaching is a promising alternative to cyanide based processes, applicable to numerous refractory ores and to environmentally sensitive sites. The process cannot be applied commercially without reliable techniques for recovery of the gold from ammoniacal thiosulfate liquors. Standard practices of precipitation or carbon adsorption are not readily applicable, whereas solvent extraction requires clarified liquors. The only technique appropriate for recovery of gold from commercial thiosulfate leach pulp is sorption onto an ion-exchange resin.

The resin processes reported thus far are not sufficient to justify broad commercial application, although low-copper oxide ores may be amenable to the recovery process developed by Placer Dome [116]. The principal difficulties in present applications arise from the competitive adsorption of unwanted anions. Not only are the gold and copper thiosulfate complexes both adsorbed onto the resins, but also the inevitable byproducts trithionate and tetrathionate. It is felt that both the costs and time involved in operating a two-stage elution process for copper and gold, and the additional requirement for the elution (and destruction) of adsorbed polythionates are commercially prohibitive. Few resins specifically intended for aurothiosulfate recovery have been made to date, and these have generally been ad-hoc preparations [48]. It would be desirable to have a resin which was insensitive to the presence of polythionates, and substantially selective for gold over copper.

1.6.1 Summary of Objectives

The main objectives of this project are as follows:

- Preparation of a series of resins with different IEX moieties on a common backbone
- Measurement of the rate and degree of gold adsorption onto these resins
- Establish a relationship between resin capacity and gold sorption for each moiety
- Identification of a relationship between functional group structure and the degree of gold sorption
- Examine the effects of copper and polythionates on gold sorption
- Develop a system for elution of gold from the resin products
- Compare the best performing novel resins with commercial IEX resins

In principle, a resin that performs well in this system should be highly selective for gold over the copper complexes ($[Cu(S_2O_3)_2]^{3-}$ and $[Cu(S_2O_3)_2]^{5-}$), thiosulfate, polythionates, and trace metal complexes such as lead and mercury thiosulfates. Particularly problematic is the copper(II) bis(thiosulfate) complex, which is similar in charge, size and structure to the gold complex. To distinguish between Au and Cu in the adsorption of $[M(S_2O_3)_2]^{3-}$ compounds, it may be necessary to exploit the stability and kinetics of the complexes. Interference by the much smaller divalent anions, such as trithionate and tetrathionate, also appears to be significant and ubiquitous, and it does not appear that this problem can be solved by the use of a sterically hindered resin moiety. The selection of target functional groups and the influence of solute ions will be addressed in Chapter 2. Details of the preparation of ligand groups and resins, and the characterisation thereof, are provided in Chapter 3.

In order to compare the behaviour of the resins, they must all be examined under the same conditions. This necessitates that an appropriate 'model liquor' be chosen from the range of possible leach liquors (See Table 1.1). The historical development of the ammoniacal thiosulfate leaching system shows an overall trend toward reagent minimisation, driven primarily by economic factors but also influenced by environmental concerns. The selection, composition and preparation of an artificial gold-bearing ammoniacal thiosulfate leach liquor for the purpose of testing resin performance will be further discussed in Chapter 4. This will also incorporate an examination of several techniques for elution of the adsorbed gold and other ions from the adsorbents. The concentration of the various components of the liquor will be followed by AAS and Ion Chromatography (IC), and an analysis of the distribution of the important ions will permit an evaluation of resin performance. In Chapter 5, the evaluation of resin performance in the artificial leach liquors will focus on the best performing subset of adsorbents, with a view to rigorous testing and optimisation of a single high-performance resin.

The competing ions $[Cu(S_2O_3)_n]^{(1-2n)}$, trithionate and tetrathionate set upper and lower size exclusion limits for an appropriate ion-exchange functional group. The structure of the resin itself may also influence selectivity and loading kinetics, although this factor will not be considered in this project. It is hoped that some selectivity for gold may be achieved by the provision of optimal steric bulk around one or more quaternary ammonium group(s), combined with ancillary pendant ligands such as 2-hydroxyethyl groups. It is intended that a wide selection of quaternary ammonium polymers be prepared and evaluated, each with minor differences in the type of alkyl group(s) anchored to the nitrogen atom. In this way, it is hoped that a systematic evaluation will reveal the ideal properties of a gold-selective resin.

References:

1. Wolfe, J.A., *Mineral Resources: A World Review*, 1st Edition; from series: *Environmental Resource Management*; D.R. Coates, Editor. Chapman & Hall (New York), 1984.
2. Marsden, J. and House, I., *The Chemistry of Gold Extraction.* First Edition. Ellis Horwood (New York), 1992.
3. Grosse, A., *Synthesis of Adsorbents for Metal Ions in Soils and Ores*, M.Sc. Thesis, 107 pp.; University of Tasmania (Hobart), 1998.
4. *Environmental Issues*, Issue #83, Minerals Engineering International (MEI), <www.min-eng.com>; March 2003.
5. AusIMM, *AusIMM Week In Review*; Week 12 (23 March), The Australasian Institute of Mining and Metallurgy, <www.ausimm.com.au>; 2003
6. Bhappu, R.B., "Hydrometallurgical processing of precious metal ores", in *Gold: Advances in Precious Metal Recovery*, N. Arbiter and Han, K.N., Editors. Gordon & Breach Science Publishers (New York), 1990. pp.66-80.
7. Avraamides, J. "Prospects for alternative leaching systems for gold: a review", in *Symposium Series Australasian Institute of Mining and Metallurgy No. 32 (Carbon in Pulp Technology for the Extraction of Gold).* Australasian Institute of Mining and Metallurgy, Melbourne, 1982.
8. La Brooy, S.R., Linge, H.G., and Walker, G.S., "Review of gold extraction from ores". *Minerals Engineering*, **7**(10): 1213-1241; 1994.
9. Sparrow, G.J. and Woodcock, J.T., "Cyanide and other lixiviant leaching systems for gold with some practical applications". *Miner. Process. Extr. Metall. Rev.*, **14**: 193-247; 1995.
10. Wan, R.Y., Le Vier, M., and Miller, J.D.: "Research and development activities for the recovery of gold from non-cyanide solutions", Chapter 27 in

Proceedings of the Milton E. Wadsworth (IV) International Symposium on Hydrometallurgy. [Hydrometallurgy : Fundamentals, Technology, and Innovations]. Salt Lake City, Utah, USA. Society for Mining, Metallurgy, and Exploration, 1993. pp. 415-436.

11. Ritchie, I.M., Nicol, M.J., and Staunton, W.P. "Are there realistic alternatives to cyanide as a lixiviant for gold at the present time?", in *Cyanide: Social, Industrial and Economic Aspects. Proceedings of a Symposium held at the Annual Meeting of TMS*, New Orleans, USA. The Minerals, Metals & Materials Society, Warrendale, PA, USA, 2001. pp. 427-440.

12. McNulty, T., "Cyanide Substitutes". *Mining Mag.*(May): 256-261; 2001.

13. Fleming, C.A., McMullen, J., Thomas, K.G., Wells, J.A. "Recent advances in the development of an alternative to the cyanidation process - based on thiosulfate leaching and resin in pulp", in *SME Annual Meeting 2001*. Denver, Colorado. SME, 2001.

14. Ferron, C.J., Turner, D.W., and Stogran, K. "Thiosulfate leaching of gold and silver ores: an old process revisited", in *CIM 100th Annual General Meeting*. Montreal, Quebec. Lakefield Research Ltd., 1998.

15. Langhans, J.W.J., Lei, K.P.V., and Carnahan, T.G., "Copper-catalysed thiosulfate leaching of low-grade gold ores." *Hydrometallurgy*, **29**: 191-203; 1992.

16. Wan, R.Y. and Brierley, J.A., "Thiosulfate leaching following biooxidation pretreatment for gold recovery from refractory carbonaceous-sulfidic ore." *Min. Eng. - Littleton*, **49**(8): 76-88; 1997.

17. Wan, R.Y. "Importance of solution chemistry for thiosulfate leaching of gold", in *World Gold '97 Conference* (Singapore). Australasian Institute of Mining and Metallurgy, Carlton, Victoria, Australia, 1997. pp. 159-162.

18. Mizoguchi, T., Takei, Y., and Okabe, T., "The chemical behaviour of low valence sulfur compounds. X. Disproportionation of thiosulfate, trithionate, tetrathionate and sulfite under acidic conditions". *Bull. Chem. Soc. Jpn.*, **49**(1): 70-75; 1976.

19. Valensi, G., "Electrochemical behaviour of sulfur. Potential-pH equilibrium diagrams of the sulfur-water system at 25°, 1 atm." *Rapports Techniques - Centre Belge d'Etude de la Corrosion*, **121**(207): 22; 1973.

20. Webster, J.G., "The solubility of Au and Ag in the system Au-Ag-S-O_2-H_2O at 25°C and 1 atm." *Geochim. Cosmochim. Acta*, **50**(9): 1837-1845; 1986.

21. Zipperian, D., Raghavan, S., and Wilson, J.P., "Gold and silver extraction by ammoniacal thiousulfate leaching from a rhyolite ore." *Hydrometallurgy*, **19**(3): 361-375; 1988.

22. Benedetti, M. and Boulegue, J., "Mechanism of gold transfer and deposition in a supergene environment". *Geochim. Cosmochim. Acta*, **55**(6): 1539-1547; 1991.

23. Aylmore, M.G. and Muir, D.M., "Thiosulfate leaching of gold - a review". *Miner. Eng.*, **14**(2): 135-174; 2001.

24. Aylmore, M.G., "Treatment of a refractory gold-copper sulfide concentrate by copper ammoniacal thiosulfate leaching". *Miner. Eng.*, **14**(6): 615-637; 2001.

25. Gundiler, I.H. and Goering, P.D. "Thiosulfate leaching of gold from copper-bearing ores", in *SME Annual Meeting*. Reno, Nevada. SME, 1993. [93-281].

26. Gowland, W., *The Metallurgy of the Non-Ferrous Metals*, 4th Edition, Volume 1. Charles Griffin & Co. (London), 1930. pp. 378-381 & 415-418.

27. Genik-Sas-Berezowsky, R.M., Sefton, V.B., and Gormely, L.S., "Recovery of precious metals from metal sulfide", US Patent (4,070,182), Sherritt Gordon Mines Limited, Toronto, Canada, 1978.

28. Arima, H., Fujita, T., and Yen, W., "Thermodynamic evaluation on gold oxidation and reduction mechanisms in ammonium thiosulfate solution", in *SME Annual Meeting 2002* [02-039]. Phoenix, Arizona. SME, 2002.

29. Ficeriova, J., Balaz, P., Boldizarova, E., Jelen, S., "Thiosulfate leaching of gold from a mechanically activated Cu-Pb-Zn concentrate". *Hydrometallurgy*, **67**: 37-43; 2002.

30. Navarro, P., Vargas, C., Villarroel, A., Alguacil, F.J., "On the use of ammoniacal/ammonium thiosulphate for gold extraction from a concentrate". *Hydrometallurgy*, **65**(1): 37-42; 2002.

31. Kerley, B.J.J., "Recovery of precious metals from difficult ores", US Patent (4,269,622), Kerley Industries, 1981.

32. *Approved Criteria for Classifying Hazardous Substances*, NOHSC (National Occupational Health and Safety Commission); Sydney, Australia, 1999.

33. Bean, S.L., "Thiosulfates", in *Kirk-Othmer Encyclopedia of Chemical Technology*, 4th Edition, Volume 24. J.I. Kroschwitz, Editor; John Wiley and Sons (New York), 1997. pp. 51-68.

34. *European MSDS: Directive 67/548/EEC*, 2001
American MSDS: 29 CFP 1910-1200, FDA (USA), 2001,

35. Elsner, L., *Jnl. f. Prak. Chem.*, **37**: 441-446; 1846.

36. Jeffrey, M.I. and Ritchie, I.M., "The leaching and electrochemistry of gold in high purity cyanide solutions." *J. Electrochem. Soc.*, **148**(4): D29-D36; 2001.

37. Fagan, P.A. and Haddad, P.R., "Reversed-phase ion interaction chromatography of Cu(I)-cyanide complexes". *J. Chromatogr. A*, **770**:

165-174; 1997.

38. Grigorova, B., Wright, S.A., and Josephson, M., "Separation and determination of stable metallo-cyanide complexes in metallurgical plant solutions and effluents by reverse phase ion pair chromatography". *J. Chromatogr.*, **410**: 419-426; 1987.

39. Hilton, D.F. and Haddad, P.R., "Determination of metal - cyano-complexes by reversed-phase ion-interaction high-performance liquid chromatography and its application to the analysis of precious metals in gold processing solutions". *J. Chromatogr.*, **361**(27): 141-150; 1986.

40. Huang, Q., Paull, B., and Haddad, P.R., "Optimisation of selectivity in the separation of metallo-cyanide complexes by ion-interaction liquid chromatography". *J. Chromatogr. A*, **770**: 3-11; 1997.

41. Cvetkovski, V., Jovanovic, L., Mitevska, N., Vukovic, M., "Recovery of gold and silver from sulfide refractory ores", in *Changing Scopes in Mineral Processing*, Kemal; A. and Akar; C., Editors; Balkema, Rotterdam, 1996. pp. 549-552.

42. Davison, J., Read, F.O., Noakes, F.D.L., Arden, T.V., "Ion exchange for gold recovery". *Trans. Institute of Mining and Metallurgy*, **70**: 247-290; 1961.

43. Torres, V.M. and Costa, R.S. "Characterisation of gold ores and cip tailings using a diagnostic leaching technique", in *Proceedings of the XIX IMPC.*, Chapter 3, SME, 1994. pp. 15-18.

44. Abbruzzese, C., Fornari, P., Massidda, R., Veglio, F., Ubaldini, S., "Thiosulfate leaching for gold hydrometallurgy." *Hydrometallurgy*, **39**: 265-276; 1995.

45. Perez, A.E. and Galaviz, H.D., "Method for recovery of precious metals from difficult ores with copper-ammonium thiosulfate." US Patent (4654078 A), 1987.

46. Gallagher, N.P., Hendrix, J.L., Milosavljevic, E.B., Nelson, J.H., "The affinity of carbon for gold complexes: dissolution of finely disseminated gold using a flow electrochemical cell." *J. Electrochem. Soc.*, **136**(9): 2546-2551; 1989.

47. Gallagher, N.P., Hendrix, J.L., Milosavljevic, Emil B., Nelson, John H., Solujic, Ljiljana, "Affinity of activated carbon towards some gold(I) complexes." *Hydrometallurgy*, **25**: 305-316; 1990.

48. Kononova, O.N., Kholmogorov, A.G., Kononov, Y.S., Pashkov, G.L., Kachin, S.V., Zotova, S.V., "Sorption recovery of gold from thiosulfate solutions after leaching of products of chemical preparation of hard concentrates." *Hydrometallurgy*, **59**: 115-123; 2001.

49. Gong, Q., Hu, J., and Cao, C., "Kinetics of gold leaching from sulfide gold concentrates with thiosulfate solution." *Trans. Nonferrous Met. Soc. China*, **3**(4): 30-36; 1993.

50. Feng, D. and Van Deventer, J.S.J., "Leaching behaviour of sulphides in ammoniacal thiosulphate systems". *Hydrometallurgy*, **63**(2): 189-200; 2002.

51. Schmitz, P.A., Duyvesteyn, S., Johnson, W.P., Enloe, L., McMullen, J., "Ammoniacal thiosulfate and sodium cyanide leaching of preg-robbing Goldstrike ore carbonaceous matter". *Hydrometallurgy*, **60**: 25-40; 2001.

52. Livingstone, S.E., "Metal complexes of ligands containing sulphur, selenium or tellurium as donor atoms". *Quarterly Reviews*, **19**: 386-397; 1965.

53. Cotton, F.A. and Wilkinson, G., *Advanced Inorganic Chemistry*, 5th Edition, John Wiley & Sons (New York), 1988.

54. *Silver Thiosulfate Complexes.*, in *Gmelins Handbuch der Anorganischen Chemie*, L. Gmelin, Editor. Verlag Chemie (Weinheim), 1973.

55. Ryabchikov, D.I., "On the structure of dithiosulphatoplatinite". *Comptes Rendus (Doklady) Acad. Sci. URSS*, **XLI**(5): 208-209; 1943.

56. Zhao, J., Wu, Z.C., and Chen, J.Y., "Extraction of gold from thiosulfate solutions with alkyl phosphorus esters". *Hydrometallurgy*, **46**(3): 363-372; 1997.

57. Jiang, T., Chen, J., and Xu, S. "Electrochemistry and mechanism of leaching gold with ammoniacal thiosulfate", in *XVIII International Mineral Processing Congress* (Sydney, Australia), Volume 5. Australian Institute of Mining and Metallurg, Parkville, Vic., 1993. pp. 1141-1146.

58. Li, J., Miller, J.D., Wan, R.Y., Le Vier, M., "The ammoniacal thiosulfate system for precious metal recovery", in *Proceedings of the XIX International Mineral Processing Congress (IMPC)* (San Francisco, CA, USA), Volume 4. SME, Littleton, CO, USA, 1995. pp. 37 - 42.

59. Thomas, K.G., Fleming, C., Marchbank, A.R., Dreisinger, D., "Gold recovery from refractory carbonaceous ores by pressure oxidation, thiosulfate leaching and resin-in-pulp adsorption."; US Patent (5,785,736), Barrick Gold Corporation, Toronto, Canada, 1998.

60. Tozawa, K., Inui, Y., and Umetsu, Y. "Dissolution of gold in ammoniacal thiosulfate solution", in *AIME 110th Annual Meeting*, 1981. [A81-25].

61. Chen, J., Deng, T., Zhu, G., Zhao, J., "Leaching and recovery of gold in thiosulfate based system--a research summary at ICM." *Trans. Indian Inst. Met.*, **49**(6): 841-849; 1996.

62. Zhu, G., Fang, Z.H., and Chen, J.Y., "Electrochemical studies on the mechanism of gold dissolution in thiosulfate solutions." *Transactions of the Nonferrous Metals Society of China*, **4**(1): 50-53, 58; 1994.

63. Briones, R. and Lapidus, G.T., "The leaching of silver sulfide with the thiosulfate-ammonia-cupric ion system." *Hydrometallurgy*, **50**: 243-260; 1998.

64. Jiang, T., Xu, S., and Chen, J. "Gold and silver extraction by ammoniacal thiosulfate catalytical leaching at ambient temperature", in *Proceedings of the First International Conference on Modern Process Mineralogy and Mineral Processing*, 1992. pp. 648-653.

65. Panayotov, V., Stamenov, S., Panayotova, M., Todorova, E., "Potentiostatic investigation of the Au and Ag dissolution", in *6th Balkan Conference on Mineral Processing.* Hotel Bellevue, Ohrid, Macedonia., 1995. pp. 172-176,

66. Aylmore, M.G. and Muir, D.M., "Thermodynamic analysis of gold leaching by ammoniacal thiosulfate using Eh/pH and speciation diagrams". *Min. Metall. Proc.*, **18**(4): 221-227; 2001.

67. Molleman, E. and Dreisinger, D., "The treatment of copper-gold ores by ammonium thiosulfate leaching." *Hydrometallurgy*, **66**(1-3): 1-21; 2002.

68. Jiang, T., Chen, J., and Xu, S., "A kinetic study of gold leaching with thiosulfate", in *Hydrometallurgy: Fundamentals, Technology & Innovations.*, Chapter 7. 1993. pp. 119-126.

69. Bhaduri, R.S., *Lixiviation of refractory ores with diethylamine or ammonium thiosulfate*, MSc. Thesis, 100 pp.; University of Nevada: (Reno), 1987.

70. Marchbank, A.R., Thomas, K.G., Dreisinger, D., Fleming, C., "Gold recovery from refractory ores by pressure oxidation and thiosulfate leaching." US Patent (5,536,297), Barrick Gold Corporation, Toronto, Canada, 1996.

71. Umetsu, Y. and Tozawa, K., "Dissolution of gold in ammoniacal sodium thiosulfate solution." *Bulletin of the Research Institute of Mineral Dressing & Metallurgy*, **28**(1): 97-104; 1972.

72. Xu, Y. and Schoonen, M.A.A., "The stability of thiosulfate in the presence of pyrite in low-temperature aqueous solutions." *Geochim. Cosmochim. Acta*, **59**(22): 4605-4622; 1995.

73. Naito, K., Shieh, M.-C., and Okabe, T., "The chemical behaviour of low valence sulfur compounds. V. Decomposition and oxidation of tetrathionate in aqueous ammonia solution." *Bull. Chem. Soc. Japan*, **43**: 1372-1376; 1970.

74. Zhang, H.G. and Dreisinger, D.B., " The adsorption of gold and copper onto ion-exchange resins from ammoniacal thiosulfate solutions". *Hydrometallurgy*, **66**(1-3): 67-76; 2002.

75. Byerley, J.A., Fouda, S.A., and Rempel, G.L., "Kinetics and mechanism of the oxidation of thiosulfate ions by copper(II) ions in aqueous ammonia solution." *J. Chem. Soc., Dalton Trans.*: 889-893; 1973.

76. Byerley, J.A., Fouda, S.A., and Rempel, G.L., "Activation of copper(II) ammine complexes by molecular oxygen for the oxidation of thiosulfate ions." *J. Chem. Soc., Dalton Trans.*: 1329-1338; 1975.

77. Johnson, P.H. and Bhappu, R.B., "Chemical mining - a study of leaching agents", in *Circular - New Mexico, Bureau of Mines and Mineral Resources.* New Mexico Bureau of Mines and Mineral Resources, 1969. pp. 1-10.

78. Flett, D.S., Derry, R., and Wilson, J.C., "Chemical study of thiosulfate leaching of silver sulfide." *Trans. Instn. Min. Metall. (Sect. C: Mineral Process. Extr. Metall.)*, **92**(Dec.): 216-223; 1983.

79. Agadzhanyan, A.E., Ter-Arakelyan, K.A., and Babayan, G.G., "Behaviour of a gold thiosulfate complex in the presence of silver and copper complexes." *Armianskii Khimicheskii Zhurnal.*, **34**(2): 112-116; 1981.

80. *Copper Thiosulfate Complexes.*, in *Gmelins Handbuch der Anorganischen Chemie*. L. Gmelin, Editor. Verlag Chemie (Berlin), 1965.

81. *Mercury Thiosulfate Complexes.*, in *Gmelins Handbuch der Anorganischen Chemie*. L. Gmelin, Editor. Verlag Chemie (Berlin), 1969.

82. *Lead Thiosulfate Complexes.*, in *Gmelins Handbuch der Anorganischen Chemie*. L. Gmelin, Editor. Verlag Chemie (Weinheim), 1972.

83. Hubin, A. and Vereecken, J., "Electrochemical reduction of silver thiosulfate complexes. Part 1: Thermodynamic aspects of solution composition". *J. App. Electrochem.*, **24**: 239-244; 1994.

84. Novakovskii, M.S. and Ryazantseva, A.P., "Cadmium complexes with thiosulfate". *Trudy Khim. Fak.*, **54**(12): 277-281; 1955.

85. Smith, R.M. and Martell, A.E., *Critical Stability Constants,* Volume 4: *Inorganic Ligands*, Plenum Press (London), 1976.

86. Tykodi, R.J., "In praise of thiosulfate". *J. Chem. Ed.*, **67**(2): 146-149; 1990.

87. Vasil'ev, A., Toropova, V.F., and Busygina, A.A., "The use of ion exchange for the separation of copper, cadmium and zinc from thiosulfate solutions". *Uch. Zap. Kazansk. Un-ta.*, **113**(8): 91-102, 1953 (CA 1956:724g)

88. Vlassopoulos, D. and Wood, S.A., "Gold speciation in natural waters: I. Solubility and hydrolysis reactions of gold in aqueous solution." *Geochim. Cosmochim. Acta*, **54**(1): 3-12; 1990.

89. *Comprehensive Coordination Chemistry*, G. Wilkinson, Editor; Pergamon Press (Oxford), 1987.

90. Williamson, M.A. and Rimstidt, J.D., "The rate of decomposition of the ferric-thiosulfate complex in acidic aqueous solutions." *Geochim. Cosmochim. Acta*, **57**(15): 3555-61; 1993.

91. Pourbaix, M.J.N., *Atlas of Electrochemical Equilibria in Aqueous Solution.* First English Edition. Pergamon Press (Oxford), 1966.

92. Finkelstein, N.P.H., R.D., "A new approach to the chemistry of gold." *Gold Bull.*, 7(3): 72-77; 1974.

93. Luo, R., "Overall equilibrium diagrams for hydrometallurgical systems: copper-ammonia-water system". *Hydrometallurgy*, **17**: 177-199; 1987.

94. Cao, C., Hu, J., and Gong, Q., "Leaching gold by low concentration thiosulfate solution." *Transactions of the Nonferrous Metals Society of China*, **2**(4): 21-25; 1992.

95. Muyunda, C.M., "Thiosulphate as an alternative lixiviant for gold - kinetics and environmental aspects", M.SC. Thesis, 185 pp.; Western Australian School of Mines, Curtin University (Kalgoorlie), 1996.

96. O'Malley, G.P. and Nicol, M.J. "Recovery of gold from thiosulfate solutions and pulps with ion-exchange resins", in *Cyanide: Social, Industrial and Economic Aspects. Proceedings of a Symposium held at the Annual Meeting of TMS* (New Orleans). TMS, Warrendale, PA, USA, 2001. pp. 469-483.

97. Mountain, B.W. and Wood, S.A. "Solubility and transport of platinum-group elements in hydrothermal solutions: thermodynamic and physical chemical constraints", in *Geo-Platinum '87* (Open University, Milton Keynes, UK). Elsevier (London), 1988. pp. 57 - 82.

98. Feng, D. and van Deventer, J.S.J., "The role of heavy metal ions in gold dissolution in the ammoniacal thiosulphate system". *Hydrometallurgy*, **64**(3): 231-246; 2002.

99. Lulham, J. and Lindsay, D., "Separation process", International Patent (WO 91/11539), Davy McKee (Stockton) Limited, Cleveland, 1991.

100. Plimer, I.R. and Williams, P.A. "New mechanisms for the mobilisation of the platinum-group elements in the supergene zone", in *Geo-Platinum '87* (Open University, Milton Keynes). Elsevier (London), 1988. pp. 83-92.

101. Anthony, E.Y. and Williams, P.A. "Thiosulfate complexing of platinum group elements", in *ACS Symposium Series 550: Environmental Geochemistry of Sulfide Oxidation,* Alpers, C.N. and Blowes, D.W., Editors. Comstock, M.J., Series Editor. American Chemical Society (Washington), 1994. pp. 551-560.

102. Muir, D.M., LaBrooy, S.R., Deng, T., Singh, P., "The mechanism of the ammonia-cyanide system for leaching copper-gold ores", in *Hydrometallurgy: Fundamentals, Technology and Innovation.* Warrendale. A.I.M.E., 1993. pp. 191-204.

103. Berezowsky, R.M.G.S. and Sefton, V.B. *Recovery of Gold and Silver from Oxidation Leach Residues by Ammoniacal Thiosulfate Leaching.* in *AIME 108th Annual Meeting.* New Orleans, Louisiana, 1979. 17 pp.

104. Kerley, B.J.J., "Recovery of precious metals from difficult ores." US Patent (4,369,061), Kerley Industries, 1983.

105. Hemmati, M., Hendrix, J.L., Nelson, J.H., Milosavljevic, E.B., "Study of the thiosulfate leaching of gold from carbonaceous ore and the quantitative determination of thiosulfate in the leached solution", in *Extraction Metallurgy '89* (London, UK). Institute of Mining and Metallurgy, London, UK, 1989.

106. Hu, J. and Gong, Q. "Substitution of sulfate for sulfite during extraction of gold by thiosulfate solution",in *Randol Gold Forum* (Cairns, Australia). Randol International Ltd. (USA), 1991. pp. 333-336

107. Cao, C., Hu, J., and Gong, Q. "Leaching gold by low concentration thiosulfate solution", in *Randol Gold Forum* (Vancouver). Randol International, Golden, Colorado, USA, 1992. pp. 293-298.

108. Wan, R.Y., LeVier, K.M., and Clayton, R.B., "Hydrometallurgical process for the recovery of precious metal values from precious metal ores with thiosulfate lixiviant", US Patent (5 354 359), Newmont Mining Corp. Denver, USA, 1994.

109. Panayotov, V.T. "A technology for thiosulfate leaching of Au and Ag from pyrite concentrate", in *Changing scopes in Mineral Processing: Proceedings of the 6th International Mineral Processing Symposium*. Kusadasi, Turkey, 1996. pp. 563 -566.

110. Groudev, S.N., Spasova, I.I., and Ivanov, I.M., "Two-stage microbial leaching of a refractory gold-bearing pyrite ore." *Miner. Eng.*, **9**(7): 707-713; 1996.

111. Yen, W.T., Stogran, K., and Fujita, T., "Gold extraction from a copper bearing ore by thiosulfate leaching." *Resources Treatment Technology*, **43**(2): 83-87; 1996.

112. Yen, W.T., Aghamirian, M.M., Deschenes, G., Theben, S., "Gold extraction from mild refractory ore using ammonium thiosulfate", from *International Symposium on Gold Recovery* (1998). Preprint manuscript supplied by W.T. Yen (11 pp.).

113. Yen, W.T., Guo, H., and Deschenes, G. "Development in percolation leaching with ammonium thiosulfate for gold extraction of a mild refractory

ore". in *EPD Congress 1999* (San Diego, USA). The Minerals, Metals and Materials Society, Warrendale, PA, USA, 1999. pp. 441-455.

114. Meggiolaro, V., Niccolini, G., Miniussi, G., Stefanelli, N., Trivellin, E., Llinas, R., Ramirez, I., Baccelle Scudeler, L., Omenetto, P., Primon, S., Visona, D., Abbruzzese, C., Fornari, P., Massidda, R., Piga, L., Ubaldini, S., Ball, S., Monhemius, A.J., "Multidisciplinary approach to metallogenic models and types of primary gold concentration in the cretaceous arc terranes of the Dominican Republic." *Trans. Inst. Min. Metall. Section B (Applied Earth Science)*, **109**: B95-104; 2000.

115. Chen, J., Zhang, Y., Lu, K., Gong, Q., Zhu, G., "Studies on environmentally friendly leaching processes in China". *Chinese J. of Chem. Eng.*, **9**(1): 5-11; 2001.

116. Ji, J., Fleming, C.A., West-Sells, P.G., Hackl, R.P., "Method for thiosulfate leaching of precious-metal containing materials." World Patent (WO 01/88212 A2), Placer Dome Technical Services Ltd., 2001.

117. Arima, H., Fujita, T., and Yen, W.T., "Gold cementation from ammonium thiosulfate solution by zinc, copper and aluminium powders". *Mater. Trans*, **43**(3): 485-493; 2002.

118. Fleming, C.A., McMullen, J., Thomas, K. G., Wells, J. A., "Recent Advances in the Development of an alternative to the cyanidation process: Thiosulfate leaching and resin in pulp". *Min. Metall. Proc.*, **20**(1): 1-9; 2003 {Preprint manuscript supplied by C. Fleming, 2002}.

119. Blasius, E. Horn, G. Knochel, A., Munch, J., Wagner, H., "Analytical chemistry of sulphur compounds", in *Inorganic Sulphur Chemistry*; G. Nickless, Editor. Elsevier Publishing Company (Amsterdam), 1968. pp.199-239.

120. Yang, T., Chen, Z., Bin, W., Chen, Q., Lu, Y., "Gold leaching in sodium polysulfide solution." *Zhongnan Kuangye Xueyuan Xuebao*, **23**(6): 687-692; 1992.

121. Earley, D. and Berdnt, M.E., "Solution mining and leaching of precious metals from ores using aqueous sulfide solutions at elevated temperatures and pressures." US Patent (363 119 A0), US Dept. of the Interior, 1995.

122. Li, H. and Ke, J., "Determination of the total concentration of polysulfide ions in the polysulfide solution of gold leaching." *Huangjin*, **19**(9): 51-53; 1998.

123. Touro, F.J. and Wiewiorowski, T.K., "Process for recovery of gold from gold ores using a complexing pretreatment and sulfurous acid leaching", US Patent (5 147 617), Freeport-McMoRan Inc., 1992.

124. Uri, N., "Thiosulfate complexes of the tervalent metals iron, aluminium, and chromium." *J. Chem. Soc.*: 335-337; 1947.

125. Awadalla, F.T. and Ritcey, G.M. "Recovery of gold from thiourea, thiocyanate or thiosulfate solutions by reduction-precipitation with a stabilized form of sodium borohydride", in *Randol Gold Forum - Randol Conference* (Squaw Valley), 1990. pp. 295-306.

126. Roy, A.B. and Trudinger, P.A., *The Biochemistry of Inorganic Compounds of Sulfur*. Cambridge University Press (Cambridge), 1970.

127. Lyons, D. and Nickless, G., "The lower oxy-acids of sulphur", in *Inorganic Sulphur Chemistry*, G. Nickless, Editor. Elsevier (Amsterdam), 1968.

128. Koh, T., "Analytical chemistry of polythionates and thiosulfate. A review". *Anal. Sci.*, **6**: 3-14; 1990.

129. Guerra, E. and Dreisinger, D.B., "A study of the factors affecting copper cementation of gold from ammoniacal thiosulfate solution." *Hydrometallurgy*, **51**: 155-172; 1999.

130. Zhang, J., Lan, K., Ding, F., Yuan, Z., Yang, L., "Leaching gold and silver by lime sulfur synthetic solution (LSSS). Part I. Synthesising the LSSS and dissolving pure gold and silver with it",*Precious Metals,* **16**: 389-393, 1992.

131. Zhang, J., Lan, X., Ding, F., Yuan, Z., Shuai, S., "Leaching gold and silver by lime sulfur synthetic solution (LSSS). Part II. Treating ores with the LSSS", *Precious Metals* **16**: 394-398.1992.

132. Lan, X., Zhang, J., Wang, G., Han, A., "Leaching gold from gold ores bearing arsenic and carbon by the LSSS", *Precious Metals,* **20**: 105-113, 1996.

133. Groves, W.D. and Blackman, L., "Recovery of precious metals from evaporite sediments." US Patent (5,405,430), 17 pp.; 1995.

134. Woollacott, L.C. and Eric, R.H., "Hydrometallurgy", in *Mineral and Metal Extraction: An Overview*, The South African Institute of Mining and Metallurgy (Johannesburg), 1994. pp. 321-370.

135. Deschenes, G. and Ritcey, G.M., "Recovery of gold from aqueous solutions" US Patent (4 913 730), Canadian Patents and Development. Ltd., 1990.

136. Zhao, J.W., Zhichun; Chen, Jiayong, "Solvent extraction of gold in thiosulfate solutions with amines." *Solvent Extraction & Ion Exchange*, **16**(2): 527-543; 1998.

137. Zhao, J., Wu, Z., and Chen, J., "Extraction of gold from thiosulfate solutions using amine mixed with neutral donor reagents." *Hydrometallurgy*, **48**: 133-144; 1998.

138. Zhao, J., Wu, Z., and Chen, J., "Gold extraction from thiosulfate solutions using mixed amines." *Solvent Extraction & Ion Exchange*, **16**(6): 1407-1420; 1998.

139. Zhao, J., Wu, Z., and Chen, J., "Separation of gold from other metals in thiosulfate solutions by solvent extraction." *Separation Science & Technology*, **34**(10): 2061-2068; 1999.

140. McPartland, J.S. and Bautista, R.G., "Concentration and reduction of Au(I) thiosulfate to metallic gold", in *Metal Separation Technologies Beyond 2000: Integrating Novel Chemistry With Processing.*, K.C.C. Liddell & D.J. Chaiko, Eds. The Minerals, Metals & Materials Society, 1999. pp.105-115.

141. Virnig, M.J. and Sierakoski, J.M., "Ammonium thiosulfate complex of gold or silver and an amine." US Patent (6 197 214), Henkel Corporation, 2001.

142. Virnig, M.J., Kordosky; G.A., Wolfe; G.A., MacKenzie; J.M., "Process of recovery of metals from aqueous ammoniacal solutions employing an ammonia antagonist having only hydrogen bond acceptor properties." US Patent (6 210 647), Henkel Corporation, 2001.

143. Mohansingh, R., *Adsorption of Gold from Gold Copper Ammonium Thiosulfate complex onto Activated Carbon and Ion Exchange Resins,* M.Sc. Thesis;. 71 pp. University of Nevada (Reno), 2000.

144. Bolinski, L. and Shirley, J. "Russian RIP technology, current status and recent developments" in *Randol Gold Forum '96*, 1996. pp. 419-423.

145. Dicinoski, G.W., "Novel resins for the selective extraction of gold from copper rich ores." *S. Afr. J. Chem.*, **53**(1): 33-43; 2000.

146. MacKenzie, J.M.W., Virnig, M.J., and Johns, M.W. "Henkel Aurix(R) resin - an update". in *Randol Gold Forum '95* (Perth, Australia), 1995. pp. 425-431.

147. Atluri, V.P., *Recovery of gold and silver from ammoniacal thiosulfate solutions containing copper by resin ion exchange method*, M.Sc. Thesis, 219 pp.; University of Arizona, 1987.

148. Degenkolb, D.J. and Scobey, F.J., "Silver recovery from photographic wash waters by ion exchange." *SMPTE Journal*, **86**(2 (February)): 65-68; 1977.

149. Lasko, C.L. and Hurst, M.P., "An investigation into the use of chitosan for the removal of soluble silver from industrial wastewater." *Environmental Science & Technology*, **33**(20): 3622-3626; 1999.

150. Mina, R., "Silver recovery from photographic effluents by ion-exchange methods.", *J. App. Photogr. Eng.*, **6**(5): 120-125; 1980.

151. Tarasova, A.A., Serova, I.B., and Leikin, Y.U.A., "Silver sorption from solutions formed in production and treatment of motion picture and photographic materials." *Russian J. App. Chem.*, **67**(6): 854-857; 1994.

152. Fleming, C.A., Wells, J., and Thomas, K.G., "Gold recovery from thiosulfate leach solutions and slurries using ion-exchange resin eluted with polythionate." US Patent (6344068), Barrick Gold Corporation, 2002.

153. Davankov, A.B., Laufer, V.M., and Zubakova, L.B., "Elution of complex silver thiosulfate ions from anion exchangers after adsorption." *Russian J. App. Chem.*, **40**(8): 1656-1659; 1966.

154. Davankov, A.B., Laufer, V.M., Zubakova, L.B, Aptova, T.A, & Mironov, A.A, "Ion exchange extraction of silver from wash waters of the motion picture film industry." *Russian J. App. Chem.*, **39**(9): 1935-1940; 1966.

155. Lurye, Y.Y. and Peremyslova, E.S., "Secondary processes occurring during ion exchange on ionites." *Russian J. App. Chem.*, **27**(11): 1143-1147; 1953.

156. Marcus, Y., "The anion exchange of metal complexes. The silver - thiosulfate system." *Act. Chem. Scand.*, **11**(4): 619-627; 1957.

157. Cooley, A.C., "Ion-exchange silver recovery for process EP-2 with nonregenerated bleach-fix." *J. Appl. Photogr. Eng.*, **7**(4): 106-110; 1981.

158. Agadzhanyan, A.E., Ter-Arakelyan, K.A., and Babayan, G.G., "Some regularities of silver thiosulfate complex sorption on AM-2B ion-exchanger." *Arm. Khim. Zh.*, **35**(3): 151-155; 1982.

159. Jay, W.H., "Process for recovery of gold and/or silver", World Patent (WO 99/13116), Everett and Goodall Electrical Pty. Ltd., 1999.

160. O'Malley, G.P., "The elution of gold from anion exchange resins", World Patent (WO 01/23626 A1), Murdoch University, Perth, WA., 2001.

161. Fagan, P., *Personal communication*: a report on the *Ballarat Gold Forum - Gold Processing in the 21st Century: An International Forum*, (Ballarat, Australia), 2000.

2. Selection and Development of Functional Resins

This chapter serves to introduce the resin functional groups used throughout this study, and the rationale behind their selection. The resin groups along with the leachate anions have been modelled using computational methods in an attempt to predict their behaviour.

In resin-based hydrometallurgical recovery processes, the range of effective functional groups is constrained by the charge of the target metal complex(es). The moieties on the adsorbent must be either neutral chelating groups capable of sequestering the target metal(s), or they must bear a charge opposite to that of the metal complex. In the case of gold recovery from ammoniacal thiosulfate leach liquors, the target complex is a trivalent anion - and therefore cationic ligands should be considered. The most readily accessible type of cationic functionality is the ammonium group, and a wide variety of ammonium based compounds can be readily affixed to a polymeric backbone.

The aurothiosulfate complex is linear with respect to the S-Au-S bonds. Gold(I) generally has a strong preference for linear complexes, as evidenced by Table 2.1. These are stabilised by the hybridisation of the large $5d_{z^2}$ orbital with the valence $6s$ and $5p_z$ orbitals of the gold(I) cation, giving a pair of linear hybrid orbitals suitable for covalent bonding [1]. The other binding orbitals are much weaker, and do not interact significantly with additional neutral ligands. It follows that gold can only be stripped from thiosulfate liquors by the use of a highly selective polymer-bound chelating ligand that displaces one or more thiosulfate ligands, or trapped by a charge-based interaction with the aurothiosulfate complex, ie. ion exchange. As shown in Table 2.1, the stability of the gold(I) thiosulfate

complex is second only to the analogous cyanide complex. Substitution of the thiosulfate ligands is therefore unlikely, and consequently there appear to be few prospects for a selective polymeric chelating group. The development of polymeric groups in this project will therefore focus on the optimisation of ion-exchange affinity for the aurothiosulfate complex. This affinity can be influenced by factors such as cavity size, steric hindrance, charge density and hydration.

Table 2.1 Physical Data for Linear Au(I) Complexes [2]

Gold Complex	β_n	E_0 (V)
$[Au(SC(NH_2)_2)_2]^+$	23.3	0.352
$[Au(CN)_2]^-$	38.3	-0.57
$[AuI_2]^-$	19.6	0.578
$[AuBr_2]^-$	12	0.960
$[AuCl_2]^-$	9	1.154
$[Au(SCN)_2]^-$	17.1	0.662
$[Au(S_2O_3)_2]^{3-}$	28.7	0.15

The bulky nature of the aurothiosulfate complex does allow some discrimination with respect to size: the large gold complex should interact with sterically hindered ligands less effectively than with smaller, more compact ligands. Unfortunately, it appears that gold forms one of the larger species in ammoniacal thiosulfate leach solutions, giving the smaller competing anions (eg. chloride, hydroxide, thiosulfate, polythionates) a kinetic and steric advantage in their access to cationic ion-exchange (IEX) sites. Sterically hindered IEX groups may provide

improvement in selectivity over the copper complexes $\{[Cu(S_2O_3)_N]^{1-2N}\}$, which are expected to be of similar size (N = 2) or even larger than the gold complex (N = 3).

The large 3- charge on the aurothiosulfate complex may also be of use in development of selective groups, as polyvalent anions are known to adsorb more strongly than singly charged anions. This is merely an effect of the concentration of coulombic potential (ie. the ratio of charge/volume), and is weakened in solutions of high ionic strength. However, this does give some prospect for differentiation between the metal complexes of the form $[M(S_2O_3)_2]^{3-}$ {M = Au(I), Ag(I) and Cu(I)}, thiosulfate and its degradation products, such as the polythionates ($S_NO_6^{2-}$; N = 3 - 5) and sulfate.

The following section seeks to develop a range of IEX groups which have the potential to discriminate between the aurothiosulfate complex and its competitors, namely the polythionates and the cuprothiosulfate complexes.

2.1 Constraints on the Substrate

The choice of functional groups is constrained by the available methods for anchoring moieties to polymer resins. Numerous treatments exist for affixing ionogenic functional groups to porous polymeric resins. These treatments are specific to a given type of substrate, such as the sulfonation, chloromethylation or bromination of polystyrene. Similarly, acrylic resins may be hydrolysed, transesterified or transaminated [3].

The most significant constraint is the limited commercial availability of reactive precursor resins. Porous polystyrene resin and the chloromethylated derivative are widely available, as are porous polyacrylic ester resins such as poly(methyl methacrylate). More obscure resins bearing reactive moieties such as

epoxide, aldehyde or aminomethyl groups are also available, but are prohibitively expensive and thus not conducive to commercial development.

A great many derivatives can be readily prepared from a chloromethylated polystyrene (Merrifield) resin in one-pot reactions, and even more via multi-step procedures [3]. Chloromethylated polystyrene was readily available in this laboratory, and was used throughout this project as the substrate upon which the resin groups were anchored. By using a common substrate, the effects of substrate, particle size, and to a lesser degree porosity, on the performance of the various IEX groups can be controlled, reduced or eliminated.

The most readily accessible reaction for the derivatisation of a chloromethylated aromatic substrate is direct S_N2 alkylation of an amine, illustrated below (Equation 2.1):

$$(\text{Polymer})CH_2Cl + NR_3 \rightarrow (\text{Polymer})CH_2NR_3^+ Cl^- \quad (2.1)$$

$$(\text{Polymer})CH_2NHR_2^+ Cl^- \rightarrow (\text{Polymer})CH_2NR_2 + HCl \quad (2.2)$$

Where the compound is a tertiary amine, the product is a polymer-bound ammonium salt and is ready for use. If primary or secondary amine compounds are employed, the resulting proton-bearing ammonium salts can readily eliminate hydrochloric acid after treatment with an alkyl halide (Eqn 2.2), and these amine sites may undergo subsequent alkylation. This is particularly undesirable if several chloromethyl groups adhere to the same amine (Eqn 3.2), as the resin structure (porosity) may be permanently distorted. A similar problem arises with the use of polyamine compounds, where different amine sites form a crosslink in the resin. These side reactions may be minimised by using a large excess of the amine

compound, which increases the likelihood of interaction between a chloromethyl group and a free amine, and allows excess amine to scavenge the free HCl.

The general synthesis procedure applied was taken from the work of Dicinoski [4]. This utilises hot DMF as the solvent to enhance the rate of S_N2 alkylation reactions between chloromethylated polystyrene and amine compounds. These conditions are also suitable for the subsequent exhaustive alkylation of the affixed amine functional groups with benzyl chloride, although milder conditions are mandated for volatile alkyl halide reagents such as methyl iodide.

2.2 *Prospects for Gold-Selective Functional Groups*

A central aim of this project was to relate the structural characteristics of resin functional groups to their efficacy for the adsorption of gold from ammoniacal thiosulfate leach liquors. This was pursued by preparing structural variations of a basic theoretical archetype of an ammonium functional group. This generic ligand is illustrated in Figure 2.1. Note that the two peripheral ammonium groups (denoted N^2 and N^3) are optional, as are the bridging components joining them.

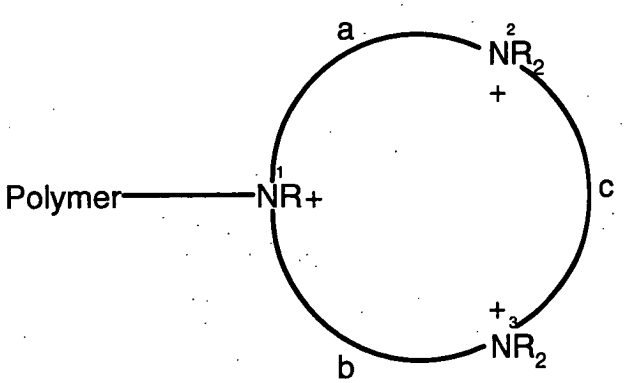

Figure 2.1 Generic (poly)Ammonium Functional Group

The optional structural components **a**, **b** and **c** represent alkyl groups affixed to the nitrogen atom(s), and may also bridge between ammonium groups. These groups may be as simple as a hydrogen or terminal alkyl group (eg. methyl), but may also be bridging $-CH_2-$ or $-CH_2CH_2-$ groups. For example, diethylenetriamine bound to a resin can be described by defining the terms **a** = **b** = $-CH_2CH_2-$ with all R groups being hydrogen atoms.

The R groups represent simple alkyl groups of two types, divided by steric bulk, namely small (methyl, ethyl) and larger (benzyl) alkyl groups. The alkylation of the ammonium groups is intended to be exhaustive – that is, to convert all weak base functional groups into strong base (ammonium) moieties. In this fashion, similar ammonium group structures can be prepared with high and low degrees of steric hindrance around the cationic centre (see Section 2.2.2).

2.2.1 Target Functional Groups

A set of 46 functional groups was chosen to examine the various possibilities illustrated by Figure 2.1, constrained by the availability of precursors and the need for a simple and consistent synthetic approach. The structures of the functional groups to be prepared are shown in Figures 2.2 – 2.6. These moieties may be grouped into six categories, arranged by common structural properties:

(1) Simple Amines and Ammonium Salts (Figure 2.2)

(2) Heterocyclic Amines and Ammonium Salts (Figure 2.3)

(3) Hydroxyalkylamines and Ammonium Salts (Figure 2.4)

(4) Linear Polyamines and Polyammonium Salts (Figure 2.4)

(5) N,N',N''-Trialkylhexahydro-1,3,5-triazine Salts (Figure 2.5)

(6) Triazamacrocylic Ligands (Figure 2.6)

A few resin preparations were attempted that were not readily classified in the above system. The N-oxide resin (**POP**) was studied as a representative product of the possible N-oxidation side-reaction, whereas the Schiff-base (**DSU**) resin was an intermediate in the preparation of the triazamacrocyclic moiety (**DTP**).

Simple Aryl- and Alkylammonium Salts:

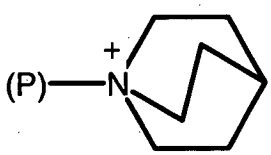

Quinuclidinium (**QNU**)

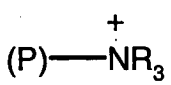

	R =
Tributylammonium (**ABU**)	$(CH_2)_3CH_3$
Trioctylammonium (**TOA**)	$(CH_2)_7CH_3$
Tribenzylammonium (**TBA**)	CH_2Ph
Triphenylammonium (**APH**)	Ph

N-oxide and Simple Amines:

Diisopropylamine (**DIP**) 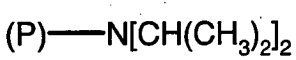

Diethylenetriamine (**DET**) 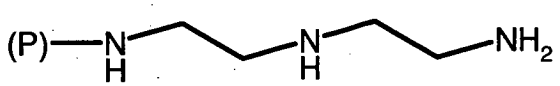

Tris(2-aminoethyl)amine (**TAA**) 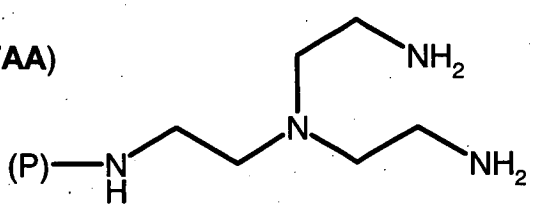

Piperidine N-oxide (**POP**) 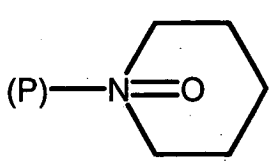

Figure 2.2 Structures of Target Ammonium Functional Groups (Part 1)

(P) = Polystyrene Backbone; Bn = benzyl (-CH_2Ph); RX = BnCl or MeI

Small Alkylammonium Heterocycles:

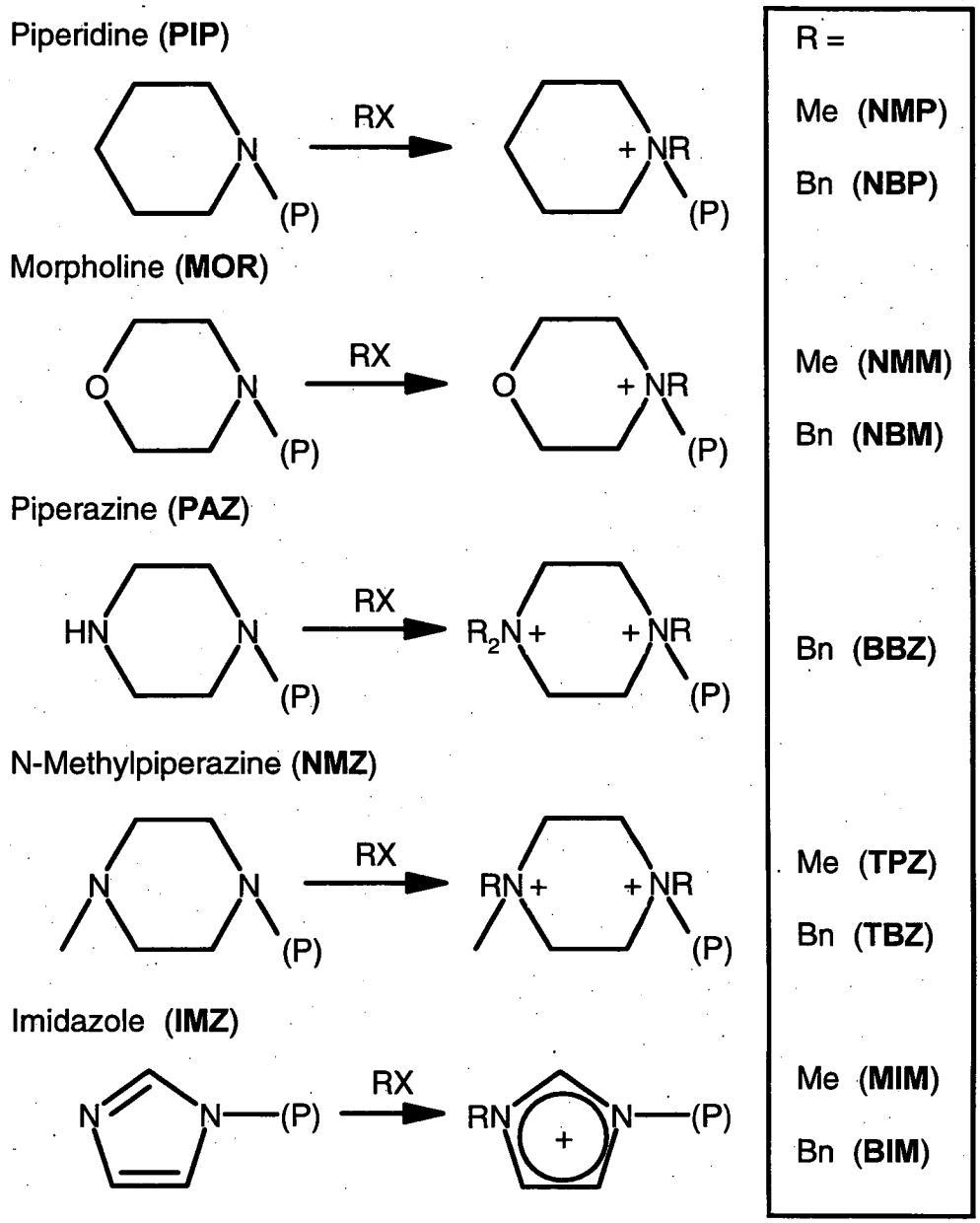

Figure 2.3 Structures of Target Ammonium Functional Groups (Part 2)

(P) = Polystyrene Backbone; Bn = benzyl ($-CH_2Ph$); RX = BnCl or MeI

Hydroxyalkylammonium salts:

Ethanolamine (**ETA**) R = Me (**ETM**) or Bn (**ETB**)

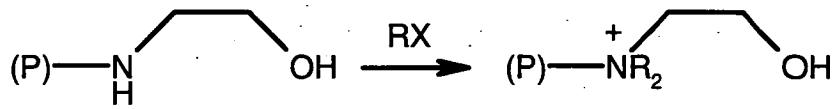

Diethanolamine (**DEA**) R = Me (**DAM**) or Bn (**DAB**)

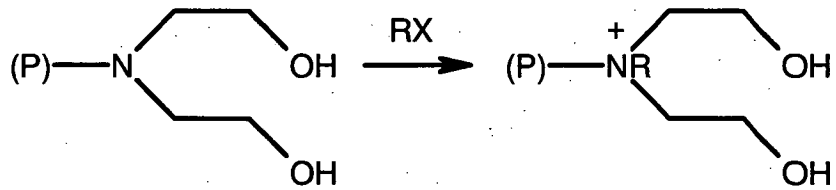

Piperidineethanol (**PET**)

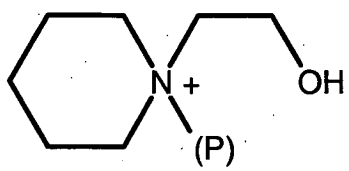

Linear Polyammonium Salts:

Tetramethyethylenediamine (**TME**) R = Me (**PME**) or Bn (**BME**)

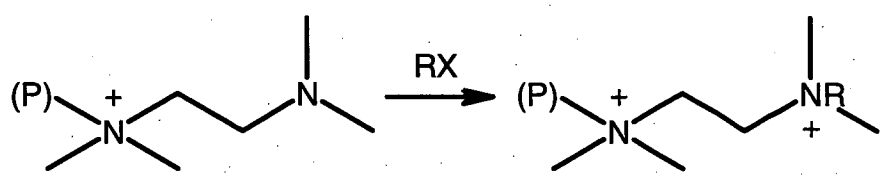

Heptamethyl Diethylenetriammonium (**DTM**)

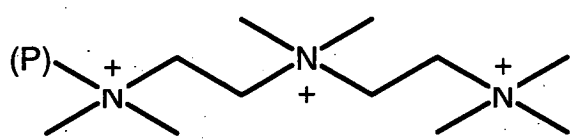

Figure 2.4 Structures of Target Ammonium Functional Groups (Part 3)

(P) = Polystyrene Backbone; Bn = benzyl (-CH_2Ph); RX = BnCl or MeI

Hexahydro-1,3,5-triazine (or hexahydro-*s*-triazine) Derivatives:

Triethyl-hexahydro-1,3,5-triazine (**TET**)

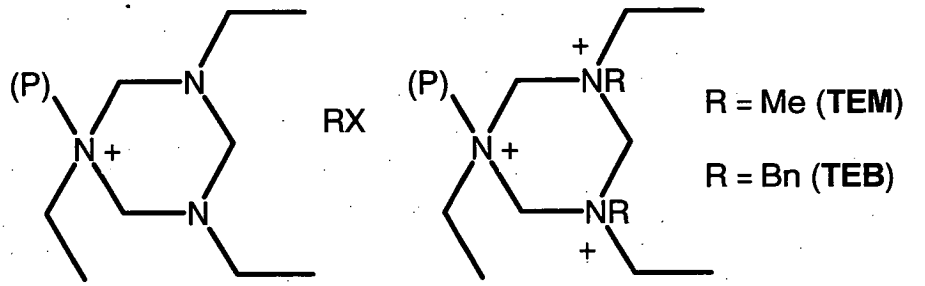

Tribenzyl-hexahydro-1,3,5-triazine (**TBT**)

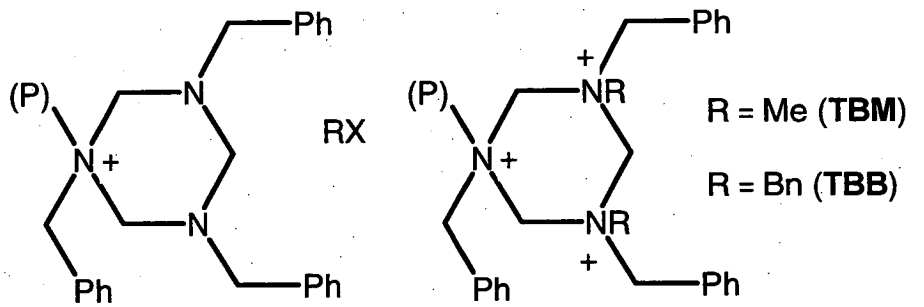

Figure 2.5 Structures of Target Ammonium Functional Groups (Part 4)

(P) = Polystyrene Backbone; Bn = benzyl (-CH_2Ph); RX = BnCl or MeI

Imines and Triazamacrocycles:

Diethylenetriamine bis(salicylidene) (**DSU**)

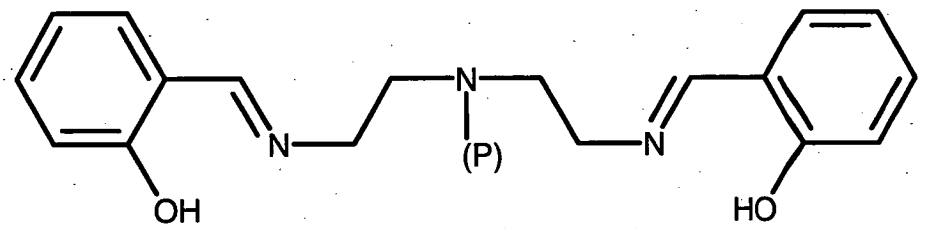

N'-Diethylenetriamine (**DST**)

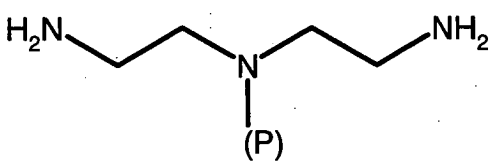

1,4,7-Triazacyclododecane (**DTP**)

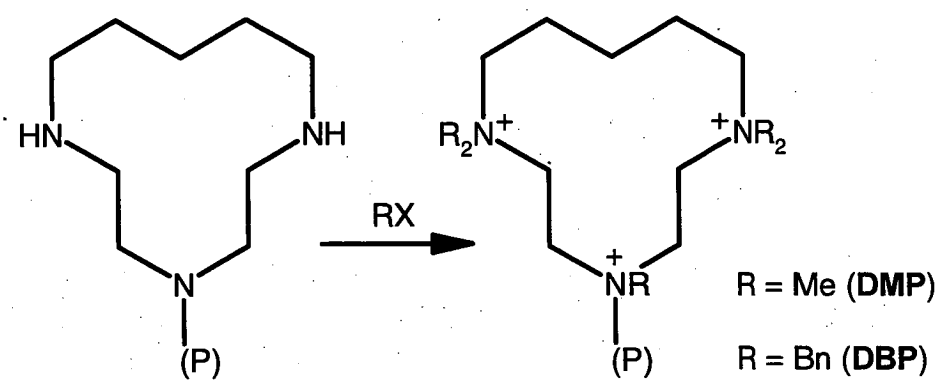

Figure 2.6 Structures of Target Ammonium Functional Groups (Part 5)

(P) = Polystyrene Backbone; Bn = benzyl (-CH_2Ph); RX = BnCl or MeI

2.2.2 Alkyl Substituents

2.2.2.1 Methyl (-CH_3)

Methylation of amine groups is a well known reaction that can be achieved using numerous reagents – eg. dimethyl sulfate, formaldehyde/formic acid, or iodomethane (methyl iodide) [5-7]. The hazardous nature of these treatments should be noted, since all these reagents are suspected carcinogens. In the present circumstances, treatment with iodomethane was preferred as the reagent is relatively

easy to handle, side reactions are few, and residues can easily be removed from the resin products under vacuo [5, 8-9]. Exhaustive methylation can also be achieved in a one-step procedure [10-11].

2.2.2.2 Benzyl (-CH_2Ph)

The benzylation of amine compounds is usually achieved using alkyl halides such as benzyl chloride or the more reactive benzyl bromide. Exhaustive alkylation may be more difficult to perform due to steric hindrance around the amine, which increases with each successive alkylation step. The steric effect of N-benzyl substitution is not completely prohibitive, as tetrabenzylpiperazinium salts have been prepared and characterised in prior studies [12].

2.2.2.3 2-Hydroxyethyl (-CH_2CH_2OH)

In addition to these simple hydrocarbon substituents, a number of moieties containing 2-hydroxyethyl groups were examined (Figure 2.4). The steric bulk of these groups may be regarded as intermediate (between methyl and benzyl). The hydroxyl group(s) may complement metal adsorption in two ways; namely by enhancing the hydrophilicity of the ligand (improved hydration), and by acting as an auxiliary ligand. It is also possible that the hydroxyethyl group will be deprotonated in leach solutions (pH 7 – 11). The resulting anionic alkoxide arm (-$CH_2CH_2O^-$) may interact with cations in solution, or form an internal salt with local ammonium groups. Neither effect is likely to enhance gold adsorption.

2.2.3 Weak Base Groups

A number of weak base resins were included in this study (Figures 2.2 – 2.6), primarily as precursors to strong base resins. These were anticipated to have pK_a values too low to be significantly protonated at pH 10 or above, and hence should show insignificant gold sorption. The gold affinity of these precursors was determined, to ensure that the gold sorption capacity of their strong base derivatives was not an artefact of residual weak-base groups.. Weak base groups with high pK_a values such as guanidine are protonated (cationic) in ammoniacal solutions, and these have been extensively examined in the past as adsorbents for gold. The recovery of gold from thiosulfate solutions using polymer based derivatives of guanidine has been claimed in a patent by Henkel [13].

Table 2.2 details the pK_a values reported in the literature (designated Ref. pK_a), [14-16] for a number of weak base groups showing the effect of alkyl group substitution on their dissociation constants. The second set of data (Calc. pK_a) were calculated using the modelling software *ACD/pKa* (version 7.02) from the I-Lab service offered by *Advanced Chemistry Development Inc.* [17]. Reasonable correlation was observed between the experimentally determined values and calculated pK_a values. Some of the structures examined (such as dimethylpiperazine) were reaction intermediates which may contaminate the final product if the alkylation step is not exhaustive.

Table 2.2 Dissociation Constants (pK_a) of Weak Base Groups

†: Ionic Strength = 0.1 (0 in all other cases); T = 25°C

Amine Compound	**Ref. pK_{a1}**	**Ref. pK_{a2}**	**Ref. pK_{a3}**	**Calc. pK_{a1}**	**Calc. pK_{a2}**	**Calc. pK_{a3}**
Diisopropylamine	11.15	-	-	10.76	-	-
Morpholine	8.33	-	-	8.97	-	-
N-methylmorpholine	7.40	-	-	7.41	-	-
Piperidine	11.16	-	-	11.24	-	-
N-methylpiperidine	10.19	-	-	9.91	-	-
N-(2-hydroxyethyl)piperidine	9.63	-	-	9.04	-	-
Piperazine	9.78	5.33	-	9.90	5.30	-
N-methylpiperazine	9.09	4.94	-	9.65	4.35	-
N,N'-dimethylpiperazine	8.54	4.63	-	8.61	4.07	-
Imidazole	10.58	6.99	-	14.10	7.18	-
1-methylimidazole	7.06	-	-	7.01	-	-
Ethanolamine	9.50	-	-	9.16	-	-
Diethanolamine	8.88	-	-	8.71	-	-
Diethylenetriamine	10.02	9.21	4.42	9.97	9.02	3.60
1,1,4,7,7-pentamethyl-diethylenetriamine†	9.22	8.41	2.09	8.84	8.10	3.40
1,1,4,4-tetramethyl-diaminoethane (TMEDA)	6.35	2.20	-	8.86	5.58	-
tris(2-aminoethyl)amine	10.03	9.13	7.85	10.00	9.27	8.53

Table 2.3 Calculated Dissociation Constants (pK_a) (25°C) [17]

‡: pK_{a4} = 1.43

Amine	**Resin**	**pK_{a1}**	**pK_{a2}**	**pK_{a3}**
N-benzyldiisopropylamine	DIP	9.95	-	-
N-benzylethanolamine	ETA	8.71	-	-
N-benzyldiethanolamine	DEA	7.68	-	-
N-benzyltetramethylethylenediamine	TME	5.53	-	-
N-benzylpiperidine	PIP	8.96	-	-
N-benzylmorpholine	MOR	7.10	-	-
N-benzylimidazole	IMZ	7.18	-	-
N-benzylpiperazine	PAZ	9.60	3.40	-
N-benzyl-N'-methylpiperazine	NMZ	8.27	3.42	-
N-benzyldiethylenetriamine	DET	9.68	8.91	3.60
N'-benzyldiethylenetriamine	DST	9.86	9.00	2.40
N-benzyltriethylhexahydro-*s*-triazine	TET	2.84	-2.59	-
N-benzyltribenzylhexahydro-*s*-triazine	TBT	1.49	-3.93	-
N-benzyltris(2-aminoethyl)amine ‡	TAA	9.84	8.98	8.71

The dissociation constants of many of the target functional groups are not known, such as the stepwise dissociation constants of the trialkylhexahydro-1,3,5-triazines (or -*s*-triazines). It would be useful to know the pK_a values of the benzylated congeners of the proposed functional groups, as it can be argued that the benzyl group is a reasonable model for the *p*-chloromethyl(polystyrene) anchor groups. The pK_a values for the amine sites of these compounds were calculated using the modelling software *ACD/pKa* (v 7.02) [17], whose accuracy has been

demonstrated by the results displayed in Figure 2.2. The results have been collected in Table 2.3 (above). The pK_a values of the hydroxyl groups (where present) have been omitted, as they describe the formation of an anion.

2.2.4 Heterocyclic Ammonium Groups

The simplest set of this class of moieties is the piperidine derivatives, which are simple trialkylammonium salts. The performance of the N-methyl and N-benzylpiperidine resins (NMP & NBP, Figure 2.3) may be compared to piperidineethanol (PET, Figure 2.4) to elucidate the structural effects of the 2-hydroxyethyl group. The introduction of the ether oxygen of morpholine and its derivatives (MOR, NMM & NBM, Figure 2.3) may also affect the sorption of metals, although ethers are quite weak chelating groups in aqueous systems.

Anchoring piperazine to a resin allows the preparation of bis(ammonium) moieties (Figure 2.3), with a fixed distance between the two ammonium groups. The alkyl groups may be mixed, allowing the possibilities shown in Figure 2.3. The bis(ammonium) ring may be unstable (particularly in leach solutions, pH ~10), and may be readily fragmented, oxidised or eliminated [12].

Imidazole is known to form a ring-delocalised cation when quaternised, which was expected to demonstrate significantly different gold sorption behaviour to the more localised ammonium groups of the other resin products.

2.2.5 Linear Polyamines

The linear polyammonium resins prepared in this work (Figure 2.4) were derivatives of tetramethylethylenediamine (TME) and diethylenetriamine (DET) resins. The flexibility of these functional groups should permit them to conform to, or accomodate the aurothiosulfate complex. These moieties are expected to be

somewhat fragile, and susceptible to fragmentation and/or elimination in a manner similar to the tetraalkylpiperazinium groups (Section 2.2.4).

2.2.6 Hexahydro-1,3,5-triazine Derivatives

These moieties were selected to facilitate the preparation of functional groups with a 3+ charge. Exhaustive alkylation of the ring nitrogens of hexahydro-1,3,5-triazines has been reported to produce tris(ammonium) moieties [18]. Steric hindrance around the amine sites of the benzylated congener may inhibit the addition of further alkyl groups. It is likely that these compounds are very susceptible to decomposition by fragmentation due to the close proximity of the ammonium groups. In acidic conditions (pH < 6.5), pure 1,3,5-triethylhexahydro-1,3,5-triazine readily breaks down into formaldehyde and ethylamine [19].

2.2.7 Macrocyclic Polyammonium Compounds

It was desirable to have a functional group that contains three fixed cationic sites embedded in a flexible macrocyclic chain. This would allow the ammonium groups to be optimally positioned around 'guest' anions, ie. encapsulating the adsorbed gold complex.

The synthesis of a subset of functionalised resins of this type may be attempted via the cyclisation of resin-bound diethylenetriamine (DST). This was pursued by anchoring diethylenetriamine by its central 2°-amine, using a known method employing Schiff-base protective groups (DSU). The resin DST may then be cyclised by the formation of a bis-imine (Schiff base) with a dialdehyde. After reducing the resulting bis-imine with sodium cyanoborohydride, the resulting triazamacrocyclic moiety (DTP) may be exhaustively alkylated in an effort to to produce tris-ammonium salts with the structures illustrated in Figure 2.6.

2.3 *Molecular Modelling of Prospective Moieties*

Each of the proposed functional groups was subjected to computer based Molecular Modelling using the program *Hyperchem* (Professional Version 5.11) [20]. The results were used to evaluate three basic parameters:

(i) the total steric energy of each group,

(ii) the steric bulk around the functional group, and

(iii) the distance between the ammonium groups (where applicable).

These calculations were performed using identical parameters and a standard treatment for each ligand, to normalise the results and facilitate direct comparison. These conditions, parameters and treatments are detailed below.

2.3.1 Molecular Modelling Parameters

Molecular mechanics applications use classical mechanics to approximate bond lengths and energies (optimised using empirical data), and thus calculate the energy of a given molecular conformation. By applying small changes to the conformation, and evaluating the change in energy that results, low-energy states for a given molecule can be determined. Rigorous and stepwise application of this procedure should lead to a low-energy optimum conformation (energy minimum), which is taken to represent the functional group in the ground state.

The resin moieties were constructed with a 4-methylbenzyl substituent to represent the anchor site of the polystyrene resin substrate (P). A fixed charge of 1+ was placed on each quaternary ammonium group; no counterions or solvent molecules were used. All structures were then optimised using the Molecular Mechanics extension of *Hyperchem*, implementing the *MM+* force field (based on the *MM2 (1977)* force field developed by Dr. Norman Allinger) [20]. Intramolecular hydrogen bonding was not included in any of these calculations.

2.3.2 Results of Molecular Modelling

The total molecular steric energy results (in kcal/mol) and the distances between ammonium groups (in Ångstroms; 10^{-10} m) in the various optimised structures are collected in Tables 2.4 – 2.6 for comparison. Changes to the orientation of the alkyl substituents (such as rotation of the benzyl -CH_2- through 180°) were not found to cause significant changes in the total energies (< 1 kcal/mol). In some cases, alkylation can produce several structural isomers where the alkyl groups may be fixed above or below the ring, relative to the polymeric backbone (eg. *syn-*, *anti-* and *mixed* N,N',N''-trisubstituted triazines), and these alternatives were examined in Table 2.6.

The total molecular energies of the various functional groups (*in vacuo*) were calculated using atomic charges, to account for the repulsion between the ammonium groups in the poly(ammonium) moieties. The molecular energy derived from a MM+ calculation has no direct physical meaning, but can be applied as a relative approximation of the enthalpy of formation between various structures [20]. These results, calculated using identical methods, can be applied as a predictor of the likely success of a given functionalisation reaction. On this basis, a series of similar molecules can be compared and estimates made of their relative stability.

A given structure is likely to be thermodynamically unstable if the MM+ energy is very high, relative to the number of atoms in the structure. The results in Tables 2.4 – 2.6 (below) indicate that the primary contribution to the energy of a polyammonium structure is from the intramolecular repulsion of ammonium groups. To estimate the threshold of stability, the energy of the bis(ammonium) moiety BBZ (Table 2.5; 164.52 kcal/mol) may be useful, as the preparation of the analogous tetrabenzylpiperazinium salt has been reported [12].

Table 2.4 MM+ Properties of Functional Groups (Part 1)

Resin Code	No. of Atoms	Total Charge	MM+ Energy
A378	18	0	0.11
ABU	57	1	39.41
APH	51	1	29.15
DIP	38	0	18.67
QNU	38	1	88.51
TBA	60	1	18.27
TOA	93	1	51.27
POP	34	0	13.17
PET	41	1	21.71
PIP	33	0	8.46
NMP	37	1	41.31
NBP	47	1	34.70
MOR	31	0	8.49
NMM	35	1	42.38
NBM	45	1	31.65
ETA	27	0	1.22
ETM	34	1	15.49
ETB	40	1	28.46
DEA	34	0	16.21
DAM	38	1	29.11
DAB	48	1	34.32

Table 2.5 MM+ Properties of Functional Groups (Part 2)

Resin Code	**No. of Atoms**	**Total Charge**	**MM+ Energy**	**N^1-N^2 (Å)**	**N^2-N^3 (Å)**
IMZ	25	0	15.53	-	-
MIM	29	1	21.56	-	-
BIM	39	1	26.29	-	-
PAZ	32	0	10.78	-	-
NMZ	35	0	13.74	-	-
TPZ	43	2	137.01	3.031	-
TBZ	63	2	143.41	3.087	-
BBZ	73	2	164.52	3.242	-
TME	41	1	21.15	-	-
PME	45	2	111.64	3.928	-
BME	55	2	108.67	4.027	-
TAA	44	0	13.45	-	-
DET	36	0	2.39	-	-
DTM	60	3	178.48	3.924	3.924
DSU	60	0	28.51	-	-
DST	36	0	14.09	-	-
DTP	49	0	25.41	-	-
DMP	67	3	282.14	3.937	5.674
DBP	117	3	307.57	4.142	5.983

Table 2.6 MM+ Properties of Functional Groups (Part 3)

Resin Code	**No. of Atoms**	**Total Charge**	**MM+ Energy**	**N^1-N^2 (Å)**	**N^1-N^3 (Å)**	**N^2-N^3 (Å)**
TET	50	1	30.00	-	-	-
syn-TEM	58	3	457.27	2.586	2.609	2.570
anti-TEM	58	3	467.93	2.528	2.531	2.552
mix-TEM	58	3	459.16	2.593	2.607	2.585
syn-TEB	78	3	477.05	2.620	2.594	2.616
anti-TEB	78	3	476.66	2.524	2.530	2.592
mix-TEB	78	3	477.95	2.605	2.600	2.622
TBT	71	1	14.32	-	-	-
syn-TBM	79	3	461.86	2.589	2.575	2.595
anti-TBM	79	3	462.20	2.513	2.513	2.575
mix-TBM	79	3	459.43	2.575	2.574	2.577
TBB	99	3	460.50	2.576	2.580	2.562

Where possible, the interatomic distances between the ammonium nitrogen atoms of the models (N^1-N^2, N^1-N^3 and N^2-N^3) were also recorded. This factor is inversely proportional to the charge-charge interaction energy of the polyammonium groups. These distances may also be useful in comparison to the charge distribution of the anions of interest (metal complexes and polythionates, Section 2.5).

The MM+ energy results show similar values for the exhaustively alkylated piperazine derivatives (Table 2.5; TPZ, TBZ and BBZ). Substitution of the methyl groups for benzyl groups (TPZ → TBZ → BBZ) increases the total energy in steps

of 6.4 and 11.1 EU respectively), and also the N^1-N^2 distance. The alkylated derivatives of tetramethyl-1,4-diaminoethane (Table 2.5; BME and PME) were much closer (within ~ 3 EU and 0.1 Å). Both these structures had a significantly greater N^1-N^2 distance than the piperazine derivatives (~ 4 Å vs. ~ 3 Å respectively), and hence lower Charge Energy. The preparation of all these groups on a polymeric resin is probably feasible.

The relatively high MM+ energy calculated for the heptamethylated diethylenetriammonium structure (DTM) (Table 2.5; 178.48 kcal/mol) may be accounted for by the interaction of two pairs of ammonium groups in the linear tris(ammonium) chain (each ~ 4 Å apart). Similar calculations were performed for the exhaustively alkylated derivatives of the macrocyclic group DTP. The N-N distances of the benzyl derivative (DBP) were found to be 0.2 - 0.3 Å greater than those of the methylated congener (DMP). The N_2-N_3 distance in these structures was ~ 6 Å, significantly greater than found in the other structures. Despite this, the charge-charge energy contributions of DMP and DBP (> 280 kcal/mol each) were also significantly greater than the linear tris(ammonium) moiety DTM. This is due to the close proximity of the third pair of ammonium groups (N^1-N^3) in the constrained ring. These tris(ammonium) structures are expected to be rather fragile.

The charge interaction contribution dominates the calculated energy of the alkylated derivatives of the hexahydro-1,3,5-triazines TET and TBT (Table 2.6). The difference in energy of the various possible isomers of each structure were found to be relatively small (< 12 kcal/mol), and a similar charge-charge contribution (~460) kcal/mol) was calculated for each. Substitution of the alkyl groups of the hexahydro-1,3,5-triazine derivatives (in order of increasing steric hindrance: methyl → ethyl → benzyl) caused only small increases in the calculated inter-ammonium distances, all within a narrow range (2.51 – 2.62 Å).

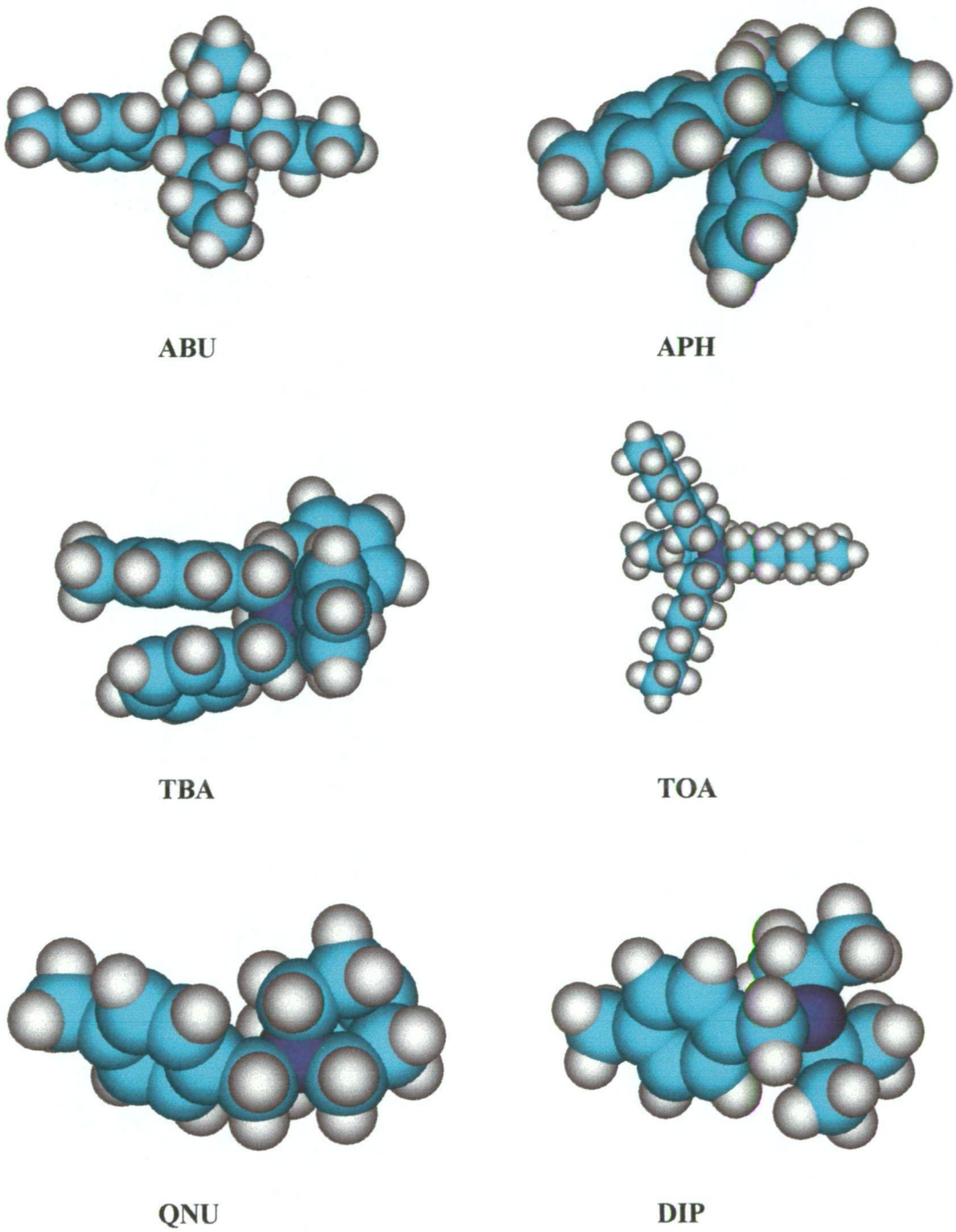

Figure 2.7 Space Filling Models of Functional Groups on Resins (Part 2)

Energy Minimised Structures (MM+) [20]

KEY: Grey = Hydrogen; Light Blue = Carbon; Dark Blue = Nitrogen

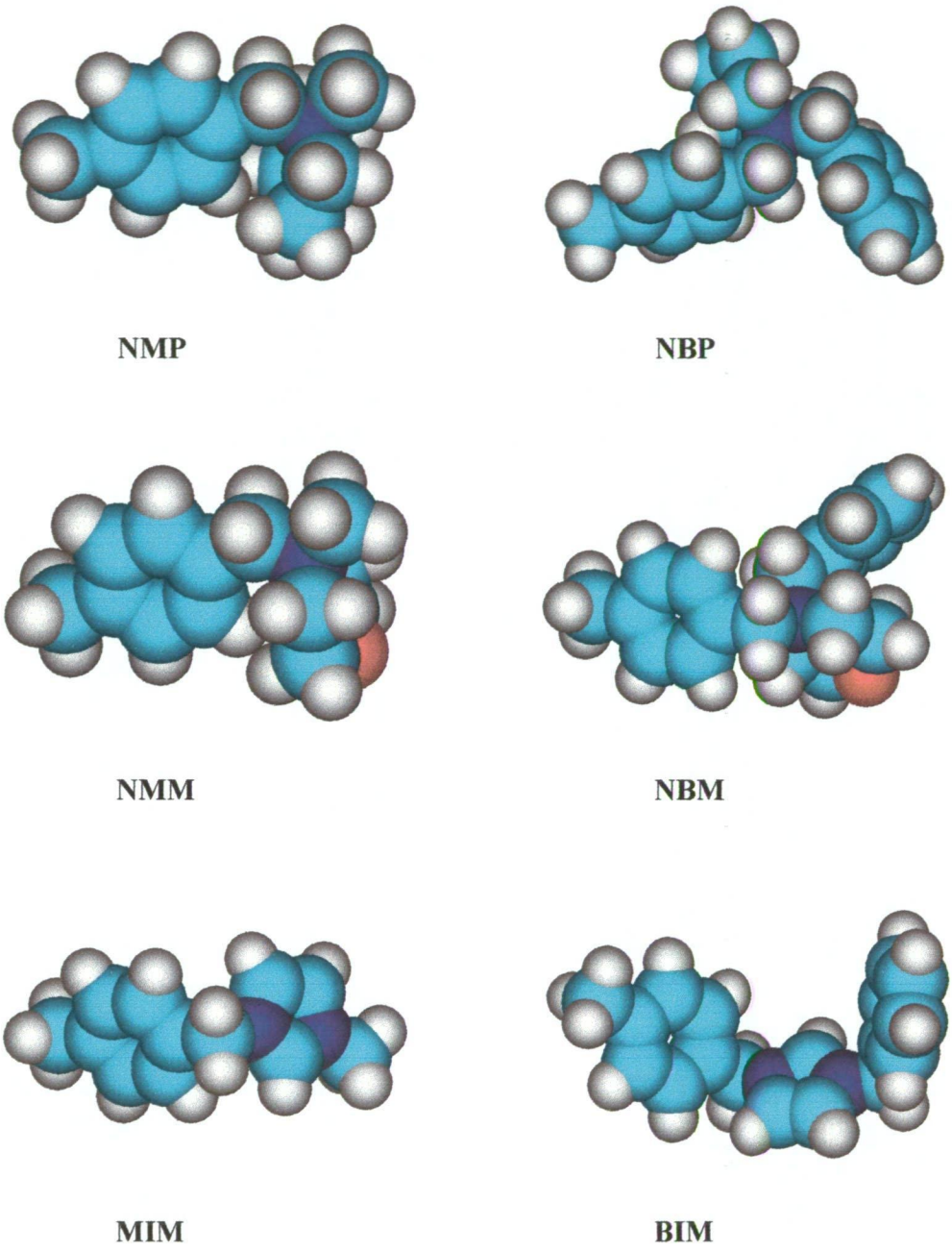

Figure 2.8 Space Filling Models of Functional Groups on Resins (Part 2)

Energy Minimised Structures (MM+) [20]

KEY: Grey = Hydrogen; Light Blue = Carbon; Dark Blue = Nitrogen; Red = Oxygen

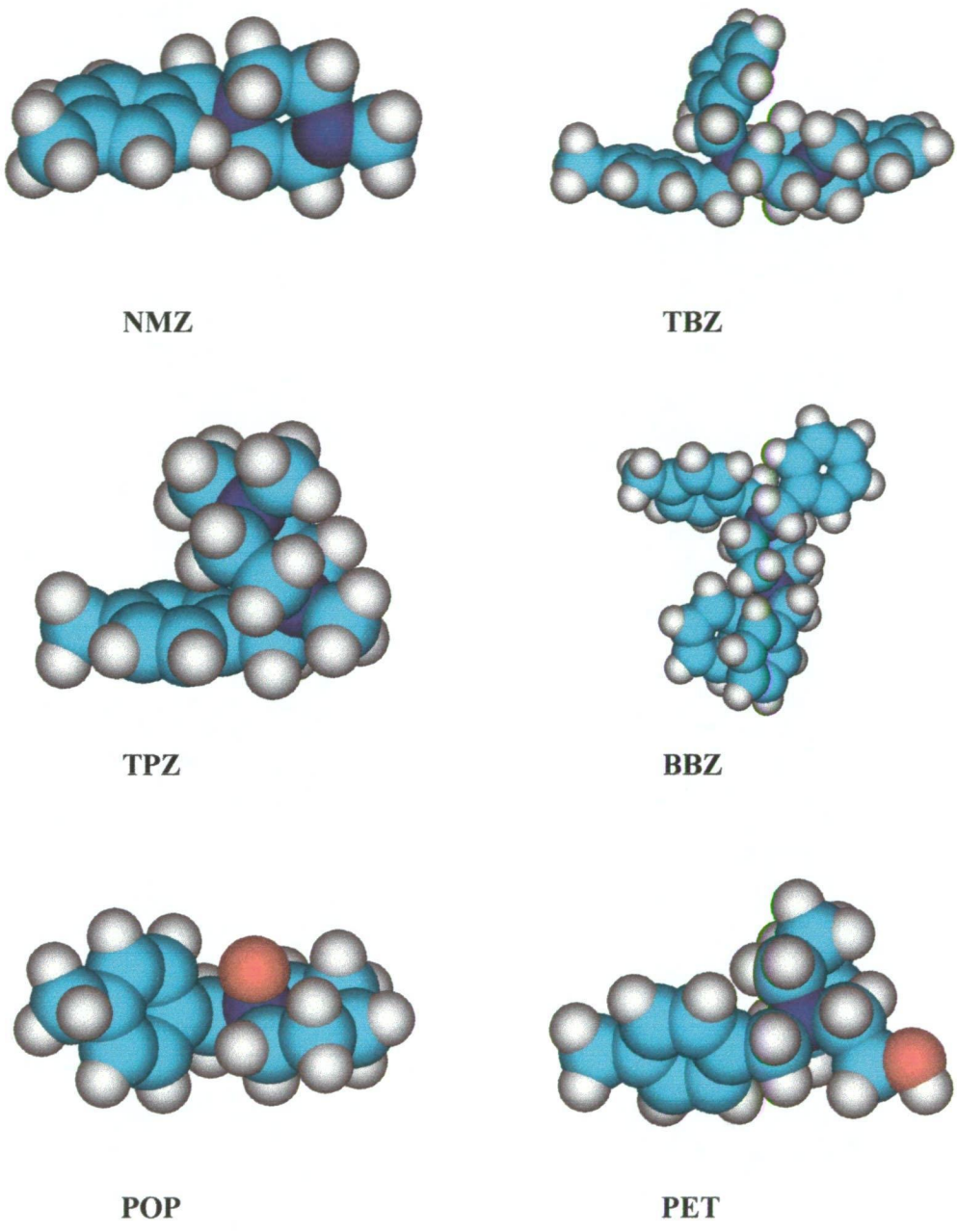

Figure 2.9 Space Filling Models of Functional Groups on Resins (Part 3)

Energy Minimised Structures (MM+) [20]

KEY: Grey = Hydrogen; Light Blue = Carbon; Dark Blue = Nitrogen; Red = Oxygen

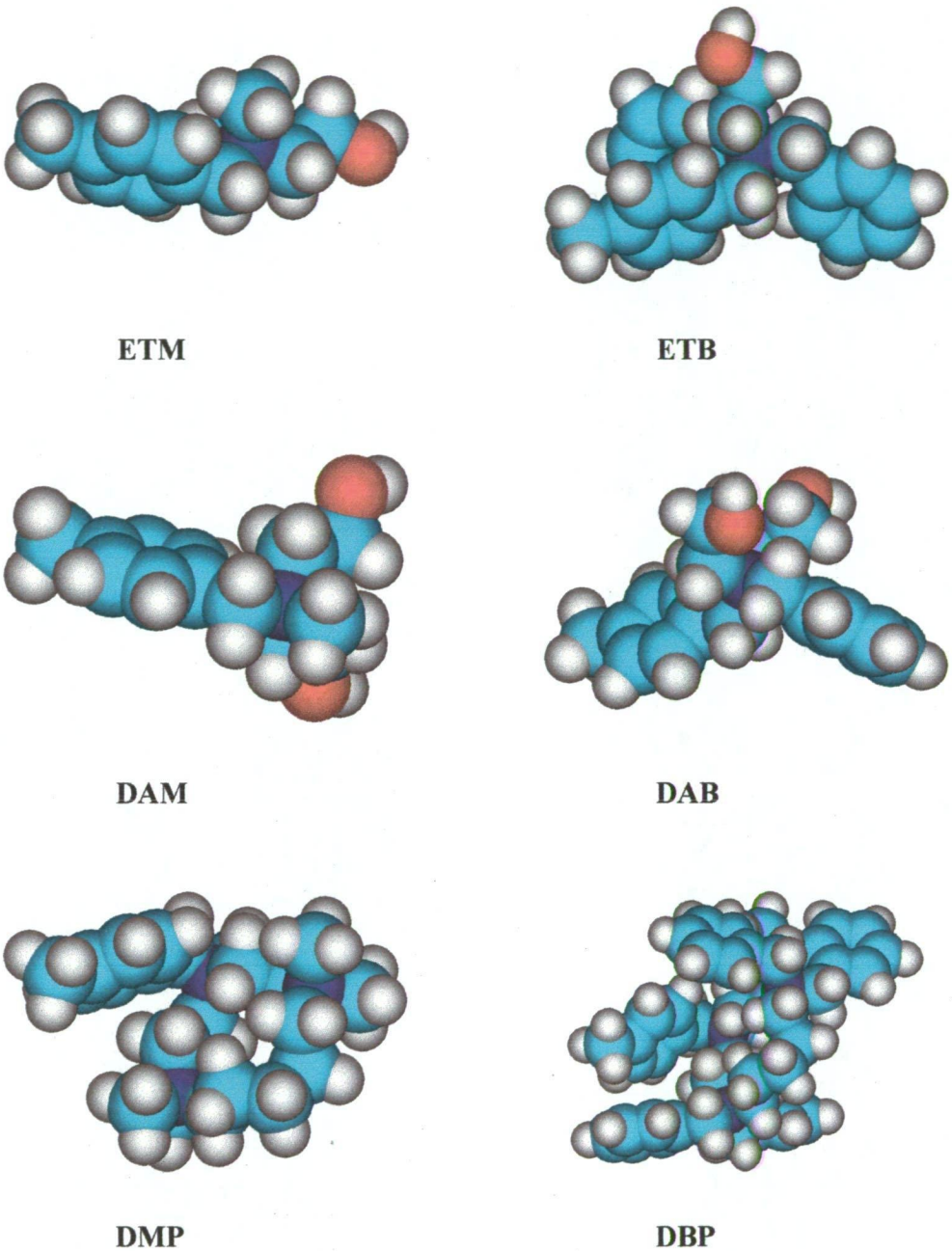

Figure 2.10 Space Filling Models of Functional Groups on Resins (Part 4)

Energy Minimised Structures (MM+) [20]

KEY: Grey = Hydrogen; Light Blue = Carbon; Dark Blue = Nitrogen; Red = Oxygen

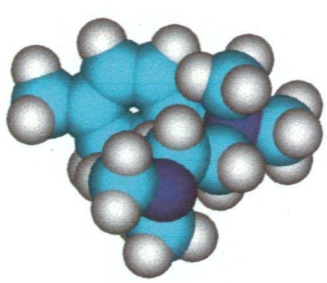

TME

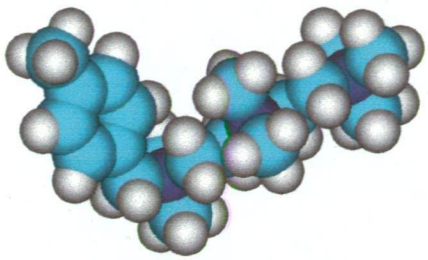

DTM

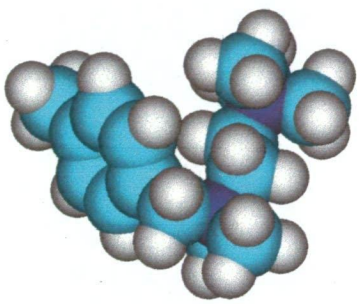

PME

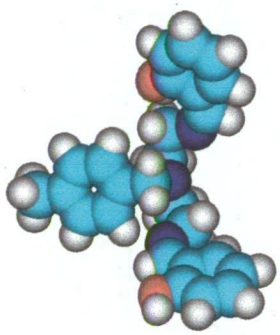

DSU

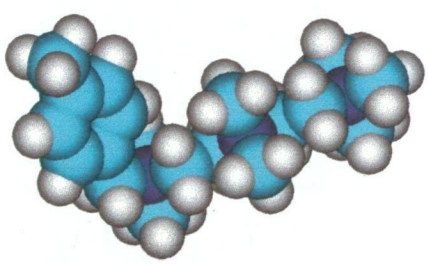

BME

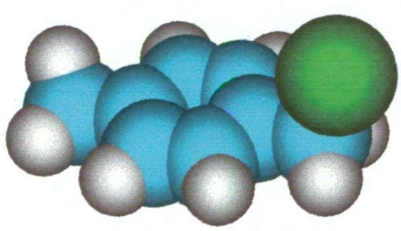

Chloromethylated Polystyrene

Figure 2.11 Space Filling Models of Functional Groups on Resins (Part 5)

Energy Minimised Structures (MM+) [20]

KEY: Grey = Hydrogen; Light Blue = Carbon; Dark Blue = Nitrogen;

Red = Oxygen; Green = Chlorine

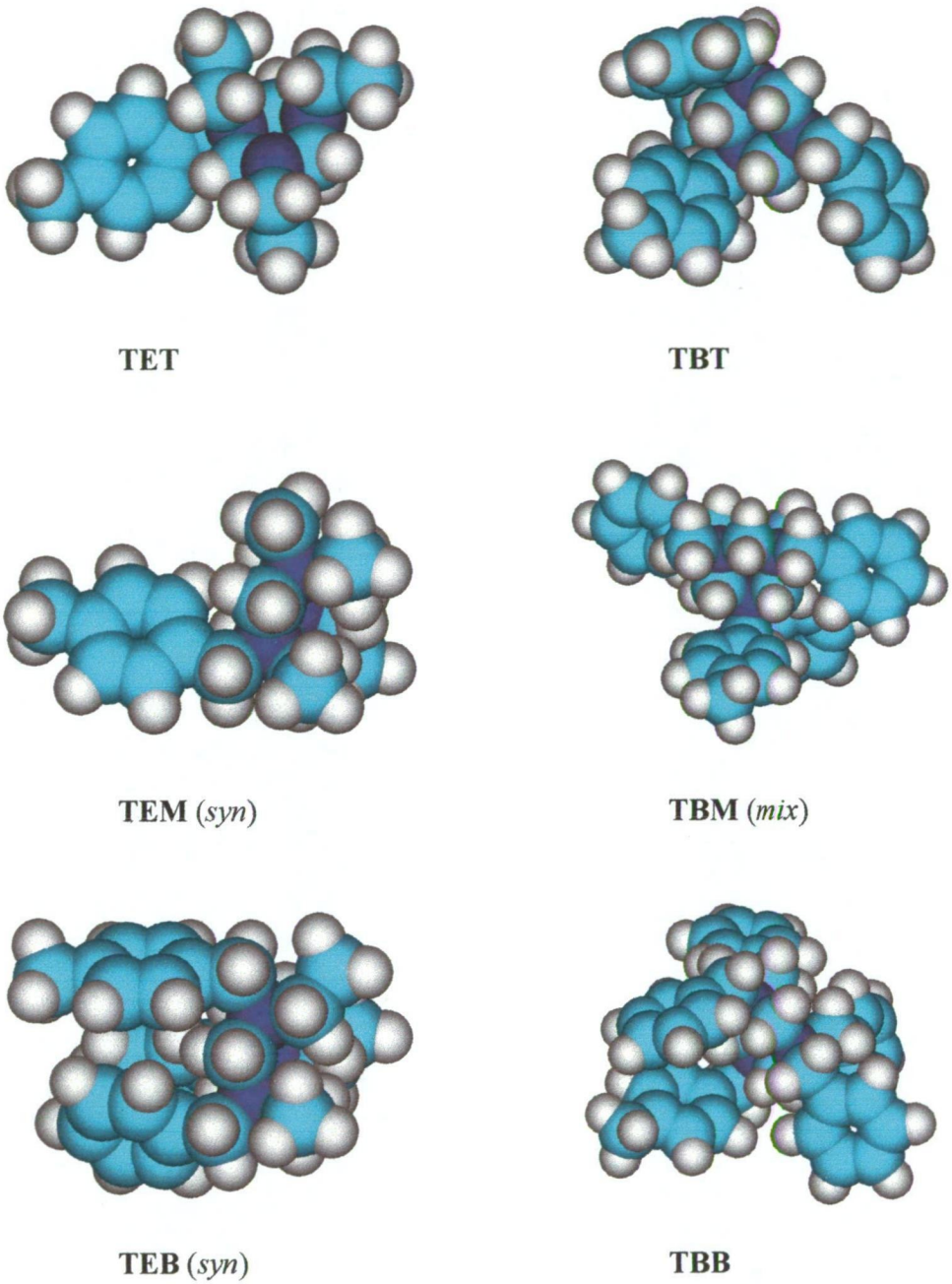

Figure 2.12 Space Filling Models of Functional Groups on Resins (Part 6)

Energy Minimised Structures (MM+) [20]

KEY: Grey = Hydrogen; Light Blue = Carbon; Dark Blue = Nitrogen

To evaluate the degree of steric hindrance around the ammonium atoms, space filling models of the optimised structures of the final IEX groups were examined. These models are provided below, as Figures 2.7 – 2.12. Only one of the three possible structural isomers of resins TBM, TEB and TEM are shown in Figure 2.12. The nitrogen atoms have been given a distinct colour (dark blue) to facilitate identification and comparison. The alkylammonium ring structures (eg. NMM, NMP, TPZ) appear more constrained, and hence less bulky than linear alkyl groups (eg. TOA, ABU). Benzylated derivatives show enhanced steric bulk near the ammonium group(s) compared to the methyl analogues. This greater bulk is less significant when the phenyl rings may move freely, and the hindrance is closer to that of a secondary carbon substituent (eg. ethyl).

2.4 Metal Equilibria in Thiosulfate Solutions

Each resin in this work must be examined in comparable conditions to allow independent assessment of the affinity of the functional group for gold. The efficacy of a resin in adsorbing gold from leach solutions depends primarily upon the affinity of the functional group for gold, the composition of the leach solution, and the rate and degree of diffusion of the solution into the resin. The latter factor may be substantially controlled by employing a common resin substrate, and performing tests using a common regime of temperature, volume, agitation and contact time. The concentrations of the various components of the leach solution must also be controlled to facilitate comparative analysis of the gold affinity of a functional resin.

A set of concentrations and conditions defining an artificial leach liquor was selected for this project (Table 2.7), and the majority of resin adsorption tests were conducted using these conditions (see Chapter 4, Section 4.1.1). The conditions

selected were at the low concentration end of reported leaching protocols, reflecting the trend toward reagent minimisation in current practice.

Table 2.7 Composition of Artificial Leach Liquor

Reagent	**Formula**	**Concentration**	**ppm**
Ammonia	NH_4OH	1.00 M	-
Ammonium Chloride	NH_4Cl	0.100 M	-
Ammonium Thiosulfate	$(NH_4)_2S_2O_3$	0.100 M	-
Cupric Sulfate	$CuSO_4.5H_2O$	3.149 mM	200
Sodium Aurothiosulfate	$Na_3[Au(S_2O_3)_2].2H_2O$	0.101 mM	20

Copper is found in ammoniacal thiosulfate solution as both Cu(I) and Cu(II) complexes, primarily as $[Cu(S_2O_3)_N]^{1-2N}$ and $[Cu(NH_3)_4]^{2+}$ respectively. In this work, the initial tests utilised a very high copper concentration (~2000 ppm), but this led to problems with accurate determinations (see Section 4.1.4.2). Subsequent tests used a dissolved copper concentration of ~200 ppm, as shown in Table 2.7.

The distribution of copper between Cu(I) and Cu(II) may be followed by UV-Vis spectroscopy, as the $[Cu(NH_3)_4]^{2+}$ complex absorbs strongly in the visible region (ν_{max} = 604 nm, molar extinction coefficient ε = 50.04 $L.mol^{-1}.cm^{-1}$). Absorbance (A) is linearly related to the concentration (c) by the relationship $A = \varepsilon.c.l$ (where l = path length in cm), so [Cu(II)] can be calculated from the absorbance at 604 nm, and [Cu(I)] may be inferred by difference. In ammoniacal solutions, Cu(I) is rapidly re-oxidised to Cu(II) by dissolved molecular oxygen, which may be minimised by utilising a closed system. Rigorous exclusion of oxygen

from the liquors in this work was not considered practical, although the leach vessels should remain closed whenever possible to keep conditions consistent.

In a control experiment, the influence of thiosulfate on the distribution of copper ions was followed by UV spectroscopy. The absorbance of a solution of $CuSO_4$ (10.00 mM) and ammonium thiosulfate (100 mM) in ammonia (0.50 M) was compared to that of a control solution of $CuSO_4$ (10.00 mM) in ammonia (0.50 M) over 96 hours. A sample of each solution was placed in a separate quartz cell, which was filled to the brim and stoppered to exclude air. The absorbance of these solutions at 604 nm was measured against a 'blank' cell of ammonia (0.50 M). The results (shown in Figure 2.13) indicate that the Cu(II) concentration had fallen to ~10% of the initial value after 96 hours at ambient temperature.

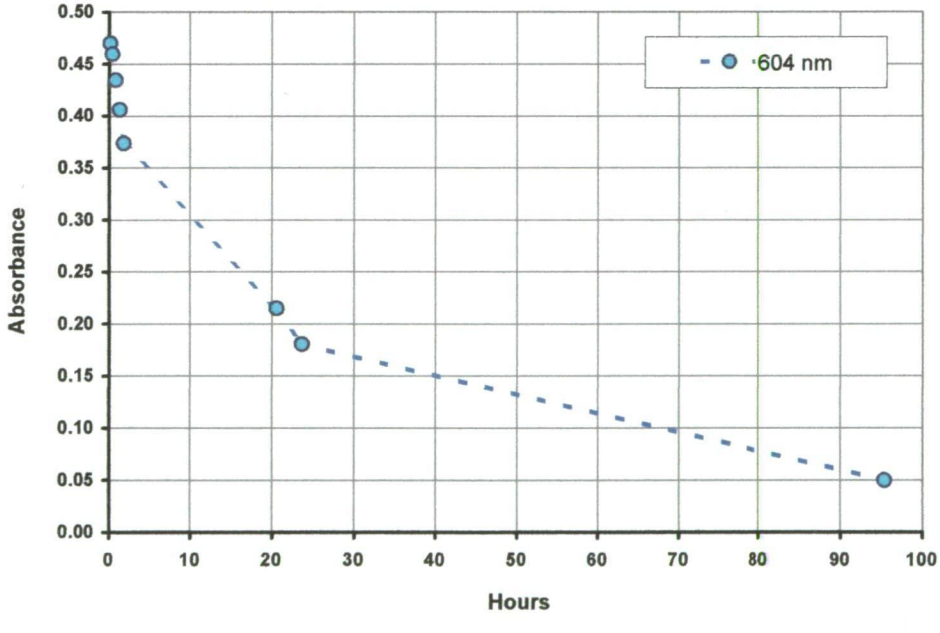

Figure 2.13 The Influence of Thiosulfate on Cu(II) in Aqueous Ammonia

The distribution of copper in ammoniacal thiosulfate solution may be predicted by simultaneously solving the equilibrium reactions between Cu(I) and

ammonia, thiosulfate, hydroxide and water ligands. The many side-reactions of thiosulfate have been excluded. The copper distribution in the leach liquor described in Table 2.7 has been calculated using the computer programs *Hydra* and *Medusa* [21-22]. The results are displayed as the fraction of total Cu(I) for each of the soluble thiosulfate complexes $[Cu(S_2O_3)]^-$, $[Cu(S_2O_3)_2]^{3-}$, $[Cu(S_2O_3)_3]^{5-}$, and the diammine complex $[Cu(NH_3)_2]^+$ (Figure 2.14). Note that the bis(thiosulfate) complex comprises approximately 20% of the soluble Cu(I). The $[Cu(S_2O_3)_2]^{3-}$ complex is similar in structure and charge to the Au(I) complex, and is expected to compete significantly for IEX sites.

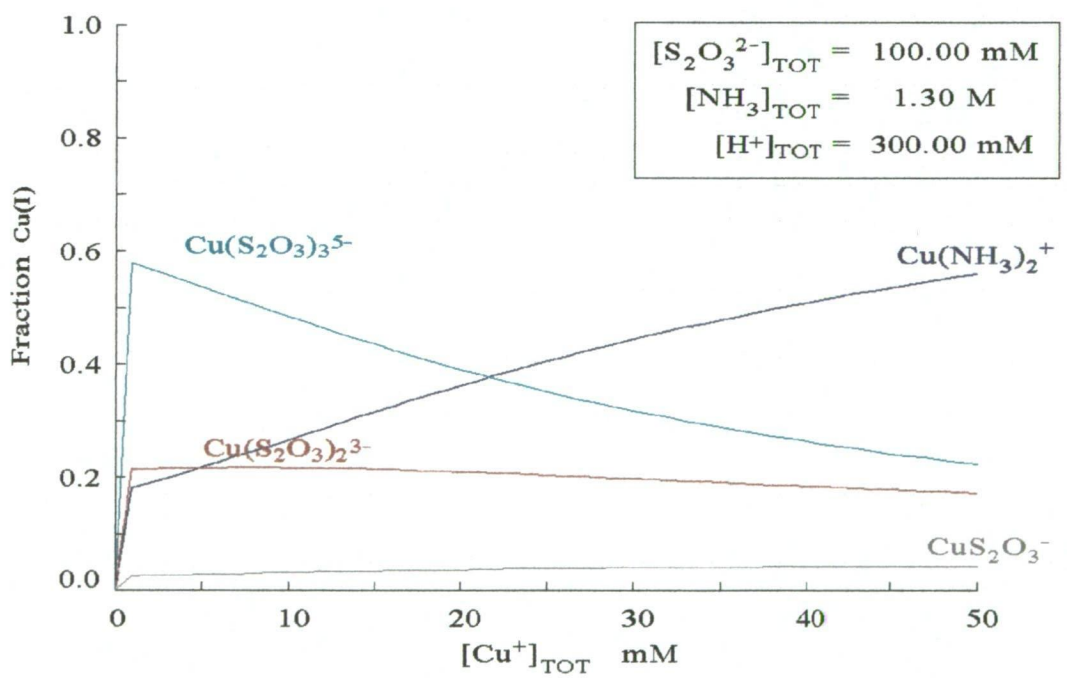

Figure 2.14 The Distribution of Cu(I) in 0.1 M Thiosulfate (pH 10.3)

In the proposed test conditions, the data in Figure 2.13 suggest that the initial 200 ppm (3.15 mM) [Cu(II)] will fall to ~20% (0.62 mM) after 24 hours. The Cu(I)

distribution is predicted to be 20% bis(ammine), 20% bis(thiosulfate) and 60% tris(thiosulfate) complex, and skewed toward the latter as [Cu(I)] decreases.

The same programs also facilitated the development of an Eh *vs* pH Predominance (Pourbaix) Diagram for copper in the liquor described in Table 2.7 (Figure 2.15). It is apparent that the low concentration of thiosulfate common in the more recent applications (see Table 1.1) increases the significance of the competing ammine complexes. The lower order copper complexes, $Cu[S_2O_3]^-$ and $Cu[S_2O_3]^{3-}$, also become more abundant as free thiosulfate becomes scarce with decreasing pH.

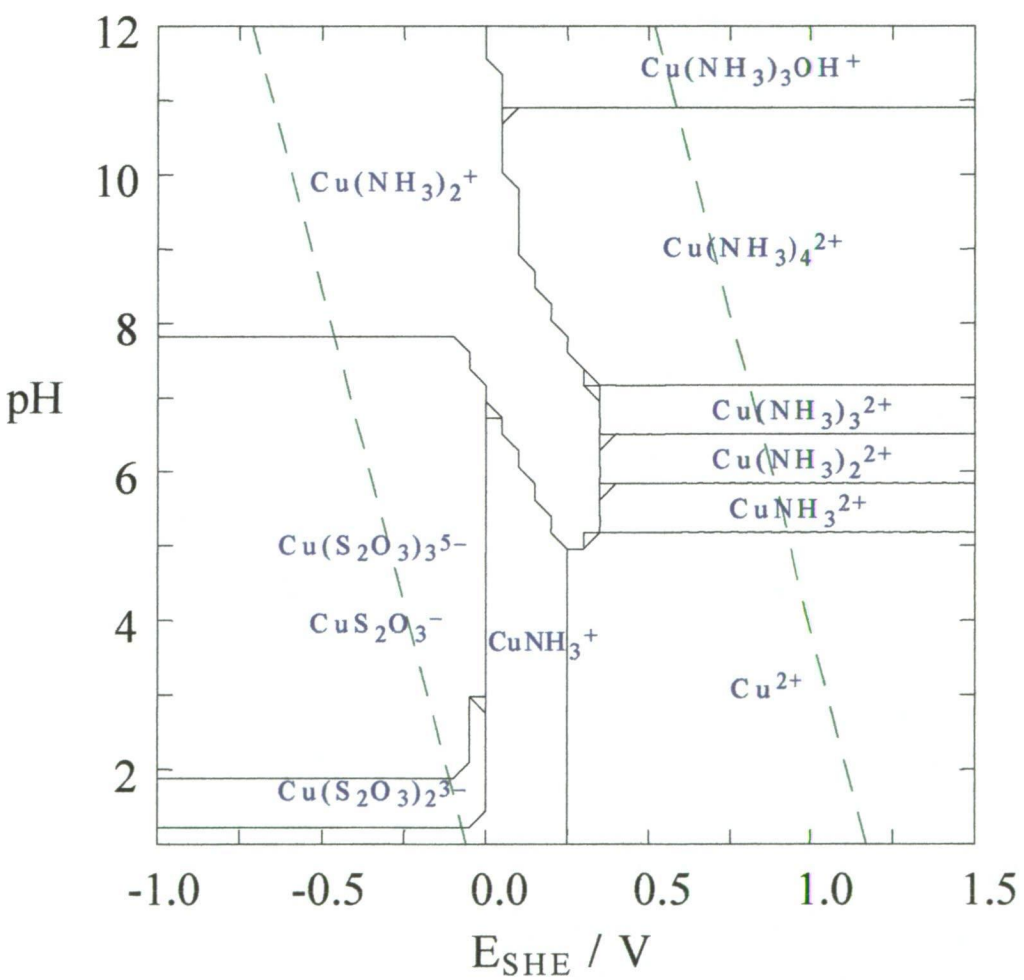

Figure 2.15 Predominance Diagram (Eh vs pH) for Cu^+/Cu^{2+}

$[S_2O_3]$ = 100 mM; $[Cu^{2+}]$ = 15 mM; $[NH_3]$ = 1.30 M; T = 25°C

2.5 Molecular Modelling of Critical Complexes

The structure and charge distribution of the gold and copper thiosulfate complexes and the important sulfoxy dianions (thiosulfate, trithionate, and tetrathionate) have been examined via computational methods. These results can be compared to the physical data from crystal studies to monitor accuracy. Electron Potential Contour (EPC) maps showing potential interaction with cations may then be derived for comparison to the functional groups developed in Sections 2.2 – 2.3.

The sulfoxy ions may be efficiently modelled by simple molecular mechanics, such as Hyperchem (MM+) [20] with a reasonable expectation of accuracy. However, molecular modelling parameter sets for transition metals are not very accurate, as the complexities of *d*-orbital interactions cannot be represented accurately using a simple mechanical model. The program *Spartan* [23] employs the semi-empirical PM3(tm) parameter set, containing additional empirical parameters to model the equilibrium geometry of transition metal compounds, and was used to simulate the cuprothiosulfate complexes. Unfortunately, gold is not included in the set of transition metals parameterised in PM3(tm).

The electronic behaviour of metal complexes may be more accurately modelled by Density Functional Theory (DFT). This quantum mechanical approach utilises pseudopotential core functions augmented by additional orbital basis sets to model the electronic wavefunction of metal atoms. Simpler atoms may be modelled in the same process using *ab-initio* techniques. The energy is minimised in a computationally intensive iterative process to arrive at an optimum self-consistent structure. The program *Gaussian03* [24] was employed to simulate the structures of the important anions, using the B3LYP/LANL2DZ level of theory (a Hartree-Fock/DFT hybrid of Becke-Perdew/Lee-Yang-Parr techniques, with pseudopotential

core functions for copper and gold) and augmented by the 6-311+G(2df) split-valence polarization basis sets (employing additional *d*- and *f*-orbital functions) on the sulfur and oxygen atoms. All DFT calculations were optimised at this level of theory (B3LYP/LANL2DZ:6-311+G(2df)) unless otherwise stated.

2.5.1 The Aurothiosulfate Complex

The complex $[Au(S_2O3)_2]^{3-}$ was initially modelled using MM+, and the resulting structure was used as the starting point for DFT optimisation. This was progressively refined by increasing the level of theory from HF/LANL1MB through BP86/LANL2DZ, and finally to B3LYP/LANL2DZ. The latter level of theory was further refined by expanding the orbital basis sets for sulfur and oxygen atoms to 6-311+G(2df), to more closely approximate the reported crystal structure [25]. The energy of the singlet state optimum was found to be E_0 = -2179.889 AU. The electron density of the optimised wavefunction was used to create the EPC maps shown in figure 2.16 [23]. These plots shows the force on a positive point charge, such as interaction with an ammonium group, superimposed on a simple ball-and-stick model of the optimised complex. Blue contours indicate regions of high attraction for a point positive charge, and red contours indicate little interaction.

Table 2.8 Structural features of the Aurothiosulfate Complex

	Au-S (Å)	**S-S (Å)**	**S-O (Å)**	**S-Au-S**	**Au-S-S**
Crystal	2.27	2.06	1.46	176.5	103.9
MM+	2.509	2.059	1.64	179.9	120.5
DFT	2.386	2.178	1.477 – 1.485	171.7	116.9

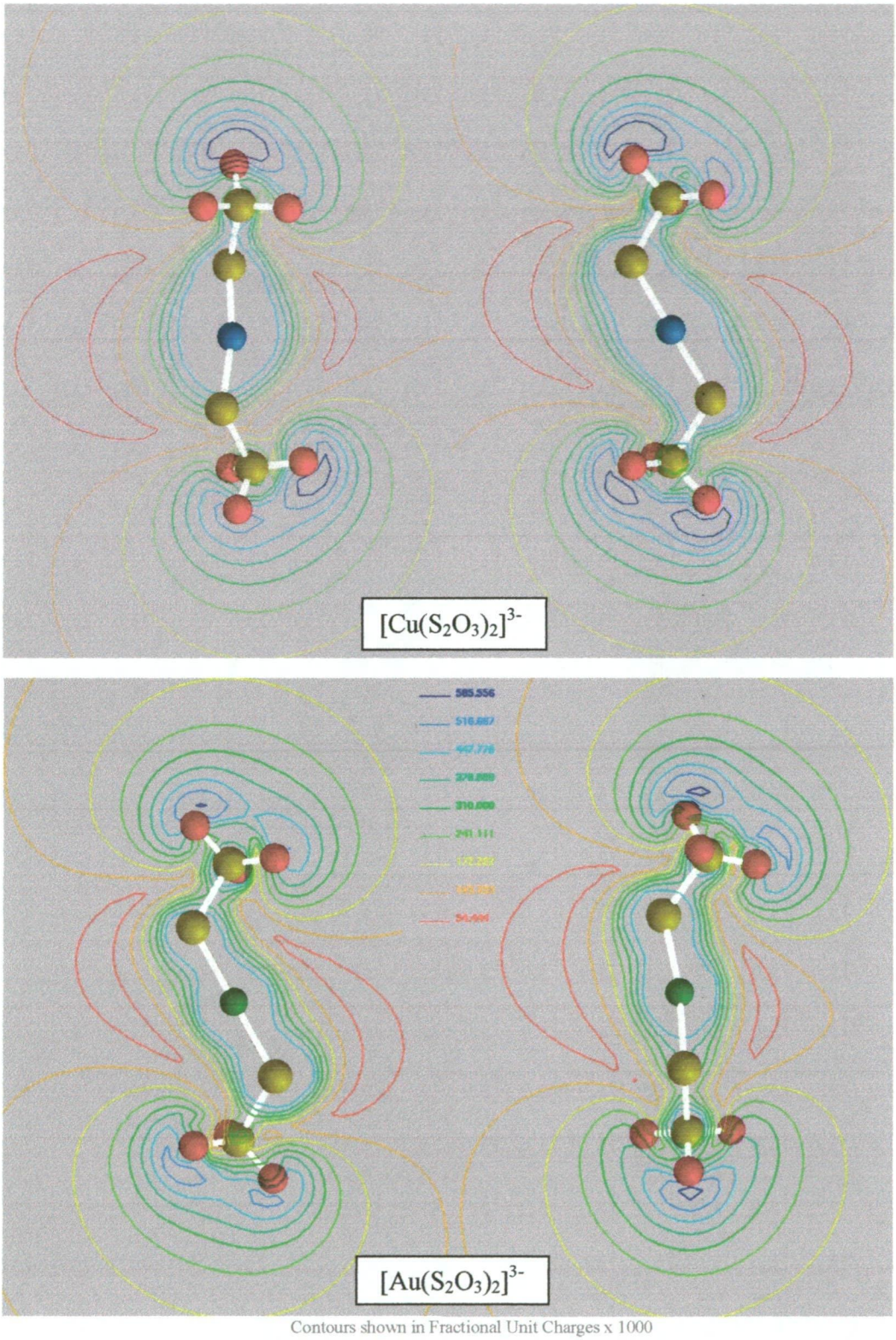

Figure 2.16 EPC Maps of DFT Models of $[M(S_2O_3)_2]^{3-}$ (M = Cu, Au)

KEY: Red = Oxygen; Yellow = Sulfur; Blue = Copper(I); Green = Gold(I)

2.5.2 The Cuprothiosulfate Complexes

The crystal structure cited below (Table 2.9) was derived from X-ray analysis of the compound $Na_3[Cu(S_2O3)_2].2NaNO_3$ [26-27]. The Cu(I) ions in this complex are tetrahedrally coordinated by bridging via the terminal sulfur atoms of the thiosulfate ligands, in a similar fashion to the silver complex (see Figure 1.2). In aqueous ammoniacal leach solutions, it is very likely that the two vacant coordinates of $[Cu(S_2O_3)_2]^{3-}$ will be taken up by solvent molecules (H_2O or NH_3) to maintain the tetrahedral geometry.

To examine the possibility of the two thiosulfate ligands occupying the four tetrahedral coordination positions, the complex was optimised from two different starting structures. The first was a 'bent' complex with only the terminal thiosulfate sulfur atoms chelating the metal. The second structure constrained the thiosulfate ligands to an angle such that oxygen atoms occupied the third and fourth coordinates. At the highest level of DFT theory applied, the two structures converged to a single optimum chelated only by the sulfur atoms. Examination of this singlet state optimum (E_0 = - 240.576 AU) revealed a linear complex, with reasonable bond lengths. EPC maps of the DFT optimised structure are shown in Figure 2.16. It is likely that the geometry of this complex is not accurately predicted, due to the absence of solvent ligands. The addition of further atoms into this calculation would significantly increase the computational complexity (and duration), and was not pursued in this work.

A more realistic approximation of the complex $[Cu(S_2O_3)_2]^{3-}$, and the related tris(thiosulfate) complex $[Cu(S_2O_3)_3]^{5-}$, may be derived from the PM3(tm) optimised structures via single-point DFT calculations at the B3LYP/LANL2DZ level of theory. These are detailed in Table 2.9, and EPC maps derived from these structures are shown in Figure 2.17.

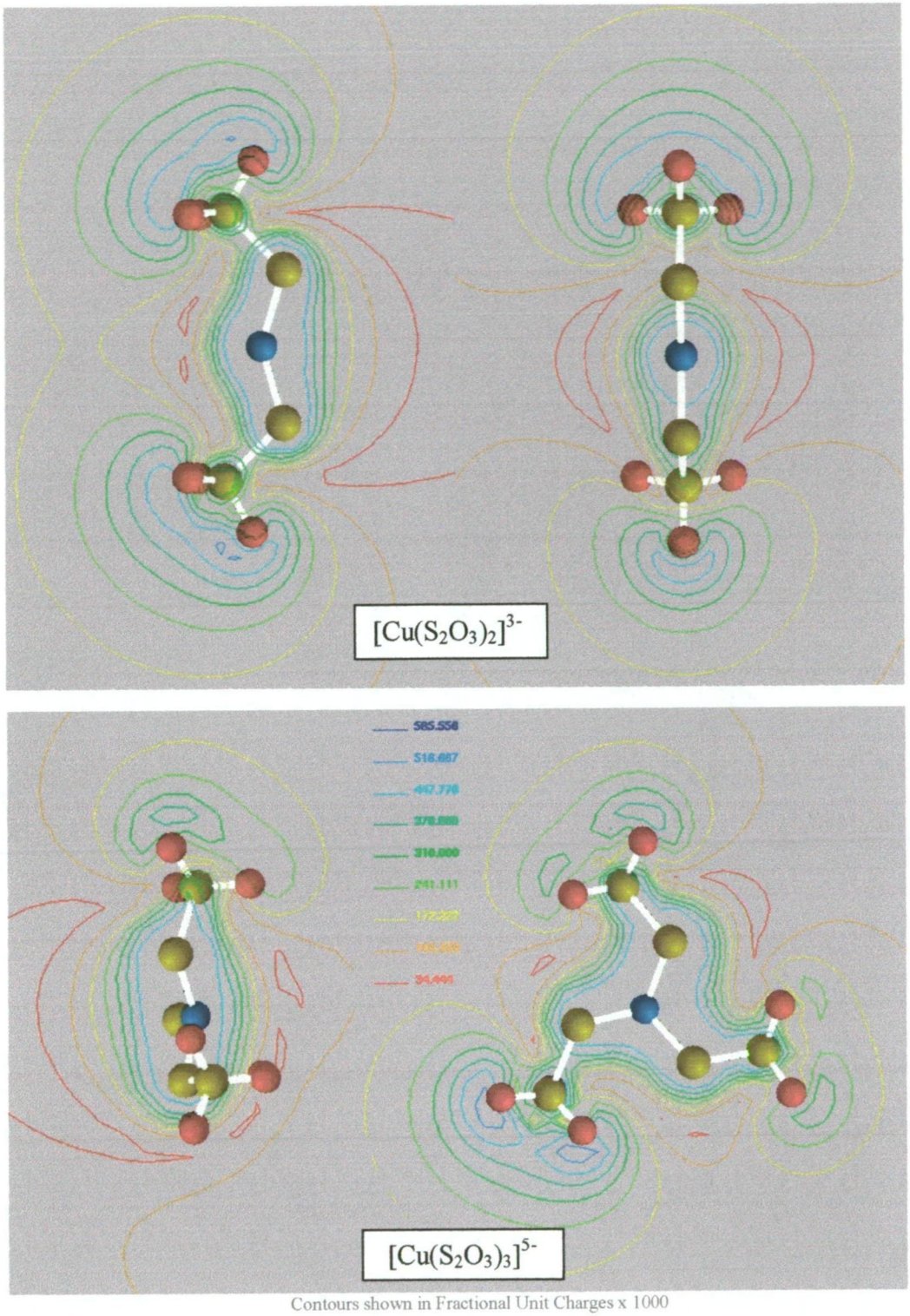

Contours shown in Fractional Unit Charges x 1000

Figure 2.17 EPC Maps of PM3 Models of $[Cu(S_2O_3)_n]^{(1-2n)-}$ (n = 2, 3)

KEY: Red = Oxygen; Yellow = Sulfur; Blue = Copper(I)

Table 2.9 Structural features of the Cuprothiosulfate Complexes

$[Cu(S_2O_3)_2]^{3-}$	Cu-S (Å)	S-S (Å)	S-O (Å)	S-Cu-S	Cu-S-S
Crystal	2.353	2.046	1.460 – 1.480	109.4 – 109.7	111.6 – 116.7
MM+	2.19	1.99	1.64	109.5	92.0
PM3(tm)	2.128	2.217	1.530	147.5	118.4
DFT	2.251	2.166	1.480	170.4	115.9
$[Cu(S_2O_3)_3]^{5-}$	Cu-S (Å)	S-S (Å)	S-O (Å)	S-Cu-S	Cu-S-S
MM+	2.31	2.06	1.64	120.1	120.4
PM3(tm)	1.997 – 2.107	2.186 – 2.264	1.482 – 1.537	112.4 – 119.5	111.6 – 118.3

2.5.3 Thiosulfate, Trithionate and Tetrathionate

It is appropriate to consider the sulfoxy anions at the same levels of computational theory as the metal complexes to facilitate direct comparison. These are presented in Table 2.10, accompanied by the structural data derived from X-ray crystallography. The data for the trithionate and tetrathionate dianions were derived from the study of crystalline Cobalt(II) complexes containing the sulfoxy anions as a counterion [28-29]. EPC maps were derived from single point DFT calculations on these optimised structures, at the B3LYP/LANL2DZ level of theory (Figure 2.18). The scale of the EPC maps may be implied from the bond lengths denoted in the corresponding Tables.

Table 2.10 Structural features of the Sulfoxy Anions

$S_2O_3^{2-}$	S-S (Å)	S-O (Å)	S-S-O
Crystal	2.013	1.468	108.9
MM+	2.127	1.430	109.2
PM3	2.121	1.554	110.5
DFT	2.128	1.491	107.8 – 111.2

$S_3O_6^{2-}$	S-S (Å)	S-O (Å)	S-S-O	S-S-S
Crystal	2.092, 2.112	1.437 – 1.449	100.7 – 107.1	102.71
MM+	2.242	1.397	105.2 – 106.6	146.0
PM3	2.275	1.494 – 1.502	104.0 – 108.7	127.7
DFT	2.208	1.465 – 1.476	97.0 – 108.2	115.8

$S_4O_6^{2-}$	S-S (Å)	S-O (Å)	S-S-O	S-S-S
Crystal	2.019; 2.132	1.417 – 1.450	100.9 – 108.2	103.4
MM+	2.100; 2.328	1.394 – 1.402	98.1 – 108.0	110.1
PM3	2.054; 2.359	1.478 – 1.489	100.0 – 108.6	114.0
DFT	2.057; 2.236	1.462 –1.474	96.4 – 109.1	110.8

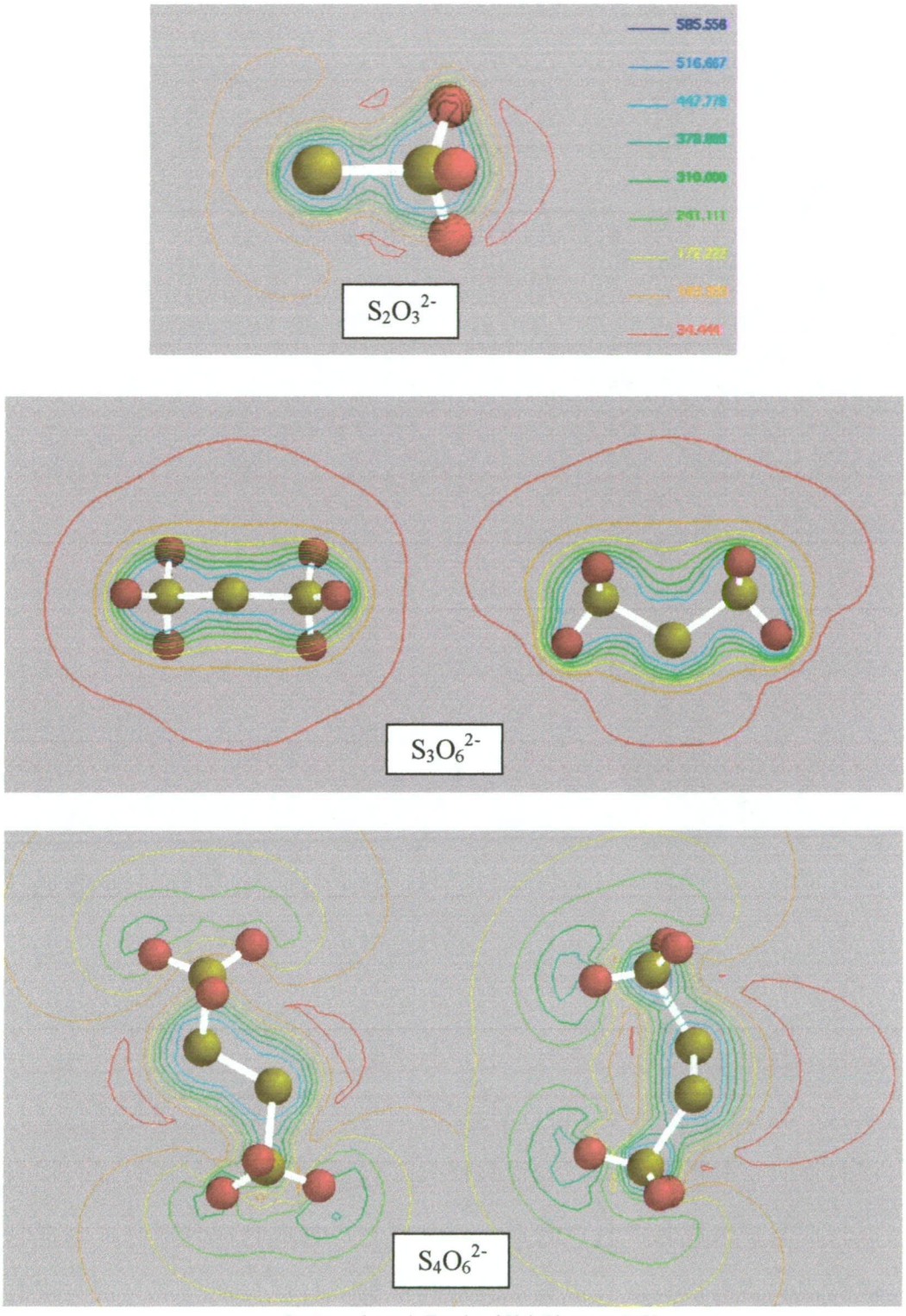

Contours shown in Fractional Unit Charges x 1000

Figure 2.18 EPC Maps of DFT Models of Polythionate Dianions

KEY: Red = Oxygen; Yellow = Sulfur

2.5.4 Comparison and Implications

A small linear Cu(I) complex, as in Figure 2.16, may significantly compete with Au(I) thiosulfate species for IEX sites. The calculated bond lengths of the Cu(I) bis(thiosulfate) complex were found to be shorter than the corresponding Au(I) complex, at both MM+ and DFT levels of theory. The opposite trend in the crystal structures (Tables 2.9 and 2.10) originates from the change to a tetrahedrally coordinated Cu(I) complex. This would be more bulky than the aurothiosulfate complex, and may be less problematic. The Cu(I) tris(thiosulfate) complex (Figure 2.16) is more bulky, but very likely to bind strongly to cationic IEX sites due to the high 5- charge.

The broad lobes of blue projecting from the oxygen atoms in the EPC maps of the various anions (Figs. 2.16 – 2.18) denote regions of strong interaction with a cation. The strong-base functional groups of a resin should favour these regions in ion-exchange interactions. The narrow bands surrounding the central sulfur and/or metal atoms shows that the overall negative charge is delocalised along this axis. The complexes $[Au(S_2O_3)_2]^{3-}$ and $[Cu(S_2O_3)_2]^{3-}$ (Figure 2.16) showed very similar interaction surfaces, with slightly broader lobes near the copper and oxygen atoms of the smaller Cu(I) complex. The oxygen lobes swell as an additional thiosulfate ligand is added in the PM3 derived EPC maps of the $[Cu(S_2O_3)_2]^{3-}$ and $[Cu(S_2O_3)_3]^{5-}$ complexes (Figure 2.17). No out-of-plane regions of favourable cationic interaction were observed when these models were rotated around the axis.

The lower charge of the polythionates was evident in the EPC maps (Figure 2.18). The projected lobes at the oxygen atoms in the tetrathionate anion were less intense than those of the metal complexes, and were smaller again in trithionate and thiosulfate. The S-O bond lengths of the polythionates (Table 2.10) were also shorter than those of the metal complexes (Tables 2.9 and 2.10) by corresponding methods.

The sulfide (-S-) sulfur atoms of these anions, particularly thiosulfate, were more attractive to a cation than those in the metal complexes. Basic IEX principles predict that the anions with higher charge {Au(I) and Cu(I) bis(thiosulfate) complexes} will interact more favourably than the sulfoxy dianions. However, polythionates are found in leach solutions at concentrations much greater than the gold (eg. 10 mM trithionate vs. 0.1 mM Au) and significantly suppress gold loading on IEX resins[30].

It is likely that the cationic IEX moieties of the resin will interact with the broader lobes at the oxygen atoms of the metal-thiosulfate complexes, and the oxygen and sulfide sulfur atoms of the polythionates. The flexibility of all these anions also allows for both ends of the molecule to interact with a cation, whereas the metal complexes are more rigid along the S-M^{+}-S axis. The $[Cu(S_2O_3)_2]^{3-}$ complex may bind more effectively in the proposed tetrahedral form, due to the lower S-M^{+}-S angle. A lower angle is also found in the $[Cu(S_2O_3)_3]^{5-}$ complex.

The relative flexibility of multiply charged nature of the anions of interest, and the presence of the favourable cation-interaction regions at the S-O lobes, suggests that a favourable IEX moiety may be multiply charged (eg. 2+ or even 3+). This may be achieved by exhaustive quaternisation of bis- and tris-amine precursors.

Some modification of the strength of the IEX interactions may also be achieved through steric hindrance around the cationic IEX sites. Bulky ammonium substituents should diminish the advantages of both smaller and more flexible anions. This may be improve selectivity for aurothiosulfate over the polythionates, but not versus cuprothiosulfates. However, the loading of copper onto strong-base IEX resins may be minimised by careful management of the leach liquor to minimise the abundance of the tris-thiosulfate complexes (ie. low $[S_2O_3]^{2-}$, and to slow the formation of polythionates (ie. low $[O_2]$ and $[Cu^{2+}]$).

References:

1. Cotton, F.A. and Wilkinson, G., *Advanced Inorganic Chemistry*, 5th.edition; John Wiley & Sons (New York), 1988.
2. Adams, M.D., Johns, M.W., and Dew, D.W., "Recovery of gold from ores and environmental aspects", *Gold: Progress in Chemistry, Biochemistry and Technology,* (Section 3); H. Schmidbaur, Editor. John Wiley & Sons Ltd. (Chichester), 1999.
3. Sherrington, D.C. and Hodge, P., Eds. *Synthesis and Separations using Functional Polymers*, 1st edition; John Wiley & Sons (Chichester), 1988.
4. Dicinoski, G.W., *Syntheses of anion exchange resins selective for gold and silver cyanide complexes*, 437 pp.; Department of Chemistry; Central Queensland University (Rockhampton, Queensland, Australia), 1995.
5. Szonyi, A. and Cambon, A., "New synthetic strategy to vesicle-forming perfluoroalkylated amphiphiles". *New. J. Chem.*, **17**: 425-434; 1993.
6. March, J., *Advanced Organic Chemistry*, 4th edition; John Wiley & Sons (New York), 1992.
7. Cope, A.C. and Trumbull, E.R., "Olefins from amines", *Organic Reactions*, (Chapter 5); A.C. Cope, Editor. John Wiley & Sons (New York), 1960.
8. Kaiser, C. and Weinstock, J., "Alkenes via Hofmann elimination: use of ion-exchange resin for preparation of quaternary ammonium hyroxides: diphenylmethyl vinyl ether"; *Organic Syntheses*, **VI**: 552-555; 1976.
9. Cope, A.C. and Bach, R.D., "*trans*-Cyclooctene". *Organic Syntheses*, **V**: 314-320; 1969.
10. Sommer, H.Z., Lipp, H.I., and Jackson, L.L., "Alkylation of amines. a general exhaustive alkylation method for the synthesis of quaternary ammonium compounds."; *J. Org. Chem.*, **36**(6): 824-828; 1971.

11. Sommer, H.Z. and Jackson, L.L., "Alkylation of amines. a new method for the synthesis of quaternary ammonium compounds from primary and secondary amines."; *J. Org. Chem.*, **35**(5): 1558-1562; 1969.

12. Kerwin, J.F., Hall, G.C., Macko, Edward, McLean, R.A., Fellows, E.J., Ullyot, G.E., "Adrenergic blocking agents. IV. B-haloethylammonium compounds"; *J. Am. Chem. Soc.*, **73** (December); 5681-5686; 1951.

13. Virnig, M.J. and Sierakoski, J.M., "Ammonium thiosulfate complex of gold or silver and an amine."; *US Patent 6 197 214*, Henkel Corporation, 2001.

14. Smith, R.M. and Martell, A.E., *Critical Stability Constants. Volume 4: Inorganic Ligands*; Plenum Press (London); 1976.

15. *Lange's Handbook of Chemistry*; Dean, J.A., Editor; 14th edition; McGraw-Hill Inc. (New York), 1992.

16. Xu, S., Otto, F.D., and Mather, A.E., "Dissociation constants of some alkanolamines"; *Canadian Journal of Chemistry*, **71**(7): 1048-1050; 1992.

17. *pKa* Software (versions 4.56 - 7.02), ACD/I-Lab service; Advanced Chemical Development, Inc. (Toronto, Canada), 2001. <www.acdlabs.com>

18. Goldann, K., Kirstahler, A., and Damm, H., "Quaternary ammonium compounds (hexahydrotriazines)"; *German Patent Index (Deutsches Patentamt),* (DE 1086709); Henkel & Cie G.m.b.H., 1960.

19. *ChemWatch* (edition 1, 2002), ChemWatch Inc. (Caulfield North, Victoria, Australia), 2002. <www.chemwatch.com.au>

20. *HyperChem* (version 5.11 Pro*)*, Hypercube Inc. (Gainesville, USA), 1996.

21. *MEDUSA* (version 25; March 1998); Puigdomenech, I., Department of Inorganic Chemistry, Royal Institute of Technology, Stockholm, Sweden; 1998. <http://www.inorg.kth.se>

22. *HYDRA*, (Student Version 10, based on CEC software written by Mingsheng Wang and Mamoun Muhammed); Puigdomenech, I. and Zagorodni, A., Department of Inorganic Chemistry, Royal Institute of Technology: (Stockholm, Sweden), 1998. <http://www.inorg.kth.se>

23. *SPARTAN* (version 5.03 x11); Wavefunction, Inc. (Irvine, CA, USA), 1997.

24. *Gaussian 03*, (revision B.03); Frisch, M.J., Trucks, G.W., et al.; Gaussian Inc. (Pittsburgh, PA, USA.), 2003.

25. Ruben, H., Zalkin, A., Faltens, M. O., Templeton, D.H., "Crystal structure of sodium gold(I) thiosulfate dihydrate, $Na_3[Au(S_2O_3)_2].2H_2O$"; *Inorg. Chem.*, **13**(8): 1836-1839; 1974.

26. Chan, E.J., Skelton, B.W., and White, A.H., "Complex coinage metal (I) thiosulfates". *Acta. Cryst.*, **A58** (Supplement): C130; 2002.

27. White, A.H.; and Chan, E.J.; Unpublished Results; Department of Chemistry, University of Western Australia (Perth, W.A.), 2004.

28. Chun, H., Jackson, W.G., McKeon, J.A., Somoza, F.B.(Jr.), Bernal, I., "The interaction between amminehalocobalt(III) cations and polythionate anions. Hydrogen-bonding patterns and S-S bond cleavage reactions". *Eur. J. Inorg. Chem.*, **1**: 189 - 193; 2000.

29. Bernal, I., Cetrullo, J., and Jackson, W.G., "The phenomenon of conglomerate crystallisation. 24. Spontaneous resolution in coordination compounds". *Inorg. Chem.*, **32**: 4098 - 4101; 1993.

30. Ji, J., Fleming, C., West-Sells, P.G., Hackl, R.P., "A novel thiosulfate system for leaching gold without the use of copper and ammonia". in *Hydrometallurgy 2003 - 5th International Conference*, Vol. 1 (Leaching and Solution Purification); TMS, 2003. pp. 227-244.

3. Synthesis and Analysis of Novel Anion Exchange Resins

A wide variety of functionalised resins have been prepared using the exhaustively chloromethylated macroporous polystyrene substrate denoted A378 (*Rohm & Haas* Duolite A378). A more detailed description and analysis of this material is given in Section 3.1.10. To permit some characterisation of the effect of this particular substrate upon the degree of functionalisation and sorption kinetics, one functionality (N-methylmorpholine, NMM) was prepared on both A378 base and also the exhaustively chloromethylated macroporous resin D2780 (*Purolite*).

Each product in this research has been given a unique code for identification. These codes consist of a three letter abbreviation of the functional group, and a batch number. In cases where a synthesis has been repeated, even using identical conditions, the new product has been given a new batch number. Each batch has been assessed separately in terms of functional group concentration (capacity). This allows for variations of capacity between batches, and also reveals degradation processes which may occur over time.

The functional groups were covalently anchored to the polymer matrix by the mono-alkylation reactions of 1°, 2° or 3° - amine compounds with the *p*-chloromethyl groups (-CH_2Cl) of the substrate(s). The attachment of primary and secondary amine reagents will produce weak base (amine) resins, whereas alkylation involving tertiary amine starting materials produces strong base (quaternary ammonium) resins. The latter may also be produced by subsequent treatment of weak base resins with alkylating agents, such as the alkyl halides iodomethane and benzyl chloride. Accordingly, the resin syntheses reported herein are divided into three categories:

- Initial Strong Base Resins (3°-amine starting materials) *Section 3.3*
- Weak Base Resins (1° or 2°- amine starting materials) *Section 3.4*
- Alkylated Resins (derivatives of the products above) *Section 3.5*

Resin syntheses are detailed individually in Sections 3.3 – 3.5. Each such synthesis is denoted by the name of the reagent to be affixed to the chloromethyl sites of the precursor. This avoids confusion in naming the resulting weak base (amine) and strong base (quaternary ammonium) compounds, and serves as a reminder of possible side reactions. Unexpected and/or unwanted nitrogen-bearing functionalities may form by processes such as oxidation, crosslinking, or elimination of alkyl groups, and these may contribute to the effective IEX capacity, or even function as chelating groups.

The synthetic procedure that was generally followed (see Section 3.1.2) was primarily intended to achieve a high degree of functionalisation. Dimethylformamide was chosen as solvent due to the following reasons (in order of priority):

(1) Many amine compounds are highly soluble in DMF

(2) S_N2 reactions are very fast in DMF [1].

(3) Crosslinked polystyrene swells well in DMF [2]

(4) Low volatility (bp. 153°C)

(5) Relatively low toxicity

(6) Non-flammable

Where DMF could not be used, the selection of solvent was based on those used in prior literature, following the above criteria. Other suitable solvents include chloroform, tetrahydrofuran, and the glyme solvents (polyethylene glycol alkyl ethers).

Air has also been excluded from these reactions to minimise the formation of N-oxides and other oxidative side reactions. There has been no significant attempt in any of these preparations to maximise the degree of apparent or effective functionalisation, minimise thermal or oxidative degradation processes, or to prevent morphological changes of the substrate such as loss of porosity. Product optimisation procedures such as these are beyond the scope of this project, and lie within the realm of a pilot-plant scale study. The intention of this project was to evaluate the efficacy of each moiety for the recovery of gold – that is, to determine gold sorption per mol of resin functionality.

Materials used and prepared have been characterised by appropriate methods, including infra-red (IR) spectroscopy, carbon-13 (^{13}C) NMR spectroscopy, mass-transfer ion exchange (IEX) analysis, combustive elemental analysis, acid-base titration, swelling in water, and competitive adsorption of gold from a standard artificial ammoniacal thiosulfate liquor. These gold adsorption studies will be provided and discussed in Chapter 4. The analytical results for each resin are given immediately following the synthetic procedure. The general procedures used for these analyses are described in Sections 3.1.1 – 3.1.10.

Finally, the resin products have been compared to several commercially available anion-exchange resins of both Type I (trialkylammonium groups) and Type II (hydroxyalkylammonium groups). The resins examined were:

- **Dowex-1** (*Dow Chemicals*), a Type I (alkylamine) strong base Gel-matrix resin bearing 3.5 meq/g trimethylammonium groups and a water content of 46%. The backbone contains 8% crosslinking reagent, while the particle size of the batch was 100-200 mesh (75-150 μm).

- **Amberlite IRA-410** (*Rohm & Haas*), a Type II (2-hydroxyalkylamine) strong base Gel-matrix resin bearing 3.4 meq/g dimethylethanolammonium groups. The water content was 42%, while the particle size of was 50-100 mesh (150-300 μm).
- **Amberlite A26** *(Rohm & Haas)*, a Type I strong base resin, with 4.2 meq/g quaternary ammonium groups and a water content of 69% in hydroxide form. The particle size of this macroreticular material was 16-45 mesh (355-1180 μm).

The A26 resin has a large size range, and was examined as supplied, while a sieved fraction (> 850 μm) was also studied. This permits comparison of the capacity and efficacy of the new materials produced herein with current commercial products being tested for this application. In particular, the large size fraction of the A26 sample was expected to show comparable kinetics to the big-bead A378 and D2780 substrates. It should also be noted that the novel resins prepared in this work have not been optimised for application to hydrometallurgical recovery processes. These materials cannot be expected to achieve commercial viability without considerable further development. In particular, the IEX capacities of the novel resins prepared herein are generally lower than those found in most commercial IEX resins. The resins of commerce generally have small functional groups, permitting relatively high IEX capacity per unit mass. The synthesis and stability of commercial IEX resins has also generally been optimised. Multi-step resin preparations are not common in industry.

The kinetics of gold adsorption in the new resins may be adversely affected by changes in the porosity or hydrophobicity of the substrate. Similarly, the effects of osmotic shock, resin fouling, and degradation of the functional group and matrix over time have not been investigated in this project due to time constraints.

3.1 Methods and Reagents:

High purity nitrogen gas (*BOC Gases*) was passed through columns of Drierite (4-mesh, *Aldrich*) and KOH pellets (LR, *Ajax*). All chemicals used were of AR quality, and glass-distilled de-ionised water (Millipore *milli-Q*, conductivity < 18 μSiemens) was used throughout, unless otherwise specified.

Abbreviations used in this work:

Arom.	Aromatic
^{13}C-NMR	Carbon 13 Nuclear Magnetic Resonance Spectrometry
DCM	Dichloromethane
DGDE	Diethylene glycol diethyl ether
Dien(Sal)$_2$	Diethylenetriamine N,N''-bis(salicylidene)
DMF	N,N-Dimethylformamide
DMSO	Dimethyl sulfoxide
EA	Elemental Analysis
EtOH	Ethanol
^{1}H-NMR	Proton Nuclear Magnetic Resonance Spectrometry
IC	Ion Chromatography
IEX	Ion Exchange
IR	Infra-Red (Spectra)
LSIMS	Liquid Secondary Ion Mass Spectra
MCPBA	*m*-Chloroperoxybenzoic acid
PDR	Persulfate Digestion Reagent

Ph.	Phenyl
PS	Polystyrene
PTFE	Poly(tetrafluoroethylene) (*Teflon*)
SS	Solid State (NMR)
TBT	1,3,5-Tribenzylhexahydro-1,3,5-triazine
TET	1,3,5-Triethylhexahydro-1,3,5-triazine
THF	Tetrahydrofuran
TLC	Thin layer Chromatography
TMEDA	Tetramethylethylenediamine *[N,N,N',N'-tetramethyl-1,2-diaminoethane]*
TPY	2,4,6-tris(2-pyridyl)-1,3,5-triazine

3.1.1 Solvent Purification

Chloroform: The solvent was left to stand over excess anhydrous granular $CaCl_2$ (LR, *BDH*) for two weeks, and then decanted and filtered to remove the solids. The solvent was then heated in a one-piece still with quartz boiling chips until ~75% was distilled. This distillate was stored in a sealed brown bottle until required.

Diethyl Ether: A batch of ether (500 mL) was refluxed over sodium wire under dry nitrogen gas for several hours to remove impurities and peroxides. The clear distillate was sealed in a glass bottle and stored in the absence of light.

Dimethylformamide: DMF (99.5, *Riedel de Häen*) for reactions and washing was initially distilled at 40-60°C using a rotary evaporator (*Büchi* Rotavapor R-114) fitted to a PTFE-lined vacuum pump (*Büchi* V-500). This was stored over 4Å molecular sieves that had been dried in vacuo for several hours at 200°C. Subsequent experiments employed clear, colourless DMF directly from fresh bottles.

Ethanol: In a typical preparation, a batch of sodium wire (~ 10 g) was placed in ethanol (300 mL; 99%) and allowed to react completely before gentle distillation under a blanket of dry nitrogen. Approximately 250 mL of anhydrous ethanol was collected.

Methanol: For use in the Soxhlet extraction of the A378 substrate, this solvent was distilled from a long path (45 cm x 2 cm) Vigreaux still. In all other applications, AR grade methanol (99 %) was used without further purification.

Tetrahydrofuran: A batch of THF (300 mL) was taken from a fresh bottle (99%, *Waters*) and refluxed over sodium wire under dry nitrogen gas for several hours to remove impurities and peroxides. Approximately 200 mL of clear distillate was subsequently collected for use in the Soxhlet extraction apparatus.

3.1.2 General Resin Synthesis Procedure

Functionalisation: The dry resin substrate (usually 10-20 mL) was decanted from a measuring cylinder into a clean, dry Schott bottle containing a small PTFE-coated magnetic stirrer bar. The reagent was then added at once under a stream of dry nitrogen, and the residue washed in with solvent (usually DMF, 50-80 mL in total). The plastic cap (with a maximum tolerance of 140°C) was securely screwed on, and the flask placed in an oil bath and magnetically stirred as the oil temperature was increased to 100°C (± 5°C). The magnetic stirrer bar did not keep the resin suspended, but merely agitated and turned over the mixture. The reactions were generally conducted for 3-7 days before allowing the flask to cool and isolating the resin products.

Washing Procedure: After reaction, the cooled reaction mixture was filtered through a porosity #3 sintered glass funnel. The residue and remaining beads were rinsed into the funnel with a small quantity of reaction solvent (eg. 2 x 10 mL DMF). Suction was applied to the funnel, and the resin allowed to drain for several minutes.

The polymer beads were then slurried with clean solvent (~ 25 mL per 20 mL resin) and allowed to stand on the frit for 10-15 minutes before suction was applied again. This was repeated twice, and the same procedure was then repeated using 2-3 batches of DCM. A third solvent wash was usually conducted using 2-3 batches of methanol, and much of this solvent was subsequently removed by suction on the frit for ~30 minutes. The remainder of the solvent was stripped from the resin by placing the products in a vacuum oven (~5 mm Hg) at 40°C for at least two hours.

Washing was sometimes varied by introducing one or more aqueous wash steps to remove water soluble by-products or impurities, or to condition the resin groups into a known ionic form. These details are supplied following each resin preparation.

Resin Conditioning: Resins were generally converted to their freebase form (1° - 3° amines), or hydroxide or chloride form (ammonium salts). For a resin bearing strong and weak base groups (ie. 1° - 3° amine *and* quaternary ammonium moieties), the resin was usually first washed with strong base to deprotonate the weak ammonium groups prior to exchanging the strong base counterions with chloride.

The procedure for conversion of a weak-base resin from a protonated (ammonium) form to the free base was the same as that for forcing strong-base resins into hydroxide form. This was usually conducted by treating the resin with 1-2 batches of aqueous NaOH (~ 1 M, 2-3 bed volumes) over 30 minutes. Resins treated in this fashion were rinsed several times with water (2-3 bed volumes), allowing 15 minutes per rinse step to allow diffusion of residual base from the matrix.

To convert the resins to the chloride form, each resin was treated with 2-3 batches of strong sodium chloride solution (~ 1 M, 2-3 bed volumes) and left to stand for 15 minutes per batch to facilitate diffusion and permit the mass-transfer driven exchange of hydroxyl and other anions with the abundant chloride anions.

3.1.3 Pulverisation of Products

Anhydrous samples of polymer materials were pulverised in a stainless steel vessel attached to a *Retsch* MM200 Ball Mill, using stainless steel ball bearings. Anhydrous powders prepared in this fashion were placed in dry stoppered vials and held in a P_2O_5-charged desiccator.

3.1.4 InfraRed Analysis

Analytical reagent quality KBr was finely ground, oven-dried at 120°C overnight, and stored in a desiccator over P_2O_5. A small quantity of this material (ca. 100-200 mg) was ground with finely powdered resin (ca. 2-4 mg) in a clean, dry agate mortar and pestle, and then pressed under 10 tons in a steel die to produce IR plates (10 mm diameter and ~ 0.5 mm thick). The peaks in each spectrum have been reported in wavenumbers ($\bar{\nu}$, cm^{-1}), with the strongest peaks denoted (s) and weak peaks denoted (w).

The structural features thought to be responsible for a given IR peak have been assigned where possible. In this context, the abbreviations *str.* (stretch) and *def.* (deformation) will be used. These assignments were made with an estimated variance of ± 3 cm^{-1}, which may exclude some overlapped peaks. The peaks associated with the backbone polymer (A378) have been omitted for clarity. Some IR bands characteristic of the new functional sites may be lost in this subtraction.

3.1.5 Solid State Carbon-13 NMR

The ^{13}C-NMR spectra were generally obtained using pulverised resins in freebase form (1° - 3° amines) and/or chloride form (ammonium salts) respectively, or in mixed form where the functional group bears both strong- and weak-base moieties.

The spectra were obtained using a *Varian-Inova* 400 MHz Wide Bore instrument fitted with a *Doty Scientific* DSIV-187 Cross-Polarisation Magic-Angle Spinning (CP-MAS) supersonic probe. The samples were placed in a silicon nitride sample holder spinning at 12-16 KHz and data was recorded using the *xpolar1* sequence using *tppm2* waveform programmed decoupling, with a contact time of 2.5 seconds and a relaxation delay of 4.00 seconds. The peaks were assigned relative to the methyl carbon peak of the external standard, hexamethylbenzene. The important peaks are reported in ppm (parts per million). It should be noted that the broad peaks (~ 5-10 ppm) are caused by the variety of differently shielded environments within the resin, and cannot be avoided. Peaks have been assigned based on predicative spectra derived from the ^{13}C-NMR modelling package *CNMR Viewer* (v. 5.12) by ACD Labs [3].

3.1.6 Elemental Analysis

3.1.6.1 Parr Bomb

Initially, elemental analysis was performed by combustion of a powdered sample of resin in an oxygen-charged Parr Bomb, and the resulting liquor was analysed by IC for nitrate and chloride [4]. The performance of the bomb was investigated using standards of triethylbenzylammonium chloride (99%), tridodecylmethylammonium chloride (98%), and powdered samples of the polymers Dowex-1 and IRA-410. Combustion experiments were conducted in platinum or silica crucibles on anhydrous materials, both in a pure state and in combination with the recommended combustion aids, benzoic acid (50-80% w/w) or decalin (tetrahydronapthalene; 25-90% w/w).

The procedure adopted was as follows: A small quantity of aqueous sodium carbonate solution (5-10 mL, 5 % w/v) was placed in a corrosion resistant bomb (*Parr Instrument Company* 1108-Cl Combustion Bomb) prior to combustion to trap the acidic

gases evolved during combustion. The bomb was fitted with a nickel-chrome or platinum fuse wire. The sample was weighed into a crucible of platinum or silica, and combined with combustion aid when required. Samples (ca. 0.1 – 0.5 g) were analysed as powders or slurried with decalin. For solid samples, the fuse was touching the top of the sample; in liquid samples, ~5 mm of cotton was suspended from the wire into the liquid. After securing the lid, the bomb was flushed twice with oxygen (5 and 20 bar) and chilled in an ice bath. The bomb was charged to 30-35 bar with oxygen, ignited, and left to stand for 5 minutes. After gentle depressurisation, the solution was washed from the bomb with water, filtered through a plug of glass wool to remove soot and fragments of the ignition wire, and the final solution pH measured. Blank determinations were obtained by performing the procedure in the absence of sample.

The liquors were diluted and analysed by IC, using a *Dionex* IC instrument consisting of an AS550 Autosampler, GP50 Gradient Pump, LC30 Column Oven, EG40 Eluent Generator, ASRS-Ultra Eluent Suppressor and CD25 Conductivity Detector, and controlled by a PC running *PeakNet* (version 6.30 SP1). This was fitted with *Dionex* analytical AS-11 and AG-11 guard columns, utilising an isocratic hydroxide eluent (6.0 mM) at a flow rate of 1.0 mL/minute with subsequent eluent suppression and conductivity detection. This was initially compared to standards of sodium nitrate, sodium nitrite and sodium chloride (0.5 - 2.5 mM). The results obtained via this procedure will be discussed in Section 3.6.1.5.

3.1.6.2 Oxidation Bomb

An alternative method for analysis of total nitrogen was to digest a powdered sample in aqueous persulfate solution in a high-pressure PTFE lined bomb at elevated temperature (110 – 150° C) [5, 6]. The procedure employed was as follows: Sodium hydroxide (0.4500 g, 11.3 mmol) was made to 200.0 mL with water. A 20.0 mL aliquot of this solution was added to a batch of potassium persulfate ($K_2S_2O_8$; 1.001 g, 3.701 mmol) and stirred with gentle heating until the solids dissolved. This solution was denoted "Persulfate Digestion Reagent" (PDR).

A sample of vacuum-dried pulverised resin (DST1; NaOH form; 0.1000 g) was weighed into the PTFE vessel (~ 50 mL capacity). The PDR reagent (6.0 mL) was added to the vessel, which was swirled to mix the reagents. The vessel was closed tightly and placed in an oven at 110°C for four hours. This was allowed to cool for 48 hours, and then carefully opened in a fume hood. The contents consisted of a yellow slurry beneath a yellowish solution, with an appearance similar to the starting material. Repetition of this procedure brought a similar result.

Neither of the above techniques was found to be fully effective when applied to the polymer samples produced in this work. Subsequently, all Elemental Analyses (EA) reported were performed on anhydrous powdered samples (1 - 2 mg) by the Central Science Laboratory (CSL) at the University of Tasmania, using a *Carlo-Erba* CHNS Elemental Analysis Instrument (employing dynamic flash combustion [7]).

3.1.7 Ion Exchange Analysis

The procedure used to determine the effective ion-exchange capacity of a functionalised resin was adapted from that described in the PhD thesis of Dr. Greg Dicinoski [8].

IEX Analysis Procedure: A weighed sample of each anhydrous polymer (ca. 1.000 g) was stirred in water (~ 50 mL) for 15 minutes, then loaded into an IEX column (~ 25 mL capacity, ~ 10 mm diameter) with a porosity #3 sintered glass frit at the bottom. The resin was conditioned with NaCl solution (1.0 M, pH 10.00) by passing 50.0 mL through the column at a flow rate of 1.0 mL/min. The column was then washed extensively with aqueous NaOH (0.1 mM, pH 10.00, 150 – 300 mL) at a flow rate of 1.0 mL/min until no chloride was detected in the effluent.

The columns bearing the polymer beads in chloride form were then eluted with sodium nitrate solution (1.0 M, pH 10.00, 50.0 mL each at 1.0 mL/min). The effluent from this step was collected and made up to 100.0 mL. Finally, the resin was quickly flushed with weak NaOH solution (0.1 mM, < 10.0 mL, 5.0 mL/min) and returned to the first step of the process. The nitrate effluent liquors were then analysed (initially by Ion Chromatography, using the same method used to analyse the Parr Bomb combustion liquor, and later by a Chloride Ion Selective Electrode) and calibrated against a set of standard chloride solutions at pH 10. The results of the Ion-Exchange capacity tests are collected in Table 3.3 (Section 3.6.1.6).

Test for Chloride: The absence of chloride in the effluent was confirmed by using the following colorimetric test: Three drops of yellow chromate solution were added to ca. 20 mL of the effluent, and silver nitrate solution was added dropwise until a red colour appeared. The absence of chloride was indicated when three or fewer drops of silver nitrate solution produced a persistent red precipitate in the effluent.

The two reagent solutions were prepared as follows:

Chromate Indicator: Anhydrous sodium chromate (Na_2CrO_4; 98%; 0.1448 g, 0.89 mmol) was made to 20.0 mL with water, giving a yellow solution (44.5 mM) which was stored in a brown glass bottle.

Silver Nitrate solution: Silver nitrate was dried in an oven at 116°C for one hour, and a sample weighed out (1.6996 g; 10.00 mmol) and made up to 100.0 mL with water. This yielded a solution containing 0.100 M $AgNO_3$, which was stored in a brown glass bottle to protect the light-sensitive reagent.

3.1.8 Titration of Functionalised Polymers

An autotitrator (*Metrohm* Dosimat E535) with a chart recorder (Potentiograph E536) was used for resin capacity and pk_a determination. An inexpensive silver/silver chloride pH meter was connected, and calibrated at pH values of 4.0, 7.0 and 10.0 using commercial buffer solutions (*BDH*).

A pre-weighed sample of the resin (~ 1.000 g) was conditioned by rinsing with excess NaOH solution (~ 1 M , ≥ 50 mL at 1.0 mL/min). The resin was then flushed thoroughly with water (≥ 100 mL at 2.0 mL/min) until the flush liquor was neutral to phenolphthalein, then dried by suction. This batch of resin was placed in the titration vessel with 10.0 mL of standardised NaOH (ca. 0.1 mM). .

Stock NaOH solution (1.000 M) was produced by diluting a standardised ConVol ampoule to one litre. Dilute sodium hydroxide solutions (0.100 M) were prepared by dilution of the stock solution, and titrated in triplicate against oven-dried potassium hydrogen phthalate (ca. 0.20 g). Solutions of HCl were prepared by diluting ~11 mL of concentrated aqueous HCl to 1000 mL, and then standardised in triplicate against sodium tetraborate decahydrate (Borax, ca. 0.20 g). These concentrations were confirmed by titration of an aliquot of the dilute NaOH solution (10 mL) with the standardised acid, with the endpoint determined with a pH electrode (pH = 7). The data was treated with the pK_a deconvolution program PKAS [9], to determine weak acid pK_a values. The results are discussed in Section 3.6.1.7.

3.1.9 Resin Swelling in Water

The resin density was obtained by weighing a well settled volume of anhydrous resin (2.00 mL). This sample was allowed to stand in water (10 mL) for 1 hour, and then settled again and measured in the same vessel.

3.1.10 Analytical Data for Precursor and Commercial Resins

3.1.10.1 Duolite A378

This material is a fully chloromethylated macroporous polystyrene (PS) substrate crosslinked with 8% divinylbenzene (DVB) produced by *Rohm & Haas* for *Mintek* (South Africa). This beads were of a large average particle size (> 850 μm), with very few particles below 500 μm. A 10 mL sample of the anhydrous resin weighed approximately 5.5 g.

A batch of this material (~220 mL, denoted A378-A) was placed in a Soxhlet extraction thimble and washed continuously with distilled methanol for 24 hours. The solvent was removed on a Rotary Evaporator with a vacuum pump to leave ~1.5 grams of residue, a mixture of pale solids and yellowish oil of unknown composition. Subsequent batches of A378 resin were used without any solvent washing.

^{13}C-NMR (SS: CP-MAS): δ (ppm) = 42 (**C**H_2**C**HAr); 48 (**C**H_2Cl); 130 (Arom.).

IR (KBr plate): $\bar{\nu}$ (cm^{-1}) = 3415 (broad; adsorbed H_2O); 3023 (Arom. CH str.); 2920 (s) & 2850 (CH_2 str.); 1611, 1510 & 1492 (w) (1,4-Arom. C-C str.); 1444 & 1420 (CH_2 def.); 1383 (CH str.); 1264 (s) (CH_2Cl def); 1212 & 1182 (w) (CH_2 wag); 1109 & 1018 (1,4-Arom. in-plane CH def.); 823 (s) (1,4-Arom CH rock.); 746 (CH_2Cl rock); 701 & 672 (s) (Arom. out-of-plane CH def.); 549.

Four samples of the A378 chloromethylated polystyrene substrate were combusted in a Parr Bomb under oxygen and were found to contain an average

4.90 meq/g Cl (± 0.40 meq/g) and a negligible level of nitrogen (< 0.20 %). In comparison, commercial elemental analysis yielded the following breakdown: Carbon (73.22 %); Hydrogen (6.62 %); Nitrogen (0.24 %); Other (19.92 %). Assuming that the 'other' component is 100% chlorine, this corresponds to a capacity of 5.62 meq/g of *p*-chloromethylated polystyrene groups. The difference in the two values for chlorine content determined above is probably due to incomplete combustion in the Parr Bomb, resulting in a diminished recovery of chloride by that technique.

The elemental compositions of *p*-chloromethylstyrene (CMS) and *p*-divinylbenzene (DVB) are shown below in Table 3.1. The A378 material fits reasonably well with the calculated values for a composition of 9% *p*-divinylbenzene.

Table 3.1 Calculated composition of *p*-chloromethylated polystyrene

Substance	**% Carbon**	**% Hydrogen**	**% Chlorine**
p-chloromethylstyrene (CMS)	70.83	5.94	23.23
p-divinylbenzene (DVB)	92.26	7.74	0
A378	73.22	6.62	19.92
91% CMS + 9% DVB	72.76	6.10	21.14

3.1.10.2 D2780

This exhaustively chloromethylated macroporous polystyrene matrix was prepared by *Purolite* (UK). Elemental analysis confirms that this substrate contains 20 - 22 % chlorine (w/w), with a particle size range 500-900 μm The batch used in this research was washed with methanol in a Soxhlet apparatus in the manner described in Section 3.1.10.1. This substrate was used only for the preparation of the NMM2 resin.

3.2 Synthesis and Characterisation of Reagents

3.2.1 Methylation of 1,3,5-triethylhexahydro-1,3,5-triazine (TET)

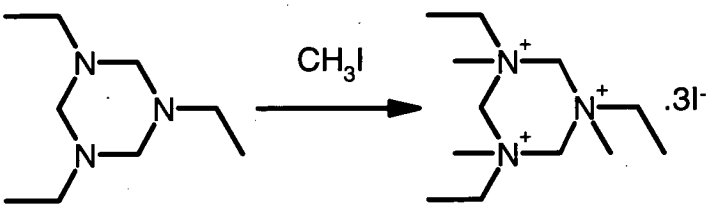

Figure 3.2.1 · Methylation of 1,3,5-triethylhexahydro-1,3,5-triazine

A sample of TET (1.029 g, 6.01 mmol) was dissolved in DCM (15 mL) in a round-bottomed flask fitted with a reflux condenser, with stirring under dry nitrogen gas. The solution was cooled to 0°C in an ice bath, and iodomethane (2.746 g, 19.3 mmol) added dropwise with stirring over 10 minutes, washing in the residue with DCM (15 mL). The mixture was stirred for a further hour, and then warmed to a gentle reflux for 1 hour, followed by heavy refluxing for a further 30 minutes. After cooling, the solvent and excess iodomethane were removed on a vacuum line at 20-45°C over 3 hours, leaving a pale yellow tar (2.508 g; < 67% theoretical yield).

^{1}H-NMR (TET; $CDCl_3$): δ (ppm) = 1.08 (triplet; 9H; J_H = 7.2 Hz); 2.49 (quartet; 6H; J_H = 7.3 Hz); 3.35 (broad multiplet, 6H).

^{1}H-NMR (TMT; $CDCl_3$ + 2 drops d^6-DMSO): 1.2 (m; 3.19H); 1.3 (m; 9H); 2.6 (m + s, 2.83H); 2.89 (s; 2.81H); 3.03 (quartet; 3.48H); 3.3 (m + s; 6.51H); 3.5 (1.74H); 3.65 (broad m; 5.17H); 4.42 (0.86H); 5.40 (DCM); 8.7 (broad m; 1.88H; *HCO*).

Electrospray MS: This technique was selected as the most appropriate for detection of polycationic species. Direct flow analysis of a sample dissolved in water gave the following major mass peaks: M/Z = 595.7; 466.7; 408.7; 338.2; 281.2; 170.0.

3.2.2 Preparation of diethylenetriamine N,N''-bis(salicylidene) [*Dien(Sal)$_2$*]

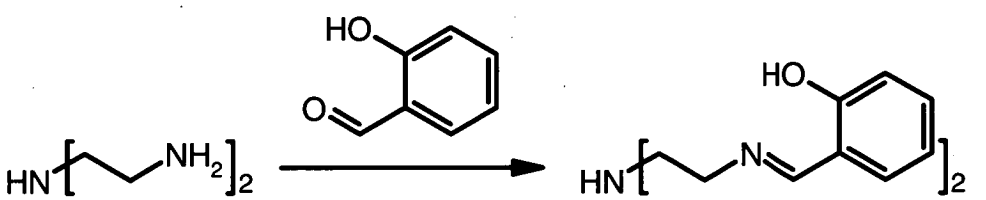

Figure 3.2.2 Reaction of diethylenetriamine and salicylaldehyde

This reagent was prepared according the method of Coleman & Taylor [10]. Salicylaldehyde (25.055 g, 205.2 mmol) was dissolved in absolute ethanol (200 mL), and diethylenetriamine (10.572 g, 102.5 mmol) dissolved in absolute ethanol (50 mL) was added dropwise over 30 minutes. The mixture became very warm (~60°C), and was left to stir for 30 minutes as it slowly cooled to room temperature (~18°C) below a $CaCl_2$ tube. The ethanol was then removed on a rotary evaporator, and the viscous yellow *Dien(Sal)$_2$* product (~32g, ca. 100%) was used shortly after preparation.

IR (KBr plate): $\bar{\nu}$ (cm^{-1}) = 3320 (NH str.), 3052 (w) (1,2-H-bonded OH str.), 3028 (Arom. CH str.), 2928 & 2844 (w) (CH str.), 1628 (s) (C=N str.), 1580, 1497 (1,2-Arom. C-C str.), 1461 (CH bend), 1337 (C-O str.), 1278 (s) (C-O str.), 1211 (C-N str.), 1150 (1,2-Arom. CH def.), 1044 (w) (1,2-Arom. CH def.), 973, 894, 856 (NH wag), 756 (s) (1,2-Arom. CH def.), 464.

3.2.3 Exhaustive Benzylation of Piperazine (TEBAZ)

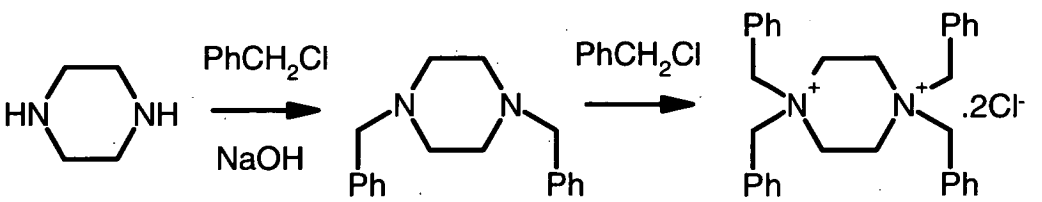

Figure 3.2.3 Stepwise Benzylation of Piperazine

3.2.3.1 Alkylation of Piperazine

A 250 mL round-bottomed flask containing a PTFE magnetic stirrer bar was placed in an oil bath and fitted with a condenser. Piperazine hexahydrate (20.2767 g, 104 mmol) was washed into the flask with DMF (50 mL) and allowed to dissolve. This was followed by tributylamine (38.1850 g, 206 mmol) also dissolved in DMF (50 mL). Finally, benzyl chloride (57.5035 g, 454 mmol) dissolved in DMF (50 mL) was rapidly added. This was left to stir overnight at room temperature, and then heated to 92°C for 19 hours. The cooled brown solution was mixed with acetone (50 mL) for 5 minutes, producing abundant white precipitate. The mixture was filtered via a porosity #3 sintered glass funnel and the solids were rinsed with acetone (2 x 50 mL). The combined filtrate was stirred with another aliquot of acetone (50 mL), and cooled in an ice-bath. A second crop of crystals was obtained, which were also washed with acetone (2 x 50 mL). The combined filtrates were reduced in volume to ~150 mL by rotary evaporation, followed by the addition of acetone (75 mL), and the mixture left to cool in a fume hood overnight. A small third crop of crystals was recovered by filtration and rinsed with acetone (2 x 25 mL). A sample was taken of each of crop of crystals and denoted **TEBAZ** crops 1, 2 and 3.

Solubility tests were conducted on samples of crop 1 (~ 20 mg) in small flasks with ~1 mL each of a range of different solvents: chloroform, DCM, DMSO, ethanol, methanol, THF and water.

The three crops were combined and stirred with a solution containing 6% DMF in acetone (250 mL) for 1 hour, warming gently to ~40°C. The mixture was immediately filtered on a porosity #3 sintered glass funnel, and washed with acetone (2 x 50 mL). The solid white product was placed in a round-bottomed flask and dried on a vacuum line for ~2 hours, leaving 7.876 g of anhydrous powder (**TEBAZ** Crop 4).

^{1}H-NMR (TEBAZ Crop 2; $CDCl_3$): δ (ppm) = 2.31 (s, 1H); 3.4 (broad m; 43.8H); 4.3 (broad m, 2.75H); 7.4 (broad, 15.9H)

LSIMS (TEBAZ Crop 4; glycerol): M/Z = 134.1 (8%); 177 (23%); 267.1 (100%)

3.2.3.2 Conversion of TEBAZ to Free Base

A solution of NaOH (AR, 4.0612 g, 102 mmol) was prepared in Milli-Q water (50 mL) in a 250 mL round-bottomed flask fitted with a reflux condenser. The TEBAZ salt prepared above was slurried with water (50 mL) and added to the caustic solution with vigorous stirring. A large volume of white precipitate formed over 30 minutes, after which DCM (50 mL) was added. The flocculate rapidly dissolved, and after 10 minutes stirring two clear liquid phases were apparent. The lower layer was separated and the aqueous layer further washed with aliquots of DCM (2 x 50 mL). The organic layers were combined and dried overnight on $CaCl_2$, filtered over calcium sulfate, and the DCM distilled to yield 5.891 g of white crystalline N,N'-dibenzylpiperazine.

3.2.3.3 Alkylation of N,N'-dibenzylpiperazine

The N,N'-dibenzylpiperazine prepared above (Section 3.2.3.2) (5.8913 g, 22.12 mmol) was slurried in DMF (50 mL) and washed into a 100 mL round-bottomed flask with additional DMF (15 mL). The mixture was magnetically stirred and heated to 45°C under dry nitrogen and a condenser, dissolving the solids. A solution of benzyl chloride (12.632 g, 101 mmol) in DMF (15 mL) was placed in a pressure-equalising dropping funnel, and added to the reaction mixture dropwise over 15 minutes. This mixture was left to stir ~70 hours at 50°C, then heated to 95°C for 4 hours. After cooling, the pinkish slurry was washed into a clean rotavap flask with DMF (3 x 15 mL) and acetone (AR, 50 mL), and the solvent removed. The residue was dried on a vacuum line for 40 minutes, leaving a yellow solid (11.8898 g) contaminated with traces of benzyl chloride. The product was shaken with 3 x 50 mL ethyl acetate, and isolated on a porosity #3 sintered glass filter. The solid product that resulted (**TEBAZ**-5) was dried on a vacuum line for 2 hours at 40°C, leaving 7.5993g of white powder. A sample of this final product was analysed by LSIMS.

LSIMS (TEBAZ-2; glycerol): M/Z = 226.1 (53%); 267.2 (39%); 357.2 (100%).

3.3 *Synthesis and Characterisation of Simple Strong-Base Resins*

3.3.1 Tributylamine (ABU)

Figure 3.3.1 Reaction of resin A378 with tributylamine

Tributylamine (7.845 g, 42.3 mmol) was dissolved in 50.0 mL of distilled DMF and added to a 100 mL Schott flask containing A378 resin (10 mL, 6.194 g). The flask was then sealed, shaken, and heated to 110°C (± 5°C) on an oil bath for 130 hours with occasional shaking. The beads were filtered off and washed successively with methanol (2 x 50 mL), water (4 x 100 mL), aqueous KOH solution (0.2 M, 250 mL) and then water (4 x 100 mL), leaving ~20 mL of swollen yellow beads (**ABU1**).

EA: Carbon (74.42 %); Hydrogen (12.20 %); Nitrogen (2.87 %); Other (8.02 %).

{Calculated for 2.05 meq/g tributylammonium hydroxide:

Carbon (77.46 %); Hydrogen (9.94 %); Nitrogen (2.87 %); Other (9.73 %)}.

^{13}C-NMR (SS: CP-MAS): δ (ppm) = 15 (3 x **C**H_3); 21 (3 x **C**H_2); 26 (3 x **C**H_2); 42 (*PS*); 61 (3 x **C**H_2 + **C**H_2*PS*); 129 (*PS*).

Predicted ^{13}C-NMR: 14 (3 x **C**H_3); 20 (3 x **C**H_2); 24 (3 x **C**H_2); 62 (3 x **C**H_2N^+); 66 (**C**H_2Ph); 129 – 133 (Arom.).

IR (KBr plate): $\bar{\nu}$ (cm^{-1}) = 3425 (H_2O str.); 2960 (CH_3 str.); 2930 & 2873 (CH_3 + CH_2 str.); 1702; 1452 (s) (CH_2 def.); 1379 (CH_3 def); 1276 & 1216 (CH_2 wag); 1176 (C-N str.); 859.

3.3.2 Triphenylamine (**APH**)

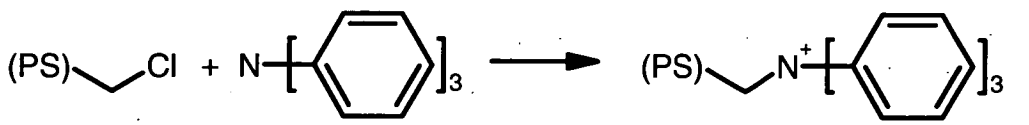

Figure 3.3.2 Reaction of resin A378 with triphenylamine

A solution of triphenylamine (9.287 g, 37.9 mmol) in distilled DMF (50 mL) was added to a 100 mL Schott flask containing A378-A (10 mL, 5.592 g). The flask was then sealed, shaken, and heated to 110°C (± 5°C) on an oil bath for 130 hours with occasional shaking. The green solution was filtered off and the polymer washed with methanol (2 x 50 mL), water (50 mL), diethyl ether (6 x 30 mL), THF (2 x 50 mL), and finally water (2 x 50 mL). The chloride counter-ions were removed by washing with a KOH solution (0.2 M, 250 mL) and then water (4 x 100 mL), leaving pale yellowish beads (**APH1**, ~10 mL).

EA: Carbon (74.83 %); Hydrogen (6.74 %); Nitrogen (0.28 %); Other (18.15 %).

{Calculated for 0.20 meq/g triphenylammonium hydroxide:

Carbon (73.33 %); Hydrogen (6.64 %); Nitrogen (0.28 %); Other (19.76 %)}.

IR (KBr plate): $\bar{\nu}$ (cm^{-1}) = 3419 (H_2O str.); 1362; 1093 (Arom. CH bend).

This spectrum appeared to be very similar to that of the original substrate.

3.3.3 1,3,5-Triethylhexahydro-1,3,5-triazine (**TET**)

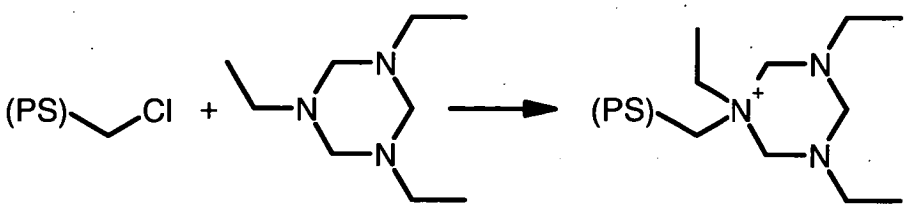

Figure 3.3.3 Reaction of A378 with 1,3,5-triethylhexahydro-1,3,5-triazine

3.3.3.1 Preparation 1

A sample of TET (6.748 g, 39.4 mmol) was dissolved in distilled DMF (50 mL) and added to a 100 mL Schott flask containing A378-A (10 mL, 5.687 g, 32.0 mmol Cl) and a small PTFE-coated magnetic stirrer bar. The flask was then sealed, shaken, and heated to 110°C (± 3°C) on an oil bath with magnetic stirring for 139 hours. After being allowed to cool to room temperature, the mixture was filtered using a porosity #3 sintered glass funnel to isolate the polymer beads, which were subsequently washed with DMF (50 mL), methanol (3 x 50 mL), water (3 x 150 mL), aqueous KOH (0.1 M, 250 mL) and finally with water (3 x 150 mL). A small sample (~1 mL) of the yellow polymer product (**TET1**, ~15 mL total) was taken, dried on a vacuum line and pulverised for subsequent analyses.

EA: Carbon (83.25 %); Hydrogen (8.62 %); Nitrogen (5.52 %); Other (2.61 %).

{Calculated for 1.31 meq/g 1,3,5-triethylhexahydro-1,3,5-triazine hydroxide: Carbon (72.74 %); Hydrogen (8.15 %); Nitrogen (5.52 %); Other (13.60 %)}.

^{13}C-NMR (SS: CP-MAS): δ (ppm) = 11 (3 x **C**H_3); 39 (*PS*); 43 (2 x **C**H_2CH$_3$); 60 (**C**H_2CH$_3$ + **C**H_2*PS*); 126-135 (PS).

Predicted ^{13}C-NMR: 9 ($\mathbf{C}H_3$); 11 (2 x $\mathbf{C}H_3$); 44 (2 x $\mathbf{C}H_2CH_3$); 55 ($\mathbf{C}H_2CH_3$); 62 ($\mathbf{C}H_2Ph$); 72 ($\mathbf{C}H_2N$); 79 (2 x $\mathbf{C}H_2N$); 129 – 132 (Arom.)

IR (KBr plate): $\bar{\nu}$ (cm^{-1}) = 3418 (H_2O str.); 2966 (CH_3 str.); 2925 & 2856 (CH_2 str.); 2786; 1684; 1606 (Arom. C-C str.); 1452 (s) (CH_2 def.); 1364 (CH_3 def.); 1308 (w); 1282 (w); 1216 & 1172 (C-N str.); 1134 (w); 1095 (C-N str.); 1042 (w); 811 (s) (1,4-Arom. CH def.); 760 (w) (CH_2 rock).

3.3.3.2 Preparation 2

A fresh sample of solvent-washed A378 resin (10 mL, 5.371 g) was swollen overnight in DMF (25 mL) in a sealed flask with a small magnetic stirrer bar. This was then combined with a solution of TET (6.521 g, 38 mmol) in DMF (25 mL). After stirring for 64 hours at room temperature, the flask was placed in an oil bath and heated to 110°C (± 3°C) for 174 hours.

After cooling, the reaction mixture was vacuum filtered on a porosity #3 sintered glass funnel, and then slowly washed with DMF (50 mL), methanol (3 x 50 mL), and water (3 x 100 mL). The yellow beads that resulted were conditioned with HCl (0.5 M; 4 x 125 mL), and rinsed with water (3 x 200 mL). Finally, the resin was solvent washed with methanol (3 x 25 mL), then DCM (3 x 25 mL). After allowing most of the residual DCM to evaporate, the sample was dried on a vacuum line at 60°C for ~2 hours. This anhydrous sample was stored in a desiccator as **TET2** (~15 mL).

EA: Carbon (72.24 %); Hydrogen (8.33 %); Nitrogen (4.86 %); Other (14.57 %).

{Calculated for 1.16 meq/g 1,3,5-triethylhexahydro-1,3,5-triazine chloride: Carbon (71.30 %); Hydrogen (7.71 %); Nitrogen (4.86 %); Other (16.13 %)}

IR (KBr plate): $\bar{\nu}$ (cm^{-1}) = 3419 (H_2O str.); 2924 (CH_2 str.); 2665; 1452 (s) (CH_2 def.); 1425 (CH_3 def.); 1217, 1192 & 1105 (w) (C-N str.); 1039 (w); 765 (w) (CH_2 rock).

3.3.3.3 Preparation 3

In a 100 mL Schott flask, washed A378 resin (20 mL) was combined with TET (6.769 g, 40 mmol) and DMF (50 mL). The lid was secured, the flask shaken, and placed in an oil bath and heated to 100°C (± 3°C) with stirring. The mixture was maintained at this temperature for 48 hours, then cooled and filtered, and washed with DMF (2 x 50 mL), DCM (3 x 30 mL), methanol (2 x 50 mL) and water (5 x 50 mL). The orange-pink resin, **TET3** (~40 mL) was stored wet in a 50 mL plastic (PS) vial.

IR (KBr plate): $\bar{\nu}$ (cm^{-1}) = 3447 (H_2O str.); 2925 (CH_2 str.); 1636; 1452 (CH_2 def.); 1218, 1189 & 1096 (w) (C-N str.); 763 (w) (CH_2 rock); 555.

3.3.4 1-Piperidineethanol (**PET**)

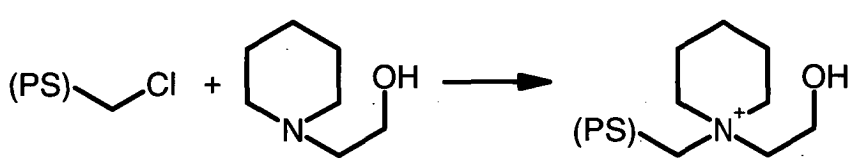

Figure 3.3.4 Reaction of A378 with 1-piperidineethanol

3.3.4.1 Preparation 1

To a batch of anhydrous A378 beads (10 mL, 5.320 g) in a 100 mL Schott flask was added a solution of 1-piperidineethanol (N-(2-hydroxyethyl)piperidine) (4.536 g, 35.1 mmol) in DMF (50 mL). A small magnetic stirrer bar was added, and the reaction vessel sealed and heated to 105°C (± 2°C) in an oil bath, with magnetic stirring, for 190

hours. The red-brown mixture was allowed to cool, then vacuum filtered on a porosity #3 sintered glass funnel. The resin was washed with DMF (2 x 50 mL), methanol (2 x 50 mL), water (2 x 200 mL), aqueous NaOH (~1 M, 5 x 100 mL), and finally water (5 x 200 mL). This left approximately 25 mL of large yellow beads (denoted **PET1**). A sample was dried on a vacuum line at 50°C for 2 hours and pulverised in a ball mill.

EA: Carbon (70.64 %); Hydrogen (8.81 %); Nitrogen (4.07 %); Other (16.48 %).

{Calculated for 2.90 meq/g N-(2-hydroxyethyl)piperidinium hydroxide:

Carbon (74.05 %); Hydrogen (9.07 %); Nitrogen (4.07 %); Other (12.81 %)}

^{13}C-NMR (SS: CP-MAS): δ (ppm) = 16 (3 x **C**H_2); 36 (*PS*); 48 (CH_2OH); 51 (**C**H_2*PS*); 59 (**C**$H_2C H_2$OH + 2 x **C**H_2); 122 (PS).

Predicted ^{13}C-NMR: 21 (3 x **C**H_2); 57 (**C**H_2OH); 63 (**C**H_2*PS*); 64 (2 x **C**H_2); 65 (**C**$H_2C H_2$OH); 128 – 133 (Arom.)

IR (KBr plate): $\bar{\nu}$ (cm^{-1}) = 3334 (OH str.), 2933 (s) & 2871(CH_2 str.); 1454 (s) (CH_2 def.); 1427 & 1365 (OH coupled CH_2 wag); 1219 & 1193 (CH_2 wag); 1095; 1050 (C-O str.); 931 (w); 914 (w); 854; 767 (w) (CH_2 rock); 606.

3.3.4.2 Preparation 2

A sample of A378 resin (50 mL) was swollen for 1 hour in DMF (100 mL) in a round-bottomed 500 mL flask whilst sparging with dry N_2 gas. The slurry was stirred mechanically via a PTFE paddle on a glass arm passing through a reflux condenser. The reagent 1-piperidineethanol (34.7101 g, 268.7 mmol) was added in one portion and washed in with DMF (150 mL). The mixture was heated to 95-100°C, with mechanical stirring, for 69 hours. After cooling, the resin was filtered on a porosity #3 sintered glass funnel and washed with DMF (2 x 50 mL) and left to stand for 30 minutes in DCM (2 x 60 mL). The resin was further washed with methanol (2 x 60 mL) before air drying

with suction over the sintered glass filter funnel. The resulting polymer beads (~100 mL) were stored in a 120 mL plastic vial and denoted **PET2**.

IR (KBr plate): $\bar{\nu}$ (cm^{-1}) = 3367, 2933 (CH_2 str.); 1662; 1454 (s) (CH_2 def.); 1427 & 1364 (OH coupled CH_2 wag); 1219 & 1193 (CH_2 wag); 1095; 1050 (C-O str.); 934 (w); 914 (w); 855; 766 (w) (CH_2 rock); 606; 554.

3.3.5 Trioctylamine (**TOA**)

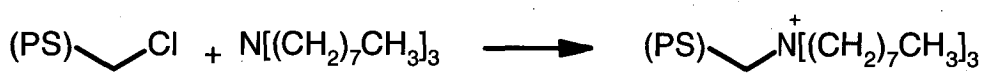

Figure 3.3.5 Reaction of A378 with trioctylamine

3.3.5.1 Preparation 1

To a batch of anhydrous A378 beads (10 mL, 5.645 g) was added trioctylamine (12.115 g, 34.3 mmol). The amine was washed in with DMF (50 mL), which was found to be immiscible with trioctylamine. The upper layer (trioctylamine) was separated and recovered, and the beads were dried on a rotary evaporator for 2 hours to strip off the DMF. After solubility testing, diethylene glycol diethyl ether (DGDE) was selected as a suitable solvent. Thus, the recovered trioctylamine was added as a solution in DGDE (50 mL), and the reaction vessel was flushed with dry nitrogen before adding a small magnetic stirrer bar. The reaction vessel was then sealed and heated to 105°C (± 2°C) in an oil bath with stirring for 190 hours. The pale yellow mixture was allowed to cool, then filtered on a porosity #3 sintered glass funnel with suction. The resin was washed with DGDE (2 x 50 mL), methanol (2 x 50 mL), water (2 x 200 mL), aqueous KOH (ca. 1 M, 5 x 100 mL), and finally water (5 x 200 mL). This left approximately 25 mL

of pale beads, denoted **TOA1**. A sample was dried on a vacuum line at 50°C for 2 hours, and pulverised in a ball mill for elemental analysis.

EA: Carbon (76.17 %); Hydrogen (7.46 %); Nitrogen (0.59 %); Other (15.78 %).

{Calculated for 0.42 meq/g trioctylammonium hydroxide:

Carbon (74.34 %); Hydrogen (7.42 %); Nitrogen (0.59 %); Other (17.64 %)}

IR (KBr plate): $\bar{\nu}$ (cm^{-1}) = 3420 (H_2O str.); 1700; 1450 (s) (CH_2 def.); 1360; 1095 (C-N str.).

3.3.5.2 Preparation 2

To a 100 mL round-bottomed flask containing A378 resin (10 mL) was added a solution of trioctylamine (8.392 g, 23.7 mmol) in THF (60 mL). A reflux condenser was fitted to the flask, and the mixture was heated in an oil bath at ~80°C, with magnetic stirring. A vigorous reflux was established, and maintained for 26 hours. The cooled yellow-orange mixture was filtered and the resin beads washed with THF (2 x 30 mL), DCM (2 x 25 mL) and methanol (2 x 30 mL). After drying on a vacuum line for two hours, the product (denoted **TOA2**, ~10 mL) was stored in a desiccator.

IR (KBr plate): $\bar{\nu}$ (cm^{-1}) = 3375 (H_2O str.); 1700; 1370.

Due to the negligible IEX capacity of this material (0.25 meq/g, see Table 3.3), this resin was not examined further.

3.3.6 1,3,5-Tribenzylhexahydro-1,3,5-triazine (**TBT**)

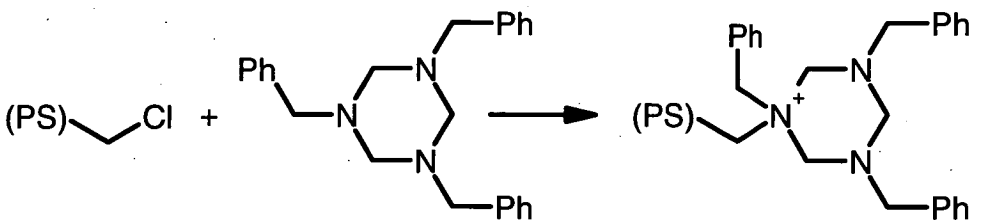

Figure 3.3.6 Reaction of A378 with 1,3,5-tribenzylhexahydro-1,3,5-triazine

3.3.6.1 Preparation 1

A solution of 1,3,5-tribenzylhexahydro-1,3,5-triazine (4.868 g) in DMF (50 mL) was added to a small batch of anhydrous A378 beads (5 mL, 2.813 g) in a Schott flask. A small magnetic stirrer bar was added, and the reaction vessel was sealed and heated to 106°C (± 2°C) in an oil bath, with stirring, for 144 hours. The resulting tan-brown suspension of beads was allowed to cool to room temperature, then vacuum-filtered on a porosity #3 sintered glass funnel, leaving rich brown beads in the funnel and a rust-coloured filtrate. The beads were washed twice more with DMF (3 x 50 mL), then methanol (2 x 60 mL), and then aqueous KOH (~0.5 M, 3 x 150 mL). Finally, the light tan beads were washed extensively with water (5 x 200 mL). The product was dried on a vacuum line for 2 hours, and denoted **TBT1** (~10 mL, OH^- form).

EA: Carbon (81.74 %); Hydrogen (7.87 %); Nitrogen (4.62 %); Other (5.77 %).

{Calculated for 1.10 meq/g 1,3,5-tribenzylhexahydro-1,3,5-triazinium hydroxide: Carbon (77.47 %); Hydrogen (7.23 %); Nitrogen (4.62 %); Other (10.68 %)}

^{13}C-NMR (SS: CP-MAS): δ (ppm) = 41 (*PS*); 61 (**C**H_2*PS* + 3 x **C**H_2Ph); 76 (**C**H_2N); 81 (2 x **C**H_2N); 128 – 135 (Arom.).

Predicted ^{13}C-NMR: 57 (2 x **C**H_2Ph); 64 (2 x **C**H_2Ph); 75 (**C**H_2N); 83 (2 x **C**H_2N); 127 – 137 (Arom.)

IR (KBr plate): $\bar{\nu}$ (cm^{-1}) = 3400 (H_2O str.); 2785 (w) (CH_2 str.); 1674 (s); 1605 (Arom. C-C str.); 1452 (s) (CH_2 def.); 1365; 1308 (w) & 1106 (C-N str.); 977(w).

3.3.6.2 Preparation 2

To a batch of dry A378 chloromethylated polystyrene resin (20 mL) swollen in DMF (50 mL) was added 1,3,5-tribenzylhexahydro-1,3,5-triazine (10.453 g, 29.24 mmol). The reaction vessel was flushed with dry nitrogen and a magnetic stirrer bar added. The Schott flask was then closed tightly, then placed in an oil bath and heated to 100°C for 168.5 hours. After cooling, the reaction mixture was filtered on a porosity #3 sintered glass funnel, and the dark red beads washed with DMF (3 x 50 mL), DCM (3 x 50 mL), methanol (3 x 50 mL), water (2 x 100 mL), aqueous NaOH (1.0 M, 3 x 100 mL), water (4 x 100 mL), and finally with methanol (2 x 40 mL). After drying in a vacuum oven at 60°C for 2 hours, the khaki resin (denoted **TBT2**, ~20 mL, OH^- form) was stored in a desiccator.

EA: Carbon (78.36 %); Hydrogen (6.99 %); Nitrogen (3.69 %); Other (10.96 %).
{Calculated for 0.88 meq/g 1,3,5-tribenzylhexahydro-1,3,5-triazinium hydroxide: Carbon (76.57 %); Hydrogen (7.10 %); Nitrogen (3.69 %); Other (12.63 %)}

IR (KBr plate): $\bar{\nu}$ (cm^{-1}) = 3394 (H_2O str.); 1674 (s); 1605 (Arom. C-C str.); 1477 & 1452 (s) (CH_2 def.); 1371; 1308 (w) (C-N str.); 1270; 1101 (C-N str.).

3.3.6.3 Preparation 3

In a 100 mL Schott flask, washed A378 resin (20 mL) was combined with 1,3,5-tribenzylhexahydro-1,3,5-triazine (11.080 g, 31 mmol) and DMF (50 mL). The lid was secured, the flask shaken, and placed in an oil bath and heated to 100°C with stirring. This reaction mixture rapidly became a purple-brown colour, and was left to stir at 100°C for 48 hours, then cooled, filtered, and washed with DMF (2 x 50 mL), DCM (3 x 30 mL), methanol (2 x 50 mL) and water (5 x 50 mL). This yielded the deep purple resin **TBT3** (~40 mL) which was stored wet in a ~ 50 mL plastic vial.

IR (KBr plate): $\bar{\nu}$ (cm^{-1}) = 3409 (H_2O str.); 2704; 1674; 1453 (s) (CH_2 def.); 1379 (w); 1312 & 1083 (w) (C-N str.); 914 (w); 853; 555.

3.3.7 N-methylpiperidine (**NMP**)

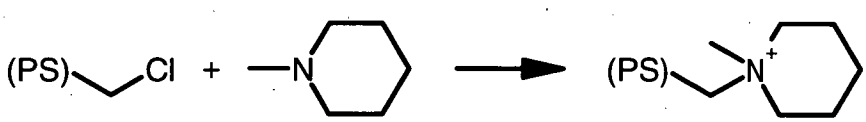

Figure 3.3.7 Reaction of A378 with N-methylpiperidine

A batch of anhydrous A378 resin (10 mL; 5.358 g) was swollen in DMF (25 mL). A sample of N-methylpiperidine (4.062 g, 40.96 mmol) was dissolved in DMF (25 mL) and the solution added to the reaction vessel, which was then flushed with dry nitrogen before being sealed tightly. The mixture was heated to 110°C in an oil bath for 168 hours whilst being agitated gently. After allowing the mixture to cool, the resin beads were rinsed onto a porosity #3 sintered glass filter with DMF (50 mL). The DMF was removed by suction, and the brown cloudy liquor discarded. The tan-brown beads

were slowly rinsed with: DCM (2 x 50 mL), methanol (2 x 50 mL, then 2 x 10 mL), water (2 x 100 mL), HCl (0.5 M aqueous, 50 mL, then 2 x 100 mL), and finally with water (3 x 100 mL). The resin (denoted **NMP1**, ~25 mL) was stored in the Cl^- form.

A sample (~10 mL) was taken and wet-loaded into a glass fritted column (10 x 150 mm) with a porosity #3 sintered glass frit and teflon tap at the base. The column was slowly flushed with NaOH (1.0 M, 500 mL at 5 mL/minute using a peristaltic pump) to convert the resin into the hydroxide form. After thoroughly flushing with water (100 mL over 20 minutes), the filtered resin was dried in vacuo at 60°C for 2 hours. A sample of the dry beads was pulverised for later analysis, and the dry beads and powder were stored in a desiccator over P_2O_5.

EA: Carbon (71.60 %); Hydrogen (8.93 %); Nitrogen (4.43 %); Other (15.04 %).

{Calculated for 3.16 meq/g N-methylpiperidinium hydroxide:

Carbon (77.15 %); Hydrogen (9.28 %); Nitrogen (4.43 %); Other (9.15 %)}

^{13}C-NMR (SS: CP-MAS): δ (ppm) = 17 (3 x $\mathbf{C}H_2$); 36 – 40 (*PS*); 55 ($N^+\mathbf{C}H_3$); 64 (2 x $\mathbf{C}H_2$ + $\mathbf{C}H_2$*PS*); 123 (Arom.).

Predicted ^{13}C-NMR: 20 (2 x $\mathbf{C}H_2$); 21 ($\mathbf{C}H_2$); 50($N^+\mathbf{C}H_3$); 65 (2 x $\mathbf{C}H_2$); 68 ($\mathbf{C}H_2$Ph); 126 – 134 (Arom.)

IR (KBr plate): $\bar{\nu}$ (cm^{-1}) = 3416 (H_2O str.); 2930 (s) (CH_3 str.); 1473 (s) (CH_3 def.); 1453 (s) (CH_2 def.); 1358 (CH_3 def.); 1273 (w) & 1221 (CH_2 wag); 1077 (w); 1028 (1,4-Arom. CH def.); 936; 881 (s) (1,4-Arom. CH def.); 860; 814; 762 (w) (CH_2 rock); 611 (w); 563.

3.3.8 N-methylmorpholine (NMM)

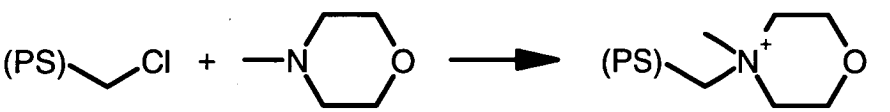

Figure 3.3.8 Reaction of A378 with N-methylmorpholine

3.3.8.1 Preparation 1

A batch of anhydrous A378 resin (10 mL; 5.486 g) was weighed, and swollen in DMF (25 mL). A sample of N-methylmorpholine (4.753 g, 46.99 mmol) was added along with DMF (25 mL). The reaction vessel was flushed with dry nitrogen before being sealed and heated to 110°C in an oil bath with gentle agitation for 168 hours. After allowing the mixture to cool, the resin beads were rinsed onto porosity #3 sintered glass filter funnel with DMF (50 mL). The DMF was removed by suction, and the yellow liquor discarded. The yellow-tan beads were slowly rinsed with: DCM (2 x 50 mL), methanol (2 x 50 mL, then 2 x 10 mL), water (2 x 100 mL), aqueous HCl (0.5 M; 50 mL, then 2 x 100 mL) and finally with water (3 x 100 mL). The resin was denoted **NMM1** (25 mL, Cl^- form).

A sample (~10 mL) was taken, washed into an IEX column (10 x 150 mm, with a porosity #3 sintered glass frit and teflon tap at the base) and eluted with NaOH (1.0 M, 500 mL at 5 mL/minute) in order to convert it into the OH^- form. After thoroughly flushing with water (100 mL over 20 minutes) followed by vacuum filtration, the resin was dried in vacuo at 60°C for 2 hours and stored in a desiccator.

EA: Carbon (67.48 %); Hydrogen (8.14 %); Nitrogen (4.25 %); Other (20.13 %).

{Calculated for 3.03 meq/g N-methylmorpholinium hydroxide:

Carbon (73.08 %); Hydrogen (8.54 %); Nitrogen (4.25 %); Other (14.14 %)}

^{13}C-NMR (SS: CP-MAS): δ (ppm) = 37 – 40 (*PS*); 57 (**C**H_3); 65 (4 x **C**H_2 + **C**H_2*PS*); 123 (Arom.).

Predicted ^{13}C-NMR: 50 (**C**H_3); 62 (2 x **C**H_2); 63 (2 x **C**H_2); 68 (**C**H_2Ph); 126 - 134 (Arom.)

IR (KBr plate): $\bar{\nu}$ (cm^{-1}) = 3383 (H_2O str.); 2883 (CH_3 str.); 1476 (s) (CH_3 def.); 1453 (s) (CH_2 def.); 1362 (CH_3 def.); 1235 (w) (CH_2 wag); 1124 (s) (ether str.); 1063; 964 (w); 890 (s) (1,4-Arom. CH def.); 857; 571.

3.3.8.2 Preparation 2

Purolite D2780 Matrix: A sample of *Purolite* D2780 resin (10 mL) was swollen in DMF (50 mL) whilst sparging with dry N_2 gas for 10 minutes in a Schott flask (100 mL). N-methylmorpholine (9.740 g, 96.3 mmol, ~3x molar excess) was added and washed in with DMF (10 mL). The cap was secured and the flask placed in an oil bath at 100°C with stirring.

After 69 hours, the reaction mixture was cooled, the resin was recovered and washed with DMF (3 x 20 mL), DCM (2 x 25 mL), and methanol (3 x 25 mL). The resin was then wet-loaded into an IEX column (as previously employed in Section 3.3.8.1), washed with water (~250 mL) and methanol (~100 mL), and dried on a vacuum line. The pale yellow product was denoted **NMM2** (~20 mL, Cl^- form).

IR (KBr plate): $\bar{\nu}$ (cm^{-1}) = 3413 (H_2O str.); 1476 (CH_3 def.); 1453 (s) (CH_2 def.); 1425 (s) & 1361 (CH_3 def.); 1286 & 1234 (w) (CH_2 wag); 1191; 1124 (s) (ether str.); 1083; 1064; 993 (w); 964 (w); 889 (s) (1,4-Arom. CH def.); 856; 826; 622; 558.

3.3.8.3 Preparation 3

N-methylmorpholine (10.7569 g, 106.3 mmol) was dissolved in DMF (60 mL), combined with A378 resin (20 mL) in a Schott flask flushed with dry nitrogen, and heated to 100°C for 72 hours with stirring. The product was filtered from the brown liquor using a porosity #3 sintered glass filter, then washed with DMF (2 x 50 mL), DCM (50 mL) and methanol (3 x 40 mL), and dried in a vacuum oven at 40°C for 2 hours. The resin was denoted (**NMM3**) (~40 mL, Cl^- form).

IR (KBr plate): $\bar{\nu}$ (cm^{-1}) = 3450 (H_2O str.); 2884 (CH_3 str.); 1659; 1476 (s) (CH_3 def.); 1453 (CH_2 def.); 1425 & 1361 (CH_3 def.); 1304 (w); 1285 (w) &1235 (CH_2 wag); 1192 (w); 1124 (s) (ether str.); 1063; 994; 964 (w); 889 (s) (1,4-Arom. CH def.); 856; 826; 764 (w) (CH_2 rock); 622; 556.

3.3.9 N,N,N',N'-tetramethylethylenediamine (**TME**)

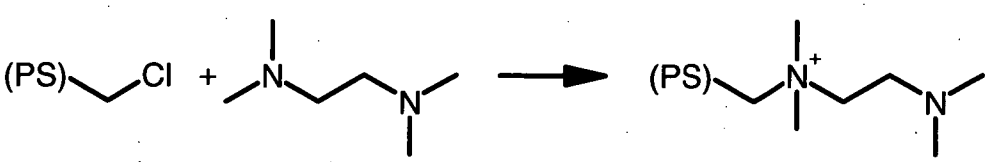

Figure 3.3.9 Reaction of A378 with N,N,N',N'-tetramethylethylenediamine

3.3.9.1 Preparation 1

A batch of anhydrous A378 resin (10 mL) was swollen in DMF (25 mL). A sample of TMEDA (6.410 g, 55.16 mmol) was washed in with DMF (25 mL) and the reaction vessel was flushed with dry nitrogen before sealing. The reaction mixture was heated to 110°C in an oil bath for 168 hours whilst being slowly agitated. After allowing the mixture to cool, the resin beads were rinsed onto a porosity #3 sintered

glass filter funnel with DMF (50 mL). The DMF was removed by suction, and the brown cloudy liquor discarded. The tan-brown beads were slowly rinsed with: DCM (2 x 50 mL), methanol (2 x 50 mL, then 2 x 10 mL), water (2 x 100 mL), aqueous HCl (0.5 M, 50 mL then 2 x 100 mL) and finally with water (3 x 100 mL). The resin was denoted **TME1** (~20 mL, Cl^- form).

A sample (~10 mL) was taken and washed into an IEX column (10 x 150 mm, with a porosity #3 sintered glass frit and teflon tap at the base), then eluted with NaOH (1.0 M, 500 mL at 5 mL/minute) to convert it into the OH^- form. After thoroughly flushing with water (100 mL over 20 minutes) and being recovered by filtration, the resin was dried in vacuo at 60°C for 2 hours. A sample of the dry beads was pulverised for later analysis, and the dry beads and powder were stored in a desiccator.

EA: Carbon (76.36 %); Hydrogen (9.32 %); Nitrogen (7.04 %); Other (7.28 %). {Calc. for 2.51 meq/g N,N,N',N'-tetramethyl-1,2-ethylenediammonium hydroxide: Carbon (73.34 %); Hydrogen (9.23 %); Nitrogen (7.04 %); Other (10.39 %)}

^{13}C-NMR (SS: CP-MAS): δ (ppm) = 41 (*PS*); 45 (2 x **C**H_3N); 54 (2 x **C**H_3N^+ + **C**H_2N); 65 (**C**H_2N^+); 70 (**C**H_2*PS*); 130 (Arom.).

Predicted ^{13}C-NMR: 44 (2 x **C**H_3N); 51 (2 x **C**H_3N^+); 54 (**C**H_2N); 60 (**C**H_2N^+); 67 (**C**H_2Ph); 129 – 134 (Arom.)

IR (KBr plate): $\bar{\nu}$ (cm^{-1}) = 3416 (H_2O str.); 2925 & 2857 (CH_2 def.); 2600; 2466; 1477 (s) (CH_2 def.); 1425 (w) (CH_3 def.); 1220, 1190 & 1114 (w) (C-N str.); 973 (w); 859 (CH_3 rock); 764 (w) (CH_2 rock); 557.

3.3.9.2 Preparation 2

A batch of anhydrous A378 resin (10 mL) was swollen in DMF (25 mL). A sample of TMEDA (6.580 g, 56.62 mmol) in DMF (25 mL) was added and the reaction

vessel flushed with dry nitrogen before being sealed. The mixture was heated at 100°C in an oil bath for 168 hours whilst being gently agitated, then allowed to cool to room temperature. The resin beads were separated on a porosity #3 sintered glass filter and washed with fresh DMF (2 x 50 mL), DCM (2 x 50 mL), methanol (3 x 50 mL), water (2 x 100 mL), aqueous NaOH (1.0 M; 3 x 100 mL), and finally with water (100 mL). The polymer was further washed by placing it in an IEX column (as employed in Section 3.3.9.1) and flushing it with 500 mL water at 5 mL/minute. The beads were rinsed with methanol (50 mL) and suction-dried prior to drying in a vacuum oven at 60°C for 2 hours. The anhydrous pale yellow resin that resulted was denoted **TME2** (~15 mL, OH^- form), and was stored in a desiccator.

EA: Carbon (74.05 %); Hydrogen (8.84 %); Nitrogen (6.93 %); Other (10.18 %). {Calc. for 2.47 meq/g N,N,N',N'-tetramethyl-1,2-ethylenediammonium hydroxide: Carbon (73.34 %); Hydrogen (9.19 %); Nitrogen (6.93 %); Other (10.55 %)}

IR (KBr plate): $\bar{\nu}$ (cm^{-1}) = 3424 (H_2O str.); 2777 (w); 1641; 1454 (s) (CH_2 def.); 1371 (CH_3 def.); 1219 (w) & 1100 (C-N str.); 856 (CH_3 rock); 763 (w) (CH_2 rock).

3.3.9.3 Preparation 3

A sample of A378-A resin (50 mL) was swollen for 30 minutes in distilled DMF (200 mL) in a round-bottomed 500 mL flask whilst sparging with dry N_2 gas. The slurry was stirred mechanically, via a PTFE paddle on a glass shaft passing through a condenser and attached to a RW-20 overhead stirrer (*IKA Labortechnik*). The reagent, TMEDA (16.6612 g, 143 mmol), was added and washed in with DMF (50 mL), and the mixture heated to 95-100°C, with stirring, for 48 hours. After cooling, the resin was filtered on a glass frit and washed with DMF (4 x 50 mL) and left to stand overnight in DCM (~50 mL), then washed with methanol (2 x 50 mL). The resin was washed with

aqueous NaOH (~3 M, 250 mL) to deprotonate the weak base groups, then with NaCl (1.0 M, 3 x 150 mL). The resin was finally washed with water (2 x 300 mL) and methanol (2 x 50 mL) before air drying with suction. The resulting ~100 mL of polymer beads were denoted **TME3**, and were stored in a plastic (PS) vial.

IR (KBr plate): $\bar{\nu}$ (cm^{-1}) = 3419; 2925 (CH_2 str.); 2784 (w); 1480 (s) (CH_2 def.); 1425 (w) & 1383 (CH_3 def.); 1221, 1191& 1102 (w) (C-N str.); 999; 858 (CH_3 rock); 828 (1,4-Arom. CH def.); 764 (w) (CH_2 rock); 705.

3.3.10 2,4,6-Tris(2-pyridyl)-1,3,5-triazine (**TPY**)

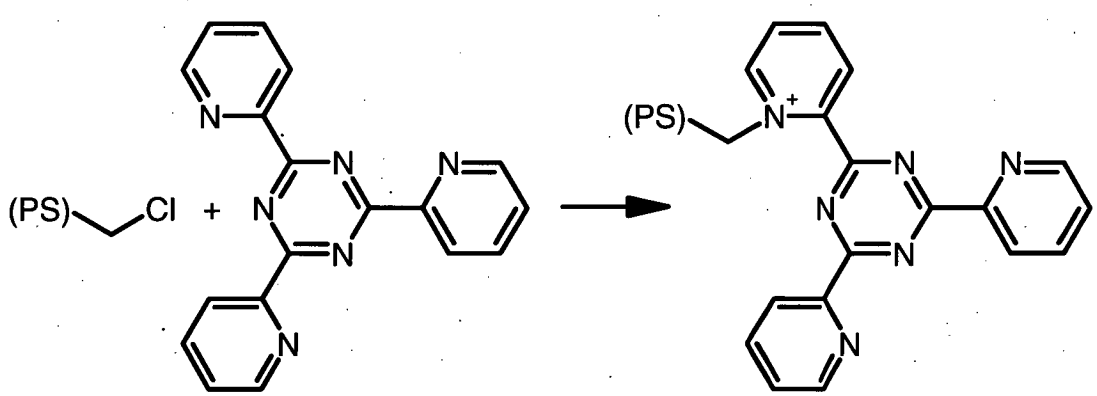

Figure 3.3.10 Reaction of A378 with 2,4,6-tris(2-pyridyl)-1,3,5-triazine

A sample of clean, dry chloromethylated polystyrene beads (A378; 10 mL; 5.235 g) was combined with a suspension of TPY (10.008 g, 32 mmol) in DMF (50 mL) under dry nitrogen. A PTFE coated magnetic stirring bar was added, the cap secured tightly, and the mixture heated to 100°C (± 5°C) with stirring for 97 hours. After cooling, the product was recovered by filtration on a porosity #3 sintered glass filter, and rinsed with the following: DMF (2 x 50 mL), DCM (5 x 50 mL), methanol (50 mL), water (100 mL), and aqueous HCl (0.5 M, 2 x 50 mL). A considerable

quantity of powdery solid remained, which was removed by placing the product on a fine wire mesh screen (<0.6 mm holes) and passing a stream of tap-water through the sieve from below, fast enough to suspend the fine particles (which were discarded) but not the polymer beads. The beads were washed with aqueous HCl (0.5 M, 50 mL) to strip any iron adsorbed from the tap water, and then water (2 x 100 mL). The bright yellow beads that remained were stored as **TPY1** (HCl form, ~4 mL), after drying on a vacuum line for 4 hours at 60°C.

IR (KBr plate): $\bar{\nu}$ (cm^{-1}) = 3413 (H_2O str.); 1721 (s); 1477 & 1450 (CH_2 def.); 1367; 1158 (s) (C-N str.); 1086 (w).

3.3.11 Quinuclidine (**QNU**)

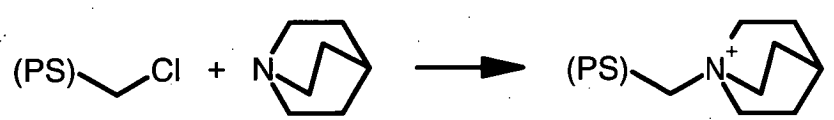

Figure 3.3.11 Reaction of A378 with quinuclidine

3.3.11.1 Preparation 1

A sample of clean, dry, chloromethylated polystyrene beads (A378; 10 mL; 5.281 g) was combined with a solution of quinuclidine (3.674 g, 33 mmol) in DMF (50 mL) under a dry nitrogen atmosphere. The mixture was stirred and heated to 100°C for 97 hours, after which the mixture was allowed to cool. The pale yellow solution was filtered on a porosity #3 sintered glass funnel, and washed with: DMF (2 x 50 mL), DCM (2 x 50 mL), methanol (2 x 50 mL), water (2 x 50 mL), aqueous HCl (0.5 M; 2 x 50 mL), and water (3 x 100 mL). The beads were denoted **QNU1** (~20 mL, Cl^- form) and were dried on a vacuum line for 4 hours at 60°C.

EA: Carbon (70.24 %); Hydrogen (8.65 %); Nitrogen (4.39 %); Other (16.72 %).

{Calculated for 3.14 meq/g quinuclidinium chloride:

Carbon (74.03 %); Hydrogen (8.36 %); Nitrogen (4.39 %); Other (13.22 %)}.

^{13}C-NMR (SS: CP-MAS): δ (ppm) = 21 (**C**H); 25 (3 x **C**H_2CH); 41 (*PS*);

55 (3 x **C**H_2N^+); 67 (**C**H_2*PS*); 128 - 133 (Arom.).

Predicted ^{13}C-NMR: 30 (3 x **C**H_2CH); 37 (**C**H); 60 (3 x **C**H_2N^+); 62 (**C**H_2Ph);

129 - 134 (Arom.).

Literature NMR [8]: 20.7 (**C**H); 24.5 (3 x **C**H_2CH); 55.0 (3 x **C**H_2N^+).

IR (KBr plate): $\bar{\nu}$ (cm^{-1}) = 3414 (H_2O str.); 2939 (s) & 2882 (w) (CH_2 str.); 1465

(CH_2 def.); 1381 (CH def.); 1347 (w), 1325 (w) & 1219 (CH_2 wag); 1073 (s) (C-N str.);

989 (w); 938 (w); 899; 834 (1,4-Arom. CH def.); 608.

3.3.11.2 Preparation 2

A sample of quinuclidine (5.4303 g) was dissolved in DMF (60 mL), combined with A378 resin (20 mL) in a Schott flask, flushed with dry nitrogen, and heated to 100°C for 72 hours with magnetic stirring. The product was filtered from the pale yellow liquor using a porosity #3 sintered glass filter funnel, and washed with DMF (2 x 50 mL), DCM (50 mL) and methanol (3 x 40 mL). The resin was dried in a vacuum oven at 40°C for 2 hours, and denoted **QNU2** (~30 mL, Cl^- form).

IR (KBr plate): $\bar{\nu}$ (cm^{-1}) = 3421 (H_2O str.); 2943 & 2882 (CH_2 str); 1660; 1465 (s)

(CH_2 def.); 1385 (CH def.); 1347 & 1325 (w) (CH_2 wag); 1291 (w); 1218 (CH_2 wag);

1119 (w); 1073 (C-N str.); 1045 (w); 988 (w); 938 (w); 899; 834 (1,4-Arom. CH def.);

816 (w); 764 (w) (CH_2 rock); 691 (w); 608; 542 (w).

3.3.12 Tribenzylamine (**TBA**)

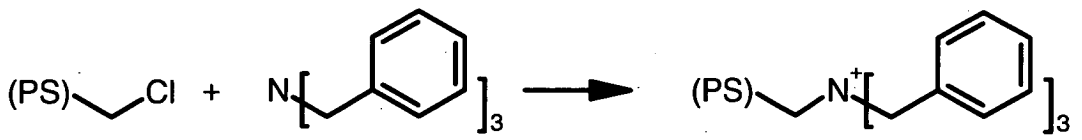

Figure 3.3.12 Reaction of A378 with tribenzylamine

To a batch of dry A378 chloromethylated polystyrene resin (10 mL) swollen in DMF (60 mL) was added tribenzylamine (11.392 g, 39.6 mmol). The reaction vessel was flushed with dry nitrogen and a magnetic stirrer bar added. The cap of the Schott flask was then tightly secured, and the reaction mixture placed in an oil bath and heated to 105°C for 168.5 hours. After cooling, the reaction mixture was filtered on a porosity #3 sintered glass funnel, and the pale yellow beads were washed with DMF (2 x 50 mL), DCM (3 x 25 mL), methanol (2 x 25 mL), water (3 x 100 mL), aqueous HCl (0.5 M, 3 x 100 mL), water (3 x 100 mL), and methanol (2 x 20 mL). The beads were dried in a vacuum oven at 60°C for 2 hours, and the polymer product (denoted **TBA1**, ~10 mL) stored in a desiccator.

EA: Carbon (75.20 %); Hydrogen (7.00 %); Nitrogen (0.94 %); Other (16.86 %).

{Calculated for 0.67 meq/g N'-tribenzylammonium chloride:

Carbon (75.40 %); Hydrogen (6.73 %); Nitrogen (0.94 %); Other (16.93 %)}.

IR (KBr plate): $\bar{\nu}$ (cm^{-1}) = 3420 (H_2O str.); 1720; 1450 (s) (CH_2 def.); 1364; 1159; 1090.

3.4 *Synthesis and Characterisation of Weak-Base Resins*

3.4.1 N-Diethylenetriamine (**DET**)

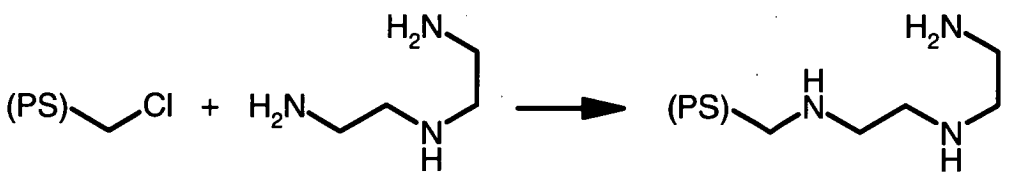

Figure 3.4.1 Reaction of A378 with diethylenetriamine

3.4.1.1 Preparation 1

Diethylenetriamine (4.019 g, 39.0 mmol) was added to a 100 mL Schott flask containing A378-A (10 mL, 5.499 g). The amine residues were washed in with distilled DMF (50 mL). The flask was then sealed, shaken, and heated to 110°C (± 5°C) in an oil bath for 48 hours, with occasional shaking. The yellow beads were filtered off and washed with methanol (3 x 50 mL), then water (3 x 50 mL). The chloride counter-ions were removed by washing with aqueous KOH (~0.3 M, 250 mL) and then the swollen yellow beads (ca. 20 mL) were rinsed with water (3 x 50 mL). The resin product was dried in a vacuum oven for 2 hours at 50°C, and denoted **DET1** (~15 mL, free base).

EA: Carbon (79.45 %); Hydrogen (8.48 %); Nitrogen (7.87 %); Other (4.20 %).

{Calculated for 1.87 meq/g N-diethylenetriamine:

Carbon (73.07 %); Hydrogen (8.02 %); Nitrogen (7.87 %); Other (11.04 %)}.

^{13}C-NMR (SS: CP-MAS): δ (ppm) = 36 (*PS*); 46 (**C**H_2NH_2 + **C**H_2NH);

53 (2 x **C**H_2NH + **C**H_2*PS*) *{Arom. region not recorded}*

Predicted ^{13}C-NMR: 41 ($\mathbf{C}H_2NH_2$); 49 ($\mathbf{C}H_2NH$); 51 (2 x $\mathbf{C}H_2NH$); 54 ($\mathbf{C}H_2Ph$); 127 - 140 (Arom.)

IR (KBr plate): $\bar{\nu}$ (cm^{-1}) = 3403 (NH str.); 2926 (s) (CH_2 str.); 2814 & 2773 (w) (NH^+ str.); 1676 (s) (1°-NH def.); 1454 & 1362 (CH_2 def.); 1175 (w); 1147 (w) (C-N str.); 1098; 812 (s) (1,4-Arom. CH rock + 1°-NH rock.); 761 (2°-NH + CH_2 rock).

3.4.1.2 Preparation 2

A Schott flask was charged with diethylenetriamine (33.080 g, 321 mmol), A378-A resin (20 mL) and DMF (50 mL). The cap was secured, and the mixture left to stir at room temperature overnight. The colourless mixture was then heated to 80°C in an oil bath for 144 hours. After cooling, the resin was washed with DMF (2 x 50 mL), DCM (2 x 50 mL), methanol (3 x 50 mL), aqueous NaOH (1.0 M, 2 x 50 mL), and water (100 mL). The resin was then wet-loaded into an IEX column (20 x 300 mm, with a porosity #3 sintered glass frit and teflon tap at the base) and washed counter-currently with water (2000 mL) for 30 minutes, removing the finer particles of shattered resin (~5 mL). The remaining **DET2** beads (~25 mL) were rinsed with methanol (2 x 25 mL) and dried in vacuo for three hours.

IR (KBr plate): $\bar{\nu}$ (cm^{-1}) = 3431 (NH str.); 2815 (CH_2 str.); 2768 (NH^+ str.); 1672 (s) (1°-NH def.); 1453 (s) (CH_2 def.); 1362 (CH_2 def.); 1308 (w); 1174 & 1146 (C-N str.); 970 (w); 942 (w); 814 (s) (1,4-Arom CH rock + 1°-NH rock.); 762 (2°-NH + CH_2 rock).

3.4.2 N-Tris(2-aminoethyl)amine (**TAA**)

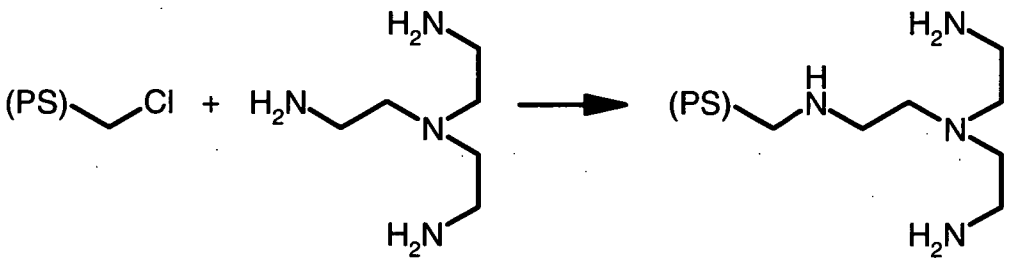

Figure 3.4.2 Reaction of A378 with tris(2-aminoethyl)amine

Tris(2-aminoethyl)amine (5.560 g, 38.0 mmol) was added to a 100 mL Schott flask containing a batch of the A378-A resin (10 mL, 5.024 g). The amine was washed in with distilled DMF (50 mL), and the flask was then sealed, shaken and heated to 110°C on an oil bath for 48 hours with occasional shaking. The tan-coloured beads were filtered off and washed with methanol (3 x 50 mL), then water (3 x 50 mL). The chloride counter-ions were removed by washing with KOH solution (~0.3 M, 250 mL) and then water (3 x 50 mL), leaving swollen light-brown beads (~20 mL).

EA: Carbon (79.00 %); Hydrogen (8.37 %); Nitrogen (8.19 %); Other (4.44 %).

{Calculated for 1.46 meq/g N',N'-bis(2-aminoethyl)-1,2-diaminoethane:

Carbon (72.04 %); Hydrogen (8.03 %); Nitrogen (8.19 %); Other (11.75 %)}.

IR (KBr plate): $\bar{\nu}$ (cm^{-1}) = 3389 (NH str.); 2813 (CH str.); 1676 (s) (1°-NH def.); 1453 (CH_2 def.); 1362; 1174 (w) (C-N str.); 814 (s) (1,4-Arom. CH def. + NH rock); 761 (CH_2 rock).

3.4.3 Diisopropylamine (**DIP**)

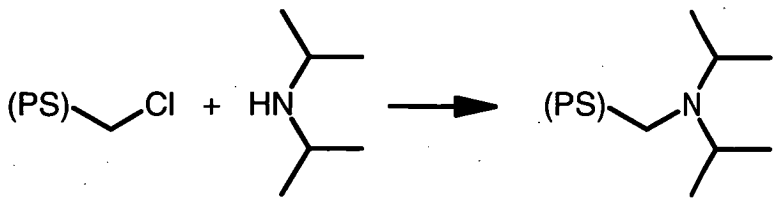

Figure 3.4.3 Reaction of A378 with diisopropylamine

Diisopropylamine (bis(2-propyl)amine) (25 mL, ca. 18 g, 180 mmol) was washed into a 100 mL Schott flask containing A378-A (10 mL, 5.288 g) with distilled DMF (40 mL). The cap was secured, and the mixture allowed to stand for 2 weeks at room temperature. The contents of the flask were then transferred to a 100 mL round-bottomed flask fitted with a reflux condenser, and heated to a mild reflux in an oil bath (100°C) for 7 hours. The cream beads and white precipitate were filtered off and washed with DMF (50 mL), methanol (3 x 50 mL), and then water (3 x 200 mL). Chloride ions were removed by washing with KOH solution (~0.2 M, 3 x 75 mL) and then water (3 x 200 mL), leaving swollen cream-coloured beads (**DIP1**, ~15 mL).

EA: Carbon (79.40 %); Hydrogen (8.86 %); Nitrogen (3.54 %); Other (8.20 %).

{Calculated for 2.53 meq/g bis(2-propyl)amine:

Carbon (79.10 %); Hydrogen (8.96 %); Nitrogen (3.54 %); Other (8.39 %)}.

IR (KBr plate): $\bar{\nu}$ (cm^{-1}) = 3385 (H_2O str.); 2965 (s) (CH_3 str.); 2925 (CH_2 str.); 2879 (w) (CH_3 str.); 1702; 1605 (Arom. C-C str.); 1452 (CH_2 def.); 1362 (CH_3 def.); 1176 (C-N str.); 957 (w); 885 (w); 760 (w) (CH_2 rock).

3.4.4 N-methylpiperazine (**NMZ**)

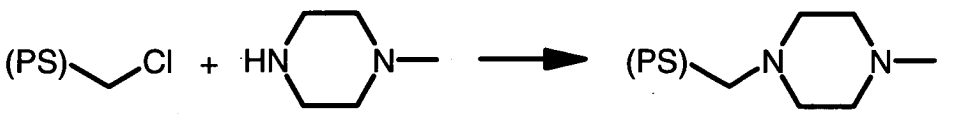

Figure 3.4.4 Reaction of A378 with N-methylpiperazine

3.4.4.1 Preparation 1

A batch of anhydrous A378 resin (10 mL) swollen in DMF (25 mL) was combined with N-methylpiperazine (5.734 g, 57.24 mmol) in DMF (25 mL), and the reaction vessel flushed with dry nitrogen before sealing. The vessel was heated to 110°C in an oil bath for 168 hours with gentle agitation. After cooling, the mixture was rinsed into a porosity #3 sintered glass filter funnel with DMF (50 mL). The DMF was removed by suction, and the brown liquor was discarded. The tan-brown beads were slowly rinsed with: DMF (2 x 100 mL), DCM (2 x 50 mL), methanol (50 mL, then 10 mL), water (2 x 100 mL), aqueous HCl (0.5 M, 50 mL, then 2 x 100 mL) and water (3 x 100 mL). The resin was denoted **NMZ1**, (~20 mL, Cl^- form).

A sample of NMZ1 resin (~10 mL) was washed into an IEX column (10 x 150 mm, with a porosity #3 sintered glass frit and teflon tap at the base), then rinsed with NaOH (1.0 M, 500 mL at 5 mL/minute) to convert it into the OH^- form. After thoroughly flushing with water (100 mL over 20 minutes) and recovery by filtration, the resin was dried in vacuo at 60°C for 2 hours and stored in a desiccator. **EA**: Carbon (80.08 %); Hydrogen (9.48 %); Nitrogen (10.24 %); Other (0.20 %). {Calculated for 3.66 meq/g N'-methylpiperazine: Carbon (78.04 %); Hydrogen (9.09 %); Nitrogen (10.24 %); Other (2.64 %)}.

IR (KBr plate): $\bar{\nu}$ (cm^{-1}) = 3392 (H_2O str.); 3012 (Arom. CH str.); 2936 (CH_3 + CH_2 str.); 2796; 1675; 1455 (s) (CH_2 def.); 1369 (CH_3 def.); 1348 (CH_2 wag); 1282 (s) (C-N str.); 1206 (w) (CH_2 wag); 1163 (s) (C-N str.); 1142; 1011 (s) (1,4-Arom. CH def.); 924 (CH_3 rock); 830; 807 (1,4-Arom. CH def.); 760 (w) (CH_2 rock); 543.

3.4.4.2 Preparation 2

A batch of anhydrous A378 resin (10 mL) was swollen in DMF (25 mL). A sample of N-methylpiperazine (5.852 g, 58.42 mmol) was washed in with DMF (25 mL) and the reaction vessel was flushed with dry nitrogen before sealing. The mixture was heated at 100°C in an oil bath for 168 hours with gentle agitation, then allowed to cool to room temperature. The resin beads were separated on a porosity #3 sintered glass filter, and washed with fresh DMF (2 x 50 mL), DCM (2 x 50 mL), methanol (3 x 50 mL), water (2 x 100 mL), aqueous NaOH (1.0 M; 3 x 100 mL), and finally water again (100 mL). The polymer was then rinsed by wet-loading it into an IEX column (as employed in Section 3.4.4.1), and washed with 500 mL water at 5.0 mL/minute. The beads were rinsed with methanol (50 mL) and suction-dried prior to placing in a vacuum oven at 60°C for 2 hours. The anhydrous yellowish resin that resulted was denoted **NMZ2** (~15 mL, OH^- form), and was stored in a desiccator.

3.4.4.3 Preparation 3

A sample of A378 resin (50 mL) was swollen for 30 minutes in distilled DMF (200 mL) in a 500 mL round-bottomed flask whilst sparging with dry N_2 gas. The flask was fitted with a PTFE paddle connected to a glass shaft passing through a *Liebig* condenser. The mixture was stirred mechanically with a RW-20 overhead stirrer (*IKA Labortechnik*). The reagent, N-methylpiperazine (27.6906 g, 276 mmol), was added and

washed in with DMF (50 mL), and the mixture heated to 95 - 100°C, with mechanical stirring, for 47 hours. After cooling, the resin was filtered on a porosity #3 sintered glass funnel and washed with DMF (2 x 50 mL) and left to stand for one hour in each of two batches of DCM (60 mL). The resin was further washed with methanol (2 x 50 mL) before air drying with suction. The resulting polymer beads (~110 mL) were stored in a plastic (PS) vial and denoted **NMZ3**.

3.4.5 Piperidine (**PIP**)

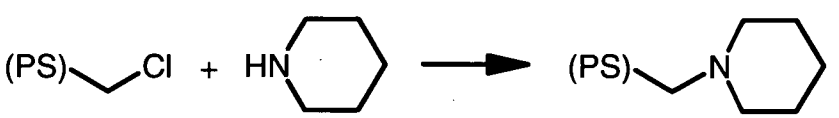

Figure 3.4.5 Reaction of A378 with piperidine

3.4.5.1 Preparation 1

A sample of dry A378 polymer beads (10 mL) was combined with a solution of piperidine (4.953 g, 58 mmol) in DMF (50.0 mL) under dry nitrogen. The cap on the flask was secured, and the mixture was stirred and heated to 100°C for 168 hours, then allowed to cool. The reaction mixture was filtered on a porosity #3 sintered glass funnel, and washed with DMF (2 x 50 mL), DCM (2 x 50 mL), methanol (50 mL), water (100 mL), aqueous HCl (0.5 M, 3 x 50 mL), water (2 x 100 mL), and methanol (20 mL). The polymer was then slurried in water, and washed with aqueous NaOH (1.0 M, 500 mL) to convert it into free-base form. The pale beads were then washed vigorously with a counter-current stream of water (~1000 mL) to suspend and remove the fines, and to remove residual NaOH. After a further wash with methanol (20 mL),

the beads were dried in a vacuum oven at 60°C for ~6 hours. The dry resin, denoted **PIP1** (~12 mL, free base), was stored in a desiccator.

EA: Carbon (83.24 %); Hydrogen (9.32 %); Nitrogen (5.69 %); Other (1.75 %).

{Calculated for 4.07 meq/g piperidine:

Carbon (82.80 %); Hydrogen (9.31 %); Nitrogen (5.69 %); Other (2.19 %)}.

^{13}C-NMR (SS: CP-MAS): δ (ppm) = 21 (3 x **C**H_2); 35 – 40 (*PS*); 50 (2 x **C**H_2N); 59 (**C**H_2*PS*); 122 - 139 (Arom.).

Predicted ^{13}C-NMR: 24 (**C**H_2); 26 (2 x **C**H_2); 55 (2 x **C**H_2N); 64 (**C**H_2Ph); 127 – 139 (Arom.).

IR (KBr plate): $\bar{\nu}$ (cm^{-1}) = 3441 (H_2O str.); 3016 (Arom. CH str.); 2930 (s) (CH_2 str.); 2791; 2752; 1368; 1342 (CH_2 def.); 1298; 1270 (w); 1153 (C-N str.); 1102 & 1038 (1,4-Arom. CH def.); 994; 862.

3.4.5.2 Preparation 2

A Schott flask was charged with piperidine (6.076 g, 71.4 mmol), clean A378 resin (10 mL) and DMF (50 mL). The cap was fitted, and the mixture left to stir overnight at room temperature (~18°C). The following day, the cloudy mixture was heated to 80°C in an oil bath, and maintained at that temperature for 144 hours. This resin was washed with DMF (2 x 50 mL), DCM (2 x 50 mL), methanol (3 x 50 mL), aqueous NaOH (1.0 M, 2 x 50 mL), and water (100 mL). The resin was then loaded into an IEX column (20 x 300 mm, with a porosity #3 sintered glass frit and teflon tap at the base) and washed counter-currently with water (~2000 mL) for 30 minutes to suspend and remove the finer particles. The **PIP2** beads (~15 mL) were rinsed with methanol (2 x 25 mL) and dried in vacuo for three hours. This material was used directly in the preparation of the N-oxide resin POP2.

3.4.6 Piperazine (**PAZ**)

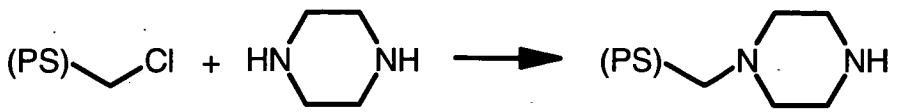

Figure 3.4.6 Reaction of A378 with piperazine

A sample of clean, dry chloromethylated polystyrene beads (A378; 10 mL) was combined with a solution of piperazine hexahydrate (9.757 g, 50 mmol) in DMF (50.0 mL) under dry nitrogen. A stirrer-bar was added, the cap secured tightly, and the mixture stirred and heated to 100°C for 168 hours, then allowed to cool. The reaction mixture was filtered on a porosity #3 sintered glass funnel, and washed with DMF (2 x 50 mL), DCM (2 x 50 mL), methanol (50 mL), water (100 mL), aqueous HCl (0.5 M, 3 x 50 mL), water (2 x 100 mL), and methanol (20 mL). The polymer was immersed in water, and washed with aqueous NaOH (1.0 M, 500 mL) to convert it into the free-base form. The cream coloured beads were then washed vigorously with a stream of water (~1000 mL) to suspend and remove the fines by counter-current flotation, and to neutralise residual NaOH. After a further wash with methanol (20 mL), the beads were dried in a vacuum oven at 60°C for approximately 6 hours, and the product (denoted **PAZ1**, ~12 mL, free base) stored in a desiccator.

EA: Carbon (81.10 %); Hydrogen (8.42 %); Nitrogen (7.90 %); Other (2.58 %).

{Calculated for 2.82 meq/g piperazine:

Carbon (76.43 %); Hydrogen (8.21 %); Nitrogen (7.90 %); Other (7.46 %)}.

^{13}C-NMR (SS: CP-MAS): δ (ppm) = 35 (*PS*); 40 (2 x **C**H_2NH); 48 (2 x **C**H_2N); 58 (**C**H_2*PS*); 123 - 139 (Arom.).

Predicted ^{13}C-NMR: 46 (2 x $\mathbf{C}H_2NH$); 56 (2 x $\mathbf{C}H_2N$); 63 ($\mathbf{C}H_2Ph$); 127 – 138 (Arom.).

IR (KBr plate): $\bar{\nu}$ (cm^{-1}) = 3402 (NH str.); 2809 (CH_2 str.); 1681 (s) (NH def.); 1607 (1,4-Arom. C-C str.); 1453 (s) (CH_2 def.); 1334 (CH_2 wag); 1141 (C-N str.); 1010 (s) (1,4-Arom. CH def.); 844 (s) (1,4-Arom. CH def. + NH rock).

3.4.7 Morpholine (**MOR**)

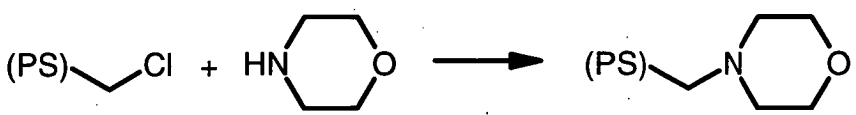

Figure 3.4.7 Reaction of A378 with morpholine

To a batch of dry A378 chloromethylated polystyrene resin (10 mL) swollen in DMF (50 mL) was added morpholine (10.345 g, 119 mmol). The reaction vessel was flushed with dry nitrogen gas and a magnetic stirrer bar added. The cap of the Schott flask was then fitted tightly, and the flask placed in an oil bath and heated to 100°C for 168 hours. After cooling, the reaction mixture was filtered on a porosity #3 sintered glass funnel, and the pale yellow beads were washed with DMF (2 x 25 mL, 50 mL), DCM (3 x 25 mL), methanol (3 x 25 mL), water (2 x 100 mL), aqueous NaOH (1.0 M, 3 x 50 mL), water (3 x 100 mL), and methanol (2 x 20 mL). The resulting polymer was dried in a vacuum oven at 60°C for 2 hours, and stored in a desiccator (denoted **MOR1**, ~15 mL, free base).

EA: Carbon (78.21 %); Hydrogen (8.48 %); Nitrogen (5.76 %); Other (7.55 %).

{Calculated for 4.11 meq/g morpholine:

Carbon (77.57 %); Hydrogen (8.49 %); Nitrogen (5.76 %); Other (8.18 %)}.

^{13}C-NMR (SS: CP-MAS): δ (ppm) = 35 (*PS*); 49 (2 x **C**H_2N); 59 (**C**H_2*PS*); 62 (2 x **C**H_2O); 123 - 140 (Arom.).

Predicted ^{13}C-NMR: 54 (2 x **C**H_2N); 63 (**C**H_2Ph); 66 (2 x **C**H_2O); 127 - 138 (Arom.).

IR (KBr plate): $\bar{\nu}$ (cm^{-1}) = 3443 (H_2O str.); 2802; 2761 (w); 1453 (CH_2 def.); 1349 & 1331 (CH_2 wag); 1286 (C-N str.); 1117 (s) (ether str.); 1070; 1007 (1,4-Arom. CH def.); 914; 866 (s) (1,4-Arom. CH def.); 795 (CH_2 rock).

3.4.8 Diethanolamine (**DEA**)

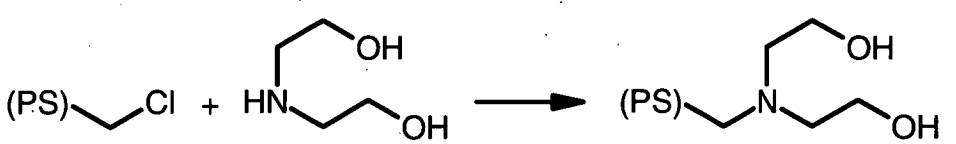

Figure 3.4.8 Reaction of A378 with diethanolamine

To a batch of dry A378 resin (20 mL) swollen in DMF (60 mL) was added diethanolamine (bis(2-hydroxyethyl)amine) (10.779 g, 102.6 mmol). The reaction vessel was flushed with dry nitrogen gas and a magnetic stirrer bar added. The cap of the Schott flask was then fitted tightly, and the flask placed in an oil bath and heated to 105°C for 168 hours. After cooling, the reaction mixture was filtered on a porosity #3 sintered glass funnel, and the cream-coloured beads were washed with DMF (2 x 100 mL), DCM (3 x 50 mL), methanol (2 x 50 mL), water (4 x 100 mL), aqueous NaOH (1.0 M, 5 x 100 mL), water (5 x 100 mL), and methanol (2 x 40 mL). The polymer beads (~30 mL, denoted **DEA1**) were then dried in a vacuum oven at 60°C for 2 hours, and stored in a desiccator.

EA: Carbon (73.60 %); Hydrogen (8.51 %); Nitrogen (4.95 %); Other (12.94 %).

{Calculated for 3.53 meq/g N,N-bis(2-hydroxyethyl)amine:

Carbon (72.46 %); Hydrogen (8.50 %); Nitrogen (4.95 %); Other (14.09 %)}

IR (KBr plate): $\bar{\nu}$ (cm^{-1}) = 3369 (s) (OH str.); 1650 (NH def.); 1604 (Arom. C-C str.); 1451 (CH_2 def.); 1364 (OH coupled CH_2 wag); 1292 (w) (CH_2 wag); 1147 (C-N str.); 1036 (s) (C-O str.); 764 (CH_2 rock); 541.

3.4.9 Imidazole (**IMZ**)

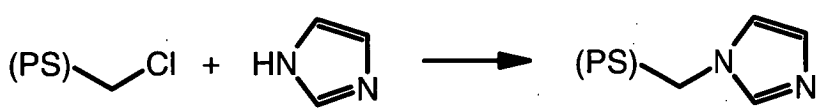

Figure 3.4.9 Reaction of A378 with imidazole

3.4.9.1 Preparation 1

To a batch of dry A378 resin (20 mL) swollen in DMF (50 mL) was added a solution of imidazole (9.460 g, 139 mmol) in DMF (25 mL). The reaction vessel was flushed with dry nitrogen and a magnetic stirrer bar added. The cap of the Schott flask was secured, and the flask placed in an oil bath and heated to 105°C for 168 hours. After cooling, the reaction mixture was filtered on a porosity #3 sintered glass funnel, and the beads were washed with DMF (2 x 50 mL), DCM (3 x 30 mL), methanol (2 x 50 mL), water (3 x 100 mL), aqueous NaOH (1.0 M, 2 x 100 mL, 50 mL), water (3 x 100 mL), and methanol (2 x 20 mL). The polymer beads were then dried in a vacuum oven at 60°C for 2 hours, and stored in a desiccator (denoted **IMZ1**, ~30 mL).

EA: Carbon (77.03 %); Hydrogen (7.03%); Nitrogen (8.79 %); Other (7.15 %).

{Calculated for 3.14 meq/g imidazole:

Carbon (77.16 %); Hydrogen (6.90 %); Nitrogen (8.79 %); Other (7.14 %)}.

^{13}C-NMR (SS: CP-MAS): δ (ppm) = 35 (*PS*); 45, 58 (**C**H_2*PS*); 123 - 140 (Arom. + 2 x **C**HN + **C**HN_2).

Predicted ^{13}C-NMR: 51 (**C**H_2Ph); 119 (**C**HN); 130 (**C**HN); 127 - 136 (Arom.); 137 (**C**HN_2).

IR (KBr plate): $\bar{\nu}$ (cm^{-1}) = 3393 (H_2O str.); 1668 (s) & 1603; (conjugated C=C str.) 1559 (C=N str.); 1449 (CH_2 def.); 1351 & 1283 (CH_2 wag); 1230 & 1145 (C-N str.); 1076; 914; 761 (CH_2 rock); 663 (alkene CH rock); 617.

3.4.9.2 Preparation 2

A sample of dry A378 resin (10 mL) was combined with imidazole (6.455 g, 94.8 mmol) in a Schott flask. DMF (50 mL) and a magnetic stirrer bar were added, the cap secured, and the mixture stirred to dissolve the imidazole. The flask was placed in an oil bath and heated to 100°C with stirring for 144 hours, then cooled and filtered on a porosity #3 sintered glass funnel. The resin was rinsed with DMF (2 x 50 mL), DCM (2 x 30 mL), methanol (2 x 30 mL) and water (3 x 100 mL). The off-white resin was converted to free-base form by washing with aqueous NaOH (1.0 M, 3 x 25 mL), then rinsed with water (5 x 100 mL). The resin product was rinsed with methanol (2 x 30 mL), then dried on a vacuum line for 2 hours (denoted **IMZ2**, ~15 mL).

IR (KBr plate): $\bar{\nu}$ (cm^{-1}) = 3428 (H_2O str.); 3054 (alkene CH str.); 1653 (C=C str.); 1560 (C=N str.); 1450 (CH_2 def.); 1345 (CH_2 wag); 1320 (w); 1282 (CH_2 wag); 1230 & 1144 (C-N str.); 1076; 913; 762 (CH_2 rock); 663 (alkene CH rock); 618; 554.

3.4.10 Ethanolamine (**ETA**)

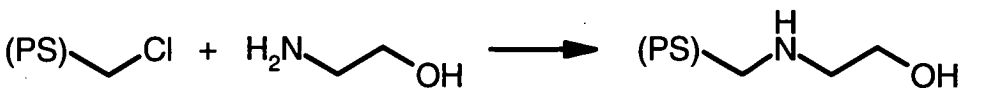

Figure 3.4.10 Reaction of A378 with ethanolamine

To a batch of dry A378 resin (20 mL) swollen in DMF (60 mL) was added ethanolamine (2-aminoethanol) (9.198 g, 150.6 mmol). The reaction vessel was flushed with dry nitrogen gas and a magnetic stirrer bar was added. The cap of the Schott flask was then secured and the flask placed in an oil bath and heated to 105°C for 168 hours. After cooling, the reaction mixture was filtered on a porosity #3 sintered glass funnel, and the beads washed with DMF (2 x 50 mL), DCM (3 x 30 mL), methanol (2 x 50 mL), water (3 x 100 mL), aqueous NaOH (1.0 M, 2 x 100 mL, 50 mL), water (3 x 100 mL), and methanol (2 x 20 mL). The polymer beads were then dried in a vacuum oven at 60°C for 2 hours and stored in a desiccator (denoted **ETA1**, ~25 mL, free base).

EA: Carbon (80.21 %); Hydrogen (8.30 %); Nitrogen (5.06 %); Other (6.43 %).

{Calculated for 3.61 meq/g ethanolamine:

Carbon (75.55 %); Hydrogen (7.82 %); Nitrogen (5.06 %); Other (11.57 %)}.

IR (KBr plate): $\bar{\nu}$ (cm^{-1}) = 3407 (OH str.); 2816 (CH_2 str.); 2780 (w); 1664 (NH def.); 1452 (CH_2 def.); 1362 (OH coupled CH_2 wag); 1259 (w) (CH_2 wag); 1173 (w) (C-N str.); 1053 (s) (C-O str.); 980 (w); 817 (NH rock); 760 (CH_2 rock).

3.4.11 Diethylenetriamine N,N''-bis(salicylidene) [*Dien(Sal)$_2$*] (**DSU**) [11]

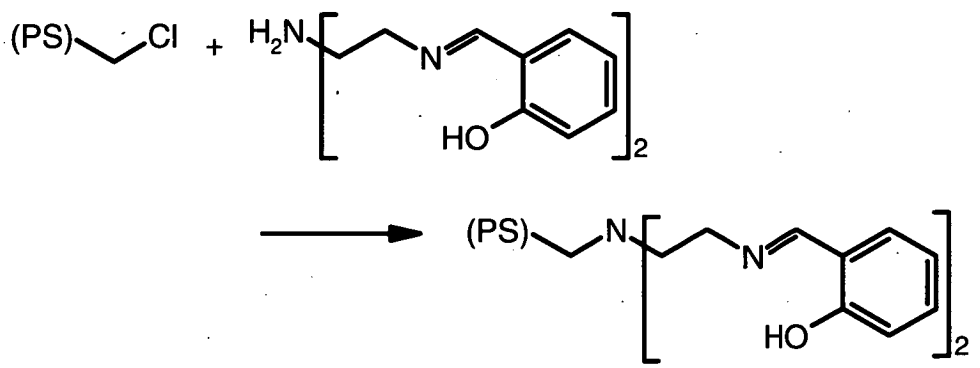

Figure 3.4.11 Reaction of A378 with *Dien(Sal)$_2$*

Dien(Sal)$_2$ (~32 g, ~102 mmol, prepared in Section 3.2.2) was combined with anhydrous A378 resin (20 mL) and DMF (200 mL). The flask was flushed with dry nitrogen gas, fitted with a condenser and a $CaCl_2$ drying tube, and heated to 100°C for 66 hours. After cooling, the brown mixture was filtered and the tan resin washed with DMF (4 x 50 mL), DCM (3 x 50 mL), methanol (3 x 50 mL), water (3 x 100 mL), aqueous NaOH (1.0 M, 3 x 150 mL, turning yellow), water (5 x 100 mL), and methanol (3 x 50 mL). The yellow resin product was denoted **DSU1** (~40 mL, free base). This product was immediately used in the preparation of resin DST1 (Section 3.4.12).

3.4.12 N'-diethylenetriamine Resin (**DST**) [11]

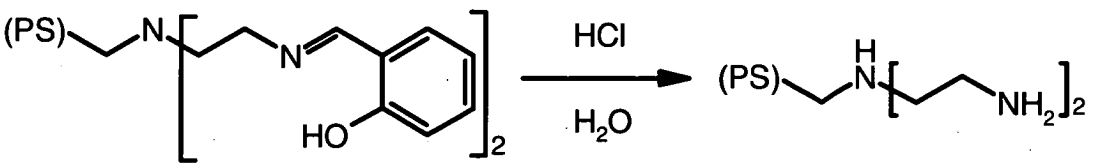

Figure 3.4.12 Hydrolysis of Schiff-base resin DSU1

Concentrated HCl (177 mL) was diluted to 300.0 mL and added to the DSU1 resin prepared in Section 3.4.11. This was placed in a 500 mL round-bottomed flask fitted with a reflux condenser, and heated in an oil bath to 60°C. The system was held at this temperature with stirring for 24 hours, then cooled and filtered on a porosity #3 sintered glass funnel. The resin washed with water (5 x 100 mL), aqueous NaOH (2.0 M; 5 x 100 mL), and water (10 x 100 mL), with the last wash being pH neutral and colourless. The resin was washed with distilled ethanol (AR, 3 x 100 mL), and air-dried on the glass sinter with suction. The resulting tan resin (~30 mL) was labelled **DST1**.

EA: Carbon (74.97 %); Hydrogen (8.22 %); Nitrogen (7.99 %); Other (8.82 %).

{Calculated for 1.90 meq/g N'-diethylenetriamine:

Carbon (73.07 %); Hydrogen (8.04 %); Nitrogen (7.99 %); Other (10.89 %)}.

^{13}C-NMR (SS: CP-MAS): δ (ppm) = 35 (*PS*); 40 (2 x **C**H_2N); 48; 53 (**C**H_2*PS* + 2 x **C**H_2N); 114 (**Ar**OH); 123 - 140 (Arom.).

Predicted ^{13}C-NMR: 39 (2 x **C**H_2N); 62 (**C**H_2Ph); 63 (2 x **C**H_2N); 127 - 139 (Arom.)

IR (KBr plate): $\bar{\nu}$ (cm^{-1}) = 3415 (s) (NH str.); 1632 (s) (1°-NH def.); 1580 (w); 1454 & 1364 (CH_2 def.); 1279 & 1150 (C-N str.); 757 (CH_2 + NH rock); 555.

3.4.13 Piperidine N-oxide (**POP**) [12]

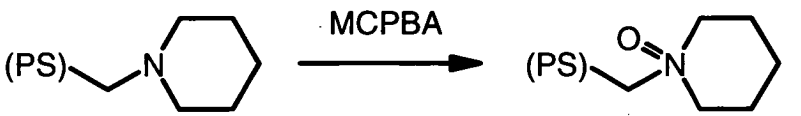

Figure 3.4.13 Oxidation of piperidine resin (PIP)

An anhydrous sample of PIP2 resin in free base form (10 mL, 5.570 g, ~23 mmol, prepared in Section 3.4.5.2) was swollen in freshly distilled chloroform (40 mL) in a 250 mL round-bottomed flask. The floating beads were stirred for 30 minutes, then additional chloroform (40 mL) was added. The mixture was cooled in an ice bath, and a solution of *m*-chloroperoxybenzoic acid (MCPBA, 85%, 10.002 g, 49 mmol) in chloroform (100 mL) was added dropwise, washing in the residue with chloroform (40 mL). The mixture was left stirring vigorously overnight (17 hours), then filtered on a porosity #3 sintered glass funnel and rinsed with chloroform (2 x 25 mL). Sodium metabisulfite (5%, 500 mL) was added with stirring to the chloroform residues and left to agitate for 2 hours to neutralise the oxidising agent (MCPBA). The resin was washed with methanol (3 x 25 mL) and dried on a vacuum line for 2 hours. The off-white resin product (~20 mL) was denoted **POP2**.

EA: Carbon (70.35 %); Hydrogen (7.52 %); Nitrogen (2.71 %); Other (19.42 %).

{Calculated for 1.93 meq/g piperidine N-oxide:

Carbon (75.48 %); Hydrogen (7.65 %); Nitrogen (2.71 %); Other (14.16 %)}.

^{13}C-NMR (SS: CP-MAS): δ (ppm) = 24 (3 x **C**H_2); 41 (*PS*); 60 (2 x **C**H_2N); 74 (**C**H_2*PS*); 129 (Arom.).

Predicted ^{13}C-NMR: 21 (2 x **C**H_2); 22 (**C**H_2); 64 (2 x **C**H_2N); 76 (**C**H_2Ph); 128 - 132 (Arom.).

IR (KBr plate): $\bar{\nu}$ (cm^{-1}) = 3422 (H_2O str.); 2931 (s) & 2858 (CH_2 str.); 1701 (w); 1602 (s) (1,4-Arom. C-C str.); 1560 (s) (3°-N=O str.); 1453 (CH_2 def.); 1376 (s) (N=O dimer str.); 1291 (w); 1245; 1140 (C-N str.); 1069; 1038 (w) (1,4-Arom. CH def.); 956; 904 (w); 860 (1,4-Arom. CH def.); 762 (s) & 731 (s) (CH_2 rock); 707 (w); 678 (w); 655; 593 (w); 544; 435.

3.5 *Synthesis and Characterisation of Alkylated Resins*

3.5.1 Methylated N-methylpiperazine (**TPZ**)

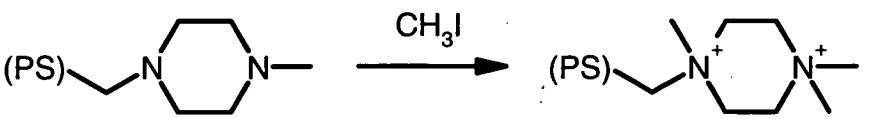

Figure 3.5.1 Methylation of N-methylpiperidine resin (TPZ)

3.5.1.1 Preparation 1

A sample of anhydrous NMZ1 resin (OH^- form, 5 mL, 2.727 g, 19.9 mmol N, prepared in Section 3.4.4.1) was placed in a 3-necked round-bottomed flask (100 mL) fitted with a gas inlet and a reflux condenser topped with a drying tube filled with granular $CaCl_2$. The resin was stirred and swollen in DMF (50 mL) under a dry nitrogen atmosphere for 20 minutes. A pressure equalising dropping funnel was used to add a solution of methyl iodide (MeI, 4.04 g, 28.5 mmol) in DMF (10 mL) over a 10 minute period. A further 15 mL of DMF was used to wash in the MeI residues, and the mixture was then stirred for 72 hours at room temperature. The flask was then heated to 45 - 50°C for 2½ hours, then cooled and then resin recovered on a porosity #3 sintered glass funnel. The resin was washed with DMF (3 x 50 mL), DCM (50 mL), methanol (2 x 50 mL), water (2 x 80 mL), aqueous HCl (0.5 M; 5 x 100 mL), and water (3 x 100 mL). The resin, denoted **TPZ1** (~11 mL),was stored wet until required.

EA: Carbon (59.36 %); Hydrogen (8.02 %); Nitrogen (6.87 %); Other (25.75 %).

{Calculated for 2.45 meq/g N,N',N'-trimethylpiperazinium dichloride:

Carbon (64.46 %); Hydrogen (8.12 %); Nitrogen (6.87 %); Other (20.56 %)}.

IR (KBr plate): $\bar{\nu}$ (cm^{-1}) = 3418 (H_2O str.); 3015 (Arom. CH str.); 1475 (s) (CH_2 + CH_3 def.); 1360; 1221 (C-N str.); 1188 (w); 1105 (C-N str.); 966; 923 (CH_3 rock); 885 (w); 852 (w) (1,4-Arom. CH def.); 826 (w).

3.5.1.2 Preparation 2

A batch of NMZ3 beads (100 mL, ~370 mmol N, prepared in Section 3.4.4.3) were swollen for 30 minutes in DMF (100 mL) in a 500 mL round-bottomed flask whilst sparging with dry N_2 gas. The flask was fitted with a condenser, and the slurry was agitated with a RW-20 overhead stirrer (*IKA-Labortechnik*) holding a PTFE paddle on a glass arm. The reagent, methyl iodide (74.1495 g, 522 mmol), was added dropwise over one hour with stirring at room temperature, and washed in with DMF (3 x 50 mL). This mixture was then heated to 60°C for 14 hours with vigorous stirring. The cloudy yellow mixture was then cooled and filtered, and the polymer isolated from the yellow precipitate by washing extensively with water (5 x 60 mL), then methanol (2 x 60 mL) and DCM (2 x 60 mL). The yellowish resin was finally dried by suction over a porosity #3 sintered glass funnel, and denoted **TPZ2** (iodide form).

The entire batch of resin was stirred for one hour in a solution of aqueous sodium hydroxide (250 mL, ~3 M), then rinsed with water (5 x 100 mL). The resin was then stirred for one hour in each of three portions of NaCl solution (1.0 M, 150 mL), and flushed again with water (3 x 300 mL). After removing most of the water by suction filtration on a porosity #3 sintered glass funnel, the product was washed with methanol (2 x 60 mL) and dried by suction for an hour, leaving ~90 mL of resin.

^{13}C-NMR (SS: CP-MAS): δ (ppm) = 41 (*PS*); 46 (**C**H_3N^+); 53 (2 x **C**H_3N^+); 62 (4 x **C**H_2N^+); 70 (**C**H_2*PS*); 129 (Arom.).

Predicted ^{13}C-NMR: 50 ($\mathbf{C}H_3N^+$); 51 (2 x $\mathbf{C}H_3N^+$); 56 (2 x $\mathbf{C}H_2N^+Me$); 57 (2 x $\mathbf{C}H_2N^+Me_2$); 67 ($\mathbf{C}H_2Ph$); 125 – 135 (Arom.)

IR (KBr plate): $\bar{\nu}$ (cm^{-1}) = 3425 (H_2O str.); 3012 (Arom. CH str.); 1476 (CH_2 + CH_3 def.); 1360; 1219 & 1104 (C-N str.); 965 (w); 922 (CH_3 rock); 879; 853 (1,4-Arom. CH def.); 764 (CH_2 rock); 647 (w).

3.5.2 Benzylated N-methylpiperazine (**TBZ**)

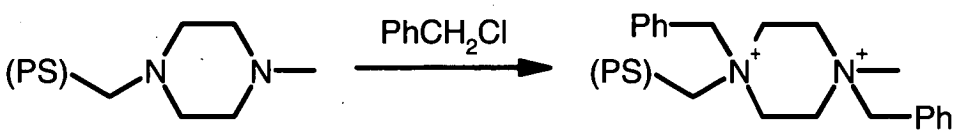

Figure 3.5.2 Benzylation of N-methylpiperidine resin (TPZ)

A sample of anhydrous NMZ2 resin (OH^- form; 10 mL, 6.545 g, ~48 mmol N, prepared in Section 3.4.4.2) was placed in a 3-necked 100 mL round-bottomed flask fitted with a gas inlet and a condenser vented through an oil bubbler. The resin was stirred and swollen in DMF (50 mL) under dry nitrogen gas whilst heating to 50°C. A pressure equalising dropping funnel was used to add benzyl chloride (9.346 g, 73.8 mmol) over 10 minutes as a solution in DMF (15 mL). A further 10 mL of DMF was used to wash in the residues, and the mixture heated to 60°C for 24 hours. The mixture was then cooled and filtered on a porosity #3 sintered glass funnel, and washed with DMF (2 x 50 mL), DCM (2 x 50 mL), methanol (3 x 50 mL), water (3 x 100 mL), aqueous HCl (0.5 M; 5 x 100 mL), water (3 x 100 mL), and methanol (2 x 50 mL). The resulting resin product was air-dried and denoted **TBZ1** (~12 mL).

EA: Carbon (71.86 %); Hydrogen (8.25 %); Nitrogen (6.70 %); Other (13.19 %). {Calculated for 2.39 meq/g N,N'-dibenzyl-N'-methylpiperazinium dichloride: Carbon (72.32 %); Hydrogen (7.62 %); Nitrogen (6.70 %); Other (13.37 %)}.

^{13}C-NMR (SS: CP-MAS): δ (ppm) = 39 (*PS*); 42; 45 (**C**H_3N^+); 58 (4 x **C**H_2CH_2); 68 (2 x **C**H_2Ph + **C**H_2*PS*); 127 (Arom.).

Predicted ^{13}C-NMR: 50 (**C**H_3N^+); 56 (2 x **C**$H_2CH_2N^+$Me); 57 (2 x CH_2**C**H_2N^+Me); 62 (2 x **C**H_2Ph); 67 (Ph**C**H_2N^+); 125 – 135 (Arom.)

IR (KBr plate): $\bar{\nu}$ (cm^{-1}) = 3413 (H_2O str.); 1635; 1475 + 1454 (CH_2 + CH_3 def.); 1358 (CH_3 def.); 1217; 1189 (w) & 1105 (C-N str); 1028 (Arom. CH def.); 986 (s); 884; 855 (w); 768 (CH_2 rock); 711 (Phenyl CH def.).

3.5.3 Benzylated N,N,N',N'-tetramethylethylenediamine (**BME**)

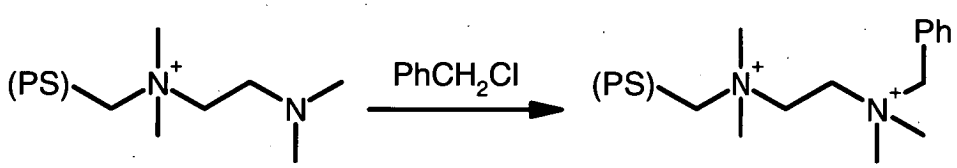

Figure 3.5.3 Benzylation of TMEDA resin (**TME**)

The anhydrous resins TME1 (OH^- form, ~5 mL, prepared in Section 3.3.9.1) and TME2 (OH^- form, ~12 mL, prepared in Section 3.3.9.2) were combined. A sample of this resin (9 mL) was calculated to have approximately 11.3 mmol N as tertiary amine groups (based on elemental analysis, 7.04% N). A 3-necked 100 mL round-bottomed flask was fitted with a reflux condenser, flushed with dry nitrogen gas, then charged with the batch of mixed TME resin (9.0 mL, 4.520 g). The resin was then swollen in DMF (50.0 mL), followed by the addition of benzyl chloride (4.350 g, 34 mmol). The

mixture was stirred gently and heated at 100°C for 24 hours, then left to cool under a blanket of dry nitrogen gas.

The beads were recovered on a porosity #3 sintered glass funnel, and washed with DMF (2 x 50 mL), DCM (3 x 50 mL), methanol (2 x 50 mL), aqueous HCl (0.5 M, 2 x 50 mL), water (3 x 100 mL + 2 x 50 mL), and methanol (20 mL). The product was dried on a vacuum line for 4 hours at 60°C and denoted **BME1** (~12 mL, HCl form).

EA: Carbon (71.41 %); Hydrogen (8.27 %); Nitrogen (5.09 %); Other (15.23 %). {Calculated for 1.82 meq/g N'-benzyl-N,N,N',N'-tetramethyl-1,2-ethylenediammonium chloride: Carbon (69.40 %); Hydrogen (7.88 %); Nitrogen (5.09 %); Other (17.64 %)}.

^{13}C-NMR (SS: CP-MAS): δ (ppm) = 38 (*PS*); 44 (2 x **C**H_3N^+); 50 (2 x **C**H_3N^+); 57 (2 x **C**$H_2CH_2N^+$); 63 (Ph**C**H_2N^+ + CH_2*PS*); 127 (Arom.).

Predicted ^{13}C-NMR: 50 (4 x **C**H_3N^+); 60 (2 x **C**$H_2CH_2N^+$); 67 (2 x **C**H_2Ph); 128 - 135 (Arom.)

IR (KBr plate): $\bar{\nu}$ (cm^{-1}) = 3417 (H_2O str.); 2630 (w) (CH_2 str.); 1478 (Arom. C-C str.); 1453 (CH_2 def.); 1425 (w) (CH_3 def.); 1273 (w) & 1217 (CH_2 wag); 1084 (w) (Phenyl CH def.); 922 (w) (CH_3 rock); 858 (1,4-Arom. CH def.).

3.5.4 Benzylated 1,3,5-triethylhexahydro-1,3,5-triazine (**TEB**)

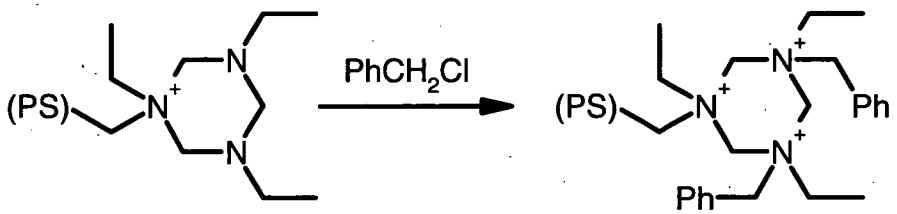

Figure 3.5.4 Benzylation of 1,3,5-triethylhexahydro-1,3,5-triazine resin (TET)

A sample of anhydrous TET1 resin (OH form; 10 mL, 4.222 g, 16.6 mmol N, prepared in Section 3.3.3.1) was placed in a 100 mL round-bottomed flask fitted with a condenser and swollen in DMF (50 mL) with stirring under a dry nitrogen atmosphere. Benzyl chloride (3.693g, 29.2 mmol) was added, and the mixture allowed to stir at room temperature for 72 hours, then heated to 100°C for 24 hours, cooled, and filtered on a porosity #3 sintered glass funnel. The resin was washed with DMF (2 x 50 mL), DCM (2 x 50 mL), methanol (2 x 50 mL), water (2 x 100 mL), aqueous HCl (0.5 M, 2 x 100 mL), water (3 x 100 mL), and methanol (20 mL). After drying in a vacuum oven at 60°C for 4 hours, the resin (denoted **TEB1**, ~10 mL) was stored in a desiccator.

EA: Carbon (75.84 %); Hydrogen (8.05 %); Nitrogen (3.87 %); Other (12.24 %). {Calc. for 0.92 meq/g 3,5-dibenzyl-1,3,5-triethylhexahydro-1,3,5-triazinium trichloride: Carbon (70.16 %); Hydrogen (7.26 %); Nitrogen (3.87 %); Other (18.71 %)}.

^{13}C-NMR (SS: CP-MAS): δ (ppm) = 8 (3 x **C**H_3); 38 (*PS*); 43; 54 (3 x **C**H_2CH$_3$); 62 (**C**H_2*PS* + 2 x **C**H_2Ph); 127 (Arom.).

Predicted ^{13}C-NMR: 7 (3 x **C**H_3); 56 (3 x **C**H_2CH$_3$); 63 (3 x **C**H_2Ph); 87 (3 x N^+**C**H_2N^+); 129 – 131 (Arom.).

IR (KBr plate): $\bar{\nu}$ (cm^{-1}) = 3404 (H_2O str.); 2861 (w) (CH_2 def.); 2613 (w); 1454 (s) (CH_2 def.); 1190 (w) & 1096 (C-N str.); 852 (w); 756 (CH_2 rock); 554.

3.5.5 Methylated 1,3,5-triethylhexahydro-1,3,5-triazine (**TEM**)

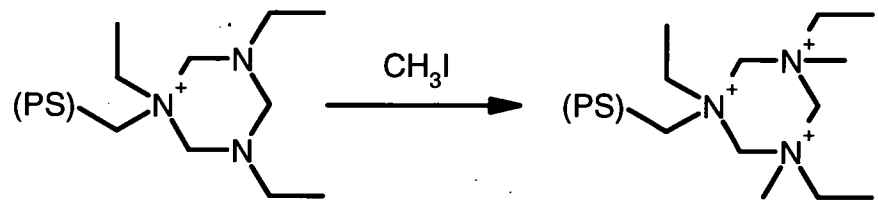

Figure 3.5.5 Methylation of 1,3,5-triethylhexahydro-1,3,5-triazine resin (TET)

A sample of anhydrous TET1 resin (OH^- form; 8 mL, ~13.3 mmol N, prepared in Section 3.3.3.1) was swollen in DMF (50 mL) in a 3-necked 100 mL round-bottomed flask under a dry nitrogen atmosphere with stirring. Methyl iodide (4.0 mL, ~9.12 g, 64 mmol) was added, and the reaction mixture heated to 50°C for 24 hours. The mixture was then cooled and the resin recovered on a porosity #3 sintered glass funnel. The resin was washed with DMF (2 x 50 mL), DCM (3 x 25 mL), methanol (2 x 50 mL), water (2 x 100 mL), aqueous HCl (0.5 M, 3 x 100 mL), water (3 x 100 mL), and methanol (2 x 20 mL). The resin, denoted **TEM1** (~10 mL), was then dried in a vacuum oven at 60°C for 4 hours and stored in a desiccator.

EA: Carbon (64.27 %); Hydrogen (7.42 %); Nitrogen (4.22 %); Other (24.09 %). {Calc. for 1.00 meq/g 3,5-dimethyl-1,3,5-triethylhexahydro-1,3,5-triazinium trichloride: Carbon (66.75 %); Hydrogen (7.50 %); Nitrogen (4.22 %); Other (21.52 %)}.

^{13}C-NMR (SS: CP-MAS): δ (ppm) = 10 (3 x **C**H_3CH_2); 41 (*PS*); 52 (2 x **C**H_3N^+); 60 (3 x **C**H_2CH_3 + **C**H_2*PS*); 74 (3 x N^+**C**H_2N^+); 128 (Arom.).

Predicted ^{13}C-NMR: 7 (2 x **C**H_3CH_2); 8 (**C**H_3CH_2); 49(2 x **C**H_3N^+); 55 (**C**H_2CH_3); 56 (3 x **C**H_2CH_3); 63 (**C**H_2Ph); 87 (2 x N^+**C**H_2N^+); 88 (N^+**C**H_2Ph); 129 - 131(Arom.).

IR (KBr plate): $\bar{\nu}$ (cm^{-1}) = 3420 (H_2O str.); 2697 (w); 1452 (CH_2 def.); 859 (w); 559.

3.5.6 Benzylated 1,3,5-tribenzylhexahydro-1,3,5-triazine (**TBB**)

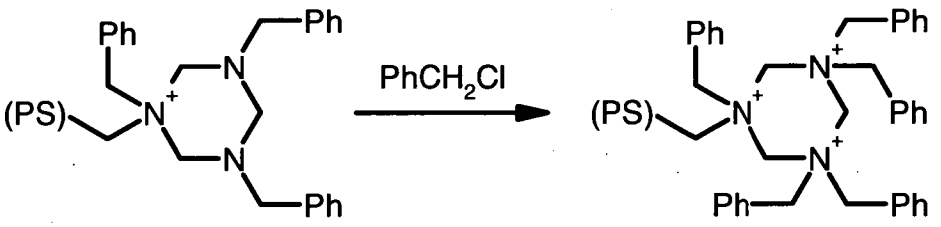

Figure 3.5.6 Benzylation of 1,3,5-tribenzylhexahydro-1,3,5-triazine resin

A sample of anhydrous TBT2 resin (OH^- form; 10 mL, 5.168 g, 13.6 mmol N, prepared in Section 3.3.6.2) was swollen in DMF (25 mL) in a 3-necked 100 mL round-bottomed flask under a dry nitrogen atmosphere with stirring. A solution of benzyl chloride (6.940 g, 54.8 mmol) in DMF (25 mL) was added, and the reaction mixture heated to 100°C for 24 hours under a stream of dry nitrogen gas, then cooled and filtered on a porosity #3 sintered glass funnel. The collected resin was washed with DMF (3 x 50 mL), DCM (3 x 25 mL), methanol (2 x 50 mL), aqueous HCl (0.5 M, 5 x 100 mL), water (3 x 100 mL), and methanol (2 x 25 mL). The resin was dried in a vacuum oven at 60°C for 4 hours and stored in a desiccator (denoted **TBB2**, ~10 mL).

EA: Carbon (77.07 %); Hydrogen (7.42 %); Nitrogen (3.12 %); Other (12.39 %). {Calc. for 0.74 meq/g 1,3,3,5,5-pentabenzylhexahydro-1,3,5-triazinium trichloride: Carbon (73.88 %); Hydrogen (6.68 %); Nitrogen (3.12 %); Other (16.32 %)}.

^{13}C-NMR (SS: CP-MAS): δ (ppm) = 38 (*PS*); 44; 56; 66 (**C**H_2Ph); 127 (Arom.).

Predicted ^{13}C-NMR: 65 (6 x **C**H_2Ph); 90 (3 x N^+**C**H_2N^+); 130 – 132 (Arom.).

IR (KBr plate): $\bar{\nu}$ (cm^{-1}) = 3414 (H_2O str.); 1691; 1678; 1605 (Arom. C-C str.); 1370; 1088 (C-N str.); 916 (w).

3.5.7 Methylated 1,3,5-tribenzylhexahydro1,3,5-triazine (**TBM**)

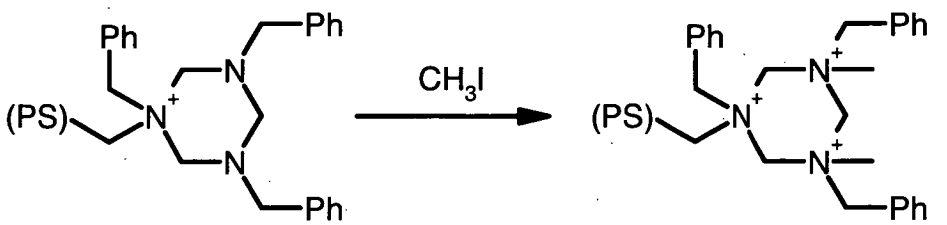

Figure 3.5.7 Methylation of 1,3,5-tribenzylhexahydro-1,3,5-triazine resin

A sample of anhydrous TBT2 resin (OH^- form; 10 mL, ~13.6 mmol N, prepared in Section 3.3.6.2) was swollen in DMF (25 mL) in a 3-necked 100 mL round-bottomed flask under a dry nitrogen atmosphere with stirring. Methyl iodide (4.0 mL, 9.12 g, 64 mmol) was added at once, washing in with DMF (25 mL). The reaction mixture was then heated to 55°C for 24 hours under a stream of dry nitrogen gas, then cooled in an ice-bath and filtered on a porosity #3 sintered glass funnel. The recovered resin was washed with DMF (3 x 50 mL), DCM (5 x 30 mL), methanol (2 x 40 mL), water (2 x 100 mL), aqueous HCl (0.5 M, 3 x 100 mL), water (3 x 100 mL), and methanol (2 x 25 mL). After drying in a vacuum oven at 60°C for 4 hours, the resin (denoted **TBM2**, ~12 mL) was stored in a desiccator.

EA: Carbon (66.29 %); Hydrogen (6.70 %); Nitrogen (2.93 %); Other (24.08 %). {Calc. for 0.70 meq/g 3,5-dimethyl-1,3,5-tribenzylhexahydro-1,3,5-triazinium $3Cl^-$: Carbon (71.68 %); Hydrogen (6.81 %); Nitrogen (2.93 %); Other (18.58 %)}.

^{13}C-NMR (SS: CP-MAS): δ (ppm) = 7; 37 (*PS*); 55 (2 x **C**H_3); 71 (**C**H_2*PS* + 3 x **C**H_2Ph); 125 (Arom.).

Predicted ^{13}C-NMR: 50 (2 x **C**H_3); 65 (2 x **C**H_2Ph); 66 (2 x **C**H_2Ph); 91 (2 x N^+**C**H_2N^+); 92 (N^+**C**H_2N^+); 130 – 132 (Arom.).

IR (KBr plate): $\bar{\nu}$ (cm^{-1}) = 3420 (H_2O str.); 1673; 1606 (Arom. C-C str.); 1475 (CH_2 def.); 1452 & 1376 (CH_3 def.); 1085 (C-N str.); 916 (w) (CH_3 rock); 854.

3.5.8 Benzylated Diethanolamine (**DAB**)

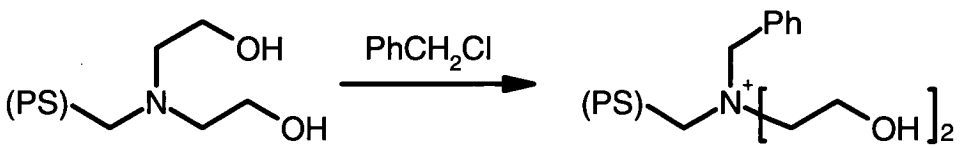

Figure 3.5.8 Benzylation of diethanolamine resin (DEA)

A sample of DEA1 resin (anhydrous free base form, 10 mL, ~18 mmol N, prepared in Section 3.4.8) was placed in a Schott flask with a magnetic stirrer bar, and stirred with DMF (50 mL) for 20 minutes to allow full swelling of the resin matrix. After this time, benzyl chloride (10.333 g, 81.6 mmol) was added and washed in with additional DMF (10 mL). The cap was secured and the mixture left to stir overnight at room temperature, before being placed in an oil bath at 100°C for 72 hours. After cooling, the pale pink resin was slowly rinsed with DMF (2 x 50 mL), then DCM (2 x 25 mL), methanol (3 x 50 mL), water (3 x 100 mL), aqueous NaOH solution (1.0 M, 3 x 50 mL), and water (5 x 100 mL). The resin product was dried in a vacuum oven for 2 hours at ~50°C and was denoted **DAB1** (~12 mL, OH^- form).

EA: Carbon (75.38 %); Hydrogen (8.80 %); Nitrogen (3.24 %); Other (12.58 %). {Calc. for 2.31 meq/g N-benzyl-N,N-bis(2-hydroxyethyl)ethylammonium hydroxide: Carbon (73.81 %); Hydrogen (8.04 %); Nitrogen (3.24 %); Other (14.91 %)}.

^{13}C-NMR (SS: CP-MAS): δ (ppm) = 38 (*PS*); 58 (2 x $\mathbf{C}H_2OH$ + $\mathbf{C}H_2Ph$ + $\mathbf{C}H_2$*PS*); 68 (2 x $\mathbf{C}H_2CH_2OH$); 126 (Arom.).

Predicted ^{13}C-NMR: 57 (2 x CH_2OH); 63 (2 x CH_2Ph); 66 (2 x CH_2CH_2OH); 128 - 134 (Arom.).

IR (KBr plate): $\bar{\nu}$ (cm^{-1}) = 3383 (OH str.); 1653; 1452 (CH_2 def.); 1364 (OH coupled CH_2 wag); 1287 (CH_2 wag); 1040 (C-O str.); 738 (w) (CH_2 rock).

3.5.9 Benzylated Ethanolamine (**ETB**)

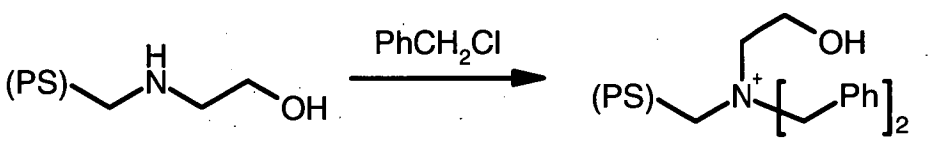

Figure 3.5.9 Benzylation of ethanolamine resin (ETA)

A sample of ETA1 resin (anhydrous free base form; 10 mL, ~18 mmol N, prepared in Section 3.4.10) was placed in a Schott flask with a magnetic stirrer bar, and stirred with DMF (50 mL) for 20 minutes to allow full swelling of the resin matrix. Benzyl chloride (11.094 g, 87.6 mmol) was then added and washed in with additional DMF (10 mL). The flask was sealed and left to stir overnight at room temperature, before being placed in an oil bath at 100°C for 72 hours. The pale pink resin was recovered and rinsed with DMF (2 x 50 mL), DCM (2 x 25 mL), methanol (3 x 50 mL), water (3 x 100 mL), aqueous NaOH solution (1.0 M, 3 x 50 mL), water (5 x 100 mL), methanol (2 x 25 mL), and DMF (2 x 25 mL).

The resin was washed back into the Schott flask with DMF (25 mL), and a further batch of DMF (25 mL) and benzyl chloride (11.365 g, 89.8 mmol) was added, along with a magnetic stirrer bar. The screw-cap fitted securely before the flask was again placed in an oil bath at 100°C for a further 94 hours. The flask was cooled, and

the contents filtered on a porosity #3 sintered glass funnel, rinsing with DMF (10 mL, then 3 x 25 mL), methanol (2 x 25 mL), DCM (2 x 25 mL), methanol (2 x 25 mL) and water (2 x 100 mL). The resin was then shaken with three portions of aqueous NaOH (1.0 M, 25 mL), followed by a water (5 x 100 mL). The resin product was denoted **ETB1** (~12 mL, OH^- form).

EA: Carbon (79.07 %); Hydrogen (8.52 %); Nitrogen (3.23 %); Other (9.18 %). {Calculated for 2.31 meq/g N,N-dibenzyl-N-(2-hydroxyethyl)ammonium hydroxide: Carbon (79.65 %); Hydrogen (7.82 %); Nitrogen (3.23 %); Other (9.30 %)}.

^{13}C-NMR (SS: CP-MAS): δ (ppm) = 38 (*PS*); 42; 58 (**C**H_2OH + 2 x **C**H_2Ph); 70 (**C**$H_2$$CH_2$OH + **C**$H_2$*PS*); 126 (Arom.).

Predicted ^{13}C-NMR: 57 (**C**H_2OH); 64 (3 x **C**H_2Ph); 68 (**C**$H_2$$CH_2$OH); 129 - 134 (Arom.).

IR (KBr plate): $\bar{\nu}$ (cm^{-1}) ≈ 3404 (OH str.); 1668 (s); 1605 (Arom. C-C str.); 1452 (CH_2 def.); 1363 (OH coupled CH_2 wag); 1055 (C-O str.); 738 (Phenyl CH def.).

3.5.10 Crosslinking N'-Diethylenetriamine resin with Glutaraldehyde (**DTP**)

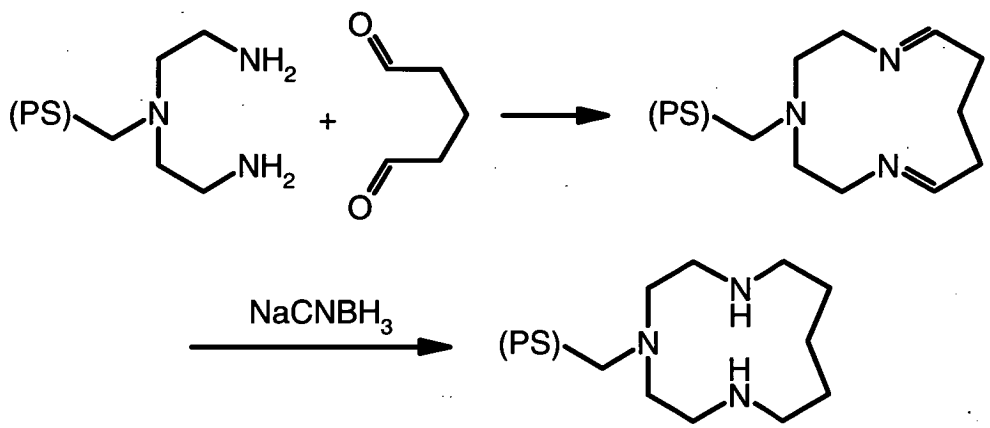

Figure 3.5.10 Crosslinking of N'-Diethylenetriamine resin

The entire batch of DST1 resin (~30 mL, free base, prepared in Section 3.4.12) was washed with absolute ethanol (~100 mL). The residual solvent was removed on a vacuum line over several hours, leaving the anhydrous resin (12.601 g).

Sodium tetraborate decahydrate (2.3846 g, 6.25 mmol) was dissolved in 200.0 mL of water, producing a 31 mM borate buffer solution (pH ~9). Beneath a blanket of dry nitrogen gas, the DST1 resin was washed into a 3-neck round-bottomed 250 mL flask with methanol (AR, ~40 mL). This was stirred gently for 10 minutes as it was heated to ~30°C in an oil bath. A glass syringe and steel needle were used to deliver 5.0 mL of glutaraldehyde solution (50% in water, 27.6 mmol) dropwise over 10 minutes. The residue in the syringe was rinsed in with additional methanol (~5 mL). Sodium cyanoborohydride (AR, 3.222 g, 51.3 mmol) was dissolved in ~150 mL of the borate solution, then added to the reaction mixture. The residue was washed into the reaction vessel with the borate buffer solution (~10 mL), then methanol (~5 mL). The

reaction temperature was stabilised at 37°C, and the mixture was left to stir under an atmosphere of dry nitrogen gas for 24 hours.

Saturated aqueous $NaHCO_3$ (~50 mL) was slowly added, with stirring, to quench the reaction. As the mixture cooled over the next 30 minutes, the nitrogen atmosphere was removed. The resin was isolated by vacuum filtration on a porosity #3 sintered glass funnel, and rinsed with saturated aqueous $NaHCO_3$ (50 mL), then water (2 x 100 mL). The reaction liquor and wash residues were neutralised by adding to an equal volume of 2% $Na_2S_2O_3$ solution. The resin was then washed with water (2 x 100 mL), methanol (AR, 3 x 50 mL), DCM (2 x 50 mL), and THF (2 x 50 mL, then 5 x 25 mL) until the washes were colourless. The resin was again washed with methanol (20 mL), and then with water (200 mL, dropwise over several hours). The reaction vessel and all the equipment used to handle the cyanoborohydride reagent were cleaned and neutralised by steeping in a 2% $Na_2S_2O_3$ solution in a fume hood for 10 minutes to neutralise any cyanide residues.

The resin was shaken with aqueous NaOH (1.0 M, 50 mL), and the yellow solution drained after 15 minutes. This was repeated twice, after which the resin was stirred with NaOH solution (1.0 M, 100 mL) for 30 minutes. After filtration, the resin was twice more treated with 50 mL of the NaOH solution. The resin was eluted with NaOH (1.0 M, 400 mL) over four hours, and then with water (400 mL). Finally, the resin was rinsed with methanol (AR, 2 x 50 mL), and dried on a rotary evaporator (denoted **DTP1**, ~32 mL, free base).

EA: Carbon (69.58 %); Hydrogen (7.66 %); Nitrogen (7.26 %); Other (15.50 %).

{Calculated for 1.73 meq/g 1,4,10-triazadodecane:

Carbon (74.80 %); Hydrogen (8.51 %); Nitrogen (7.26 %); Other (9.42 %)}.

^{13}C-NMR (SS: CP-MAS): δ (ppm) = 26 (3 x **C**$H_2CH_2NH_2$); 34 - 41 (*PS*); 46 (2 x **C**H_2CH_2N + 2 x **C**H_2N); 53 (2 x **C**H_2CH_2N); 63 (**C**H_2*PS*); 121; 129 - 137 (Arom.).

Predicted ^{13}C-NMR: 29 (**C**$H_2CH_2CH_2N$); 30 (2 x CH_2**C**H_2CH_2N); 46 (2 x **C**$H_2CH_2NCH_2Ph$); 47 (2 x CH_2CH_2**C**H_2N); 55 (2 x CH_2**C**H_2NCH_2Ph); 62 (**C**H_2Ph); 127 – 139 (Arom.).

IR (KBr plate): $\bar{\nu}$ (cm^{-1}) = 3365 (NH str.); 3018 (Arom. CH str.); 2929 (s) & 2856 (CH_2 str.); 2819 (w); 1672 (NH def.); 1454 (s) (CH_2 def.); 1364; 756 (CH_2 rock); 555.

3.5.11 Benzylated Crosslinked N'-Diethylenetriamine (**DBP**)

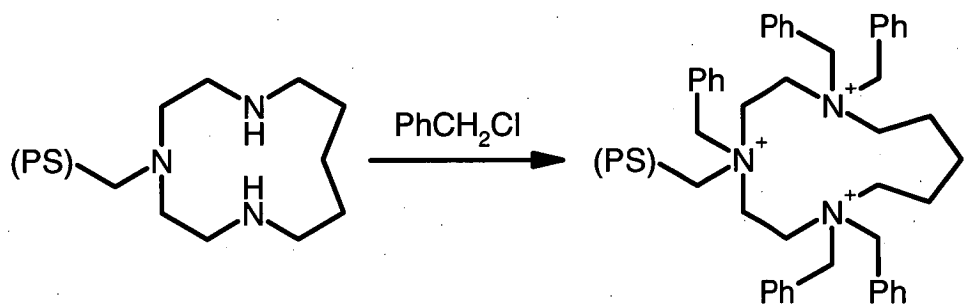

Figure 3.5.11 Benzylation of Triazamacrocycle resin (DTP)

A batch of DTP1 resin (16 mL, free base, ~41 mmol N, prepared in Section 3.5.10) was swollen in DMF (~20 mL) and placed in a Schott flask. Benzyl chloride (11.436 g, 90.6 mmol) was added and washed in with DMF (50 mL), followed by a magnetic stirrer bar. The lid was secured and the flask was placed in an oil bath at 100°C, with stirring, for 96 hours, then cooled and filtered on a porosity #3 sintered glass funnel.

The resulting orange-yellow resin was slowly rinsed with DMF (2 x 50 mL), then DCM (2 x 25 mL), methanol (3 x 50 mL), water (3 x 100 mL), and then with

aqueous NaOH (1.0 M, 3 x 50 mL) to strip HCl from the benzylated weak-base groups. The resin was rinsed again with water (5 x 100 mL), methanol (2 x 25 mL) and DMF (2 x 25 mL). The polymer was then washed into a glass IEX column (20 x 300 mm, with a porosity #3 glass frit and teflon tap at the base) with methanol (50 mL) and rinsed with water (2 x 50 mL, then 100 mL dropwise over 30 minutes). It was then flushed with aqueous NaCl (5.0 M, 100 mL), to replace the hydroxide counterions on the strong-base groups, and with water (250 mL, dropwise over one hour). The resin was again rinsed with methanol (2 x 25 mL), then DMF (2 x 25 mL), suction filtered, and transferred to a Schott flask with DMF (25 mL).

A further batch of DMF (25 mL) was used to wash in benzyl chloride (11.630 g, 91.9 mmol). A magnetic stirrer bar was added and the screw-cap secured before the flask was again placed in an oil bath at 100°C for 94 hours. After the flask was cooled, the contents were filtered on a porosity #3 sintered glass funnel, and rinsed with DMF (10 mL, then 3 x 25 mL), methanol (2 x 25 mL), DCM (2 x 25 mL), methanol (2 x 25 mL) and water (2 x 100 mL). The resin was then shaken with three portions of aqueous NaOH (1.0 M, 25 mL), filtering after each addition, then washed with water (5 x 100 mL). The resin product was dried on a vacuum line for 2 hours, and denoted **DBP1** (~15 mL, OH^- form).

EA: Carbon (78.16 %); Hydrogen (8.59 %); Nitrogen (5.13 %); Other (8.12 %). {Calc. for 1.22 meq/g 1,4,4,10,10-pentabenzyl-1,4,10-triazadodecanetriammonium $3OH^-$: Carbon (80.50 %); Hydrogen (8.33 %); Nitrogen (5.13 %); Other (6.03 %)}.

^{13}C-NMR (SS: CP-MAS): δ (ppm) = 21 (3 x $CH_2\mathbf{C}H_2CH_2$); 35 - 40 (*PS*); 48 (2 x $CH_2\mathbf{C}H_2N$); 53 (4 x $CH_2\mathbf{C}H_2N$); 65 (5 x $\mathbf{C}H_2Ph$ + $\mathbf{C}H_2$*PS*); 123 - 140 (Arom.).

Predicted ^{13}C-NMR: 20 (2 x $CH_2\mathbf{C}H_2CH_2N$); 22 ($\mathbf{C}H_2CH_2CH_2N$); 52 (2 x $N\mathbf{C}H_2CH_2N$); 53 (2 x $CH_2CH_2\mathbf{C}H_2N$); 54 (2 x $NCH_2\mathbf{C}H_2N$); 61 (2 x $\mathbf{C}H_2Ph$); 63 (4 x $\mathbf{C}H_2Ph$); 128– 135 (Arom.).

IR (KBr plate): $\bar{\nu}$ (cm^{-1}) = 3393 (H_2O str.); 2817 (w) (CH_2 str.); 1653; 1603 (Arom. C-C str.); 1453 (s) (CH_2 def.); 1364; 1310 & 1268 (w) (CH_2 wag); 1103 (C-N str.); 845 (w).

3.5.12 Benzylated Imidazole (**BIM**)

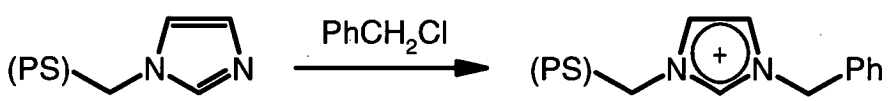

Figure 3.5.12 Benzylation of Imidazole resin (IMZ)

A sample of IMZ1 resin (anhydrous free base form; 10 mL, 31 mmol N, prepared in Section 3.4.9.1) was placed in a Schott flask with a magnetic stirrer bar. Benzyl chloride (18.282 g, 144 mmol) was added and washed in with DMF (60 mL). The lid was fitted to the flask, which was placed in an oil bath at 100°C for 72 hours. After cooling, the mixture was filtered on a porosity #3 sintered glass funnel, and washed with DMF (2 x 25 mL), DCM (2 x 25 mL), methanol (2 x 25 mL), water (5 x 100 mL), and more methanol (2 x 25 mL). The beads were dried on a vacuum line for 2 hours, and were denoted **BIM1** (~12 mL, Cl^- form).

EA: Carbon (70.60 %); Hydrogen (7.34 %); Nitrogen (6.32 %); Other (15.74 %).

{Calculated for 2.26 meq/g N'-benzylimidazolium chloride:

Carbon (74.16 %); Hydrogen (6.53 %); Nitrogen (6.32 %); Other (12.99 %)}

^{13}C-NMR (SS: CP-MAS): δ (ppm) = 38 (*PS*); 51 ($\mathbf{C}H_2Ph$ + $\mathbf{C}H_2$*PS*); 127 (Arom.).

Predicted ^{13}C-NMR: 53 (**C**H_2Ph); 60 (**C**H_2Ph); 123 (CH**C**HN); 124 (**C**HCHN); 130 - 134 (Arom.); 138 (N**C**HN).

IR (KBr plate): $\bar{\nu}$ (cm^{-1}) = 3403 (H_2O str.); 1653 & 1616 (conjugated C=C str.); 1558 (s) (C=N str.); 1496 (Arom. C-C str.); 1454 (s) (CH_2 def.); 1353 (CH_2 wag); 1323 (w) (Arom. C-C str.); 1187 (w) (CH_2 wag); 1148 (s) (C-N str.); 762 (CH_2 rock); 616.

3.5.13 Benzylated Morpholine (**NBM**)

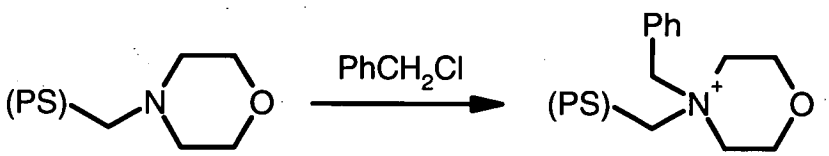

Figure 3.5.13 Benzylation of Morpholine resin (MOR)

A sample of MOR1 resin (free base form; 10 mL, ~21 mmol N, prepared in Section 3.4.7) was placed in a Schott flask with a magnetic stirrer bar. Benzyl chloride (6.869 g, 54.3 mmol) was added and washed in with DMF (60 mL). The lid was secured, and the flask placed in an oil bath at 100°C for 72 hours. After cooling, the mixture was filtered on a porosity #3 sintered glass funnel, and washed with DMF (2 x 25 mL), DCM (2 x 25 mL), methanol (2 x 25 mL), water (5 x 100 mL), and methanol (2 x 25 mL). The beads were dried on a vacuum line for 2 hours, and were denoted **NBM1** (~15 mL, Cl-form).

EA: Carbon (70.09 %); Hydrogen (7.91 %); Nitrogen (3.32 %); Other (18.68 %).

{Calculated for 2.37 meq/g N-benzylmorpholinium chloride:

Carbon (73.75 %); Hydrogen (7.39 %); Nitrogen (3.32 %); Other (15.55 %)}.

^{13}C-NMR (SS: CP-MAS): δ (ppm) = 38 (*PS*); 44; 58 (**C**H_2Ph + CH_2*PS*); 61 (4 x CH_2**C**H_2); 125 (Arom.).

Predicted ^{13}C-NMR: 62 (2 x **C**H_2Ph); 63 (4 x CH_2**C**H_2O); 128.9 - 133.8 (Arom.).

IR (KBr plate): $\bar{\nu}$ (cm^{-1}) = 3413 (H_2O str.); 2867 (w) (CH_2 str.); 2545 (w); 2464 (w); 1453 (s) (CH_2 def.); 1352, 1306 & 1216 (CH_2 wag); 1126 (s) (ether str.); 1082 (Phenyl CH def.); 1053; 964 (w); 912; 866 (1,4-Arom. CH def.); 764 (w) (CH_2 rock); 556.

3.5.14 Benzylated Piperidine (**NBP**)

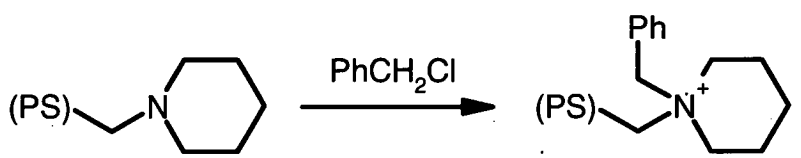

Figure 3.5.14 Benzylation of Piperidine resin (PIP)

A sample of PIP1 resin (anhydrous free base form; 10 mL, ~20 mmol N, prepared in Section 3.4.5.1) was placed in a Schott flask with a magnetic stirrer bar. Benzyl chloride (4.460 g, 35.2 mmol) was added and washed in with DMF (50 mL). The lid was secured, and the flask was placed in an oil bath at 100°C for 72 hours. The mixture was filtered on a porosity #3 sintered glass funnel, and washed with DMF (2 x 50 mL), DCM (2 x 25 mL), methanol (2 x 25 mL), water (3 x 100 mL), and methanol (2 x 25 mL). The beads were dried on a vacuum line for 2 hours, and were denoted **NBP1** (~10 mL, Cl^- form).

^{13}C-NMR (SS: CP-MAS): δ (ppm) = 19 (3 x **C**H_2**C**H_2); 38 (*PS*); 58 (**C**H_2*PS* + 3 x **C**H_2N); 126 (Arom.).

Predicted ^{13}C-NMR: 20 ($\mathbf{C}H_2CH_2CH_2N$); 21 (2 x $\mathbf{C}H_2CH_2N$); 63 (2 x $\mathbf{C}H_2Ph$); 65 (2 x $CH_2\mathbf{C}H_2N$); 130 – 134 (Arom.).

IR (KBr plate): $\bar{\nu}$ (cm^{-1}) = 3413 (H_2O str.); 2928 (s) & 2861 (CH_2 def.); 2637 (w); 2536 (w); 1615 (1,4-Arom. C-C str.); 1455 (s) (CH_2 def.); 1272 (w) & 1216 (CH_2 wag); 1032 (1,4-Arom. CH def.); 936; 856 (1,4-Arom. CH def.); 816; 763 (CH_2 rock).

3.5.15 Benzylated Piperazine (**BBZ**)

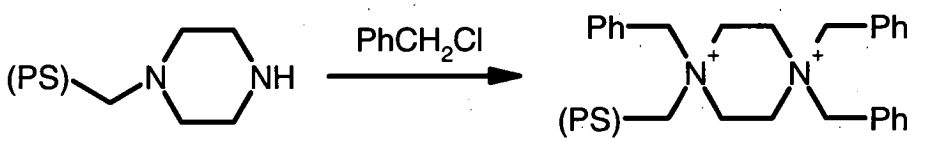

Figure 3.5.15 Benzylation of Piperazine resin (PAZ)

A sample of PAZ1 resin (anhydrous free base form; 10 mL, ~28 mmol N, prepared in Section 3.4.6) was placed in a Schott flask containing a magnetic stirrer bar. Benzyl chloride (10.730 g, 84.8 mmol) was added and washed in with DMF (50 mL). The lid was secured on the flask, which was placed in an oil bath at 100°C for 72 hours. After cooling, the mixture was filtered on a porosity #3 sintered glass funnel, and washed with DMF (2 x 50 mL), DCM (2 x 25 mL), methanol (2 x 25 mL), water (3 x 100 mL), and methanol (2 x 25 mL).

The resin was shaken with aqueous NaOH (1.0 M, 50 mL) for 1 hour to convert the remaining weak base groups into their free base form. The resin was then filtered, washed with water (5 x 50 mL) and methanol (2 x 25 mL), and dried in a vacuum oven (~50°C) for one hour.

The resin was swollen in DMF (50 mL) in a Schott flask whilst sparging with dry nitrogen gas. Benzyl chloride (12.600 g, 99.5 mmol) was added to the flask, the system sealed and heated to 100°C for 72 hours. When the mixture was cool, the resin was recovered on a porosity #3 sintered glass funnel and rinsed with DMF (2 x 25 mL), DCM (3 x 20 mL) and methanol (2 x 25 mL), then dried on a vacuum line for 2 hours at 40°C (denoted **BBZ1,** ~7 mL).

EA: Carbon (70.45 %); Hydrogen (8.24 %); Nitrogen (5.00 %); Other (16.31 %).

{Calculated for 1.78 meq/g N,N',N'-tribenzylpiperazinium chloride:

Carbon (75.42 %); Hydrogen (7.18 %); Nitrogen (5.00 %); Other (12.40 %)}

^{13}C-NMR (SS: CP-MAS): δ (ppm) = 38 (*PS*); 47; 58 (**C**H_2CH_2N + **C**H_2Ph + **C**H_2*PS*); 127 (Arom.).

Predicted ^{13}C-NMR: 58 (4 x **C**H_2CH_2N); 62 (2 x **C**H_2Ph); 130 – 134 (Arom.).

IR (KBr plate): $\bar{\nu}$ (cm^{-1}) = 3433 (H_2O str.); 2925 (s) (CH_2 str); 2562; 1668 (s); 1615 (w) (Arom. C-C str.); 1454 (s) (CH_2 def.); 1357; 1271 (w); 1219 & 1190 (w) (CH_2 wag); 1158 (w) (C-N str.); 1083 (w) (Phenyl CH def.); 963; 854 (w); 829 (1-Arom. CH def.); 750 (Phenyl CH def.).

3.5.16 Methylated Crosslinked N'-Diethylenetriamine (**DMP**)

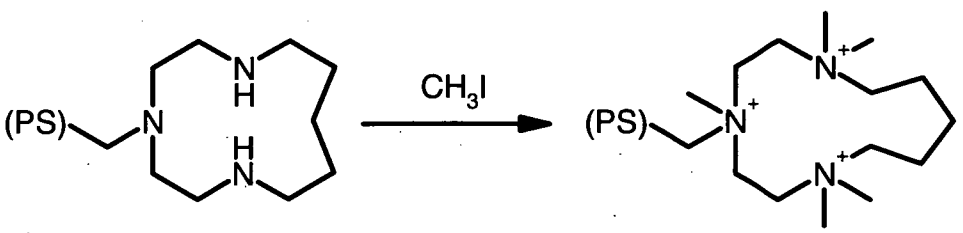

Figure 3.5.16 Methylation of Triazamacrocycle resin (DTP)

A sample of DTP1 resin (anhydrous free base form; 16 mL, ~41 mmol N, prepared in Section 3.5.10) was swollen in DMF (50 mL) and placed in a 250 mL round-bottomed flask with a magnetic stirrer bar. Methyl iodide (14.080 g, 99.2 mmol) was added and washed in with DMF (50 mL). The flask was stoppered, shaken, and left to stand for 72 hours. After this time, the reaction mixture was placed in a heating mantle, and the mixture heated to 60°C (± 5°C) for 2.5 hours, becoming a deep red colour. The mixture was cooled and filtered over a porosity #3 sintered glass funnel and washed with DMF (2 x 25 mL), DCM (2 x 25 mL), methanol (2 x 25 mL), water (2 x 50 mL), NaOH (2.0 M; 2 x 50 mL), aqueous NaCl (2.0 M; 2 x 50 mL), water (3 x 100 mL) and methanol (2 x 25 mL). The beads were dried on a vacuum line for 2 hours, and denoted **DMP1** (Cl^- form).

IR (KBr plate): $\bar{\nu}$ (cm^{-1}) = 2927 (s); 2857; 1455 (s); 1371; 1220; 1105; 852; 762.

The batch of DMP1 resin was shaken with aqueous NaOH (1.0 M, 50 mL) for 1 hour to convert the resin into free base form. The resin was recovered by filtration on a porosity #3 sintered glass funnel, and washed with water (5 x 50 mL) and methanol (2 x 25 mL), before drying in a vacuum oven for 1 hour at ~50°C.

The resin was swollen in DMF (50 mL) in a Schott flask whilst sparging with dry nitrogen gas. Methyl iodide (21.503 g,152 mmol) was added to the flask bearing the **DMP1** polymer (5.0894 g). The cap was secured, the flask wrapped in aluminium foil to exclude light, and the slurry stirred for 64 hours at room temperature. The flask was then placed in an oil bath at 50°C for 6 hours, and then cooled and the resin recovered. The resin was washed with DMF (2 x 25 mL), DCM (3 x 20 mL), methanol (25 mL) and water (2 x 25 mL). To remove the iodide counterions, the polymer was sequentially washed with aqueous solutions of Na_2SO_4 (1.0 M; 2 x 50 mL), $NaNO_3$ (1.0 M; 2 x 50 mL), and NaOH (1.0 M, 2 x 50 mL). The resin was then flushed with water (2 x 50 mL) and methanol (2 x 25 mL), and dried on a vacuum line for two hours at 40°C. The final product was denoted **DMP2** (~10 mL, OH^- form).

EA: Carbon (62.01 %); Hydrogen (7.86 %); Nitrogen (5.21 %); Other (24.92 %). {Calc. for 1.24 meq/g 1,4,4,10,10-pentamethyl-1,4,10-triazadodecanetriammonium $3OH^-$: Carbon (70.64 %); Hydrogen (8.92 %); Nitrogen (5.21 %); Other (15.23 %)}.

^{13}C-NMR (SS: CP-MAS): δ (ppm) = 19 (3 x $CH_2\mathbf{C}H_2CH_2$); 36 (*PS*); 40; 49 ($\mathbf{C}H_3NCH_2$*PS*); 57 (4 x $\mathbf{C}H_3N$ + 4 x $\mathbf{C}H_2N$); 64 ($\mathbf{C}H_2$*PS*); 124 (Arom.).

Predicted ^{13}C-NMR: 19 (2 x $CH_2\mathbf{C}H_2CH_2N$); 22 ($\mathbf{C}H_2CH_2CH_2N$); 50 ($\mathbf{C}H_3NCH_2Ph$); 52 (4 x $\mathbf{C}H_3N$); 53 (4 x $N\mathbf{C}H_2CH_2N$); 54 (2 x $CH_2CH_2\mathbf{C}H_2N$); 67 ($\mathbf{C}H_2Ph$); 124 - 135 (Arom.).

IR (KBr plate): $\bar{\nu}$ (cm^{-1}) = 3414 (H_2O str.); 3019 (Arom. CH str.); 2927 & 2859 (w) (CH_2 str.); 1671; 1476 (w) & 1453 (CH_2 def.); 1384 (s) (CH_3 def.); 1220 (w) (CH_2 wag); 1088 (w); 855 (w); 828 (1,4-Arom CH rock); 762 (CH_2 rock); 554.

3.5.17 Methylated N,N,N',N'-tetramethylethylenediamine (**PME**)

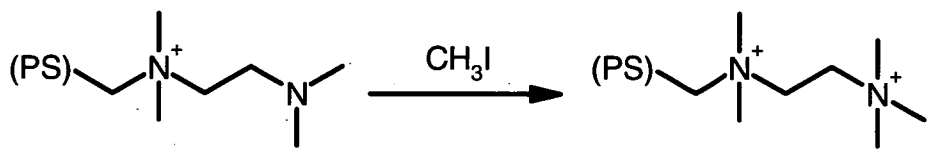

Figure 3.5.17 Methylation of TMEDA resin (TME)

The remaining batches of TME1 resin (~4 mL, prepared in Section 3.3.9.1) and TME2 (~4 mL, prepared in Section 3.3.9.2) were combined (total 10.1 mmol as NR_3 groups). This was placed in a Schott flask, and swollen in DMF (~10 mL). Methyl iodide (5.251 g, 37.0 mmol) was added and washed in with DMF (40 mL). The flask was sealed and the rapidly yellowing solution was left to stir. After 96 hours, the mixture was cooled, filtered and rinsed with DMF (2 x 50 mL), DCM (2 x 25 mL), methanol (2 x 30 mL), water (3 x 100 mL), aqueous NaCl (2.0 M; 2 x 50 mL), water (3 x 100 mL), methanol (2 x 30 mL) and diethyl ether (20 mL). The product was dried on a vacuum line for an hour, and denoted **PME2** (~8 mL, Cl-form).

EA: Carbon (52.92 %); Hydrogen (8.05 %); Nitrogen (4.60 %); Other (34.43 %). {Calculated for 1.64 meq/g N,N,N',N',N'-pentamethylmethyl-1,2-ethanediammonium $2Cl^-$: Carbon (67.23 %); Hydrogen (7.90 %); Nitrogen (4.60 %); Other (20.27 %)}.

^{13}C-NMR (SS: CP-MAS): δ (ppm) = 42 (*PS*); 51 (2 x $\mathbf{C}H_3N$); 55 (3 x $\mathbf{C}H_3N$); 59 ($\mathbf{C}H_2CH_2NMe_3$); 69 ($\mathbf{C}H_2$*PS*); 129 (Arom.).

Predicted ^{13}C-NMR: 50 (2 x $\mathbf{C}H_3N$); 53 (3 x $\mathbf{C}H_3N$); 59 ($\mathbf{C}H_2CH_2NMe_3$); 60 ($\mathbf{C}H_2NMe_3$); 67 ($\mathbf{C}H_2Ph$); 128 – 135 (Arom.)

IR (KBr plate): $\bar{\nu}$ (cm^{-1}) = 3427 (H_2O str.); 3011 (Arom. CH str.); 1477 (s) (CH_2 def.); 1425 (CH_3 def.); 1220 (CH_2 wag); 1114 (w); 1082 (w); 969; 922 (w) (CH_3 rock); 858 (1,4-Arom. CH def.); 827; 765 (w) (CH_2 rock); 705; 554.

3.5.18 Methylated Ethanolamine (**ETM**)

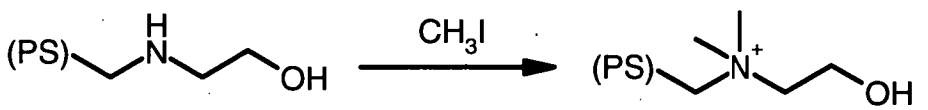

Figure 3.5.18 Methylation of Ethanolamine resin (ETA)

A sample of ETA1 resin (anhydrous free base form; 10 mL, ~18 mmol N, prepared in Section 3.4.10) was swollen in DMF (20 mL) in a Schott flask containing a magnetic stirrer bar. Methyl iodide (12.235 g, 86.2 mmol) was added and washed in with DMF (30 mL). The cap was secured and the flask covered by aluminium foil to minimise degradation of the photosensitive alkyl iodide. The reaction mixture was left to stir at room temperature for 12 hours, then placed in an oil bath and heated to 60°C for 24 hours. The reaction mixture was cooled, filtered on a porosity #3 sintered glass funnel, and washed with DMF (3 x 50 mL), DCM (2 x 25 mL), methanol (3 x 25 mL), an aqueous mixture of NaOH (0.5 M) and NaCl (2.0 M; 3 x 75 mL), water (5 x 100 mL) and methanol (2 x 30 mL). The beads were dried on a vacuum line for 2 hours, then swollen in DMF (50 mL) in a Schott flask whilst sparging with dry nitrogen gas.

A second batch of methyl iodide (19.856 g, 140 mmol) was added to the flask containing the resin (5.0295 g). The cap was fitted, the flask was wrapped in aluminium foil to exclude light, and stirred for 64 hours at room temperature. The flask was then

placed in an oil bath at 50°C for 6 hours. The reaction mixture was then cooled and filtered, and the resin washed with DMF (2 x 25 mL), DCM (3 x 20 mL), methanol (25 mL) and water (2 x 25 mL). To remove the iodide counterions, the resin was then sequentially washed with aqueous solutions of Na_2SO_4 (1.0 M; 2 x 50 mL), $NaNO_3$ (1.0 M; 2 x 50 mL), and NaOH (1,0 M, 2 x 50 mL). The resin was subsequently rinsed with water (2 x 50 mL) and methanol (2 x 25 mL), and dried on a vacuum line for 2 hours at 40°C. The product, containing a number of shattered beads, was denoted **ETM2** (~8 mL, OH^- form).

EA: Carbon (66.27 %); Hydrogen (8.25 %); Nitrogen (4.28 %); Other (21.20 %). {Calculated for 3.05 meq/g N,N-dimethyl-(2-hydroxyethyl)ammonium hydroxide: Carbon (72.14 %); Hydrogen (8.78 %); Nitrogen (4.28 %); Other (14.80 %)}.

^{13}C-NMR (SS: CP-MAS): δ (ppm) = 36 (*PS*); 49 (2 x **C**H_3N); 52; 56 (**C**H_2OH); 64 (**C**H_2*PS* + **C**H_2CH_2OH); 124 (Arom.).

Predicted ^{13}C-NMR: 52 (2 x **C**H_3N); 57 (**C**H_2OH); 69 (**C**H_2Ph); 70 (**C**H_2CH_2OH); 128 – 134 (Arom.)

IR (KBr plate): $\bar{\nu}$ (cm^{-1}) = 3379 (OH str.); 2945 (CH_3 str.); 2926 (CH_2 str.); 2862 (CH_3 str.); 1660; 1475 (w); 1452 (CH_2 def.); 1376 (CH_3 def.); 1359 (OH coupled CH_2 wag); 1217 (w); 1191 (w); 1093 (C-O str.); 975 (w); 888 (w); 829 (1,4-Arom. CH rock); 763 (w) (CH_2 rock); 553.

3.5.19 Methylated Diethanolamine (**DAM**)

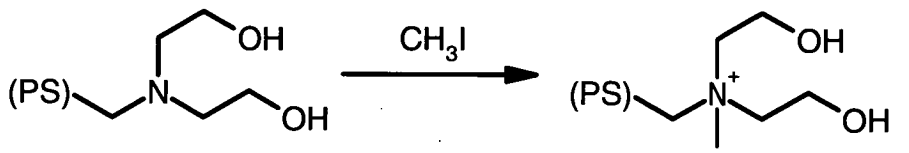

Figure 3.5.19 Methylation of Diethanolamine resin (DET)

A sample of DEA1 resin (anhydrous free base form, 10 mL, ~18 mmol N, prepared in Section 3.4.8) was swollen in DMF (20 mL) in a Schott flask containing a magnetic stirrer bar. Methyl iodide (9.333 g, 65.8 mmol) was added and washed in with DMF (30 mL), the cap secured and the flask wrapped in aluminium foil. The reaction mixture was left to stir overnight at room temperature, then placed in an oil bath and heated to 60°C for 24 hours. The mixture was then cooled, filtered on a porosity #3 sintered glass funnel, and the resin washed with DMF (3 x 50 mL), DCM (2 x 25 mL), methanol (3 x 25 mL), an aqueous mixture of NaOH (0.5 M) and NaCl (2.0 M; 3 x 75 mL), water (5 x 100 mL) and methanol (2 x 30 mL). The beads were dried on a vacuum line for 2 hours, and were denoted **DAM1** (~12 mL, Cl^- form).

EA: Carbon (59.97 %); Hydrogen (8.10 %); Nitrogen (3.10 %); Other (28.33 %). {Calculated for 2.21 meq/g N,N-bis(2-hydroxyethyl)-N-methylammonium chloride: Carbon (67.56 %); Hydrogen (7.71 %); Nitrogen (3.10 %); Other (21.64 %)}.

^{13}C-NMR (SS: CP-MAS): δ (ppm) = 37 (*PS*); 45 (**C**H_3N); 52 (2 x **C**H_2OH); 62 (**C**H_2*PS* + 2 x **C**H_2CH_2OH); 124 (Arom.).

Predicted ^{13}C-NMR: 51 (**C**H_3N); 57 (2 x **C**H_2OH); 68 (**C**H_2Ph); 73 (2 x **C**H_2CH_2OH); 124 – 134 (Arom.).

IR (KBr plate): $\bar{\nu}$ (cm^{-1}) = 3324 (OH str.); 2929 (s) (CH_3 str); 1648 (s); 1453 (s) (CH_2 def.); 1425 (w) & 1370 (s) (CH_3 def.); 1219 (w) (CH_2 wag); 1088 (s) (C-N str.); 1050 (C-O str.); 980 (w); 911 (CH_3 rock); 853 (w); 827 (1,4-Arom. CH def.).

3.5.20 Methylated N-Diethylenetriamine (**DTM**)

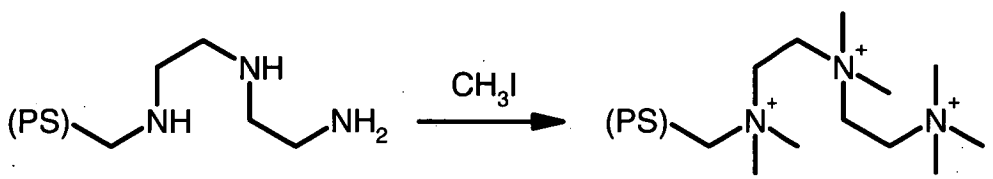

Figure 3.5.20 Methylation of N-Diethylenetriamine resin (DET)

A sample of DET2 resin (freebase, 10 mL, ~28 mmol N, prepared in Section 3.4.1.2) was placed in a 100 mL round-bottomed flask fitted with a reflux condenser, and swollen in DMF (50 mL) with magnetic stirring for 1 hour under a blanket of dry nitrogen gas. Over an hour, a solution of methyl iodide (35.85 g, 253 mmol) in DMF (10 mL) was added dropwise, and rinsed in with additional DMF (10 mL). The mixture was then heated in an oil bath until a gentle reflux commenced (at an oil temperature of ~65°C). After 20 hours, this mixture was cooled and filtered, and the resin was washed with DMF (3 x 30 mL), DCM (2 x 30 mL), methanol (3 x 30 mL) and water (3 x 80 mL), and left to stand in aqueous NaOH (1.0 M, 50 mL) for 18 hours. The resin was recovered by filtration and further rinsed with aqueous NaOH (1.0 M, 2 x 50 mL), water (3 x 100 mL), and methanol (2 x 25 mL).

The resin was dried by suction over a porosity #3 sintered glass funnel, then transferred to a 100 mL round-bottomed flask fitted with a reflux condenser, and swollen in DMF (50 mL) for 30 minutes under a blanket of dry nitrogen gas. Methyl

iodide (29.976 g, 211 mmol) was added, and washed in with DMF (~30 mL). The mixture was immersed in an oil bath at 65°C and stirred for 14 hours. After allowing the mixture to cool, the solids were recovered on a porosity #3 sintered glass filter and washed with DMF (2 x 30 mL), DCM (2 x 30 mL), methanol (2 x 30 mL), water (2 x 100 mL), aqueous NaOH (1.0 M, 3 x 40 mL), water (3 x 100 mL) and methanol (2 x 25 mL).

This resin was swollen in DMF (40 mL) under a blanket of dry nitrogen gas for 30 minutes, then methyl iodide (18.857 g, 133 mmol) was added, washing in the residues with additional DMF (40 mL). The mixture was stirred and heated in an oil bath at 70°C for 20 hours. After cooling and filtration, the resin was washed with DMF (2 x 30 mL), DCM (3 x 25 mL), methanol (2 x 30 mL) and water (2 x 100 mL).

A considerable amount of fine powder and shattered beads were present, hence the resin was sorted by counter-current flotation as follows: The resin was slurried with water and wet-loaded into a glass IEX column (20 x 400 mm, with a porosity #3 sintered glass frit and teflon tap at the base). De-ionised water was introduced from the bottom of the column. The top of the column was connected to an overflow hose leading to a 5-litre beaker. The flow rate was adjusted until the suspended fragments escaped the top of the column, whilst the intact spheres remained in the lower half of the column. After three hours, approximately 12 mL of whole beads were retained in the column. The resin was washed with aqueous NaCl (~2 M, 3 x 33 mL) to convert the counter-ions on the quaternary ammonium groups from iodide to chloride form, then rinsed with water (3 x 80 mL) and methanol (2 x 25 mL). The product was dried by suction over a the sintered glass filter funnel, then on a vacuum line for 2 hours (denoted **DTM2**, ~8 mL).

EA: Carbon (53.78 %); Hydrogen (7.61 %); Nitrogen (4.90 %); Other (33.71 %). {Calc. for 1.17 meq/g 1,1,4,4,7,7,7-heptamethyldiethylenetriammonium trichloride: Carbon (65.48 %); Hydrogen (7.87 %); Nitrogen (4.90 %); Other (21.75 %)}.

^{13}C-NMR (SS: CP-MAS): δ (ppm) = 36 (*PS*); 45; 49 (7 x **C**H_3N); 64 (4 x **C**H_2CH_2 + CH_2*PS*); 125 (Arom.).

Predicted ^{13}C-NMR: 50 (2 x **C**H_3NCH_2Ph); 51 (2 x **C**H_3N); 53 (3 x **C**H_3N); 57 (**C**H_2CH_2NMe_3 + **C**H_2NCH_2Ph); 58 (**C**H_2CH_2NCH_2Ph + (**C**H_2NMe_3); 67 (**C**H_2Ph); 128 – 135 (Arom.).

IR (KBr plate): $\bar{\nu}$ (cm^{-1}) = 3436 (H_2O str.); 3010; 1666; 1476 (s) & 1454 (w) (CH_2 def.); 1382 (CH_3 def.); 1220 (CH_2 wag); 973; 922 (CH_3 rock); 888; 857; 826 (1,4-Arom. CH rock); 705; 555.

3.5.21 Methylated Imidazole (**MIM**)

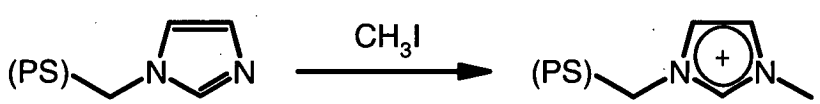

Figure 3.5.21 Methylation of Imidazole resin (IMZ)

The remaining batch of anhydrous IMZ2 resin (11 mL, ~35 mmol N, prepared in Section 3.4.9.2) was washed into a 100 mL 3-neck round-bottomed flask with DMF (50 mL). The flask was fitted with a condenser, and stirred for 30 minutes to permit swelling of the polymer. A dropping funnel containing a solution of iodomethane (15.392 g, 108 mmol) in DMF (10 mL) was fitted to the flask, and the contents added dropwise over 10 minutes. Residues were washed in with another aliquot of DMF (10 mL), and the mixture was left to stir for ~20 hours at room temperature, then in an

oil bath at 45°C for 4 hours. The cooled mixture was filtered, and the solids rinsed with DCM (4 x 25 mL) and methanol (2 x 25 mL), then air-dried on a glass frit with suction.

To remove the strongly retained iodide counter-ion, the resin was loaded into a large glass IEX column (20 x 300 mm, with a porosity #3 sintered glass frit and teflon tap at the base), shaken to remove entrained air bubbles, then eluted with an aqueous Na_2SO_4 solution (1.0 M) at 2.0 mL/min for 90 minutes. The resin was then flushed with a $NaNO_3$ solution (1.0 M) at 2.0 mL/min for 60 minutes. Finally, the resin was washed with a NaCl solution (1.0 M, pH 10.00) at 2.0 mL/min for 25 minutes, and the residual salts removed with a water wash at 2.0 mL/min for 2 hours. The resin product was recovered by filtration and rinsed with water (200 mL), then methanol (2 x 25 mL), and dried by suction on the filter. The product was dried further on a vacuum line for 2 hours (denoted **MIM2**, ~12 mL, Cl^- form).

EA: Carbon (65.37 %); Hydrogen (7.34 %); Nitrogen (7.66 %); Other (19.63 %).

{Calculated for 2.73 meq/g N'-methylimidazolium chloride:

Carbon (70.00 %); Hydrogen (6.78 %); Nitrogen (7.66 %); Other (15.56 %)}.

^{13}C-NMR (SS: CP-MAS): δ (ppm) = 41 (*PS* + **C**H_3N); 53 (**C**H_2*PS*); 129 (Arom. + 2 x **C**HN); 146 (N**C**HN).

Predicted ^{13}C-NMR: 36 (**C**H_3N); 60 (**C**H_2Ph); 123 (CH**C**HN); 124 (**C**HCHN); 129 - 133 (Arom.); 139 (N**C**HN).

IR (KBr plate): $\bar{\nu}$ (cm^{-1}) = 3416 (H_2O str.); 3138 (imidazolium CH str.); 3053 (w) (alkene CH str.); 1561 (s) (C=N str.); 1451 (CH_2 def.); 1424 & 1341 (s) (CH_3 def.); 1156 (s) (C-N str.); 827 (CH_2 rock); 764 (CH_2 rock); 705 (Arom. CH def); 620; 555.

3.6 *Results and Discussion*

The efficacy of each of the analytical procedures and reaction schemes requires evaluation. This section comprises a critical analysis of the methods used to characterise the various products (Section 3.6.1), and also of the efficacy of the preparations (Sections 3.6.2 – 3.6.13). In the case of the resin products, these have been grouped by the type of reaction used to derive the resin, such as single-step methylation and benzylation. Resins with unusual structure, such as imidazole resins and derivatives, have been grouped separately to facilitate easier comparison.

3.6.1 Comments on Analytical Methods

3.6.1.1 Infra-Red Analysis

In each of the IR spectra of the pulverised polymers, a strong absorption band was observed around 3350 - 3450 cm^{-1}, which is consistent with the presence of 1° or 2° amines (NH) or hydroxyl groups (OH). This problem proved to be ubiquitous, and could be explained by five possible mechanisms:

(1) adsorbed water on the surface of the strongly hydrophilic functionalised resins.

(2) a small amount of hydrolysis of the chloromethyl groups of the substrate directly into hydroxymethyl groups, (Eqn. 3.1),

$$(\text{Polymer})CH_2Cl + H_2O \rightarrow (\text{Polymer})CH_2OH + HCl \qquad (3.1)$$

(3) thermally induced *Hofmann* elimination of a quaternary ammonium moiety, yielding an alkene, a tertiary amine, and water (Eqn. 3.2) [13]. This is only possible if an alkyl substituent (R) bears a β-hydrogen (eg. R = $CH_2C\mathbf{H}_2OH$).

$$(\text{Polymer})CH_2N^+R_3 + OH^- \ (\Delta)\rightarrow \ (\text{Polymer})CH_2NR_2 + \text{alkene} + H_2O \qquad (3.2)$$

(4) nucleophilic substitution by the anion on alkyl substituents without β-hydrogens, also a common side-reaction in *Hofmann* eliminations (Eqns. 3.3 & 3.4) [13]. Reactions 3.3 – 3.4 are also known to proceed to a lesser degree in the presence of other anions, such as chloride, leading to halogenated elimination products.

$$(\text{Polymer})CH_2N^+R_3 + OH^- \ (\Delta)\rightarrow \ (\text{Polymer})CH_2NR_2 + ROH \qquad (3.3)$$

$$\text{or} \quad (\text{Polymer})CH_2N^+R_3 + OH^- \ (\Delta)\rightarrow \ (\text{Polymer})CH_2OH + NR_3 \qquad (3.4)$$

(5) the presence of primary or secondary amine groups on the resin, as a result of incomplete quaternisation or by decomposition of existing groups.

(6) Oxidation of the dry pulverised resin at former cross-link sites or functional moieties into carboxylic acid, aldehyde or hydroxyl groups.

The IR spectra of several resins (A378, TBA1, TET1, QNU1) were compared before and after drying in a vacuum oven (40 – 60°C) for 2 hours. This treatment caused little change in the area of the peak at ~3400 cm^{-1} for most resins, and a slight increase in that of A378. The extremely hygroscopic nature of the quaternary ammonium groups may explain the difficulty in drying the functionalised resins, but the effect of vacuum oven drying on the A378 resin is consistent with mechanism (2). It is worth noting that hydroxybenzyl groups (such as proposed in Eqn. 3.1) should display no significant IEX properties at conventional pH ranges ($pK_a >> 12$), but may serve to enhance the hydrophilic nature of the resin (ie. 'wetting').

Resins that were dried in hydroxide form may have suffered some degree of amine group elimination via mechanism (3). This was minimised by maintaining low vacuum oven temperatures ($\leq 60°C$).

There were a number of other peaks common to many of the resin products which may be attributed to structural changes in the bulk resin (such as loss of porosity) or decomposition processes, as indicated by mechanisms (4) and (5). These peaks were often found in failed resin syntheses (such as TBA1 and TOA1), and in a control sample of A378 resin after heating in DMF at 100°C for ~160 hours (**A2**).

These peaks have been given the following tentative assignments:

IR (**A2**; KBr plate): ν (cm^{-1}) = 1718 (C=O def.; carboxylic acid), 1665 (C=O def.; aldehyde), 1475 & 1452 (CH_2 def), 1161 (aliphatic C-O str.).

The unexpected peaks found at 1700-1720 cm^{-1} may be attributed to the carbonyl group of a carboxylic acid moiety, introduced via air oxidation at a benzylic site. The peak found at ~1665 cm^{-1} may be associated with the oxidation of hydroxymethyl groups to aldehydes, as a similar peak is found in the IR spectra of resins ETA1, ETB1, PET1, and PET2.

3.6.1.2 Resin Conditioning and Ionic Form

Many of the resins in this work were initially stored in hydroxide form to facilitate titration, and combustive analysis for subsequent chloride determination. Removal of chloride counterions leaves all remaining chlorine associated with the matrix (chloromethyl sites), permitting an evaluation of the efficacy of the reactions. Due to problems with the combustion techniques, this was not pursued, and many resins were left in anhydrous hydroxide form. This is believed to have led to a number of

resins with diminished capacity, due to degradation of the quaternary ammonium groups by elimination and/or oxidative processes (see Section 3.6.1.1). Subsequently, chloride counter-ions were preferred. When strong-base IEX resins are stored in chloride form, the decomposition of quaternary ammonium groups by *Hofmann* elimination is minimised, although elimination of alkyl chlorides may be possible [13]. The interference by hydroxyl groups in the IR spectra of the resin products is also minimised. In the case of a number of strong-base resins, this end was pursued by treatment with an aqueous solution of chloride ions, such as HCl or NaCl.

There are a number of resins bearing a mixture of weak- and strong-base groups, such as TME1. This also includes those resins treated with alkylating agents to quaternise the amine groups, where there has been incomplete quaternisation. In these cases, it was desirable to have the weak-base groups present as free amines. This was readily achieved by treatment with a caustic solution, but has the disadvantage of converting the quaternary ammonium groups to the less stable hydroxide form.

The latter problem was minimised in several resins by subsequent treatment of the resin with a moderately concentrated solution of sodium chloride (eg. 1 - 2 M). The mass action of the relatively high concentration of chloride ions forces the resin into chloride form. An additional refinement of this procedure was to modify the solution pH to 10 with sodium hydroxide, to minimise protonation of weak bases.

3.6.1.3 Solid-State Carbon NMR

The backbone peaks (PS-DVB) of A378 derivatives were found in different positions to the unfunctionalised resin. Examination of a number of ^{13}C-NMR spectra of the functionalised IEX resins yields the following approximate peak assignments for the *p*-chloromethylated polystyrene backbone (see Section 3.1.10.1 for resin A378):

δ (ppm) = 35 – 42 (**C**H_2**C**H); 44 - 48 (**C**H_2Cl); 126 - 132 (Aromatic).

This shift may be attributed to the effect of functional groups on the backbone, or slight variations in peak assignment relative to the external NMR reference standard. Some peak broadening was also evident due to overlap of adjacent alkyl group peaks in some products (eg: DTM2, PAZ1, PME2, TET1, TME1). The region following the alkyl backbone peak was commonly a strongly tailed shoulder of the peak at 36 - 42 ppm, and trailing off around 60 - 70 ppm.

Unexpected peaks were also found at ~145, ~156, and ~162 ppm in most of the pulverised products. For example, a peak at 147 ppm was found in the carbon NMR spectrum of A378. These weak peaks are probably due to a small degree of air-induced oxidation of the finely divided polymer at benzylic sites to aldehyde and carboxylic acid groups, particularly those sites adjacent to a broken divinylbenzene crosslink.

3.6.1.4 Elemental Analysis

Calculated percentages of carbon, nitrogen, hydrogen and other (oxygen and chlorine) for each resin were derived from the elemental proportions of the precursor resin A378. A proportion of the 'other' percentage of the substrate was replaced by equimolar quantities of the functional moiety (and counter-ion), broken into their relative elemental proportions, and the elemental percentages renormalised. The degree of functionalisation was calculated to agree with the observed values for %N.

It should be noted that some oxidative degradation of the functional groups may have occurred during storage. This has some bearing on the results of elemental analysis, which may reflect a slightly higher oxygen content (and lower nitrogen content) than the original product(s).

Parr Bomb: To monitor the performance of the bomb in converting organic chlorine (*p*-chloromethylpolystyrene) to inorganic chloride, the final solution pH was recorded after a number of the tests. The carbonate solution had an initial pH of 10.99, falling to a minimum pH of 7.30 for a sample of A378 (0.1516 g). This indicates that sufficient carbonate was present to neutralise the HCl released by combustion.

In many cases, the solution had a brown hue, and a red-brown or greenish precipitate. This is consistent with the presence of dissolved iron, introduced by corrosion of the wall of the steel vessel. The formation of these solids and the soluble complexes from which they were formed may interfere with the accurate determination of anions, by sequestering carbonate, chloride and nitrate from the bulk liquor.

Insignificant levels of nitrite were observed in ion chromatographic analysis of the initial sample liquors, and hence nitrite was omitted from further IC standards.

The results of the combustion tests employing pure quaternary ammonium salts, and a number of related resin combustion tests, are shown in Table 3.2.

Despite the use of a new corrosion-resistant bomb and investigations with the various combustion aids, the reliable determination of either element was not achieved. In particular, the level of nitrate found after combustion of standard samples were well below expectation (3-30%), and showed poor reproducibility. This is consistent with the results of Fung and Dao [14, 15], who could not achieve reliable oxidations of the nitrogenous substances. They concluded that "elemental analysis of N is not possible due to the variable oxidation of atmospheric N_2 during bomb combustion". Consequently, the Parr Bomb method was discontinued.

Table 3.2 Results of Parr Bomb Combustion Test (*via* IC)

Substrate Analysed	Combustion Aid Used	Chloride (mM)		Nitrate (mM)	
		calc.	found	calc.	found
$[CH_3(CH_2)_{11}]_3N^+CH_3\ Cl^-$	Neat pellet	0.720	0.742	0.720	0.128
$[CH_3(CH_2)_{11}]_3N^+CH_3\ Cl^-$	1:1 $PhCO_2H$	0.429	0.537	0.429	0.055
$(CH_3CH_2)_3N^+CH_2Ph\ Cl^-$	1:1 $PhCO_2H$	1.740	1.962	1.740	0.362
$(CH_3CH_2)_3N^+CH_2Ph\ Cl^-$	1:1 $PhCO_2H$	1.707	1.912	1.707	0.056
$(CH_3CH_2)_3N^+CH_2Ph\ Cl^-$	1:6 decalin	2.250	1.836	2.250	0.494
$(CH_3CH_2)_3N^+CH_2Ph\ Cl^-$	1:6 decalin	0.940	0.888	0.940	0.264
Dowex-1 (3.5 meq/g N^+)	1:10 decalin	0.738	0.857	0.738	0.266
IRA-410 (3.4 meq/g N^+)	1:10 decalin	0.813	0.846	0.813	0.207
A378 (meq/g Cl)	Neat powder	5.618	5.539	0.123	0.073

Oxidation Bomb: This procedure is intended to produce completely soluble products. The considerable volume of solid in the mixture after treatment indicated that the polymer had not been significantly digested by the first treatment.

A second batch of freshly prepared PDR was added to the mixture in the PTFE vessel. A graduated pipette was used to deliver 6.0 ml of PDR into the vessel, which was swirled about to mix with the slurry already present. The vessel was closed again, tightly sealed, and placed in an oven at 120°C for four hours. After overnight cooling, the vessel was opened to reveal a yellow slurry very similar to the starting materials. It was decided that the reagent is not sufficiently reactive toward polystyrene matrices. Therefore, this procedure was abandoned.

3.6.1.5 Ion Exchange Analysis

The exchange of soluble counterions in aqueous solution is the most appropriate method for characterisation of the ion-exchange capacity of an IEX resin. This takes into account the accessibility of the IEX sites to the aqueous phase, which is often lower than the theoretical capacity based on elemental analysis. This results since there are often some functional groups that are heavily sterically hindered or 'sandwiched' between layers of the polystyrene matrix, and virtually inaccessible to the aqueous phase. Assessment of the IEX capacity of the resin products should also take into account the pH at which the materials are to be utilised. Hence, it was decided to investigate the exchange of chloride ions for nitrate ions at pH 10.00 (0.1 mM NaOH). This is similar to the initial pH (~10.3) of the artificial leach liquor used in this study.

The use of a buffer to maintain solution pH was briefly investigated, but the buffer ions examined (~50 mM acetate or carbonate) were found to compete significantly with the analyte ions for IEX sites on the resin. The results reported in this work were obtained using solutions augmented to pH 10.00 using NaOH.

The concentrations of the NaCl and $NaNO_3$ solutions were both 1.00 M, to keep the ionic strength of the solution consistent. To allow diffusion of the solution into the polymer matrix, each solution was passed through the IEX column containing the resin sample (~1.0 g) at a flow rate of 1.0 mL/minute over 50 minutes. These analyses were conducted in duplicate to ensure reproducibility.

After initial conditioning with NaCl solution, the resins were flushed with dilute NaOH (pH 10.00) until chloride was no longer found in the effluent. This usually required ca. 150 mL of dilute NaOH, although some resins (namely BBZ1, BIM1, DMP2, DTM2, NBM1, NBP1, PME2, TBT1, TBT3, TBZ1 and TPZ1) required over 300 mL, due to poor diffusion kinetics within the modified polymer matrix. It may be

inferred from the common structural features of these resins that the presence of benzylated IEX groups is often associated with diminished porosity.

For comparative purposes, duplicate analysis of a control sample of A378 resin by this method found a negligible IEX capacity of 0.13 meq/g. All the Ion-Exchange capacity results are collected below in Table 3.3.

Table 3.3 Functionalised Resins and their IEX Capacities

SB: strong base groups per moiety; WB: weak base groups per moiety;

C_M: Ion Exchange Capacity of resin (see Section 3.1.7); NR: not recorded

Resin	Functional Group	WB	SB	C_M (meq/g)
ABU1	Tributylamine	0	1	1.39
APH1	Triphenylamine	0	1	Nil
BBZ1	Tribenzylpiperazine	0	2	1.32
BIM1	N'-benzylimidazole	1	1	2.22
BME1	N'-benzyl-TMEDA	0	2	2.27
DAB1	N-benzyl-bis(2-hydroxyethyl)amine	0	1	0.59
DAM1	N-methyl-bis(2-hydroxyethyl)amine	0	1	3.01
DBP1	Pentabenzyl Triazamacrocycle	0	3	1.40
DEA1	Diethanolamine	1	0	NR
DET1	N-diethylenetriamine	3	0	NR
DIP1	Diisopropylamine	1	0	NR
DMP2	Pentamethyl Triazamacrocycle	0	3	2.70
DST1	N'-diethylenetriamine	3	0	NR
DTM2	Heptamethyldiethylenetriamine	0	3	3.57

Table 3.3 Functionalised Resins and their IEX Capacities *(continued)*

Resin	Functional Group	WB	SB	C_M (meq/g)
DTP1	Crosslinked N'-diethylenetriamine	3	0	NR
ETA1	Ethanolamine	1	0	NR
ETB1	N,N-dibenzyl-(2-hydroxyethyl)amine	0	1	0.49
ETM2	N,N-dimethyl-(2-hydroxyethyl)amine	0	1	2.74
IMZ1	Imidazole	2	0	NR
MIM2	N'-methylimidazole	1	1	3.13
MOR1	Morpholine	1	0	NR
NBM1	N-benzylmorpholine	0	1	1.98
NBP1	N-benzylpiperidine	0	1	2.25
NMM1	N-methylmorpholine	0	1	2.70
NMM2	N-methylmorpholine	0	1	2.90
NMP1	N-methylpiperidine	0	1	3.09
NMZ1	N'-methylpiperazine	2	0	NR
PAZ1	Piperazine	2	0	NR
PET1	N-(2-hydroxyethyl)piperidine	0	1	2.30
PET2	N-(2-hydroxyethyl)piperidine	0	1	2.44
PIP1	Piperidine	1	0	NR
PME2	Pentamethyl-1,2-diaminoethane	0	2	3.83
POP2	Piperidine N-oxide	0	1	2.26
QNU1	Quinuclidine	0	1	3.07
TAA1	Tris(2-aminoethyl)amine	4	0	NR

Table 3.3 Functionalised Resins and their IEX Capacities *(continued)*

Resin	Functional Group	WB	SB	C_M (meq/g)
TBA1	Tribenzylamine	0	1	Nil
TBB2	3,5-dibenzyl-TBT	0	3	0.80
TBM2	3,5-dimethyl-TBT	0	3	1.57
TBT1	1,3,5-tribenzyl,1,3,5-hexahydrotriazine	2	1	2.09
TBT2	1,3,5-tribenzyl,1,3,5-hexahydrotriazine	2	1	1.67
TBT3	1,3,5-tribenzyl,1,3,5-hexahydrotriazine	2	1	1.59
TBZ1	N'-methyl-N,N'-dibenzylpiperazine	0	2	2.24
TEB1	3,5-dibenzyl-TET	0	3	1.86
TEM1	3,5-dimethyl-TET	0	3	0.85
TET1	1,3,5-triethyl-1,3,5-hexahydrotriazine	2	1	3.64
TET2	1,3,5-triethyl-1,3,5-hexahydrotriazine	2	1	3.33
TET3	1,3,5-triethyl-1,3,5-hexahydrotriazine	2	1	1.77
TME1	Tetramethyl-1,2-diaminoethane	1	1	1.83
TME2	Tetramethyl-1,2-diaminoethane	1	1	3.72
TME3	Tetramethyl-1,2-diaminoethane	1	1	2.15
TOA1	Trioctylamine	0	1	Nil
TOA2	Trioctylamine	0	1	0.25
TPY1	Tris(pyridyl)triazine	2	1	NR
TPZ1	Trimethylpiperazine	0	2	3.58
TPZ2	Trimethylpiperazine	0	2	2.27

Table 3.3 Functionalised Resins and their IEX Capacities *(continued)*

Resin	Functional Group	WB	SB	C_M (meq/g)
Dowex-1	Trimethylamine (Gel Matrix)	0	1	4.10
IRA410	(2-hydroxyethyl)dimethylamine	0	1	3.62
A26	Trimethylamine (Macroporous Matrix)	0	1	3.90

3.6.1.6 Titration

The principal objective of the titration of IEX resins was the determination of the pK_a values of the resin-bound functional group; the related resin IEX capacity may be accurately determined by simple ion exchange. However, titration of a resin from basic form (pH ~12) to the acidic form (pH ~ 2) also permits an assessment of the strong base capacity as the hydroxide counterions are neutralised by hydrogen ions.

Although the strong base capacity was readily measured from the titration curves obtained, it became apparent whilst processing the data using the program PKAS [9] that the weak base pK_a plateaus could not be consistently identified. It is well known that resin pK_a values are expected to be broader than the respective monomers due to the variety of the resin sites (ie. chemical environments) in which they occur. In addition to this, the slow diffusion kinetics of the resin cause the titration range of weak base groups to be much broader unless a long time is allowed for the permeation of reagents into the matrix [16]. These effects have apparently combined to render resin pK_a plateaus scarcely perceptible from the baseline. It has been suggested that such titrations need to be conducted even more slowly - over 12 hours or more - to elucidate the pK_a values of the resin moieties [8]. The *Metrohm* titration apparatus employed had a

minimum titre delivery of 10 ml over 200 minutes, which appears to be too fast to permit pK_a evaluation of the functionalised resins prepared in this work.

3.6.1.7 Resin Swelling in Water

The functional groups of an IEX resin are generally hydrophilic, and the adsorption of water into the resin structure causes expansion of the entire matrix. These calculations also take account of the degree of *swelling* induced by rehydration of an anhydrous resin, usually defined as 'wetting'. Swelling will be defined herein as the volume occupied by a batch of fully wetted resin divided by the initial volume of the same resin batch (of known mass) in an anhydrous state.

Throughout this project, the performance of the resins has been evaluated on the basis of mass. The IEX capacity of each resin has been presented in the units of *milli-equivalents per gram* (C_M, meq/g). Commercial IEX resins are often also evaluated by volume, *milli-equivalents per mL* (C_V, meq/mL). The latter term is often more useful to industry, where the volume of a containment vessel is not easily altered. In particular, resin treatments are often assessed by 'bed-volumes' – the volume of interstitial liquor that can be contained in a given volume of resin. Given a resin in a fixed ionic form (eg. free base), these two terms are linearly related as follows (Eqns. 3.5 & 3.6):

$$C_M(\text{meq/g}) \times D_R(\text{wet}) = C_V(\text{meq/mL}). \qquad (3.5)$$

where

$$D_R(\text{wet}) \times \text{Swelling} = D_R(\text{dry}) \qquad (3.6)$$

In this calculation, D_R(wet) denotes only the mass of resin per unit volume, and should not be confused with the density of the bulk wet resin - which would also include the mass of adsorbed and entrained water.

Commercial resins are rarely supplied in anhydrous form; however, the resins prepared and characterised in this project were supplied as, and referenced to, their anhydrous state. Therefore the dry density and swelling of a limited set of resins were measured, as well as C_M, to permit the derivation of C_V. The data provided in Table 3.4 relate to the testing of a refined set of resin adsorbents, the selection of which is detailed in Chapters 4 and 5.

Table 3.4 Swelling and Density of Promising Adsorbents

RESIN	**C_M(dry)** meq/g	**D_R(dry)** g/mL	**Swelling**	**C_V(wet)** meq/mL
DAM1	3.01	0.586	1.43	1.24
NMM1	2.70	0.596	1.53	1.06
MIM2	3.13	0.531	1.35	1.23
PET2	2.44	0.508	1.20	1.03
QNU1	3.07	0.507	1.53	1.02
TME3	2.15	0.474	1.00	1.02
TPZ2	2.27	0.563	1.00	1.28
Dowex-1	4.10	0.551	2.00	1.13
IRA-410	3.62	0.675	1.70	1.43

3.6.1.8 Analysis of Precursors and Commercial Resins

A378: In alternative technique to determine the degree of functionalisation (capacity), a modified version of a technique reported by Stewart and Young [17] was applied. Samples of A378 were treated with excess anhydrous pyridine, and the chloride counterions from the resulting resin were precipitated with silver nitrate. The excess silver nitrate was back-titrated with a standard solution of ammonium thiocyanate, using ferric ammonium sulfate as indicator. This analysis was performed by Dr. Matthew Shaw, who determined the capacity to be 4.13 meq/g Cl.

Although lower than the results observed by combustive techniques (Parr bomb: 4.90 meq/g Cl; Elemental Analysis: 5.62 meq/g), this is not unexpected. The reaction with pyridine reveals only those chloromethyl sites that are accessible to the reagent. The morphology of ion-exchange resins permits some reactive sites to be physically inaccessible, and a high degree of functionalisation can exacerbate this effect by steric crowding of the resin micropores.

For derivatisation purposes, the chlorine content of A378 resin was estimated as 20%, hence each batch of 10.0 mL contained roughly 31 mmol of reactive chloromethyl sites. This figure was used to confirm an excess of amine was present during synthesis.

A26: An initial batch of A26 (50 mL, Cl^- form) resin was dried in a vacuum oven (~5 mm Hg) for 2 hours at 40°C prior to use.

A larger batch of A26 resin (~ 500 mL) was sieved through a 850 μm screen. The beads that were retained (> 850 micron, ~50 mL) were dried in a vacuum oven for 2 hours at 40°C, leaving ~30 mL of large pale yellow beads (denoted **A26 Big**).

3.6.2 Evaluation of Non-Polymer Products

3.6.2.1 Methylated 1,3,5-triethylhexahydro-1,3,5-triazine (TET)

It should be noted that three alkylated products are possible (mono-, di- and trimethylated congeners). Of these products, the di- and tri-methylated species have two possible structural isomers. In addition, the mono-methylated product and one of the dimethyl congeners occur as pairs of stable nitrogen invertomers, which would complicate NMR results. The absence of sharp groupings of methyl protons in the observed ^{1}H-NMR spectrum is not consistent with the 2-4 sharp peaks at ~3.6 ppm expected from a fully methylated hexahydrotriazinium salt.

Although the product appears heavily methylated according to ^{1}H-NMR, the high molecular weight fragments in the mass spectrum are more consistent with polymerisation. The ions pairs (595.7, 466.7) and (408.7, 281.2) differ by ~128 mass units - consistent with the loss of HI. However, neither the expected molecular ion (597.0) nor any of the cations (1^{+}: 470.2; 2^{+}: 171.6; $^{3+}$: 72.1) were observed. There is some evidence of aldehydic character in the product NMR spectrum, and it is known that acid catalysis can decompose TET into formaldehyde and ethylamine [18]. It is suspected that the degradation products underwent cationic polymerisation in a Mannich-type condensation reaction, giving products of high mass. It is possible that resin products bearing the TET moiety will decompose in a similar fashion.

3.6.2.2 Benzylated Piperazine (TEBAZ)

The first crop of the first preparation was found to be insoluble in chloroform, DCM and THF; slightly soluble in methanol and DMSO; and fully soluble in water and ethanol. A proton NMR spectrum of each crop of TEBAZ (1-3) was recorded (~10 mg in d^6-DMSO), revealing approximately half the aromatic character that was expected, and little trace of the butyl groups of the acid scavenger (tributylamine) [1, 19]. Most of the third crop of precipitate was found to be insoluble in DMSO, which may indicate a polymeric byproduct.

A sample of the combined recrystallised product TEBAZ Crop 4 was submitted for LSIMS analysis, which revealed that the product consisted principally of the hydrochloride salt of N,N'-dibenzylpiperazine. The protonated molecular ion of N,N'-dibenzylpiperazine (M/Z = 267.1) was the most abundant peak in the spectrum.

After further treatment with benzyl chloride, LSIMS analysis of the product (TEBAZ-5) indicated that the product was primarily N,N,N'-tribenzylpiperazinium chloride (87% yield). The N,N,N'-tribenzylpiperazinium cation (M/Z = 357.2) was the most abundant peak in the spectrum. There was no evidence to support the formation of the bis-quaternary tetrabenzyl-piperazinium adduct (M/Z = 211.1).

3.6.3 Evaluation of Single Step Weak Base Resins

This comprises the following weak-base resins:

{DEA1, DET1, DET2, DIP1, ETA1, MOR1, NMZ1, PAZ1, PIP1, PIP2}.

3.6.3.1 Diethanolamine (DEA)

The presence of the diethanolamine moiety on the resin DEA1 can be inferred from vibrations in the IR spectrum at 3369 (O-H str.), 1147 (C-N str.) and 1036 cm^{-1} (C-O str.). An unexpected peak at 1650 cm^{-1} may be associated with the OH group, via protonation of the tertiary amine ($H\text{-}N^{+}$) or from oxidative degradation (C=O), as discussed in Section 3.6.1.2. A vibration in a similar position has been found in the IR spectra of several of the resins with the fragment (NCH_2CH_2OH) in their intended structure (eg. ETA1, PET2). Elemental analysis yielded results close to calculated values, with a slight increase in carbon possibly attributed to oxidation.

3.6.3.2 Diethylenetriamine (DET)

The IR spectra of resins **DET1** (prepared in Section 3.4.1.1) and **DET2** (Section 3.4.1.2) reveal common features consistent with the presence of N-(polystyryl)-diethylenetriamine. Several C-N stretching bands (1174 & 1146 cm^{-1}) were evident, derived from the various 1°- and 2°-amine environments present in the ligand. The peaks observed at ~2770 cm^{-1} in both resins are believed to originate from the N-H stretch of an amine site protonated by residual water (ie. $pK_a \sim 9.68$, Table 2.3, Chapter 2). The peaks observed in the carbon NMR spectrum were found to be very similar to the calculated values, but are too broad to permit a qualitative assessment of the degree of N-substitution.

Elemental analysis of DET1 revealed a higher proportion of carbon and hydrogen, and a lesser quantity of chlorine in the product than calculated. Crosslinking of the reagent, by reaction of one molecule of diethylenetriamine with two chloromethylated sites on the resin, can result in lower chlorine content as these ions are displaced from weak-base sites. This accounts for the shortfall in chloride and the consequent increase in carbon and hydrogen. A large excess of diethylenetriamine (5:1) was used in the second preparation (DET2) to minimise this effect.

Many fragmented beads were observed in both DET products, probably caused by osmotic shock during wash stages, including rapid hydration of the dry, highly functionalised beads. Counter-current washing of the resin batch **DET2** resulted in the removal of ~5 mL of fine fragments from a sample of ~30 mL.

3.6.3.3 Diisopropylamine (DIP)

A large quantity of white precipitate was observed in the reaction mixture after cooling, consisting of excess diisopropylamine precipitated as the hydrochloride salt. The IR spectrum contains the distinctive vibrations of the isopropyl group (2965, 2879 and 1362 cm^{-1}), and the C-N stretch at 1176 cm^{-1}. The peak found at.1702 cm^{-1} may be due to minor oxidative side-reactions. Elemental analysis values of the final dry polymer (free base) were all within 0.3% of the expected results.

3.6.3.4 Ethanolamine (ETA)

The presence of 2-hydroxyethylamine groups on this resin is confirmed by the peaks in the IR spectrum at 3407 cm^{-1} (O-H str.), 1664 cm^{-1} (N-H def.), 1173 cm^{-1} (C-N str.) and 1053 cm^{-1} (C-O str.). The peak at 2780 cm^{-1} may originate from a small degree of protonation of the amine by the adjacent hydroxyl group. When compared to

calculated values, the elemental analysis indicated unexpectedly high levels of carbon (+4.66%) and hydrogen, and a deficit of chlorine + oxygen (-5.14 %). This is believed to result from the hydrolysis of many of the remaining chloromethylated sites on the resin (Eqns. 3.1 and 3.4).

3.6.3.5 Morphiline (MOR)

The Infra-Red spectrum of the MOR1 resin was consistent with the presence of resin-bound morpholine, evidenced by the ether stretch at 1117 cm^{-1}. The in-plane and out-of-plane aromatic C-H def. peaks of the substrate (1007 & 866 cm^{-1}) were also shifted by the substitution. The peak at 2802 cm^{-1} may indicate a small degree of protonation to form morpholinium groups.

The major peaks in the ^{13}C-NMR spectrum also fell within 5 ppm of the calculated values. Elemental analysis of the resin gave results reasonably close to the calculated values, with a slight deficit in chlorine (-0.64%) elevating the observed proportion of carbon. During the aqueous work-up, it was noted that a small fraction of the batch of MOR1 beads (~ 0.5 mL) persistently floated in water, indicating air entrapped within the matrix.

3.6.3.6 N-Methylpiperazine (NMZ)

The reagent N-Methylpiperazine may be affixed to the resin in three ways:

(1) N-alkylation at the 2°-amine site, yielding a moiety with 2 x 3°-amines,

(2) N-alkylation at the 3°-amine site, yielding a moiety with a quaternary ammonium group and a 2°-amine group, or

(3) N-alkylation at both amine sites, yielding a moiety with a quaternary ammonium group and a 3°-amine group.

The elemental analysis results of NMZ1 (after base work-up) show a negligible amount of chlorine in the product, indicating that the expected pathway (1) was followed. The difference between calculated and observed values for hydrogen (0.39%) and carbon (2.04%), may be due to the hydrolysis of the few remaining chloromethylated sites. The nitrogen content of NMZ1 corresponds to a capacity of 3.66 meq/g of N'-methylpiperazine groups, each bearing two weak base (tertiary amine) groups. IEX analysis of this resin was not pursued.

The affixment of N-methylpiperazine has altered the position of many of the regular IR vibrations of the substrate. This included the aromatic C-H stretch (3012 cm^{-1}), the alkyl C-H stretch (2936 cm^{-1}), and the in-plane and out-of-plane aromatic C-H bends (1011 & 807 cm^{-1}). Two strong C-N stretch vibrations were also observed (1282 and 1163 cm^{-1}). Unexpected peaks at 2796 and 1675 cm^{-1} may originate from protonated ammonium groups ($pK_a \sim 8.27$, Table 2.3, Chapter 2).

The two subsequent preparations (NMZ2 and NMZ3) followed the same synthetic procedure, and were not subjected to the same rigorous analyses. Cursory IR spectra were found to be the same as the initial preparation. It was noted that a small proportion of the NMZ2 beads became light brown and glassy after drying in the vacuum oven. This glassy look disappeared when the resin was rehydrated.

3.6.3.7 Piperazine (PAZ)

Functionalisation of the resin PAZ1 resulted in the loss of the IR peaks of the polystyrene substrate, such as the in-plane and out-of-plane aromatic C-H def. peaks (1010 & 844 cm^{-1}). This vibrational damping may be due to a high degree of functionalisation. The CH_2 deformation band at 1452 cm^{-1} was particularly enhanced. The amine features were confirmed by the N-H stretch and deformation peaks (3402

and 1681 cm^{-1}), and the C-N stretch peak at 1141. The ^{13}C-NMR was consistent, with the peaks of the piperazine ring assigned ~6 ppm upfield of the calculated values.

The proportions of carbon and chlorine found by elemental analysis differ from calculated values in a complementary fashion (+4.67% C and -4.88% Cl). Crosslinking, by reaction of resin-bound piperazine groups to adjacent chloromethyl groups may account for some of this, although the strong N-H peak in the IR spectrum indicates this is not the major product. The hydrolysis of residual chloromethyl groups probably accounts for the deficit of chlorine in the resin.

3.6.3.8 Piperidine (PIP)

The high degree of functionalisation of resin PIP1 (4.07 meq/g, based on EA) has apparently shifted some of the IR peaks of the substrate, such as the aromatic C-H stretch (3016 cm^{-1}) and the CH_2 stretch (2930 cm^{-1}). The C-N stretch was found at 1153 cm^{-1}, while vibrations at 2791 and 2752 cm^{-1} probably derive from protonated ammonium groups. The ^{13}C-NMR peaks of the piperidine resin were all assigned ~5 ppm downfield of their calculated values. The elemental composition of the resin PIP1 was very similar to calculated values, with a slight excess of carbon (0.44%), balanced by the loss of chlorine.

Resin PIP2 was prepared using similar conditions to the previous batch (PIP1), however, a lower reaction temperature (80°C) was employed. After cooling, many fragmented beads were observed in this product. This was probably caused by the grinding action of the stirrer bar during synthesis. Counter-current washing of the batch of PIP2 resin resulted in the loss of ~4 mL of fine fragments from the initial sample volume (~20 mL). The PIP2 resin was presumed to have properties similar to PIP1, and was immediately used to prepare resin POP2.

3.6.4 Evaluation of Single Step Strong-Base Resins

This comprises the following strong-base resins: {ABU1, APH1, NMM1, NMM2, NMM3, NMP1, PET1, PET2, QNU1, QNU2, TBA1, TOA1, TOA2}

3.6.4.1 Tributylamine (ABU)

The presence of butyl groups is evidenced by the new aliphatic C-H stretch peaks in the IR spectrum at 2960, 2930 & 2873 cm^{-1}. The peak at 1176 cm^{-1} is believed to originate from C-N stretching. The IR vibration at 1702 cm^{-1} probably derives from a carbonyl group introduced via an oxidative decomposition process; this corresponds to the weak peaks observed in the ^{13}C-NMR at 148 & 167 ppm . The remaining ^{13}C resonances were found to be within 5 ppm of the predicted chemical shifts.

The percentage of hydrogen found in the product ABU1 was ~2.3% higher than calculated, while carbon was ~3% lower. This loss of hydrogen indicates some form of reductive process, such as elimination of 1-butene from the ammonium salt (Eqn. 3.2). Tributylamine itself contains 14.68% hydrogen, and the presence of butyl groups unaccompanied by counterions would cause an increased hydrogen content. The capacity of the resin was 2.05 meq/g by elemental analysis, but the observed IEX capacity was only 1.39 meq/g, consistent with the degradation of some strong base sites into tertiary amines.

3.6.4.2 Triphenylamine (APH)

During work-up of resin APH1, the addition of water caused the flocculation of white solids amongst the resin beads. This material, presumed to be residual triphenylamine, was removed by subsequent solvent washes. Analysis of the final resin

product by IR and IEX indicated that the product was unchanged starting material (A378). This was supported by Elemental Analysis of an anhydrous pulverised sample.

3.6.4.3 N-methylpiperidine (NMP)

During drying in vacuo, some of the resin beads became slightly darker and took on a glassy appearance. These resin beads returned to their former dull yellow appearance when permitted to rehydrate in water.

Infra-red analysis of the product NMP1 confirmed the intended structure, revealing CH_3 str. and def. peaks (2930, 1473 & 1358 cm^{-1}). Some of the backbone aromatic C-H def. vibrations were shifted (1028 & 881 cm^{-1}) due to the high degree of functionalisation. The ^{13}C-NMR spectrum also contained peaks consistent with the anticipated N-methylpiperidinium moiety.

The elemental composition of this product contains significantly less carbon than expected (-5.55% C). This believed to be caused by the presence of residual water. Despite the poor correlation with carbon, the calculated resin capacity (3.16 meq/g) agreed well with the observed IEX capacity (3.09 meq/g).

3.6.4.4 N-methylmorpholine (NMM)

As with pervious polymers, some of the beads of the NMM1 resin were observed to become darker and glassy after drying in a vacuum oven, although this change was again reversed when the resin was immersed in water for 30 minutes.

Characteristic peaks of the N-methylmorpholinium moiety were observed in the IR spectra of resins NMM1, NMM2 and NMM3. The more important of these peaks were found at 2883 cm^{-1} (CH_3 str.), 1476 & 1362 cm^{-1} (CH_3 def.), and 1124 cm^{-1}

(ether str.). Functionalisation of the resin also consistently displaced the 1,4-aromatic C-H stretch of the substrate to 890 cm^{-1}.

The ^{13}C-NMR peaks of resin NMM1 were found close to the predicted values, although the methyl carbon was found 6 ppm downfield of the predicted chemical shift. Elemental analysis of the resin found less carbon than calculated (–5.60% C), which may be accounted for by the presence of residual water and/or chloride ions. The observed IEX capacity of this resin (2.70 meq/g) was close to the value calculated from the nitrogen content (3.03 meq/g).

A number of new minor peaks were recorded in the IR spectrum of resins NMM2 and NMM3, probably due to the better quality of the KBr plate. There were no significant differences between the IR spectra of resins NMM2 and NMM3 and the first preparation (NMM1). Resin NMM3 yielded a very similar spectrum, with an additional peak at 1659 cm^{-1} that may arise from the N-H def. of a decomposition product.

The precursor resin, D2780, was employed in the preparation of NMM2 to examine the effects of differences in the swelling and hydrophilicity of the matrix, and in the size and distribution of porosity. These properties may have significant effects upon the affinity of the functionalised resin products for different ions (selectivity). This resin had an effective IEX capacity of 2.90 meq/g, close to that of resin NMM1

3.6.4.5 Piperidineethanol (PET)

The IR spectra of resins PET1 and PET2 contained common features that can be assigned to the N-(2-hydroxyethyl)piperidinium moiety. This includes peaks arising from the O-H stretch (~3350 cm^{-1}), CH_2 stretch (2933 cm^{-1}), C-O stretch (1050 cm^{-1}), and weak OH-coupled CH_2 wagging (1427 & 1365 cm^{-1}). The IR spectrum of PET2

featured an additional peak at 1661 cm^{-1} (C=O str.) derived from a minor degree of oxidative decomposition.

The various peaks of the ^{13}C-NMR spectrum of PET1 were found in positions ~5 ppm upfield of their predicted values. The EA results of PET1 indicated a deficit of carbon (-3.41% C) compared to calculated values, and the calculated capacity of 2.90 meq/g was somewhat higher than the observed IEX capacity of 2.30 meq/g. This is probably due to the fragmentation of some IEX groups (eg. via Eqn. 3.2). A similar IEX capacity was found with the second preparation, resin PET2 (2.44 meq/g).

3.6.4.6 Quinuclidine (QNU)

Numerous shattered beads were found amongst the product QNU1 after aqueous washing, probably the result of osmotic shock as the pH or solvent was rapidly changed. The second preparation (QNU2) was not washed with acid or aqueous solvents prior to IR analysis, and less shattered beads resulted in the final product.

Infra-red analysis of the products, QNU1 and QNU2, yielded similarities that also corresponded well with the reference spectrum for this resin [8]. The spectrum of resin QNU2 held additional vibrations at 1660 cm^{-1} (C=O str.), 1119 and 816 cm^{-1} (Arom. CH def.) consistent with a minor degree of oxidative decomposition.

The Carbon NMR spectrum of QNU1 was also found to be in good agreement with the reference spectrum (±1 ppm). Correlation with the predicted carbon peaks was within ~5 ppm, except in the case of the tertiary carbon (~16 ppm). Elemental analysis of QNU1 was found to be contain less carbon than calculated (-3.79% C), probably due to the effects of residual water. The calculated capacity (3.14 meq/g) was very close to the observed IEX capacity (3.07 meq/g).

3.6.4.7 Tribenzylamine (TBA)

IR and IEX analyses of resin TBA1 indicated no evidence of any significant concentration of quaternary ammonium functional groups, and were not significantly different from those of the precursor resin (A378). Elemental Analysis revealed a negligible degree of functionalisation (0.94 % N, ca. 0.67 meq/g). The steric bulk of the benzyl groups significantly impedes interaction of the central amine site with a bulky polymeric resin, resulting in a poor yield of quaternary ammonium sites.

3.6.4.8 Trioctylamine (TOA1)

The usual method of anchoring an amine group to the A378 resin was modified for the preparation of TOA resins, due to the low solubility of trioctylamine in DMF. Solubility tests (~10% v/v) established that trioctylamine is apparently soluble in diethylene glycol diethyl ether (DGDE), and tetrahydrofuran (THF). The preparation of the resin, TOA1, was performed using the glycol ether solvent, DGDE. In attempt to improve the degree of functionalisation, THF was employed as the solvent in the preparation of resin TOA2. This modification yielded similar results.

The IR spectra of TOA2 and TOA1 were very similar, showing little evidence of trioctylammonium groups. The peak at 1700 cm^{-1} (C=O str.) is reasonable evidence of an oxidative side reaction; this and the peak at ~1365 are the only features distinguishing the resins from the starting material.

The results of elemental analysis of TOA1 showed the presence of only 0.59% Nitrogen (0.42 meq/g), and slightly elevated carbon (+1.83% C). Ion exchange tests revealed both resins had an effective capacity of less than 0.25 meq/g. It was decided that the resins TOA1 and TOA2 possess no significant degree of functionalisation, and were unsuitable for subsequent testing.

3.6.5 Evaluation of Simple Methylated Derivative Resin

This comprises the following set of strong-base resins:{DAM1, TPZ1, TPZ2}. Each resin in this set was exhaustively alkylated with methyl iodide.

3.6.5.1 Methylated Diethanolamine (DAM)

The IR spectrum of resin DAM1 shared few similarities with that of the precursor resin (DEA1). The presence of methyl groups is supported by the peaks at 2929 cm^{-1} (CH_3 str.), 1425 and 1370 cm^{-1} (CH_3 def.) and 911 cm^{-1} (CH_3 rock). The peak of the C-O stretch is now found at 1050 cm^{-1} and the C-N stretch at 1088 cm^{-1}. The presence of the relatively strong peak at 1648 cm^{-1} (NH def.), also found in the precursor resin, indicates that quaternisation of the diethanolamine sites may have been incomplete. However, this may also be associated with degradation of the resin.

Most of the peaks found in the ^{13}C-NMR of product DAM1 corresponded well with the predicted values, all offset by ~5 ppm upfield. The two $HOCH_2\mathbf{C}H_2N^+$ carbons were found ~10 ppm below their predicted values, although this may be due to poor estimation of the chemical shifts of these groups by the software.

Elemental analysis of this resin gave results significantly different to the predicted results. A deficit of carbon (-7.59% C) was offset primarily by an excess of chlorine and/or oxygen (+7.19% other). This, and the slight excess of hydrogen (+0.40% H), is consistent with two mechanisms: the presence of a significant amount of residual water, and the incomplete exchange of the initial strongly bound iodide counterions with chloride. The relative mass ratio of these ions (4:1) will influence the apparent IEX capacity. This may explain the difference between the IEX capacity calculated from the elemental analysis result (as above; 2.21 meq/g), and that obtained from a conditioned sample of resin by IEX testing (Cl^- form; 3.01 meq/g).

3.6.5.2 Methylated N-methylpiperazine (TPZ)

A considerable amount of pale yellowish precipitate formed as the reaction mixture of resin TPZ2 cooled. This solid was found to be insoluble in DMF, but soluble in water, hence the resin was thoroughly washed with water. It is suspected that this solid was a mixture of quaternary ammonium salts produced by fragmentation and/or cleavage of the resin-bound functional group. This resulted from the longer reaction time (+12 hours) and slightly higher temperature (+10°C) of the second preparation. Bis(quaternary) piperazinium salts are difficult to prepare in high yield [20].

The iodide counter-ions produced during synthesis are expected to have a strong affinity for the quaternary ammonium sites [21]. Resin TPZ1 was treated with HCl (0.5 M) to exchange the iodide counter-ions with chloride. The iodide counter-ions were removed from resin TPZ2 via successive treatment with aqueous solutions of NaOH and NaCl (1.0 M), relying on mass-action ion exchange.

The IR spectra of the two products were very similar, and shared little in common to that of the precursor resin NMZ1. Evidence supporting the proposed structure were peaks at ~3015 cm^{-1} (Arom. C-H str.), 1476 cm^{-1} (CH_2 + CH_3 def.), 1220 & 1105 cm^{-1} (C-N str.), 923 cm^{-1} (CH_3 rock) and 852 cm^{-1} (1,4-Arom. C-H def.).

The carbon NMR peaks of resin TPZ2 were found within 5 ppm of predicted values, with a pair of adjacent peaks (predicted at 56 & 57 ppm) subsumed into a single peak (62 ppm). The broad nature of these peaks probably originates from the contribution of byproducts from degradation of the bis-ammonium groups. Elimination of ethylene from the tetramethylpiperazinium salt in the presence of hydroxide ions (via Eqn. 3.2) leads to a weak-base (N,N',N,-trimethylethylenediamine) moiety [20]

Elemental analysis of resin TPZ1 found 5.10% less carbon than expected, and a corresponding increase in the 'other' content, due to a combination of residual water

and degradation. The capacity calculated from the nitrogen content (4.90 meq/g) was greater than that obtained from IEX analysis (3.58 meq/g), indicating that some IEX sites were inaccessible or degraded by *Hofmann* elimination. The second preparation (TPZ2) was performed at a higher temperature and for longer, and resulted in a somewhat lower IEX capacity of 2.27 meq/g. This is believed to be due to increased thermal and/or photochemical degradation of the quaternary ammonium functional sites during the alkylation step.

3.6.6 Evaluation of Simple Benzylated Derivative Resins

This comprises the following set of strong-base resins: {DAB1, NBM1, NBP1, TBZ1}. Each resin in this set was exhaustively alkylated with benzyl chloride.

3.6.6.1 Benzylated Diethanolamine (DAB)

Treatment of the resin DEA1 with benzyl chloride caused minor changes in the IR spectrum of the product, resin DAB1. New vibrations were observed at 1287 cm^{-1} (CH_2 wag), 1040 cm^{-1} (C-O str.), and 738 cm^{-1} (CH_2 rock), although the peak at 1653 cm^{-1} ($H\text{-}N^+$ def) indicates that some weak-base groups remain as protonated ammonium salts. There was no conclusive evidence of aromatic contributions (eg. phenyl) distinct from the resin backbone.

Carbon NMR resonances were found close to predicted values. It is difficult to differentiate the presence of a benzyl group on a polystyrene substrate, as the new peaks occur very close to those of the backbone. Consequently, the CH_2 peaks of the substrate and substituent overlap and have been assigned together with the CH_2OH peaks of the bis(2-hydroxyethyl)ammonium group (58 ppm).

Excess carbon (+1.57% C) and hydrogen (+0.76% H) were found in resin DAB1, probably due to a small degree of oxidative degradation of chloromethylated sites. There is also a large discrepancy between the resin capacity calculated from the nitrogen content (2.31 meq/g) versus that obtained via IEX testing (0.59 meq/g). It is clear that less than one third of the diethanolamine sites of the resin were successfully converted into quaternary ammonium groups. It is suspected that the 2-hydroxyethyl groups hinder reaction of the amine site with the bulky alkylating agent.

3.6.6.2 Benzylated Morpholine (NBM)

The IR peaks observed in the spectrum of resin NBM1 were consistent with the proposed structure. Characteristic peaks of the morpholine resin are found at 1126 cm^{-1} (ether str.), 1352 cm^{-1} (CH_2 def.), with the 1,4-aromatic C-H def. being at 866 cm^{-1}. The peaks at 2867 cm^{-1} (CH_2 str.) and 1082 cm^{-1} (Phenyl C-H def.) provide some evidence of benzylation. There is some evidence of protonated ammonium groups (weak vibrations at 2545 & 2464 cm^{-1}), indicating some degradation of the morpholine sites.

The predicted ^{13}C-NMR spectrum was very narrow, with all non-aromatic carbon peaks between 62 – 63 ppm. The observed peaks of the carbon spectrum of product NBM1 were found within 5 ppm of this region, although an extra peak was found at 44.3 ppm – probably due to the by-product, *p*-hydroxymethyl(polystyrene).

Less carbon was found in the product that expected (-3.66% C) and more hydrogen (+0.52%), probably due to residual water and a small degree of oxidation. The capacity of resin NBM1 calculated from the nitrogen content (2.37 meq/g) was slightly greater than that found during IEX analysis (1.98 meq/g). This reflects the more restricted nature of the resin pores in aqueous solution, although some of this difference can be ascribed to weak-base functional sites.

3.6.6.3 Benzylated Piperidine (NBP)

The IR spectrum of NBP1 held few features in common with the precursor resin (PIP1), with most of the ring CH_2 and aromatic C-H vibrations found in new positions. Definitive IR vibrations of the functional groups may be subsumed into those of the backbone. There may be some cleavage of the piperidine ring, as evidenced by the relatively weak vibrations at 2673 and 2536 cm^{-1} ($H\text{-}N^+$ stretch).

The ^{13}C-NMR peaks of the product were found in the predicted positions, save for the α-carbons of the piperidine ring, which were found ~7 ppm upfield of their calculated positions. Ion exchange tests revealed a capacity of 2.25 meq/g, predictably lower than the calculated capacity of the precursor resin (PIP1, 4.07 meq/g).

3.6.6.4 Benzylated N-Methylpiperazine (TBZ)

Significant changes were observed in the IR spectrum of the resin TBZ1 when compared to the precursor resin (NMZ2). There benzyl character evident by vibrations at 1028 & 711 cm^{-1} (Phenyl C-H def.), and of methyl substitution at 1475 & 1358 cm^{-1} (CH_3 def.). The peak at 1635 cm^{-1} indicates the presence of NH groups, possibly caused by thermal decomposition of the bis-ammonium salt. Moreover, the IR spectrum of this resin is similar to that of the methylated congeners (TPZ1 and TPZ2), indicating related products (and degradation pathways). Degradation of the piperazinium ring by the elimination of ethylene yields a tetrasubstituted ethylenediamine moiety [20].

Peaks were found in the anticipated positions in the ^{13}C-NMR spectrum of TBZ1, although the benzyl carbons ($PhCH_2$) were assigned ~ 6 ppm upfield of their calculated places. An unexpected peak found at 42 ppm is probably caused by side-products (hydroxymethyl sites). The elemental composition of resin TBZ1 was not far removed from the calculated values, lacking 0.46% carbon and containing an additional

0.63% Hydrogen. The capacity calculated from this result (4.78 meq/g) greatly exceeds the observed IEX capacity of the resin (2.24 meq/g). This difference arises from incomplete alkylation and/or thermal degradation of the piperazine sites, both pathways leading to weak-base sites.

3.6.7 Evaluation of Multi-Step Alkylations

This comprises the following set of strong-base resins: {BBZ1, DTM2, ETB1, ETM2}. Each resin in this set was exhaustively alkylated in several steps. The alkylating agents utilised were benzyl chloride or methyl iodide.

3.6.7.1 Benzylated Piperazine (BBZ)

In this preparation resin PAZ1 was treated with benzyl chloride in DMF, converted to freebase form, and treated with benzyl chloride a second time. This process appears to have caused the resin to suffer a significant degree of osmotic shock. The final product (resin BBZ1) was observed to consist primarily of shattered or broken beads. IR analysis of this product showed a surprisingly large number of minor peaks, indicative of a large variety of side reactions. Some evidence of the phenyl character of the benzyl groups was found at 1083 & 750 cm^{-1} (Phenyl C-H def.). The broad peak at 2562 cm^{-1} ($H\text{-}N^{+}$ str.) and the strong peak at 1668 cm^{-1} (N-H def.) are not consistent with the intended structure, and must result from degradation of the piperazine ring. This may occur via the elimination of ethylene [20], resulting in weak-base tribenzylated ethylenediamine groups (with low pK_a).

The ^{13}C-NMR of resin BBZ1 was similar to the predicted spectrum, although all the calculated peaks fell within 5 ppm of the broad peak observed at ~58 ppm. The extra peak at 47 ppm indicates that significant side reactions have taken place.

When the elemental analysis result of resin BBZ1 was compared to calculated values, carbon was found to be deficient (-4.97% C) and hydrogen in excess (+1.06% H). This suggests the resin contains a lower proportion of benzyl groups than intended, and that the resin preparation has not been successful. The capacity calculated from the nitrogen content (3.57 meq/g) did not agree well with that found during IEX analysis (1.32 meq/g), which indicates primarily weak-base sites resulting from incomplete alkylation and/or *Hofmann* elimination. The diminished carbon content is indicative of the latter process, although some oxidation may also contribute.

The exhaustive quaternisation of free piperazine with benzyl chloride in similar conditions could not be effected, even in the presence of a sacrificial base (Section 3.2.3). The functional groups on the resin are most likely a mixture of the N-benzyl piperazine adduct and the N,N'-dibenzylated quaternary ammonium salt, and degradation products such as tetrasubstituted ethylenediamine moieties. It is apparent that the resin BBZ1 does not bear a significant capacity of the desired tribenzylated bis(ammonium) moiety.

3.6.7.2 Methylated Diethylenetriamine (DTM)

The resin DTM2 was prepared by treating the precursor resin (DET2) with methyl iodide in DMF and subsequently converting the remaining weak base groups to freebase form with NaOH. This process was repeated three times in total to ensure full alkylation, although the resin appears to have suffered a significant degree of osmotic shock as a result. After the first alkylation and caustic wash, the resin batch contained a significant amount of powder, presumably from shattered resin beads. The finer fragments (~2 mL) were removed from the final product via countercurrent flotation,

and the resin was treated with NaCl to exchange the iodide counterions for chloride before the product was analysed.

The IR spectrum contains features consistent with methylated ammonium groups, with vibrations at 1382 & 922 cm^{-1} (CH_3 def. & rock), and a trace of the diethylenetriamine skeleton, with a peak at 1476 cm^{-1} (CH_2 def.). The peaks at 1666 and 857 cm^{-1} (NH def & rock) reveal some degradation of the functional sites.

The ^{13}C-NMR spectrum of DTM2 contained a strong peaks at ~50 ppm that correlates moderately well with the predicted cluster of methyl carbon peaks. The cluster of methylene carbon peaks predicted at ~57 ppm was not found, although this may be subsumed into the peak at ~64 ppm. The unexpected peak at 45 ppm is consistent with some degradation of the functional sites.

Elemental analysis revealed a large increase in chlorine and oxygen (+11.96%), matched by a deficiency in carbon. This may be due to incomplete removal of iodide counterions. Despite this, the resin capacities calculated from the nitrogen content (3.50 meq/g) and from IEX analysis (3.57 meq/g) are in very good agreement.

3.6.7.3 Benzylated Ethanolamine (ETB)

The resin ETB1 was prepared by treating the precursor resin (ETA1) with benzyl chloride in DMF, converting the remaining weak base groups to freebase form with NaOH, and then treating resin again with benzyl chloride. The IR spectrum of the resin showed some peaks consistent with the benzylated 2-hydroxyethylammonium structure at 1055 cm^{-1} (C-O str.) and 738 cm^{-1} (Phenyl CH def.), and possibly an OH-coupled CH_2 wag at 1363 cm^{-1}. The strong peak at 1668 cm^{-1} may be due to oxidative degradation of the 2-hydroxyethylamine group (ie. C=O str. or NH def.), because a lesser peak is found in a similar position in the spectrum of the precursor resin.

Carbon-13 NMR analysis of the resin showed broad carbon peaks in positions close to the values predicted by software, but an extra peak at 42 ppm indicates the presence of by-products. The elemental analysis results were close to the calculated values, with a slight excess of hydrogen (0.70%) betraying some degraded functional sites. More importantly, the effective IEX capacity (0.49 meq/g) is much lower than that derived from the nitrogen content of the resin (2.31 meq/g).

3.6.7.4 Methylated Ethanolamine (ETM)

In this preparation, the precursor resin (ETA1) was treated with methyl iodide in DMF, then washed with NaOH to deprotonate the remaining weak base sites. The resin was then treated with methyl iodide a second time, washed with solutions of Na_2SO_4, $NaNO_3$, and NaOH, and denoted ETM2. This latter treatment was performed to ensure the complete removal of the strongly bound iodide ions.

Methylation of the resin was confirmed by vibrations in the IR spectrum at 2945 and 2862 cm^{-1} (CH_3 str.), and at 1376 cm^{-1} (CH_3 def.). The product held few peaks in common with the precursor resin, with the C-O stretch moved from 1053 to 1093 cm^{-1}. The peak at 1660 cm^{-1} is associated with some oxidative degradation of the 2-hydroxyethylamine group. The broad peaks in the ^{13}C-NMR spectrum fell close to the predicted values, but the $\mathbf{C}H_2N^+$ peaks were assigned ~7 ppm further upfield. A small peak at 52 ppm is probably due to oxidation of some functional groups.

Discrepancies between the results of elemental analysis and the calculated values (C: -5.87%, and H: –0.53%) may derive from some oxidation of the resin. The effective IEX capacity (2.74 meq/g) was reasonably close to that calculated from the nitrogen content found by elemental analysis (3.05 meq/g).

3.6.8 Evaluation of TET Resin and Derivatives

This comprises the following set of resins: {TET1, TET2, TET3, TEM1, TEB1}, each being a derivative of 1,3,5-triethylhexahydro-1,3,5-triazine.

3.6.8.1 1,3,5-triethylhexahydro-1,3,5-triazine (TET)

The IR spectra of the three preparations (TET1, TET2 & TET3) were very similar, each showing features characteristic of this treatment. Consistently, peaks were found at 2925 cm^{-1} (CH_2 str.), 1216 ,1172 & 1095 cm^{-1} (C-N str.), and 760 cm^{-1} (CH_2 rock). Evidence of the degradation of some triazine functional sites into weak base groups is evident in all three resins. The IR spectrum of TET1 contained vibrations at 2786 cm^{-1} ($H\text{-}N^+$ str.) and 1684 cm^{-1} (N-H def.), while TET2 features a vibration at 2665 cm^{-1} ($H\text{-}N^+$ str.), and TET3 shows a vibration at 1636 cm^{-1} (N-H def.).

The predicted ^{13}C-NMR corresponded reasonably well with the observed spectrum of resin TET1. However, the resonances of the triazine ring carbons were not observed in the expected position (72 ppm). These signals may be lost beneath the shoulder of the broad peak at 60 ppm, although cleavage of the sterically strained triazine ring would also explain the loss of these peaks.

The capacity calculated from elemental analysis of TET1 (1.31 meq/g strong base groups) was far below the initial IEX analysis result of 3.64 meq/g. This unexpectedly high capacity may be due to fragmentation of the unstable TET functional group into simpler ammonium groups. Subsequent IEX testing of this resin after one and four months yielded capacities of 3.23 and 1.31 meq/g, respectively. It is evident that the resin group (in hydrated state) is prone to oxidative decomposition in storage due to the actions of light, air and water. The same behaviour was noted in resin TET2: the capacity from nitrogen content (1.16 meq/g) being lower than that obtained through

IEX analysis (3.33 meq/g). Four months later, the IEX capacity had fallen to only 1.05 meq/g. Resin TET3 was prepared using a shorter reaction time, and the corresponding IEX capacity was initially found to be 1.77 meq/g.

3.6.8.2 Methylated TET (TEM)

The IR of resin TEM1 lacked any distinctive features of a methylated quaternary ammonium group. The weak peak at 2697 cm^{-1} ($H\text{-}N^+$ str.) reveals the degradation of the functional groups. The carbon-13 NMR is moderately consistent with the predicted spectrum, with the triazine ring carbon peak found at 74 ppm. This is not consistent with the predicted peaks around ~88 ppm, and confirms that the IEX sites were not converted to the desired tris(quaternary ammonium) groups. The resin was also found to contain less carbon than calculated (-2.48%), probably due to oxidation and elimination reactions. The nitrogen content gave a calculated capacity of (3.01 meq/g), whereas the observed IEX capacity was far lower (0.85 meq/g). Most of this is believed to derive from small strong base groups, derived from fragmentation of the TET moiety during the methylation step (see Section 3.6.2.1)

3.6.8.3 Benzylated TET (TEB)

There were no definitive signs of the presence of a benzylammonium group in the IR spectrum of resin TEB1. The weak peak at 2613 cm^{-1} ($H\text{-}N^+$ str.) indicates the presence of weak base groups derived from degradation of the functional sites. Analysis by carbon NMR revealed peaks similar to the predicted spectrum, with an additional resonance evident at 43 ppm. The triazine ring carbon signal predicted at 87 ppm could not be found. Elevated levels of carbon (+5.68%) and hydrogen (0.79%) in the resin are a result of substantial degradation of the functional sites. This is confirmed by

comparing the resin capacity calculated from elemental analysis (2.76 meq/g) with that found by IEX analysis (1.86 meq/g).

3.6.9 Evaluation of TBT Resin and Derivatives

This comprises the following set of resins: {TBT1, TBT2, TBT3, TBM2, TBB2}, each being a derivative of 1,3,5-tribenzylhexahydro-1,3,5-triazine.

3.6.9.1 1,3,5-tribenzylhexahydro-1,3,5-triazine (TBT)

Common features in the IR spectra of resins TBT1, TBT2 and TBT3 were found at 1605 cm^{-1} (Arom. C-C str.), 1308 & 1105 cm^{-1} (C-N str.). Each product also featured a peak around ~1370 cm^{-1}, tentatively assigned as a benzyl CH_2 wag. The strong peak at 1674 cm^{-1} found in each product originates from the NH def. of a fragmented functional group. The products TBT1 and TBT3 also featured NH^+ stretch peaks at 2785 and 2704 cm^{-1}.

The ^{13}C-NMR spectrum of resin TBT1 was entirely consistent with the predicted spectrum, including the triazine ring carbons at 76 & 81 ppm.

Elemental analysis of resin TBT1 was less consistent with calculated results, finding excess carbon (+4.27%) and hydrogen (+0.64%) indicating functional group degradation, eg. via substitution (Eqn. 3.3). The observed IEX capacity (2.09 meq/g) was initially greater than that derived from the nitrogen content (1.10 meq/g), probably due to rearrangement of functional sites in a similar fashion to resin TET1 (Section 3.6.5.1). Four months later, the capacity of the same resin had fallen to 1.67 meq/g, as these unstable IEX sites decomposed in storage. Similar results were found when resin TBT2 was examined by elemental analysis (0.88 meq/g) and IEX testing (1.67 meq/g). This resin also contained more carbon (+1.79%) than calculated.

3.6.9.2 Methylated TBT (TBM)

This resin retained many features of the precursor resin (TBT2) in the IR spectrum, including the by-product peak at 1673 cm^{-1}. There was little clear evidence of methylation of the weak base sites, with only the peaks at 1376 cm^{-1} (CH_3 def.) and 916 cm^{-1} (CH_3 rock) providing any indication. The absence of the expected triazine ring peaks (~91 ppm) from the carbon-13 NMR spectrum and the poor fit of the Ph**C**H_2 peaks indicates significant decomposition of the functional groups. The unexpected peak at 7 ppm is probably the β-carbon of an alkylammonium degradation product. Elemental analysis of resin TBM2 showed a theoretical capacity of 2.09 meq/g, based on the nitrogen content, reasonably close to the 1.57 meq/g found by IEX testing. These IEX groups are probably the result of the fragmentation of the triazine ring.

3.6.9.3 Benzylated TBT (TBB)

There were no peaks in the IR spectrum that definitively confirm the presence of the intended tris-ammonium moiety. Vibrations associated with by-products were found at 1691 and 1678 cm^{-1} (C=O str. or N-H def.), and at 1088 cm^{-1} (also found in resin TBM2). The latter is probably due to the C-N stretch of a common decomposition product. The ^{13}C-NMR spectrum of TBB2 also correlated quite poorly with the predicted peaks. Extra peaks from degradation products were found at 44 & 56 ppm, and the triazine ring carbons (expected at ~ 90 ppm) were absent.

Elemental analysis showed a theoretical capacity (2.23 meq/g) far greater than the observed IEX capacity (0.80 meq/g). It can be inferred from the results of the treatment of monomeric piperazine with benzyl chloride in DMF (Section 3.6.2.2) that the product TBB2 is unlikely to have been exhaustively alkylated. The spectra recorded are more consistent with decomposition via fragmentation of the triazine ring.

3.6.10 Evaluation of Imidazole Resin and Derivatives

This comprises the following set of resins: {IMZ1, IMZ2, BIM1, MIM2}, each being a derivative of imidazole.

3.6.10.1 Imidazole (IMZ)

The IR spectra of the two products (IMZ1 & IMZ2) were nearly identical, showing signs of the imidazole group at 1668 and 1603 cm^{-1} (conjugated C=C str.), 1559 cm^{-1} (C=N str.), and a suspected alkene C-H rock at 663 cm^{-1}. A vibration due to alkene C-H stretching (3054 cm^{-1}) was observed in the second preparation (IMZ2).

^{13}C-NMR analysis of IMZ1 did not correlate well with the peaks predicted at 51 ppm (**C**H_2*PS*) and 119 ppm (**C**HN). The former was assigned at ~58 ppm, and the imidazole ring carbons were subsumed in the aromatic shoulder at 123 ppm. The unexpected peak at 45 ppm is probably a product of functional site degradation. Elemental analysis of resin IMZ1 yielded results within 0.2% of the calculated values.

3.6.10.2 Benzylated Imidazole (BIM)

The IR spectrum of resin BIM1 apparently retained the conjugated C=C and C=N stretch peaks of the heterocyclic structure (1653, 1616, and 1558 cm^{-1}). Many of the peaks differed from those of the precursor resin (IMZ1), but there was little clear evidence of benzylation.

The ^{13}C-NMR spectrum of this resin was not as predicted, with the **C**H_2Ph peak expected at 60 ppm assigned ~9 ppm upfield, and the resonances for the heterocyclic carbon atoms were not found in their anticipated positions (~124 - 138 ppm). The predicted spectra may be inaccurate in this latter case, as the software used to predict the spectra could not simulate the delocalised charge of the imidazolium salt.

Less carbon (-3.56%) and more hydrogen (+0.81%) was found in the resin BIM1 than was expected, probably due to some degradation of the resin via oxidation, or elimination and rearrangement of the moiety (via Eqn. 3.2). Despite these results, the resin capacity calculated from the nitrogen content (2.26 meq/g BIM) was very close to the measured IEX capacity (2.22 meq/g).

3.6.10.3 Methylated Imidazole (MIM)

The conjugated C=C stretch peaks of the group of the precursor resin (IMZ2) were absent from the IR spectrum of resin MIM2, although a strong C=N peak was present at 1561 cm^{-1}. The vibration at 3138 cm^{-1} is probably the C-H stretch of the imidazolium ring. Many of the peaks differed from those of the precursor, and there were indications of methylation at 1424 & 1341 cm^{-1} (CH_3 def.).

Analysis of this resin by ^{13}C-NMR indicated that the **C**H_2*PS* peak was moved ~7 ppm upfield, while the methyl groups were obscured by the resonances of the resin skeleton. This spectrum was similar to resin BIM1, with low confidence in the predicted values of the imidazolium ring carbon peaks (123 – 139 ppm).

Resin MIM2 contained less carbon (-4.63%) and more hydrogen (+0.56%) than calculated, as was found with the benzylated analogue (BIM1). This is consistent with some degradation of the resin or imidazolium moiety. The observed IEX capacity of this resin (3.13 meq/g) exceeded that calculated from elemental analysis (2.73 meq/g). The surplus IEX capacity indicates the presence of some strong base groups derived from fragmentation of the imidazole group.

3.6.11 Evaluation of TMEDA Resin and Derivatives

This comprises the following set of resins: {TME1, TME2, TME3, BME1 PME2}, each being a derivative of N,N,N',N'-tetramethylethylenediamine.

3.6.11.1 Tetramethylethylenediamine (TME)

Some of the beads of resin batches TME1 and TME2 became darker and glassy whilst drying, although this was reversed when the resins were allowed to rehydrate for an hour. It is possible that the TMEDA group could become crosslinked, by reaction with an adjacent chloromethyl site, to form a bis-ammonium salt.

A number of common features were found in the IR spectra of TME1 and TME3, particularly the vibrations at 2925 cm^{-1} (CH_2 str.) 1477 and 1425 cm^{-1} (CH_3 def.),and 1190 cm^{-1} (C-N str.). Only the vibrations at 1220 cm^{-1} (C-N str.) and 859 cm^{-1} (CH_3 rock) were held in common with resin TME2. All the resins displayed broad peaks around 2800 – 2450 cm^{-1} ($H\text{-}N^+$ stretch) that are thought to originate from ammonium group degradation products. Resin TME2 also showed signs of weak-base character at 1641 cm^{-1} (N-H def.).

^{13}C-NMR analysis of resin TME1 agreed reasonably with the simulated spectrum. However, the resin carbon content was greater than calculated (+3.02%), and the theoretical capacity (2.51 meq/g) was significantly greater than the observed IEX capacity (1.83 meq/g). It is clear that some of the functional groups on the resin have decomposed, possibly caused by washing the resin with relatively strong HCl (0.5 M).

Although the elemental analysis result fits well with expectation, the calculated capacity of resin TME2 (2.47 meq/g) was lower than the IEX result (3.72 meq/g). This data, and the differences in the IR spectrum of this resin, indicate that side reactions are significant in this product. There may be some degree of crosslinking, by reaction of the

pendant weak-base groups (-$CH_2CH_2NMe_2$) with residual chloromethylated sites, increasing the effective IEX capacity. The resin capacity diminished to 3.50 meq/g on standing over four months, probably due to *Hofmann* degradation (Eqn. 3.2).

The resin TME3 was treated with TMEDA for less than one third of the time that the other resins, and had a more reasonable IEX capacity of 2.15 meq/g.

3.6.11.2 Benzylated Tetramethylethylenediamine (BME)

The precursor for resin was a mixture of TME1 & TME2 resins, and the IR spectrum of BME1 shares a number of peaks with these resins. There were no definitive peaks demonstrating successful benzylation. There was also some evidence of protonated ammonium groups (N-H^+ str. at 2639 cm^{-1}) produced by degradation of the functional group.

The peaks of the ^{13}C-NMR spectrum of resin BME1 were similar to those of the predicted spectrum, but shifted upfield by ~5 ppm. The symmetry of the model structure makes the calculated spectrum simpler than the resin-bound analogue, resulting in more resonances in the recorded spectrum. Some functional group decomposition is evident from the elemental analysis of the resin (+2.01% carbon). The difference between capacity derived from this (3.63 meq/g) and the IEX analysis (2.27 meq/g) is primarily due to the presence of weak base sites.

3.6.11.3 Methylated Tetramethylethylenediamine (PME)

A combined batch of resins TME1 and TME2 was used to prepare resin PME2. This sample of TME resin (8 mL) was calculated to have ~10.1 mmol tertiary amine groups (based on EA, 7.04% N), and was treated with an excess of iodomethane.

The IR spectrum of resin PME2 featured numerous peaks) in common with the benzylated congener (BME1), such as the peaks at 1425, 1384 and 922 cm^{-1} (CH_3 def. & rock). The peak at 1082 cm^{-1} in both resins may be due to a C-N stretch. It is difficult to confirm the presence of an additional methyl group in this resin. However, the peaks of the ^{13}C-NMR spectra were found within 3 ppm of the predicted peaks.

The elemental analysis of resin PME2 revealed a 14.31% shortfall in carbon, compared to calculated values, indicating the presence of residual iodide counterions and/or substantial oxidative degradation. The capacity calculated from the nitrogen content (3.28 meq/g) was lower than the observed IEX capacity (3.83 meq/g). This result indicates rapid degradation of the functional sites has occurred in the pulverised resin, with loss of volatile amine compounds resulting in a diminished nitrogen content.

3.6.12 Evaluation of Triazamacrocycle Resin and Derivatives

This comprises the following set of resins: {DSU1, DST1, DTP1, DBP1, DMP2}. These were prepared in the following sequence:

DSU1 → DST1 → DTP1 → DBP1 & DMP2.

3.6.12.1 Diethylenetriamine Bis(salicylidene) (DSU)

This synthesis utilises the reagent *Dien(Sal)*$_2$, (Section 3.2.2), employed in a modification of the Schiff-base resin preparation reported by Suzuki & Yokayama [11]. The resin product, DSU1, was used shortly after preparation, and was not studied by NMR, IR or IEX prior to hydrolysis into resin DST1.

3.6.12.2 N'-Diethylenetriamine (DST)

The hydrolysis procedure for the Schiff-base resin DSU1 is based on the method employed by Suzuki & Yokayama [11]. After hydrolysis with hydrochloric acid, the resin DST1 was washed with aqueous NaOH to deprotonate the ammonium groups. This process released a great deal of yellow material from the resin into the solutions, including residual Dien(Sal)$_2$ and salicylaldehyde. Subsequent washes with ethanol did not release any further coloured matter from the resin.

The IR spectrum was consistent with the anticipated structure, with a strong peak at 1632 cm^{-1} caused by primary N-H bending, and C-N stretching peaks at 1279 and 1150 cm^{-1}. However, the ^{13}C-NMR spectrum of this resin was not as expected. The **C**H$_2$N$^+$ peaks expected around ~63 ppm were assigned ~10 ppm upfield of the theoretical value, and an unknown peak was present at 48 ppm. There was also some evidence of salicylaldehyde residues at 114 ppm (**Ar**OH), but little evidence of imine H**C**=N peaks (~166 ppm). Elemental analysis found more carbon (+1.90%) than expected, supporting the presence of aromatic residues.

3.6.12.3 Glutaraldehyde Crosslinked N'-Diethylenetriamine (DTP)

EA results show that the batch of precursor resin, DST1, contained 47.9 mmol RNH$_2$ groups. A slight excess of the crosslinking agent (glutaraldehyde, 27.6 mmol) was applied to permit complete alkylation, prior to in-situ reduction of the imine. This preparation left a yellow residue in the product that was soluble in aqueous base. This material is likely to be a mixture of reduction byproducts of glutaraldehyde. After extensive washing, the yellow solute was flushed from the resin (DTP1) with 1.0 M NaOH at ~1 mL/minute over four hours, as indicated by a colourless eluate.

IR analysis of resin DTP1 confirmed the presence of NH groups by the vibrations at 3365 cm^{-1} (N-H str.) and 1672 cm^{-1} (N-H def.). There were few other peaks of significant diagnostic value, although the alkyl C-H stretch peaks (2950 – 2850 cm^{-1}) differed considerably from the precursor. Polymerisation of glutaraldehyde is know to form hydroxylated polymers that may also have occurred as side-reaction products in this preparation, and complicated the spectrum.

Carbon NMR analysis of DTP1 yielded resonances relatively close to predicted values, although the peaks in the alkyl region (~30 – 60 ppm) were particularly broad. The minor peak at ~121 ppm may be due to reduction byproducts. The elemental composition of the resin was deficient in carbon (–5.22%) and hydrogen (-0.85%) due to the presence of oxygen in side-reaction products of glutaraldehyde.

3.6.12.4 Methylated DTP1 (DMP)

Resin DMP2 retains the IR stretch peaks of the CH_2 groups of the crosslinking treatment (2927 & 2859 cm^{-1}). The presence of methyl groups is suggested by the strong vibration at 1384 cm^{-1}, although there are also signs of residual NH groups (1671 & 855 cm^{-1}). Analysis by ^{13}C-NMR found the $\mathbf{C}H_2N^+$ carbons at ~57 ppm, downfield from the predicted ~52 - 54 ppm. An extra resonance at ~40 ppm (also found in resin DTP1) may be a shoulder of the broad PS backbone resonance, or a component of polymeric glutaraldehyde residues. Elemental analysis found less carbon (-8.63%) and hydrogen (-1.06%) than calculated, indicating the presence of oxygen in side-reaction products of glutaraldehyde. The nitrogen content yielded a capacity (3.72 meq/g) significantly higher than the observed IEX capacity (2.70 meq/g), indicating that not all the nitrogen present in the resin was found as the expected strong base groups.

3.6.12.5 Benzylated DTP1 (DBP)

The IR spectrum of resin DBP1 was distinct from that of the precursor (DTP1) but contained no clear evidence of benzylation. There were signs of NH groups present at 1653 cm^{-1} (N-H def.) and 845 cm^{-1} (N-H rock), however, these must originate from degradation of the functional group (Eqns. 3.2 – 3.3). The resonances found in the ^{13}C-NMR spectrum approximated the predicted values of the intended macrocyclic tris(quaternary ammonium) structure, overlaid on the characteristically broad PS backbone resonance.

The difference between the capacity of the resin calculated from nitrogen content (3.67 meq/g) and IEX testing (1.40 meq/g) indicates the decomposition of the functional group. This group was clearly unstable, as the IEX capacity had fallen to only 0.51 meq/g one month later. This is attributed to rapid eliminative degradation of the initial tris(quaternary ammonium) moiety (via Eqns. 3.2 – 3.4).

3.6.13 Evaluation of Piperidine N-Oxide and TPY Resins

This comprises the following two resins: {POP2, TPY1}

3.6.13.1 Piperidine N-oxide (POP)

This resin was prepared according to known procedures [12]. The IR spectrum of resin POP2 was substantially different to that of the piperidine resin PIP1. There was evidence of the proposed N-oxide moiety in the strong vibrations at 1560 cm^{-1} (3°-N=O str.) and 1376 cm^{-1} (N=O dimer str.). The numerous minor peaks indicate a small degree of oxidative decomposition of the piperidine ring.

Analysis by ^{13}C-NMR revealed resonances very similar to those of the predicted spectrum, but elemental analysis revealed significantly less carbon than expected

(-5.13%), probably due to oxidative degradation in the bulk resin. The initial IEX capacity (2.26 meq/g) was greater than that calculated from the nitrogen content (1.93 meq/g). This is unusual in itself, as the N-oxide group carries no formal charge for ion exchange. Degradation of the functional sites was evident as the IEX capacity fell to 1.80 meq/g one month later, and to 0.87 meq/g after a further 3 months. Amine oxides such as POP2 may undergo elimination of an alkene and formation of a hydroxylamine resin, via the *Cope* reaction (Eqn. 3.7)[13].

$$(\text{Polymer})CH_2R_2N{=}O + OH^- \ (\Delta)\rightarrow \ (\text{Polymer})CH_2RNOH + \text{alkene} \qquad (3.7)$$

3.6.13.2 2,4,6-Tris(2-pyridyl)-1,3,5-triazine (TPY)

The final reaction mixture consisted of yellow polymer beads (TPY1) buried in voluminous pale yellow precipitate. This was standing under a dark green liquor, with some yellowish crystallisation on the flask walls. It appears that treatment of the resin in DMF at elevated temperature has caused the pulverisation of a significant fraction of the beads. This may be caused by osmotic shock as the resin swelled due to the formation of quaternary ammonium groups. Resin TPY1 became significantly more yellow after washing with hydrochloric acid (0.5 N). The presence of this chromophore may indicate significant decomposition of the moiety.

The IR spectrum of this resin revealed numerous peaks indicative of degradation or side-reactions, such as the strong peak at 1721 cm^{-1} (C=O str.). Due to the substantial physical damage to this resin and the small volume remaining, the product TPY1 was not examined by NMR, elemental analysis or IEX analysis.

3.7 Summary and Conclusions

The common approach used for the synthesis (DMF at 100°C for 7 days) and work-up procedures in this chapter gave a common control on the side-reactions and effects of this treatment on the resin. However, the side-reactions and degradation processes of the individual functional groups could not be controlled in such a fashion. Optimisation of each individual reaction was beyond the scope of this project, so a summary of the pertinent results is warranted.

3.7.1 Viable Resin Preparations

Most preparations resulted in resins with IEX capacities greater than 1.0 meq/g (Table 3.3). Many of the preparations yielded resins with reasonably high effective IEX capacities (~3.0 meq/g: eg. QNU1), in a similar range to commercial products such as Dowex-1, IRA-410 and Amberlite A26.

Characterisation of the functional groups was difficult due to the natural broadening of polymeric ^{13}C-NMR resonances, and the shortage of definitive IR bands for quaternary ammonium salts in general. Elemental analysis and determination of the effective IEX capacity of the product was required to support the proposed reaction scheme in many cases.

Most of the functionalised resins prepared in this work have not been reported in the literature, although it is likely that resins bearing similar structures have been examined in proprietary commercial research. The functionalisation schemes applied in this chapter should apply to comparable chloromethylated polystyrene substrates. A series of recommendations for improvement of resin synthesis and handling procedures is provided in Section 6.1.2. Most of the resins prepared herein have properties that may

be influenced by the common substrate (A378) employed in synthesis, and also by the procedures applied in preparation and work-up.

The two substrates used for the preparation of N-methylmorpholinium resins (A378 → NMM1, and D2780 → NMM2) yielded resins with similar IEX capacities. Their behaviour in leaching tests (Chapter 4) will determine if the two substrates are significantly different in their affinity with the anions of interest.

3.7.2 Problematic Resin Preparations

The difficulty in titration (Section 3.6.1.7) reveals poor kinetics, and is considered reasonable evidence of lower porosity relative to commercial products. However, this is believed to be a product of the common synthesis procedure, and hence comparative analysis of the various resins is still valid.

The simplified reaction schemes for most resins (S_N2-alkylation in most cases) leaves few side-reactions available to complicate characterisation. The extent of an alkylation reaction was assessed by the discrepancy between the results of IEX and nitrogen content by Elemental Analysis (IEX/EA %). This was most apparent the benzylated resins {ETB1 (21%); DAB1 (26%); BBZ1 (37%); DBP1 (38%); TBZ1 (47%); BIM1 (49%); BME1 (63%) and NBM1 (84%)}. The presence of weak-base groups due to incomplete alkylation complicated the IR spectra of most of these resins.

Methylated derivatives did not follow this trend, although several resins {DMP2 (73%); TPZ1 (73%) and ETM2 (90%)} showed lower IEX capacities than calculated. Some loss of effective IEX capacity may also derive from sites inaccessible to the bulk solution, due to limitations of the swollen resin matrix. Several high-capacity single-step resin preparations also showed a low IEX/EA ratio {ABU1 (68%); TME1 (73%); PET1 (79%) and NMM1 (89%)}, consistent with this effect.

Some of the functional groups attempted were reasonably fragile. Hexahydro-1,3,5-triazine resins (TET and TBT) showed evidence of rapid degradation, with fragmentation of the triazine ring resulting in a low IEX capacity relative to the nitrogen content {TET1 (35%); TBT1 (53%); TBT2 (53%)}. This trend followed to their alkylated derivatives{TEM1 (28%); TEB1 (67%); TBB2 (36%) and TBM2 (75%)}. Several of these resins lost IEX capacity on storage, and it is possible that the triazine ring may even decompose in the leach solution (pH ~10).

A few resins showed an IEX capacity greater than EA results would suggest. In the case of resins PME2 (117%) and TME2 (151%), this appears to be caused by some bridging of chloromethyl sites by the diamine reagent (TMEDA). The surprisingly high IEX capacity of resins POP2 (117%), MIM2 (115%), and DAM1 (136%) can only be ascribed to degradation of the functional groups, via elimination of alkyl fragments and/or rearrangement resulting in low-mass quaternary ammonium groups. These degradation products were not readily characterised, due to their minor presence relative to the intended functional group.

Lower levels of carbon than expected were found in many products, consistent with elevated levels of oxygen in the products. Some resins were poorly characterised due to significant oxidative degradation of the resin during synthesis or work-up. The carbonyl peaks noted in the IR spectra of the control resin A2 ($\bar{\nu}$ = 1665, 1718 cm^{-1}) apparently originate from uncharacterised oxidative degradation, and appeared to some degree in most products. Chloromethylated sites may be oxidised to carbonyl groups (aldehyde or carboxylic acid) at elevated temperatures in the presence of amine oxides [13]. A proposed reaction sequence for this oxidation is shown below (Eqn. 3.8).

$$(\text{Polymer})CH_2Cl \rightarrow (\text{Polymer})CHO \rightarrow (\text{Polymer})CO_2H \qquad (3.8)$$

The elimination of chlorine was sometimes identified by Elemental Analysis, such as in resins A2, NMZ1, ETA1, and NBM1. Some degree of hydrolysis of the chloromethyl groups of the precursor resin (A378) is evident (Eqn. 3.1), perhaps compounded by subsequent treatments (Equations 3.2 – 3.4). Most perturbations of the elemental analysis results appears to be derived from oxidation, or the presence of recalcitrant counter-ions (eg. I^- on DAM1).

Alkyl fragments may be eliminated from quaternary ammonium groups as alkyl halides (Cl^- form, Eqn. 3.3) or alkenes (particularly in OH^- form, Eqn. 3.2). The latter give rise to possible alkene vibrations in the IR spectra ($\bar{\nu}$ = 1640 – 1675 cm^{-1}), although this identification is not definitive. Storage of resins in the hydroxide form also complicated characterisation due to the broad O-H vibrations in the IR spectrum, and some loss of IEX capacity by alkene elimination. Fragmentation of quaternary ammonium functional groups by the elimination of tertiary amines, alkenes, alkyl halides, or by oxidation, leads to moieties with little or no IEX character at the high pH of leach liquors (ie. NR_3, $R_2C{=}CR_2$, RCHO and RCOOH groups). The degradation of the resins in this fashion often led to relatively poor correlations between EA results and functional capacity. The effective IEX capacity of each resin was used throughout to evaluate the behaviour of the functional groups.

References:

1. Sommer, H.Z., Lipp, H.I., and Jackson, L.L., "Alkylation of amines. A general exhaustive alkylation method for the synthesis of quaternary ammonium compounds."; *J. Org. Chem.*, **36**(6): 824-828; 1971.
2. Santini, R., Griffith, M.C., and Qi, M., "A measure of solvent effects on swelling of resins for solid phase organic synthesis"; *Tetrahedron Letters*, **39**: 8951-8954; 1998.
3. *pKa* software version 4.56, ACD/I-Lab service (www.acdlabs.com); Advanced Chemistry Development (ACD) Inc. (Toronto, Canada), 2001.
4. Colman, D.M., "Determination of low chlorine concentration in plastics"; 5 pp.; U.S. Atomic Energy Commission (Livermore, California, USA), 1958.
5. de Medina, H.L., de Vargas, M.C., Marin, J., Pirela, D., "Determination of total nitrogen in water samples by means of high-pressure bombs and ion chromatography"; *J. Chromatogr. A*, **671**: 287-293; 1994.
6. de Vargas, M.C., de Medina, H.L., Villalobos, E., Gutierrez, E., "Determination of total nitrogen in sediments by using high-pressure bombs and ion chromatography"; *Analyst*, **120**(March): 761-763; 1995.
7. Harris, D.C., *Quantitative Chemical Analysis.*, 6th Edition.; W. H. Freeman & Co. (New York), 2003.
8. Dicinoski, G.W., *Syntheses of anion exchange resins selective for gold and silver cyanide complexes*; PhD. Thesis (Chemistry); 437 pp.; Central Queensland University (Rockhampton, Queensland, Australia), 1995.
9. *PKAS* software (FORTRAN); Motekaitis, R.J., 1991.

10. Coleman, W.M. and Taylor, L.T., "Pentadentate ligands. I. Nickel(II) complexes of the linear schiff base ligands derived from substituted salicylaldehydes and diethylenetriamine and 2,2'-bis(aminopropyl)amine.";
Inorg. Chem., **10**(10): 2195 - 2199; 1971.

11. Suzuki, T.M. and Yokoyama, T., "Preparation and complexation properties of polystyrene resins containing diethylenetriamine derivatives.";
Polyhedron, **3**(8): 939 - 945; 1984.

12. Leadbeater, N.E. and van der Pol, C., "Preparation of resin-bound amine N-oxides and demonstration of their use in synthetic carbonyl cluster chemistry.";
Chem. Comm., (7): p. 599-600; 2001.

13. March, J., *Advanced Organic Chemistry*, 4th edition.; John Wiley & Sons (New York), 1992.

14. Fung, Y.S. and Dao, K.L., "Elemental analysis of chemical wastes by oxygen bomb combustion - ion chromatography"; *Anal. Chim. Acta*, **334**(1-2): 51-56; 1996.

15. *AAS Analytical Methods Manual*; Publication No. 05-100009-00;
Varian Australia Pty. Ltd. (Mulgrave, Victoria, Australia), 1989.

16. Harland, C.E., *Ion Exchange: Theory and Practice*, 2nd.Edition;
The Royal Society of Chemistry (Cambridge, UK), 1994.

17. Stewart, J.M. and Young, J.D., *Solid Phase Peptide Synthesis*.; W.H. Freeman & Co. (New York), 1969.

18. *ChemWatch* MSDS database (www.chemwatch.com.au); Chemwatch (Caulfield North, Victoria, Australia), 2002.

19. Sommer, H.Z. and Jackson, L.L., "Alkylation of amines. A new method for the synthesis of quaternary ammonium compounds from primary and secondary amines."; *J. Org. Chem.*, **35**(5): 1558-1562; 1969.

20. Kerwin, J.F., Hall, G.C., Macko, E., McLean, R.A., Fellows, E.J., Ullyot, G.E., "Adrenergic blocking agents. IV. β-haloethylammonium compounds"; *J. Am. Chem. Soc.*, **73**(December): 5681-6; 1951.

21. Breadmore, M.C., Macka, M., Avdalovic, N., Haddad, P.R., "On-capillary ion-exchange preconcentration of inorganic anions in open-tubular capillary electrochromatography with elution using transient-isotachophoretic gradients. 2. Characterisation of the isotachophoretic gradient."; *Anal. Chem.*, **73**: 820-828; 2001.

4. Performance of Resins in Leach Liquors

In Chapter 3, a large set of resins were prepared and characterised in terms of functional group and IEX capacity. In this chapter, an evaluation of the affinity of each novel resin for gold in the target environment (ammoniacal thiosulfate leach liquors) was made. This was achieved by monitoring the concentration of gold in a standard test solution before, during and after a batch of adsorbent (resin) was added. This procedure was intended to be a screening test, from which the more promising products could be identified and directed to more rigorous evaluation. The degree of gold sorption may then be related to the IEX capacity of each resin, and hence a relationship can be drawn between the structure of each functional group and its' affinity (and selectivity) for the aurothiosulfate complex. This process can elucidate structural features and trends which favour the selective adsorption of this complex from ammoniacal thiosulfate leach liquors. The elution of gold from a number of resins was also examined, using nitrate and thiourea eluents (Section 4.3).

Each novel resin produced was examined in a *Bottle Roll Test,* in which a known mass of resin was contacted with a fixed volume of artificial thiosulfate leach liquor with vigorous agitation. Small samples of known volume were taken at fixed intervals to follow the distribution of gold between the solution and the adsorbent. Bottle Roll (herein denoted B/R) Tests are a standard procedure for the testing of an adsorbent in a hydrometallurgical process, and are used extensively in research and industry. Although such tests do not necessarily reflect the conditions in which a resin may eventually be applied, they allow direct comparison of the fundamental chemical properties of the adsorbents in common experimental conditions. When normalised relative to the IEX capacity, the best performing adsorbents can be identified and directed toward further development.

4.1 Equipment and Apparatus

4.1.1 Common Reagents and Conditions

De-ionised water was used in all the experiments described in this Chapter, unless specified otherwise. Ambient laboratory temperature was approximately 18°C (± 5°C). Prior to use, all glass sample vials were soaked in concentrated aqua regia (a 1:1 mixture of concentrated HCl and HNO_3) for several minutes, then thoroughly rinsed with water, and oven-dried at 80 - 100° C. The polyethylene bottles and caps were similarly rinsed with aqua regia, then soaked in three batches of water for an hour each, and oven dried at 40° C for several days.

Gold standards in a hydrochloric acid matrix were prepared from an AAS standard solution of Au (1015 ppm) in 5% HCl (w/w) (*Aldrich*). These were acidified with small volumes of concentrated aqueous HCl (AR, 32 %, *BDH*). Pure trisodium aurothiosulfate dihydrate ($Na_3[Au(S_2O_3)_2].2H_2O$, 99.9%, *Alfa-Aesar*) was used to prepare gold standards in the ammoniacal thiosulfate matrix, and to prepare the artificial leach liquors for Bottle-Roll Tests. Copper was introduced to the leach liquor as $Cu(NO_3)_2.2½H_2O$ (AR, ≥ 96%, *Ajax*), $Cu(OH)_2$ (ca. 87%, 56-57% Cu, *Aldrich*) or $CuSO_4.5H_2O$ (AR, *Aldrich*). AAS standards for copper were prepared using the latter reagent in dilute nitric acid (~ 0.5%, AR, *BDH*).

Thiourea eluent solution was prepared using AR quality thiourea (≥ 96%, *Fluka*) and concentrated aqueous hydrochloric acid (AR, 35.4%, *BDH*). Nitrate eluents were prepared from sodium nitrate (AR, 98%, *Griffin*), and in some cases the eluent was spiked with sodium thiosulfate (AR, 99.5%, *BDH*). Hydrogen peroxide (AR, 30%, *Ajax*) and concentrated hydrochloric acid (AR, 32%, *BDH*) were used to digest sulfide precipitates.

4.1.2 Constitution of Artificial Leach Liquors

In order that the resins are evaluated under appropriate conditions, approximating those employed industrially, the leach environments and reagent concentrations used in industry were examined (see Table 1.1). Many of the reported leaching systems utilise very high copper concentrations, of the order of several grams per litre (~ 2000 ppm). B/R Test #2 undertaken using a similar copper concentration yielded unexplainable AAS results, probably due to copper deposition. Small subsets of the resins were studied in liquors containing 10 and 20 ppm Au (Section 4.2.1) and 20 ppm each of Au and Cu (Section 4.2.2). The conditions used in these developmental tests have been summarised in Table 4.1. In all cases, thiosulfate was added as $(NH_4)_2S_2O_3$. To facilitate direct AAS analysis whilst keeping a realistic leach solution, it was decided to use a concentration of approximately 200 ppm copper in all subsequent B/R Tests.

Table 4.1 Developmental Gold Adsorption Tests

Copper added as: $^{\dagger}Cu(NO_3)_2$; $^{\ddagger}Cu(OH)_2$; $^{*}CuSO_4$

B/R Test #	Gold (ppm)	Copper (ppm)	NH_4OH (M)	NH_4Cl (mM)	$[S_2O_3]$ (mM)	Time (minutes)
1	10.02	0	0.809	300	100	1465
2	11.78	1905 †	0.800	300	100	1480
3	19.76	0	1.001	100	100	1457
4	20.11	200.0 ‡	0.802	300	100	1457
5	20.08	176.6 ‡	0.802	300	100	1440
6	20.02	20.00 *	1.001	100	100	360

After these initial examinations, it was decided to use a liquor with the concentrations shown on Table 4.2. The results of tests using this leach liquor formulation are shown in Section 4.2.3.

Table 4.2 Standard Bottle Roll Artificial Liquor Concentrations

Reagent	**Formula**	**Concentration**	**ppm**
Ammonia	NH_4OH	1.00 M	-
Ammonium Chloride	NH_4Cl	0.100 M	-
Ammonium Thiosulfate	$(NH_4)_2S_2O_3$	0.100 M	-
Cupric Sulfate	$CuSO_4.5H_2O$	3.149 mM	200
Sodium Aurothiosulfate	$Na_3[Au(S_2O_3)_2].2H_2O$	0.101 mM	20

The liquor concentrations detailed above are intended to be a representative sample of current practice in thiosulfate leaching research, and were used in bottle roll tests 7-10. The gold concentration is twice the typical ~10 ppm, to permit easier monitoring by AAS.

The artificial leach liquor was generally made up in one batch, allowing at least 500.0 mL for each polymer sample to be studied. This mother liquor was made up immediately prior to the commencement of the bottle-roll tests. The reagents were combined in the following sequence, to prevent precipitation of copper salts and minimise the oxidation of thiosulfate in solution prior to the commencement of the experiment:

(i) Ammonia was added and made up to ~50% of the final volume with water.

(ii) Ammonium chloride was added and dissolved in the solution.

(iii) Copper sulfate (or other copper salt) was washed in with water (50-100 mL). The formation of a pale blue precipitate ($Cu(OH)_2$) was often observed; this redissolved when the liquor was vigorously shaken.

(iv) Ammonium thiosulfate was added rapidly, and swirled gently to dissolve.

(v) Sodium aurothiosulfate was washed in and rapidly dissolved. The entire mixture was then made up to the final volume with water.

Generally, ~10 mL of the mother liquor was retained as the time zero sample. There was no attempt made to minimise or control the concentration of dissolved oxygen, nor to prevent the diffusion of atmospheric oxygen into the artificial leach solution other than by capping the bottles between sampling. As such, oxygen should only permeate into the solution when it was opened for sampling.

4.1.3 Bottle Roll Test Conditions

Anhydrous polymer samples of approximately one gram (± 250 mg) were accurately weighed to four decimal places (± 0.3 mg), and rehydrated with water (~10 mL). After 30 minutes of immersion, the interstitial water was removed by suction. Each of these polymer samples was washed into a clean 500 mL polyethylene bottle using several ~20 mL aliquots from a 500.0 mL batch of the mother liquor. The moment when the last of this batch of liquor was added to the bottle containing the resin was taken to be Time Zero. A small sample of the mother liquor was retained as the Time Zero Sample (T_0, ~ 10 mL).

The cap was screwed onto the bottle, leaving ~20 mL headspace above the liquor. The bottle was fixed onto an orbital shaker (Model SO1, *Stuart Scientific*) and agitated at 175 rpm for 24 hours. The bottles were kept out of direct sunlight, but were under constant indoor fluorescent light over the course of the trial. The

solutions were only exposed to air during sampling, for an equivalent time for each sample.

Table 4.3 Sampling Intervals for Bottle Roll Tests

Sample	**1**	**2**	**3**	**4**	**5**	**6**	**7**	**8**	**9**	**10**
Minutes	30	60	90	120	180	240	360	480	720	1440
Hours	½	1	1½	2	3	4	6	8	12	24

Each batch was sampled at approximately the same time intervals, as detailed in Table 4.3, with the sampling time recorded (± 5 minutes). The sampling procedure was as follows: the bottle was removed from the shaker and the resin allowed to settle for one minute; approximately 10 mL (± 1 mL) was decanted into a glass vial and sealed with a plastic cap; the bottle cap was replaced, and the bottle returned to the shaker to re-suspend the resin. Samples were kept in the acid-washed glass vials with clean, airtight polyethylene caps and stored in a dark, cool place prior to analysis. The results obtained from these tests are presented in Section 4.2.

4.1.4 AAS Analysis of Leach Liquors

4.1.4.1 AAS Methods for Gold Determination

The operational parameters of the two wavelengths commonly used for the atomic absorption spectroscopy detection and determination of gold are in Table 4.4. The error margins given are estimates of those observed in practice from replicate samples when studying artificial ammoniacal thiosulfate leach liquors as described in Table 4.2.

Table 4.4 Gold Detection Parameters for Varian AAS System

AAS Wavelength (nm)	**Linear Range** (ppm)	**Error Margin** (ppm)
242.8	0.1 – 30 ppm	0.2 ppm
267.6	0.2 – 60 ppm	0.4 ppm

The Au(I) concentration in the artificial leach liquors employed (0 - 20 ppm) falls within the range of the more sensitive wavelength (242.8 nm). The leach liquor samples were analysed directly via this method, and compared to a set of standard solutions of $[AuCl_4]^-$ in aqueous HCl (5 %). A comparison of gold standards in this chloride matrix and in artificial leach solutions is detailed in Section 4.1.4.2.

In a typical preparation, the following quantities were used (Table 4.5):

Table 4.5 Preparation of Gold Standards in Hydrochloric Acid Matrix

†: *prepared by diluting the 5.075 ppm Au solution (1:10).*

Au solution (mL)	**HCl solution** (32%)	**Final Volume** (mL)	**Final [Au]** (ppm)
(10.0)†	1.00	100.0	0.5075
1.00	1.00	200.0	5.075†
1.00	1.00	100.0	10.15
2.00	1.00	100.0	20.30
5.00	2.00	200.0	25.38
5.00	1.00	100.0	50.75

Once prepared, these standard solutions were stored in a dark cool place in *Nalgene* bottles (High Density Polyethylene, HDPE) with sealed screw-caps. These standards were used for no longer than two months, minimising contamination and evaporation. The instrument zero and blank solutions (0 ppm Au) were obtained using dilute nitric acid (0.1 %), which was also used to flush the burner between measurements.

Liquors derived from elution studies were also compared to the standards of $[AuCl_4]^-$ in 5% aqueous HCl. Some dilutions were required to achieve a gold concentration within the linear range. Gold standards in nitrate (eluent) and chloride matrix are compared in Section 4.1.4.2.

4.1.4.2 Validation of Gold Standards

It is desirable to use a matrix in which the gold concentrations remain stable over a long period of time. This precludes the preparation of gold standards in artificial leach liquor, which would become oxidised at a significant (but uncertain) rate and may result in the unexpected precipitation of one or more components. Frequent preparation of aurothiosulfate standards would also consume considerable quantities of the gold complex. It is sufficient to know that aurothiosulfate in an aqueous ammoniacal thiosulfate matrix responds to AAS in a linear fashion, compared to the more durable standards of $[AuCl_4]^-$ in dilute HCl.

This has been performed for the ammoniacal thiosulfate matrix, and also for a dilute $NaNO_3$ eluent matrix (0.04 M). The results of these calibration experiments are shown in Figures 4.1 and 4.2, along with the linear best-fit equations.

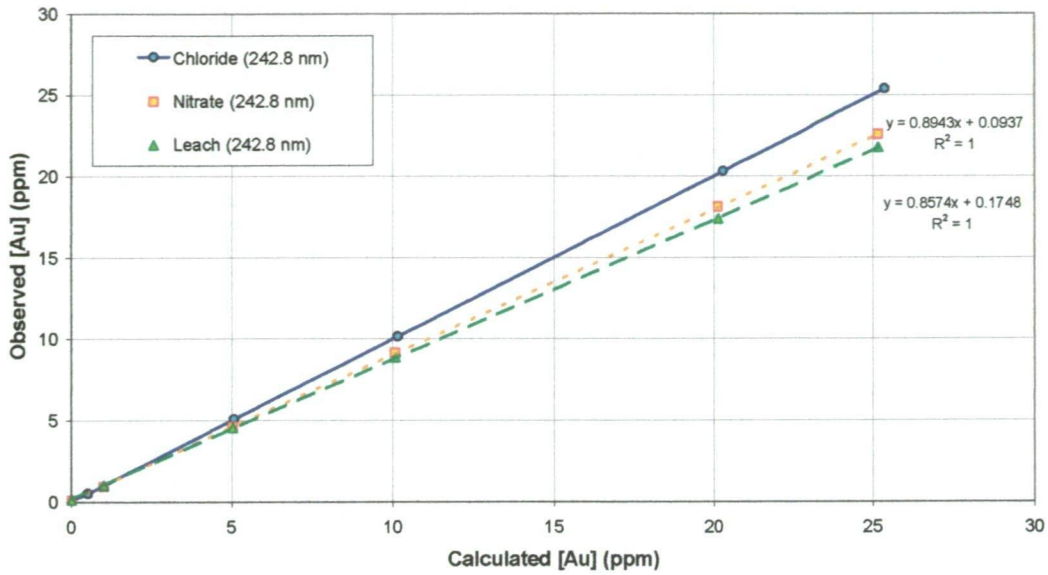

Figure 4.1 Gold AAS Calibration at 242.8 nm in Various Matrices

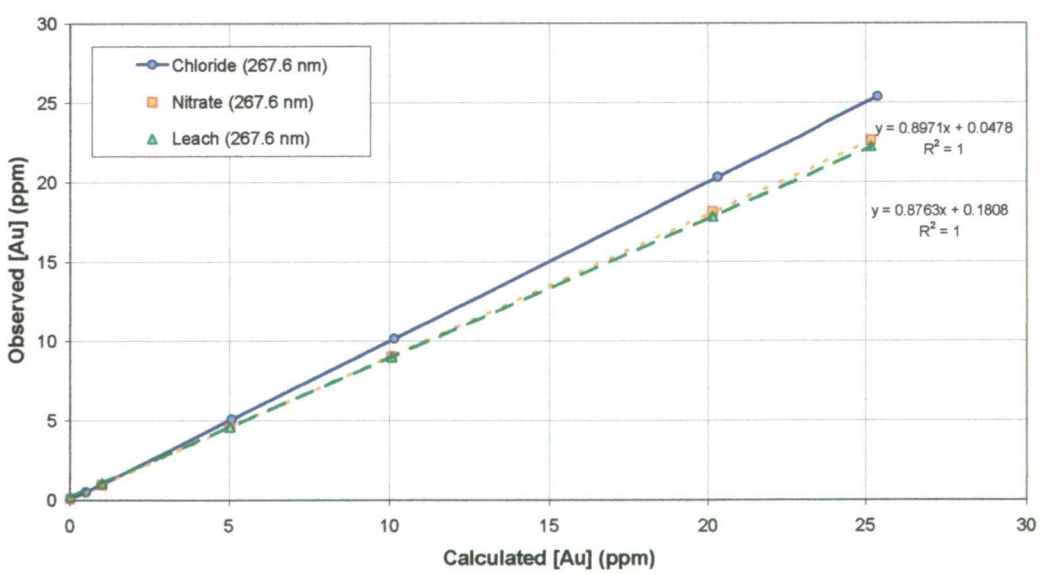

Figure 4.2 Gold AAS Calibration at 267.6 nm in Various Matrices

Table 4.6 'Blank' Leach Solution for Standard Preparation.

Reagent	**Quantity**	**Concentration**
ammonium thiosulfate	14.8211 g	0.1000 M
ammonium chloride	5.3494 g	0.1000 M
28% aqueous ammonia	68.5 mL	1.0023 M
copper sulfate pentahydrate	0.7864 g	3.149 mM (200 ppm)

To prepare a set of gold standards in ammoniacal thiosulfate solution, a batch of 'blank' (gold-free) ammoniacal thiosulfate solution was prepared by combining the reagents in Table 4.6 in the usual fashion, and making the volume up to 1000.0 mL. A small amount of the gold thiosulfate salt ($Na_3[Au(S_2O_3)_2].2H_2O$, 0.0269 g, 51.1 μmol) was made to 100.0 mL with the blank liquor to give a solution containing 101 ppm gold. Portions of this solution were diluted with 'blank' liquor to produce the Au standards (Table 4.7).

Table 4.7 Au Standards in Ammoniacal Thiosulfate Solution

†: *prepared by diluting the 10.0 ppm Au solution (1:10).*

101 ppm [Au] soln. (mL)	**Total Volume (mL)**	**Final [Au] (ppm)**
25.0	100.0	25
20.0	100.0	20
10.0	100.0	10
5.0	100.0	5
(1.0)†	100.0	1

To evaluate the response of the nitrate matrix, a set of gold standards were prepared in dilute nitrate eluent as follows: sodium nitrate (3.4003 g, 40.00 mmol) and sodium thiosulfate pentahydrate (0.9943 g, 4.006 mmol) were made to 1000.0 mL with water, giving a 'mother liquor'. A small batch of the aurothiosulfate salt (0.0269 g, 51.1 μmol) was dissolved and made to 100.0 mL using the mother liquor, yielding a solution containing 101 ppm of gold. Small portions of this solution were further diluted with mother liquor to prepare the other standards, in the same proportions as used for the leach standards (Table 4.8).

The linear calibration and correlation of the gold concentrations in these three matrices is shown in Figures 4.1 and 4.2. Each matrix gives a clear linear response at both AAS wavelengths, with least-squares fit of greater than 0.99. Both the thiosulfate and nitrate matrices show a diminished response to gold, compared to the HCl matrix.

Upon rearranging the linear best-fit equations, Equation 4.1 was formed:

$$[Au]^{T}_{CORRECTED} = (M_W . [Au]^{T}_{MATRIX}) - E_W \qquad (4.1)$$

Values for the variables M_W and E_W are provided in Table 4.8. Gold values determined in either of these matrices and correlated against standards in HCl should be scaled according to the linear conversion factors summarised in Table 4.8. In practice, the scaling factors were obtained for each Bottle Roll experiment by comparing calculated and observed values for the concentration of gold in the Time Zero sample.

Table 4.8 Calibration Factors for [Au] in Various Matrices

Solution Matrix	Wavelength (nm)	Correlation Coefficient (M_W)	Zero Correction (E_W) (ppm)
Leach	242.8	1.1663	0.2039
Leach	267.6	1.1412	0.2063
Nitrate	242.8	1.1182	0.1048
Nitrate	267.6	1.1147	0.0533

4.1.4.3 AAS Methods for Copper Determination

The operational parameters of the wavelengths commonly used for AAS determination of copper in this project are shown in Table 4.9. The error margins reported are estimates of those observed in practice when studying artificial leach liquors containing ~ 200 ppm copper, as described in Table 4.2.

Table 4.9 Copper Detection Parameters for Varian AAS System

AAS Wavelength (nm)	Linear Range (ppm)	B/R Test Number	Error Margin (ppm)
327.4	0.1 – 24	2	2.5
217.9	0.2 – 60	6	5
222.6	1 – 280	4, 5, 7, 8	10

Samples were calibrated against standards of Cu(II) in dilute nitric acid. A bulk solution of copper (1000 ppm) was prepared by dissolving $CuSO_4.5H_2O$ (3.9292 g, 15.74 mmol) in water (~100 mL), adding concentrated HNO_3 (1.5 mL,

mmol), and making the volume up to 1000.00 mL. A second portion of conc. HNO_3 (2.9 mL, 46 mmol) was diluted to 2000.00 mL and used to make up the typical solutions detailed in Table 4.10. Standards containing 10, 20, 30, 40, 50 and 60 ppm Cu(II) were freshly prepared and stored in clean polystyrene vials with a screw-caps.

Table 4.10 Preparation of Copper Standards in Dilute Nitric Acid

Cu solution (mL)	**Final Volume (mL)**	**[Cu] Final (ppm)**
1.00	250.0	4.00
1.00	100.0	10.0
1.00	50.00	20.0
10.00	250.0	40.0
25.00	500.0	50.0

Copper concentrations determined by AAS at time zero generally agreed with the calculated values (± 5 ppm). The effects of the leach matrix on copper determination are not fully known, as copper standards were not prepared in an ammoniacal thiosulfate matrix. As a result of the high margin of error relative to the small change in copper concentration expected during the B/R tests (see Figures 4.17 – 4.20), the copper concentration was not followed in subsequent tests.

4.2 Results of Bottle-Roll Tests

The loading isotherms for each resin is presented as a linear plot of $[Au]_R$ over time, with resins grouped in the same sets in which they were analysed (Figures 4.3 – 4.13). The optimum results of these tests have been summarised in Table 4.11, along with the IEX Capacity and functional group loading ($[Au]_R/C_M$) in millimols Au per mol of functional group. For a key to resin structures, refer to Appendix 1.

The initial AAS results were obtained as metal in solution in milligrams per litre (ppm), and corrected for the matrix according to Equation 4.1 (Section 4.1.4.2). The concentration of gold on the resin ($[Au]_R$, in ppm) was calculated by difference, taking into account the small quantities of gold removed in sampling aliquots. The formula for the conversion of bottle roll solution gold concentrations into resin gold loadings is provided below (Equation 4.2).

$$[Au]_R^t = \left[V_{t_0}.[Au]_S^{t_0} - V_t.[Au]_S^t - \sum_{N=t_0}^{t-1} A_N.[Au]_S^N \right] \Big/ M_R \qquad (4.2)$$

where $V_t = V_{t_0} - \sum_{N=t_0}^{t-1} A_N$ and the remaining terms are defined as follows:

t_0 = Time Zero (the moment resin was introduced to the liquor)

t = Elapsed Time since t_0 (minutes) in fixed intervals (see Table 4.3)

$[Au]_R^t$ = Gold concentration on resin at time t (ppm)

$[Au]_S^t$ = Gold concentration in solution at time t (ppm)

V_t = Volume of liquor remaining at time t (litres)

A_N = Volume of aliquot taken at time N (litres)

M_R = Mass of anhydrous resin sample (grams)

N = Time step of Sigma function

Table 4.11 Optimum Performance Characteristics of Resins

T_{max}: Time of maximum $[Au]_R$ †: *Time at end of experiment*

‡: *Tested in absence of copper* * *Capacity calculated from %N (EA)*

Resin Code	Capacity (C_M; meq/g)	T_{max} (minutes)	$[Au]_R/C_M$ (mmol/mol)	$[Au]_R$ (mg/g)	% Au Sorption
ABU1	1.39	480	9.5	2.60	27.2
BBZ1	1.32	240	3.7	0.97	9.8
BIM1	2.22	1440†	16.2	7.07	76.2
BME1	2.27	1457†	9.6	4.29	44.3
DAB1	0.59	480	10.7	1.25	12.8
DAM1	3.01	1440†	11.8	6.99	72.5
DBP1	1.40	1440†	3.5	0.96	10.0
DET1‡	5.62*	1447	0.7	0.71	3.0
DIP1‡	2.53*	347	1.5	0.73	11.0
DMP2	2.70	1440†	10.1	5.37	57.1
DTM2	3.57	360†	6.9	4.84	50.6
ETB1	0.49	1440†	5.9	0.57	6.2
ETM2	2.74	360	9.4	5.05	51.9
MIM2	3.13	360†	12.1	7.46	78.0
NBM1	1.98	360†	4.5	1.73	18.2
NBP1	2.25	1440†	7.0	3.09	31.9
NMM1	2.70	360	4.6	2.44	28.0
NMM2	2.90	1440†	11.6	6.62	67.2
NMP1	3.09	360	6.1	3.72	42.0

Table 4.11 · Optimum Performance Characteristics of Resins

[continued]

Resin Code	Capacity (C_M; meq/g)	T_{max} *(minutes)*	$[Au]_R/C_M$ (mmol/mol)	$[Au]_R$ (mg/g)	% Au Sorption
NMZ1‡	7.31*	1457†	0.5	0.65	5.9
PET1	2.30	1440†	11.9	5.38	56.0
PME2	3.83	360†	7.6	5.75	60.2
POP2	2.26	120	1.2	0.53	5.4
QNU1	3.07	371	10.8	6.51	65.9
TAA1‡	5.85*	273	0.4	0.42	7.9
TBB2	0.80	480	5.4	0.85	8.8
TBM2	1.57	1440†	3.9	1.20	12.5
TBT1	2.09	1440†	3.8	1.57	20.0
TBT2	1.67	240	2.5	0.83	14.2
TBT3	1.59	480	6.7	2.10	24.8
TBZ1	2.24	360†	7.8	3.42	35.5
TEB1	1.86	1440†	2.6	0.96	10.0
TEM1	0.85	1440	4.2	0.70	7.4
TET1	3.64	120	0.6	0.39	8.0
TET2	3.33	90	0.6	0.40	4.1
TET3	1.77	480	6.8	2.36	27.3
TME1	1.83	480	13.0	4.67	47.8
TME2	3.61	240	3.4	2.45	29.6
TOA2	0.25	90	5.5	0.27	2.8

Table 4.11 Optimum Performance Characteristics of Resins

[continued]

Resin Code	Capacity (C_M; meq/g)	T_{max} *(minutes)*	$[Au]_R/C_M$ (mmol/mol)	$[Au]_R$ (mg/g)	% Au Sorption
TPZ1	3.58	360	11.3	7.98	81.1
TPZ2	2.27	1440†	8.0	9.60	57.2
A378	Nil	90	-	0.47	4.7
A2	0.90	240	7.8	1.37	14.0
A26	3.90	180	11.8	9.10	89.6
Dowex-1	4.10	60	11.4	9.20	92.8
IRA-410	3.62	180	12.1	8.61	88.3

Using the functional group loading ($[Au]_R/C_M$) to rate resin performance, weak base resins such as DET1 and TAA1 performed the worst, and resin Au loading ($[Au]_R$) was no better than the blank substrate (A378). Resins with moieties based on hexahydro-1,3,5-triazine (TET1-2, TEB1, TEM1, TBT1-2, TBB2, TBM2) were also poor absorbents for gold. The third preparations (TET3 and TBT3) were less degraded, and performed somewhat better. The best performing resins were moderately hindered strong base groups, such as (2-hydroxyethyl)piperidinium (PET1), and imidazolium resins (BIM1, MIM2). The best of these absorbed gold as efficiently as commercial resins A26, IRA-410 and Dowex-1, but achieved maximum loading over a longer time-frame (360 – 1440 minutes).

Detailed analysis of Au and Cu loading, kinetics, and elution may be found in Section 4.4. An analysis and discussion of the functional group features associated with improved gold loading is contained in Section 4.4.5.

4.2.1 Adsorption of Gold from Copper-Free Leach Solutions {B/R #1 & #3}

Initial testing of a small subset of novel resins was performed using simplified artificial leach solutions containing no copper. The constitution of these ammoniacal thiosulfate solutions has been described in Table 4.1. It should be noted that B/R liquor #1 (Figure 4.3) contained 10 ppm gold and 0.30 M chloride, whereas B/R liquor #3 (Figures 4.4 - 4.5) held 20 ppm gold and only 0.10 M chloride. The resins examined included:

- Blank substrate: A378
- Weak base resins: TAA1, NMZ1, DET1, DIP1
- Strong base resins: ABU1, PET1, TBZ1, TPZ1, TOA1, NMM1, NMP1
- Resins bearing mixed weak- and strong-base groups: TET1, TBT1, TME1.

The results are presented as plots of the gold concentration onto each resin over the time of the test (Figures 4.3 – 4.5).

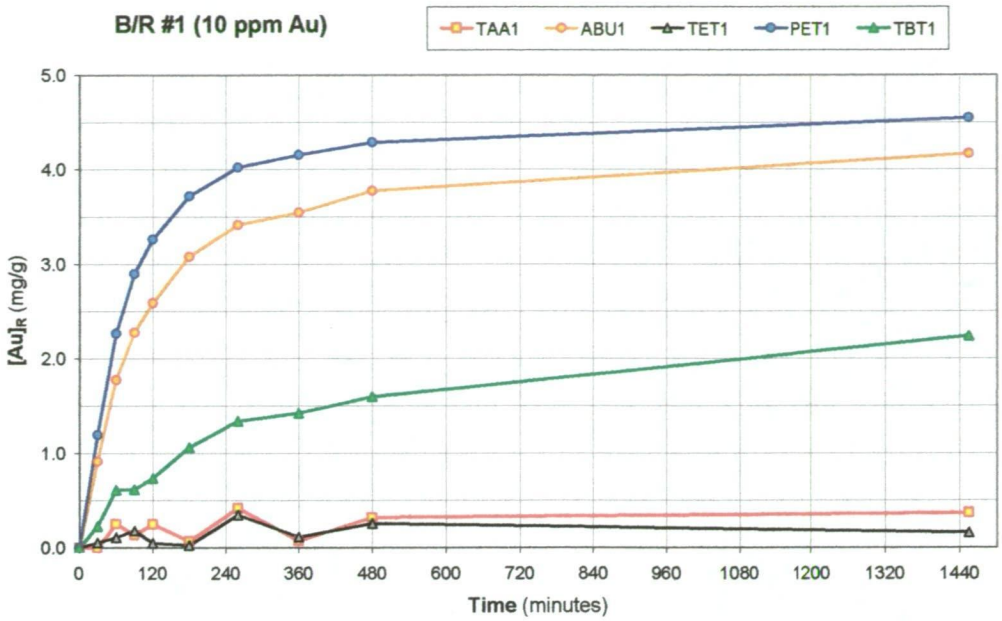

Figure 4.3 Au Sorption from Copper-Free Leach Solution {B/R #1}

(Initial $[Au]_S$ =10 ppm)

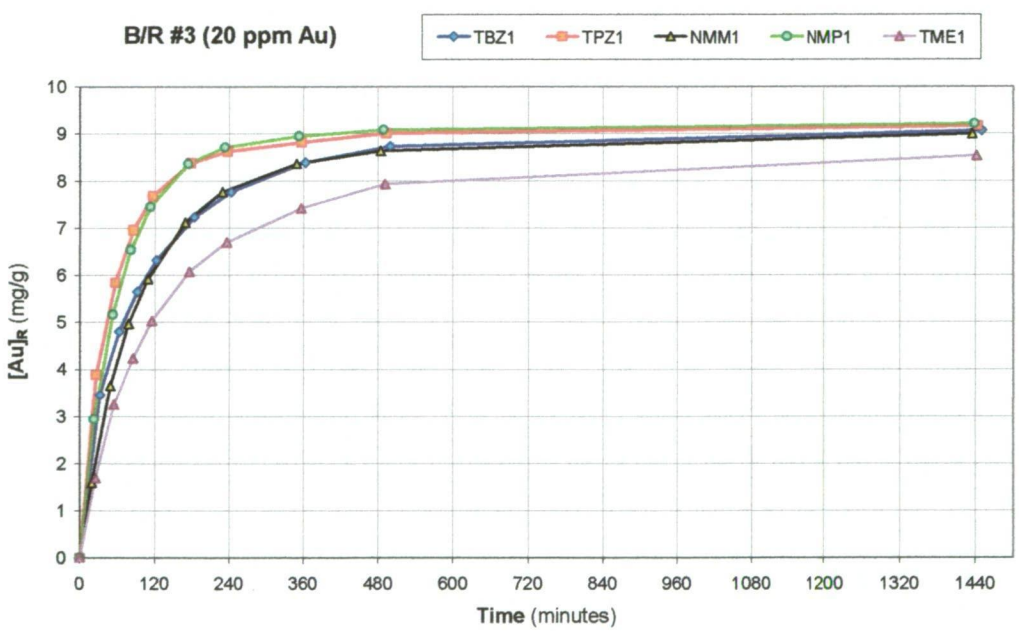

Figure 4.4 Au Sorption from Copper-Free Leach Solution {B/R #3}

Part 1 (Initial $[Au]_S$ = 20 ppm)

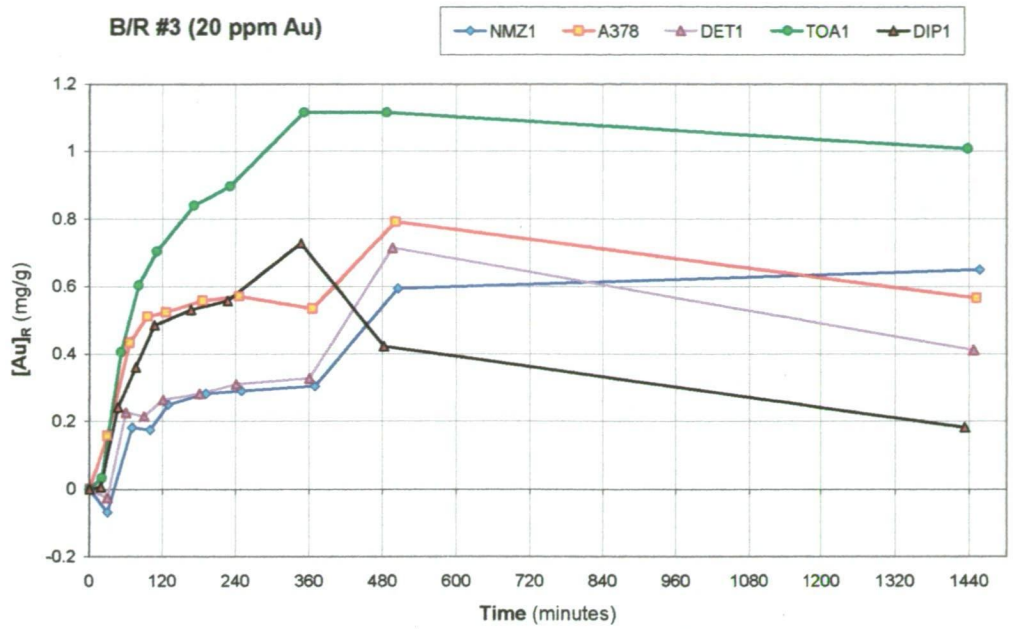

Figure 4.5 Au Sorption from Copper-Free Leach Solution {B/R #3}

Part 2 (Initial $[Au]_S$ =20 ppm)

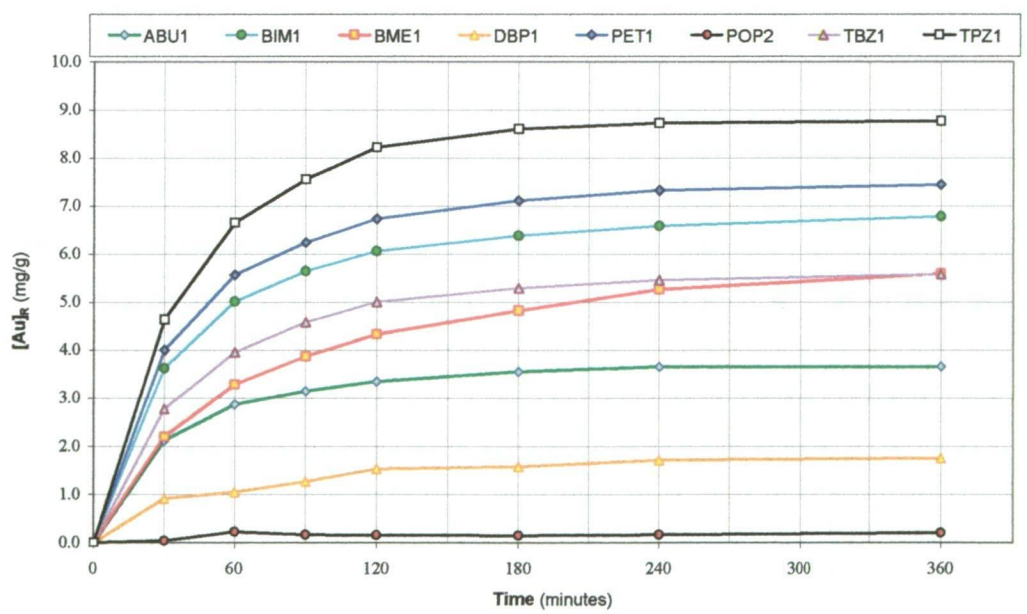

Figure 4.6 Sorption of Gold from Solution (20 ppm Cu & Au) {B/R #6}

4.2.2 Adsorption of Gold from Leach Liquor containing 20 ppm Copper {B/R #6}

A leach solution containing 20 ppm of both copper and gold was investigated in this test. The leach solution has been described in Table 4.1, with copper added as $CuSO_4.5H_2O$. The results are presented in Figure 4.6, configured as the amount of gold adsorbed per gram of resin (mg/g). These are compared with the results of prior copper-free B/R tests in Section 4.4.3.

4.2.3 Adsorption of Gold from Leach Liquors containing 200 ppm Copper

The majority of the resin testing was performed using a standard leach liquor initially containing 0.10 M thiosulfate, 200 ppm Cu and 20 ppm Au. However, the initial concentrations of ammonia species were modified after initial tests. The first two such tests (B/R #4 and #5, Table 4.1) initially contained 0.30 M chloride, 0.80 M ammonia and 0.50 M ammonium ions. More ammonia and a lower concentration of ammonium chloride (0.10 M) was used in all subsequent liquors, which started with 1.00 M ammonia, 0.10 M chloride and 0.30 M ammonium ions (from ammonium thiosulfate and ammonium chloride). The NH_4Cl concentration was reduced to minimise the concentration of chloride ions whilst retaining a buffered leach liquor. The total concentration of NH_3 and NH_4^+ remained the same in both mixtures (1.300 M).

The sorption of gold onto various resins was periodically measured at the time intervals specified in Table 4.3, and the results are presented below as plots of Au on resin (mg/g) versus time (Figures 4.7 – 4.12). The blank substrate (A378) and the control resin (A2) were also examined in Bottle Roll Test #8 (Figure 4.10).

Discussion of these results, including general trends and an analysis gold sorption kinetics, is presented in Section 4.4.2.

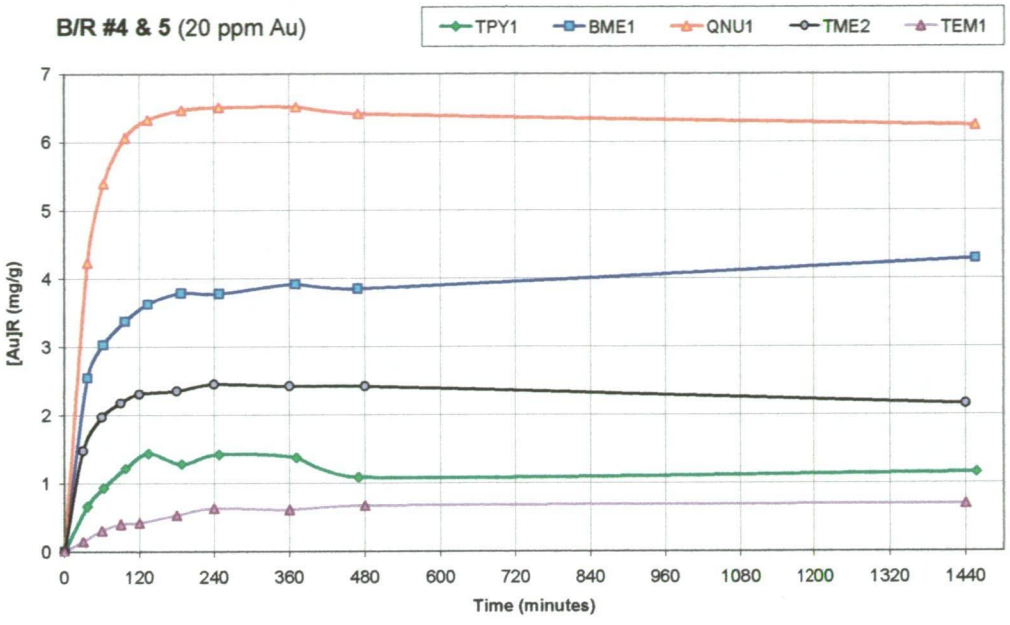

Figure 4.7 Sorption of Gold onto IEX Resins {B/R #4 & #5}

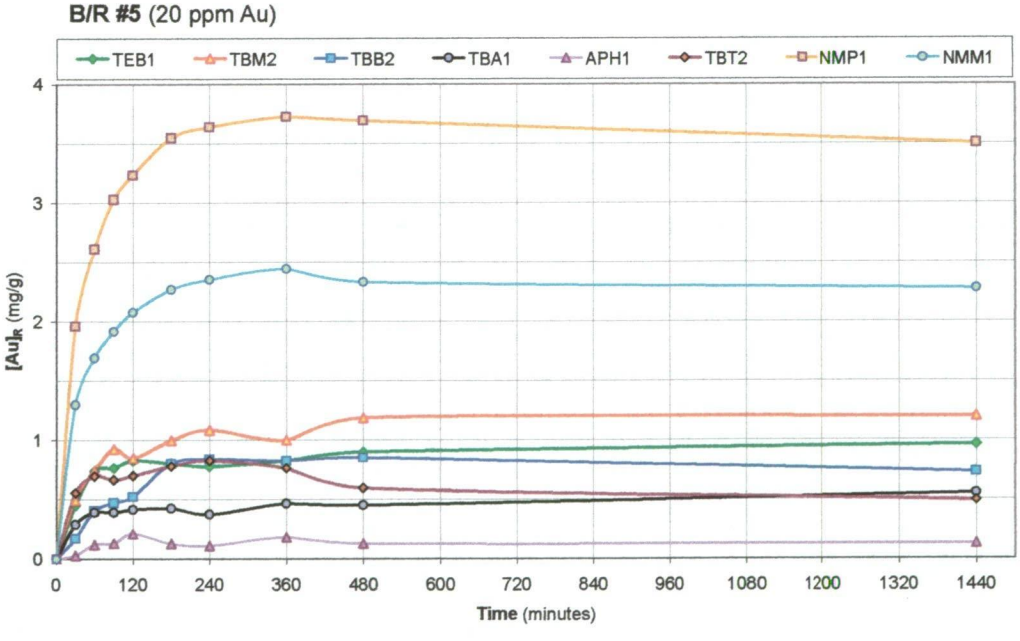

Figure 4.8 Sorption of Gold onto IEX Resins {B/R #5}

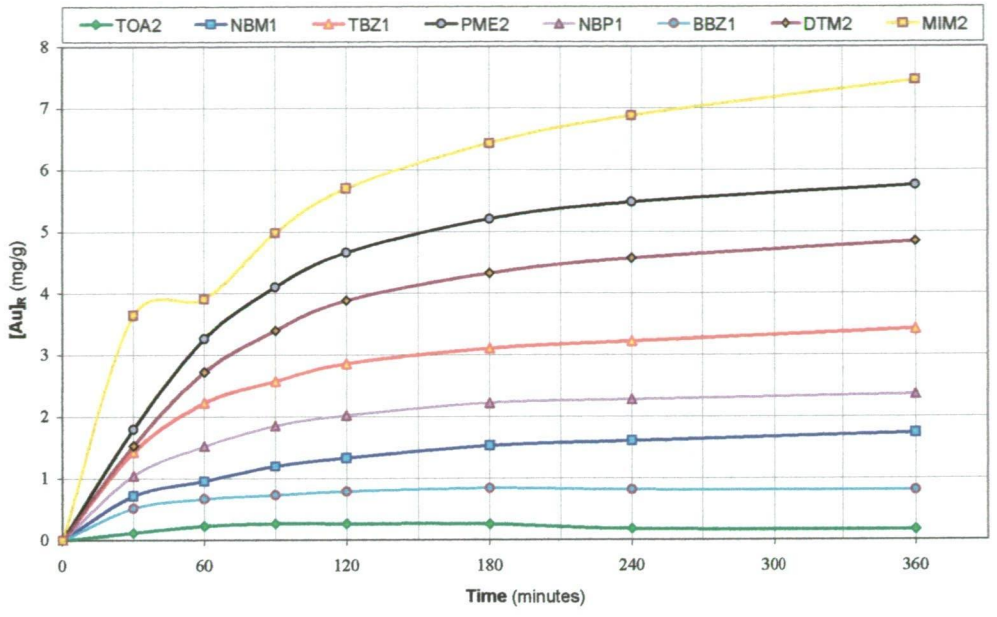

Figure 4.9 Sorption of Gold onto IEX Resins {B/R #7}

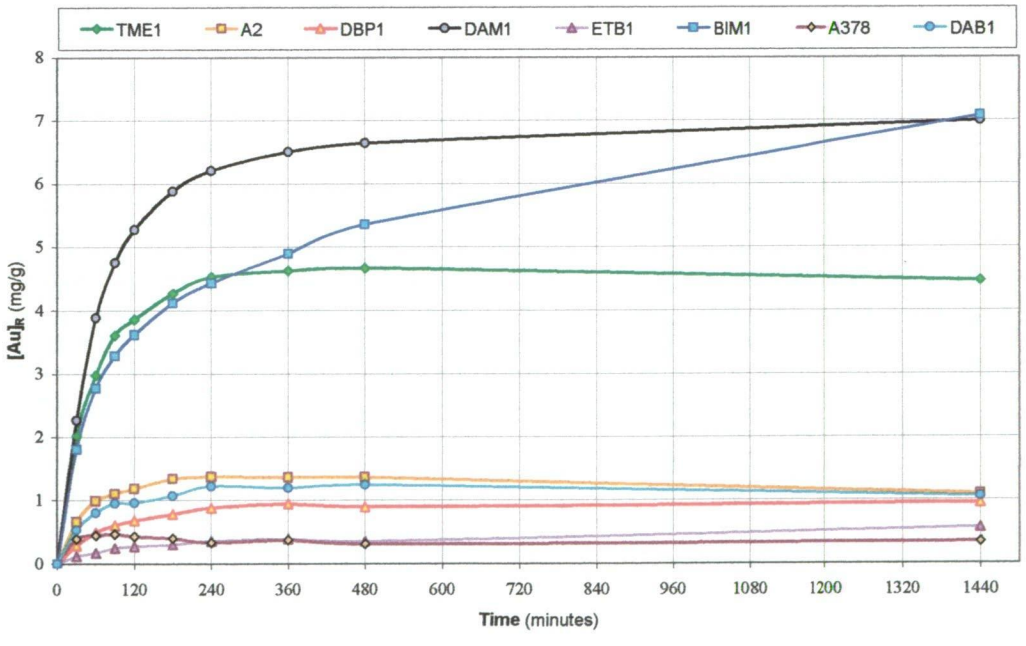

Figure 4.10 Sorption of Gold onto IEX Resins {B/R #8}

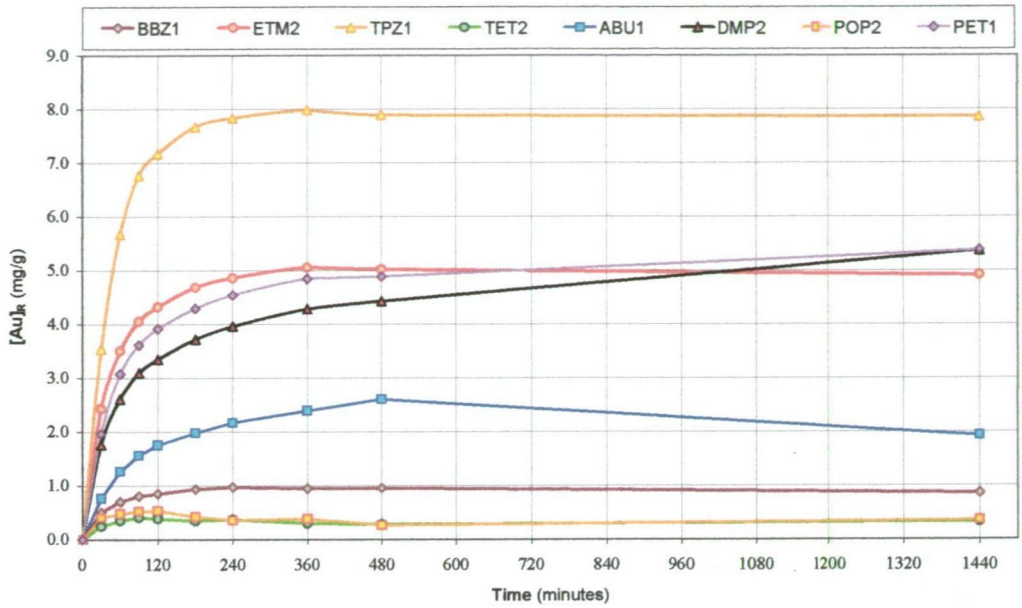

Figure 4.11 Sorption of Gold onto IEX Resins {B/R #9}

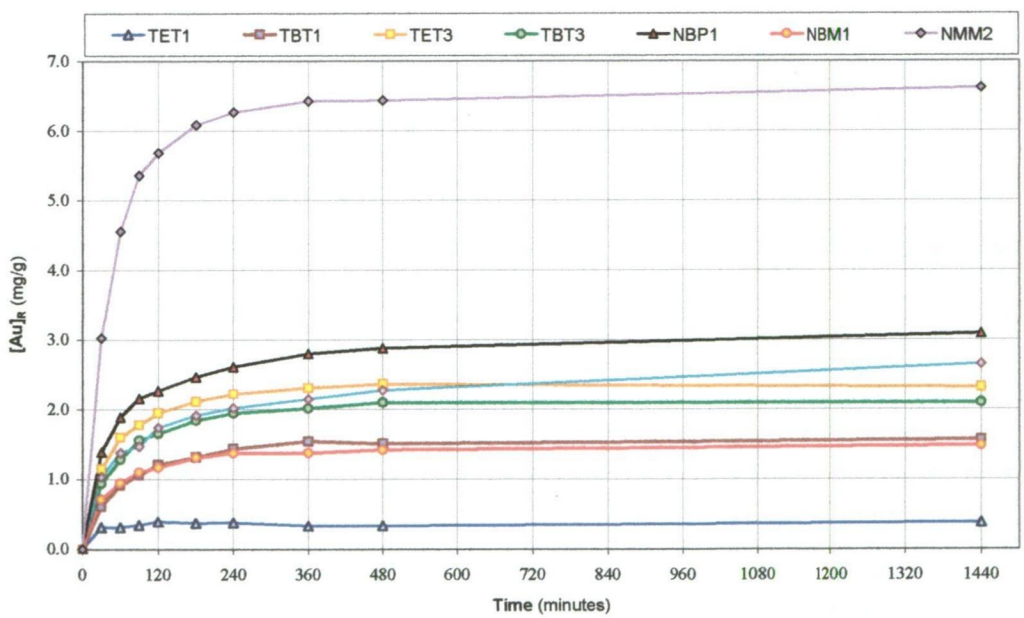

Figure 4.12 Sorption of Gold onto IEX Resins {B/R #10}

4.2.4 Sorption of Gold by Commercial Resins

A small subset of commercial ion-exchange resins have been studied in conditions identical to the novel resins prepared in this project. Commercial resins usually have quite high IEX capacities and may prove more durable than the novel resins used in this work, due to commercial product optimisation.

These commercial resins (IRA-410, Dowex-1 and A26) have already been described in Section 3.1.10. The particle sizes of these materials were generally less than that of the novel resins prepared for this project. The Dowex-1 resin particles were all very fine (75 - 150 μM), while the resins IRA-410 and A26 had a broader size distribution (150 - 300 μM and 355 - 1180 μM, respectively). The larger beads of A26 resin were separated by sieving to yield a fraction denoted 'A26 Big' ($\geq$ 850 μM), similar to the size of the common precursor resin A378 (~850 μM). The results of Bottle Roll Tests using these resins are presented in Figure 4.13. These results are compared to those of the novel resin in Section 4.4.2.

4.2.5 Reproducibility of B/R Tests

A number of duplicate tests were performed in this work to act as a control on the natural variability associated with the B/R Tests. These results may be directly compared, having been performed using fresh batches of resins in liquors with similar constitutions. The results have been arranged pairwise in Figures 4.14 - 4.16 to facilitate a visual comparison. These results are discussed in Section 4.4.2.2. Note that some of the data presented in this section has been abstracted from the trithionate selectivity tests in Chapter 5..

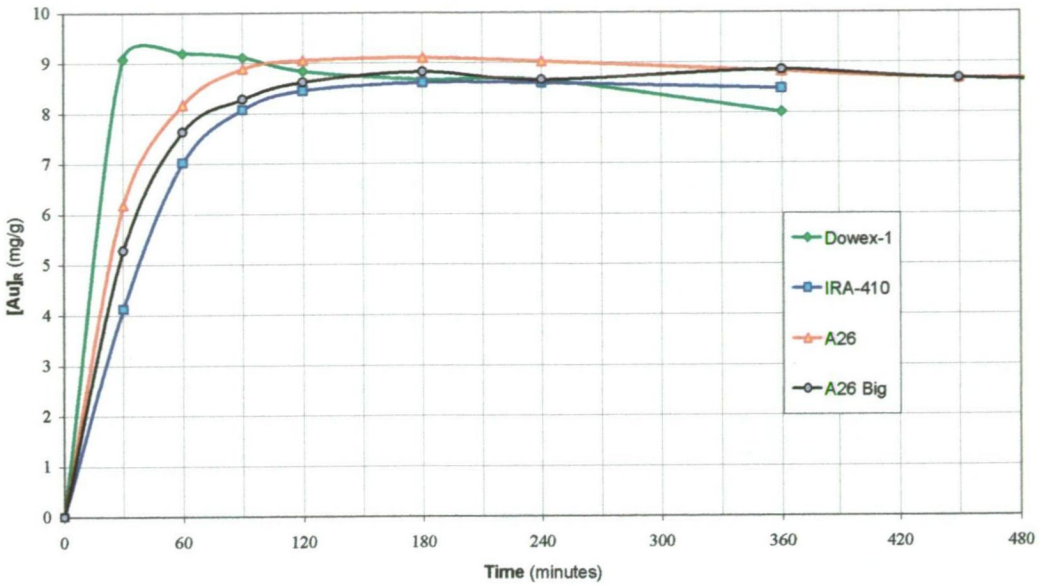

Figure 4.13 Sorption of Gold by Commercial IEX Resins

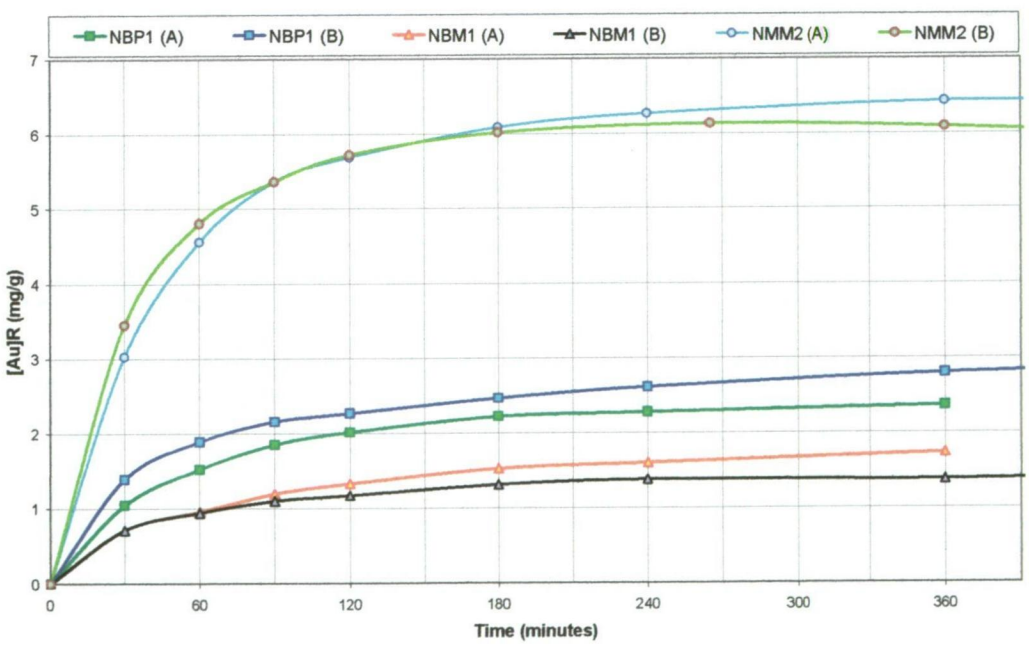

Figure 4.14 Reproducibility of Gold Sorption by Various Resins (Part 1)

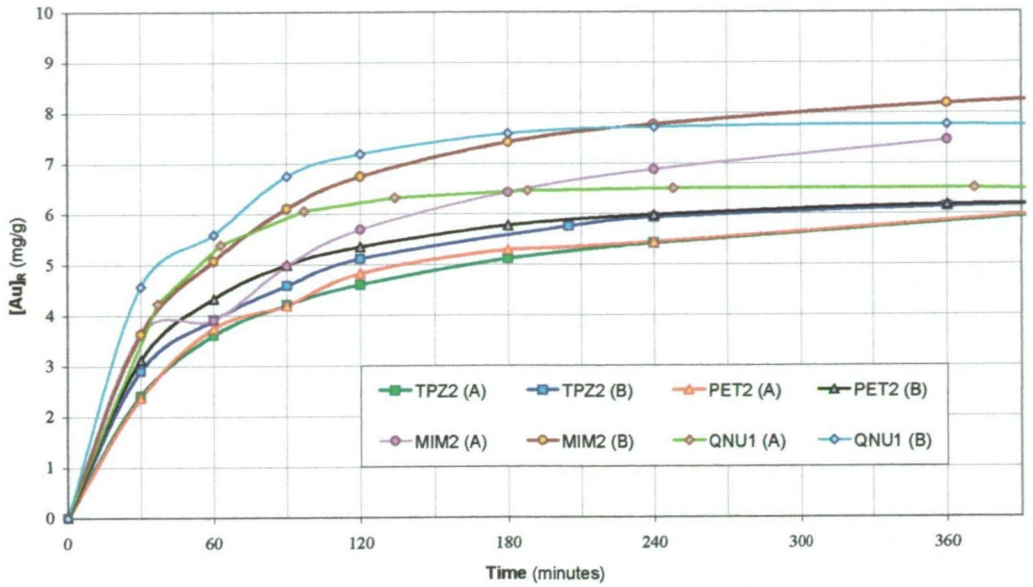

Figure 4.15 Reproducibility of Gold Sorption by Various Resins (Part 2)

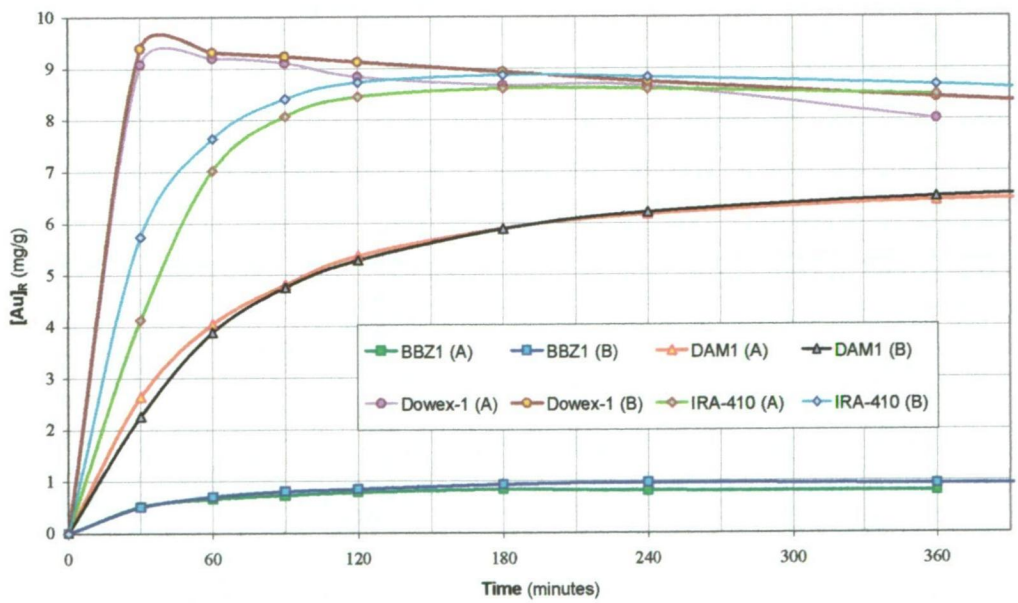

Figure 4.16 Reproducibility of Gold Sorption by Various Resins (Part 3)

4.2.6 Adsorption of Copper from Leach Liquors containing 200 ppm Copper

The concentration of copper in a number of the earlier B/R Tests was followed by AAS, as described in Section 4.1.4.2. These results are presented in Figures 4.17 – 4.20, but have not been converted into resin loadings due to the large degree of uncertainty associated with these results (discussed in Section 4.4.1.2). The adsorption of copper by the commercially manufactured resins IRA-410 and Dowex-1 are shown in Figure 4.20, along with the control results given by blank substrate resins (A378 and A2). Discussion of copper sorption results is confined to Section 4.4.3.

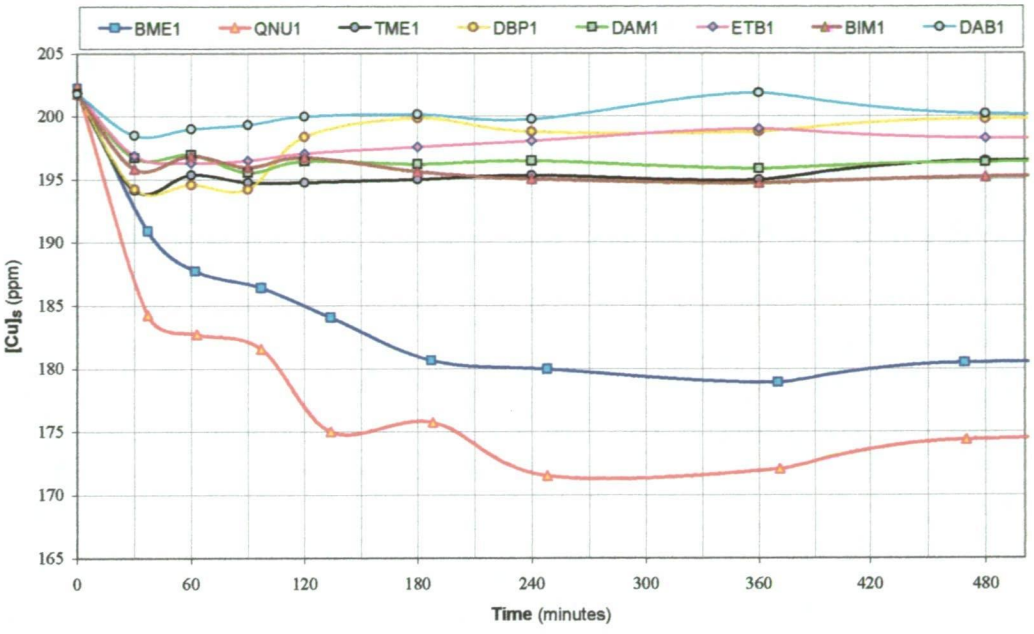

Figure 4.17 Sorption of Copper by IEX Resins {B/R #4 & 8}

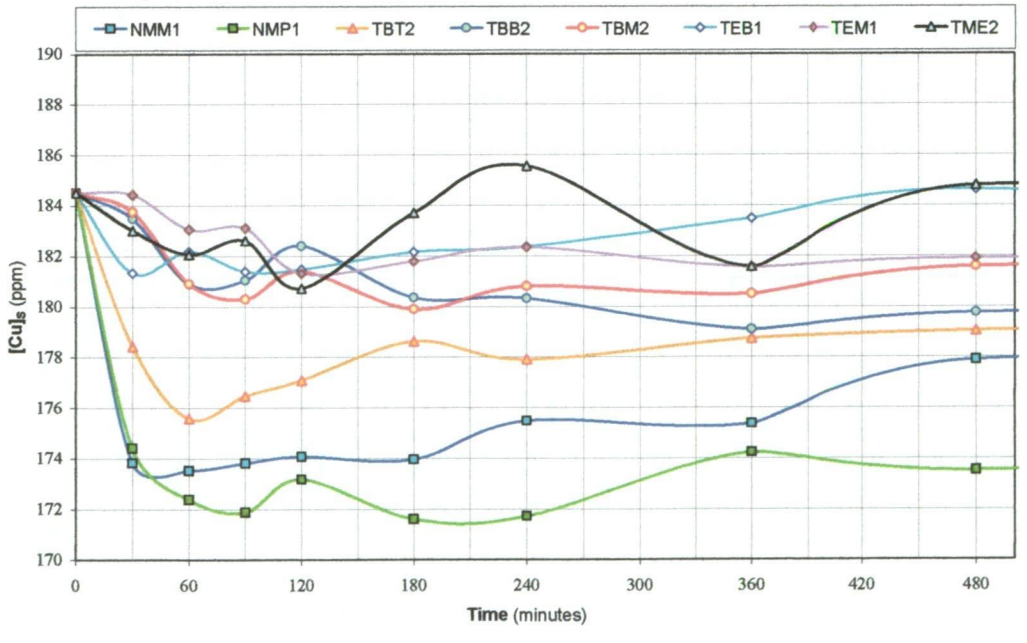

Figure 4.18 Sorption of Copper by IEX Resins {B/R #5}

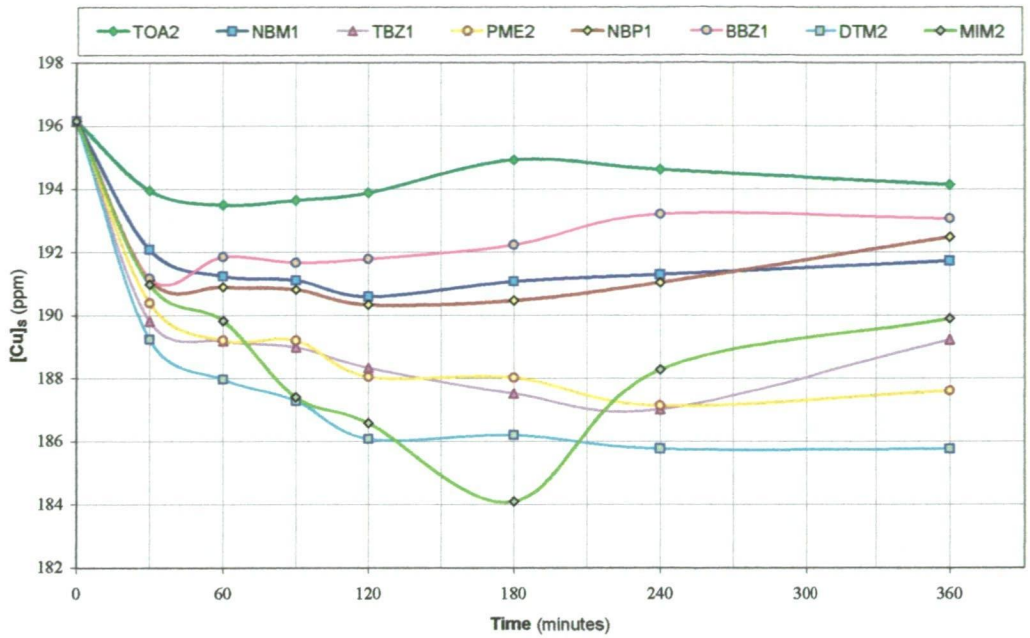

Figure 4.19 Sorption of Copper by IEX Resins {B/R #7}

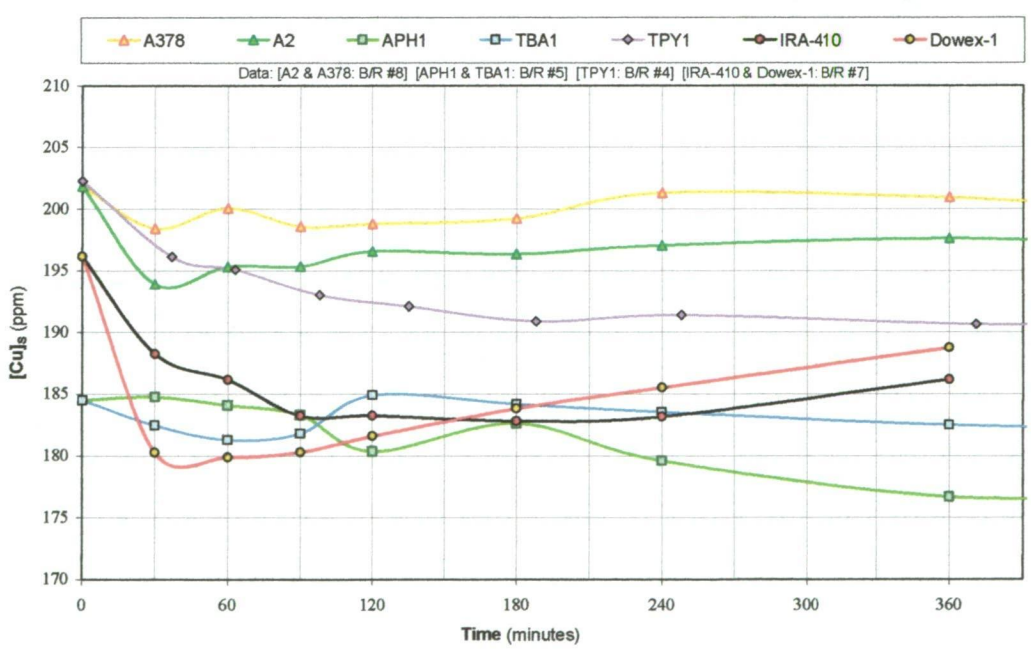

Figure 4.20 Sorption of Copper by Selected IEX Resins

4.3 Elution of Au-Loaded Polymers

Each of the B/R tests described above terminate with a sample of each resin loaded with gold. These resins were then examined in a range of elution systems, with the aim of finding a system optimal for the desorption of aurothiosulfate. The complete elution of gold from each resin was not pursued. Comprehensive elution studies are best suited to a smaller set of semi-optimal polymers, which are described and examined in Chapter 5. This section contains a general assessment of the relative elution efficiencies of the resins, and an evaluation of related chemical issues such as matrix stability and effects on AAS results.

Only a narrow range of eluent systems have been reported to strip the aurothiosulfate complex from strong base resins, and are summarised in Figure 1.4. In this work, two systems were examined for their efficacy in elution of aurothiosulfate from resins loaded during B/R Tests:

(1) 0.5 M Thiourea + 0.25 M H_2SO_4

(2) 2.0 M $NaNO_3$ + 0.2 M $Na_2S_2O_3$

The former system (1) operates by displacing the adsorbed gold with hydrogensulfate anions (HSO_4^-) and converting the aurothiosulfate complex into the corresponding thiourea complex. This system has the disadvantage of requiring an acidic pH, which can cause degradation of the resin by osmotic shock. In addition, these conditions may cause decomposition of thiosulfate into sulfur (clogging resin pores) or sulfide, permitting the loss of gold from solution by precipitation.

The latter system (2) relies upon mass-action and the standard ion-exchange affinity series to displace the adsorbed gold complex with abundant nitrate ions. In

the absence of excess complexing ligands, aurothiosulfate is likely to slowly decompose and precipitate as gold sulfide (Au_2S). Therefore, in later work the nitrate eluent was augmented with sodium thiosulfate (0.2 M) to minimise the precipitation of gold from the eluate prior to analysis.

A number of alterations in eluent make-up and flow-rate were made during the course of this work, and hence each elution batch is presented independently in Section 4.3.1 (thiourea eluent) and Section 4.3.2 (nitrate eluent). A comparison of the efficacy of the elution procedures is contained in Section 4.4.4.

4.3.1 Elution with Acidic Thiourea

4.3.1.1 Elution of Gold from Polymers in B/R Test #4

Thiourea eluent was prepared as follows: thiourea (LR, 18.031 g, 237 mmol) was added to a mixture of water (100 mL) and sulfuric acid (98%, 12.506 g, 128 mmol). The mixture was shaken until the solids dissolved, and made up to 500.0 mL with water, yielding a solution of thiourea (0.474 M) in H_2SO_4 (0.255 M).

The resins to be eluted, namely BME1, NMP1, PET1, QNU1, TBZ1, TME1, TPY1, and TPZ1, had been loaded with gold during B/R Test #4 (see Table 4.1), and were kept moist until elution. These batches of resin (~1 g) were then loaded into IEX columns (10 x 150 mm, with a porosity #3 sintered glass frit and teflon tap at the base) and immersed in water (~2 mL). Each column of resin was agitated to release entrapped air bubbles, and then eluted dropwise with the thiourea eluent solution at room temperature for 40 minutes at a rate of 1.0 mL/minute. Four fractions were at ten minutes intervals, while a fifth and final fraction of 10 mL was left to stand in the column for 1 hour before collecting the eluent.

These fractions were analysed for gold by AAS, diluting where appropriate to place the gold concentration in the linear range of the detector. These were compared

to gold standards in HCl matrix. The results of this analysis (mg Au per gram resin) are presented in Figure 4.21 for each resin in this set. The percentage of gold eluted was calculated for resins BME1 (20.3%), QNU1 (18.4%) and TPY1 (9.8%). The initial loading of gold was not well characterised for the other resins, so their elution profiles have been offset by 3.0 mg/g for clarity. An analysis of the comparative efficacy of the elution procedures is contained in Section 4.4.4.

4.3.1.2 Elution of Gold from Polymers in B/R Test #5

Fresh eluent was prepared as in Section 4.3.1.1, in this case yielding a solution of thiourea (0.500 M) in H_2SO_4 (0.250 M).

The polymers that had been loaded with gold in Bottle Roll Test #5 (see Table 4.12) were wet-loaded into IEX columns with water (~2 mL). Eluent was pumped through each column at 0.5 mL/minute, and six fractions of 10 mL each were collected at 20 minute intervals. The Au and Cu concentration in each eluate fraction was then analysed by AAS. The results have been recalculated and plotted as the concentration of gold on each polymer (Figure 4.22). The total percentage of gold eluted from each resin in this procedure is reported in Table 4.12. Copper concentrations were also followed by AAS, revealing negligible levels of copper (~5 ± 2 ppm) in the eluate of each resin.

Table 4.12 %Au Stripped by Acidic Thiourea Eluent (B/R #5)

Resin	**TEB1**	**TBM2**	**TEM1**	**TBB2**	**TBA1**
Au %	47.3	50.7	45.2	38.0	18.5
Resin	**APH1**	**TME2**	**TBT2**	**NMP1**	**NMM1**
Au %	48.1	36.7	52.6	36.6	32.5

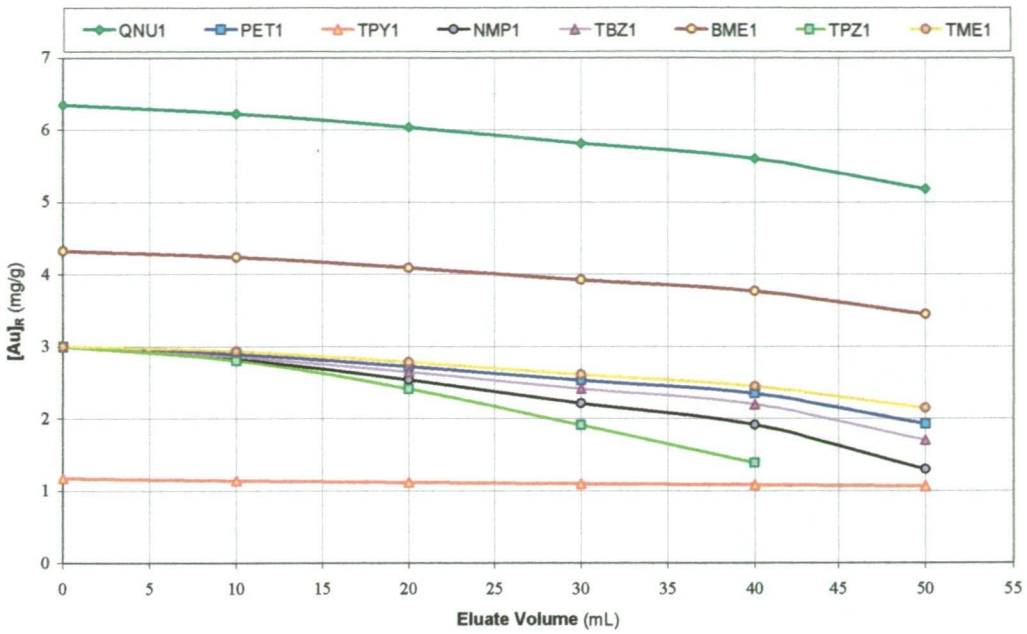

Figure 4.21 Elution of Gold from Resins using Acidic Thiourea (B/R #4)

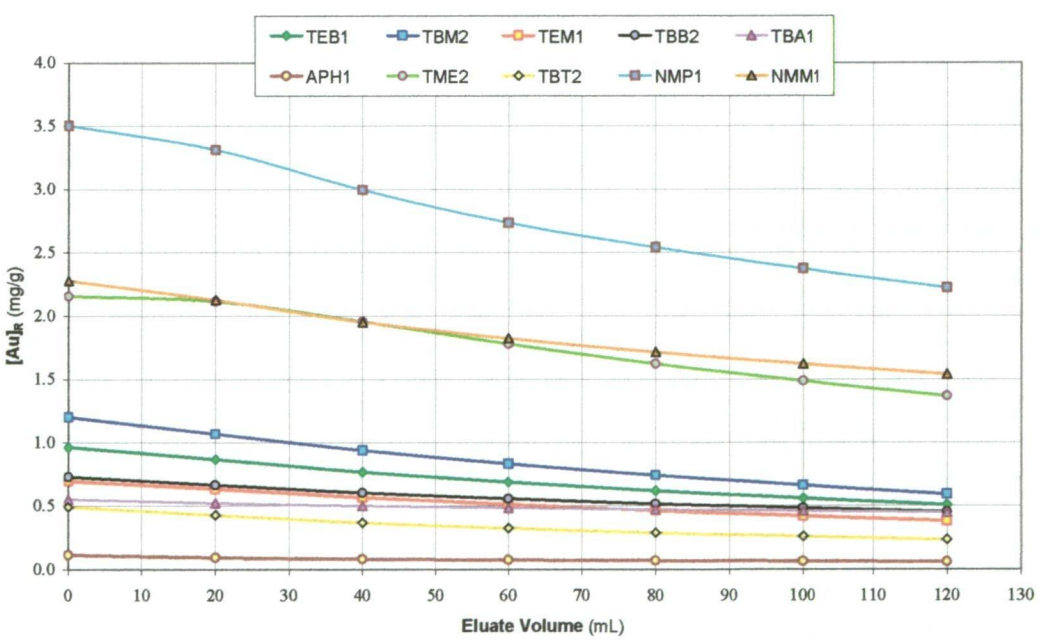

Figure 4.22 Elution of Gold from Resins using Acidic Thiourea (B/R #5)

4.3.1.3 Elution of Gold from Polymers in B/R Test #8

The eluent was prepared as in Section 4.3.1.2, yielding 500.0 mL of a solution of thiourea (0.500 M) and sulfuric acid (0.250 M). The resins used in Bottle Roll Test #8 (see Table 4.13) were packed into IEX columns, and eluted at 0.2 mL/minute. Four batches of 10 mL eluate from each resin were collected at 50 minute intervals. Some white precipitate formed in the eluate on standing overnight. To dissolve this unknown solid, the samples were combined with H_2O_2 (AR, 30%, 1-2 mL), conc. HCl (1 - 2 mL), and conc. HNO_3 (~1 mL), and refluxed for 1 minute. These samples were then made up to 100.0 mL and subjected to AAS analysis for gold. The eluate was not examined for copper.

The results are presented as the concentration of gold on the resin (mg/g) as a function of total eluate volume (Figure 4.23). The total percentage of gold eluted from each loaded resin is presented in Table 4.13.

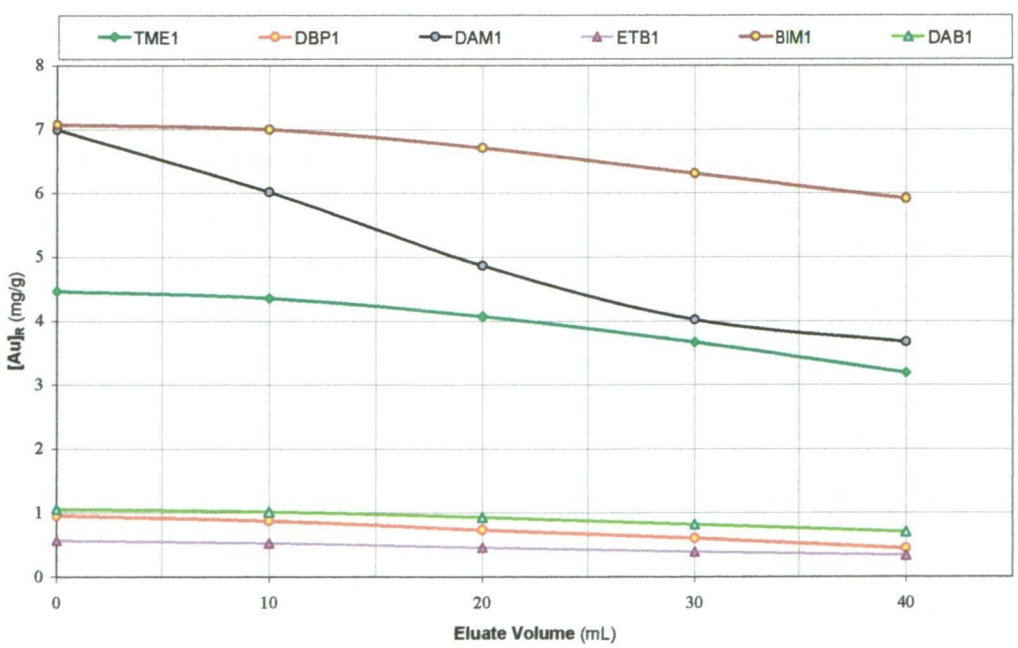

Figure 4.23 Elution of Gold from Resins using Acidic Thiourea (B/R #8)

Table 4.13 %Au Stripped by Acidic Thiourea Eluent (B/R #8)

Resin	**TME1**	**DBP1**	**DAM1**
Au %	28.6	53.2	47.6
Resin	**ETB1**	**BIM1**	**DAB1**
Au %	40.0	16.4	33.2

4.3.2 Elution with Nitrate Solution

The inefficiency and complications of the acidic thiourea eluent system made a more neutral elution process desirable. Two such systems have been examined for resins loaded with the aurothiosulfate complex. In an international patent [1], the use of concentrated nitrate solutions to displace adsorbed aurothiosulfate from commercial anion-exchange resins is claimed. This process is more direct than the two-step polythionate and sulfide treatment developed by Lakefield Research [2]. Thus, the remaining elution tests were performed using a 2.0 M nitrate eluent composed of aqueous $NaNO_3$.

4.3.2.1 Elution of Gold from Polymers in B/R Test #6

The 2.0 M $NaNO_3$ eluent was prepared by dissolving sodium nitrate (170 g, 2.00 mol) in water (~500 mL) and making the volume up to 1000.0 mL.

The batch of resins that had been loaded with gold in Bottle Roll Test #6 (see Table 4.14) were wet-loaded into IEX columns with water (~2 mL). The nitrate eluent was then pumped through each column at 1.0 mL/minute, while collecting five fractions of 20 mL each (at 20 minute intervals).

Significant amounts of brown precipitate formed in the eluates when they were left to stand overnight. This precipitate was dissolved using the following procedure. A small amount of hydrogen peroxide (30%, 5.0 mL) was added to each

sample, the vessel shaken, and left to stand for 30 minutes. The sample was then acidified with conc. HCl (5.0 mL) and refluxed for ~1 minute. The cooled samples, now free of solids, were then made to 50 mL and stored in clean polystyrene vials.

The gold concentration of each eluate was then analysed by AAS. The results are displayed in Figure 4.24 as a plot of the concentration of gold on each polymer against eluent volume. The total percentage of gold eluted from each resin in this procedure is reported in Table 4.14. Copper was not followed, as the initial leach liquor contained only 20 ppm copper.

Table 4.14 %Au Stripped using 2.0 M Nitrate Eluent (B/R #6)

Resin	**PET1**	**BME1**	**DBP1**	**POP2**
Au %	81.1	92.0	73.6	84.7
Resin	**BIM1**	**ABU1**	**TPZ1**	**TBZ1**
Au %	14.4	97.9	66.9	93.6

4.3.2.2 Elution of Gold from Polymers in B/R Test #7

The polymers that were loaded with gold in Bottle Roll Test #7 were loaded into IEX columns as before. All the resin samples were eluted with aqueous sodium nitrate solution (2.0 M, prepared as in Section 4.3.2.1) at 1.0 mL/minute, collecting the eluate in five batches of 20 mL. These were diluted to 100 mL (1:5) to place the gold in the AAS linear detection range. The results are presented in Figure 4.25, configured as the loading of gold on resin (mg/g). The total percentage of gold eluted from each resin is shown in Table 4.15.

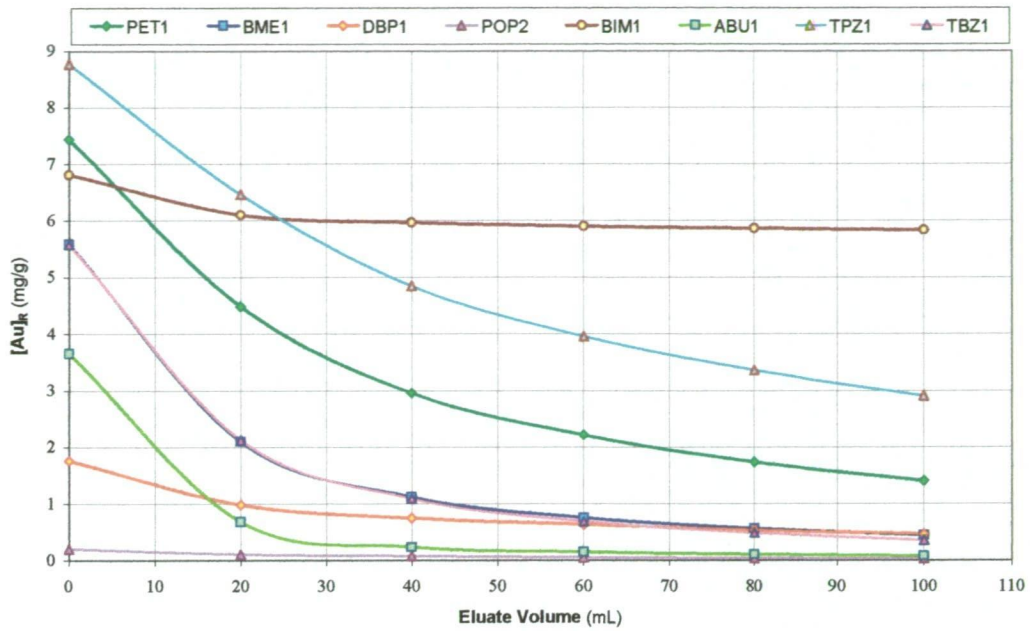

Figure 4.24 Elution of Gold from Resins using 2.0 M Nitrate (B/R #6)

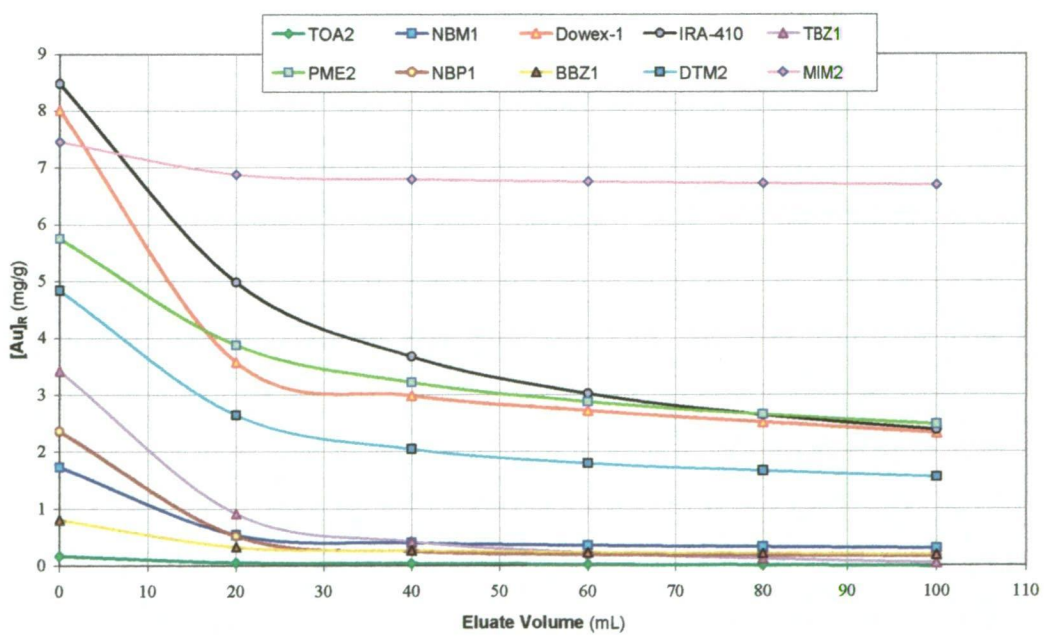

Figure 4.25 Elution of Gold from Resins using 2.0 M Nitrate (B/R #7)

Table 4.15 %Au Stripped using 2.0 M Nitrate Eluent (B/R #7)

Resin	**TOA2**	**NBM1**	**Dowex-1**	**IRA-410**	**TBZ1**
Au %	~100	82.5	70.8	71.8	98.7
Resin	**PME2**	**NBP1**	**BBZ1**	**DTM2**	**MIM2**
Au %	56.7	93.0	77.0	67.8	10.1

Both resins DTM2 and PME2 had a bluish hue after the B/R Test, and remained so after elution with nitrate. This was removed by eluting the resins with aqueous ammonia (~3 M) at 1.0 mL/minute for 20 minutes. A blue eluate was discharged, and the reasons are discussed in Section 4.4.3.

4.3.2.3 Elution of Gold from Polymers in B/R Test #9

This modified eluent was prepared by dissolving sodium nitrate (84.99 g, 1.000 mol) and sodium thiosulfate pentahydrate (6.2070 g, 25 mmol) in ~100 mL of water. These were combined and made to 500.0 mL, giving a solution containing 2.00 M nitrate ions and 50 mM thiosulfate ions. This was used to elute gold from the resins used in Bottle Roll Test #8, using the method detailed in Section 4.3.1.1. Six aliquots of 10 mL eluate were collected from the resins over 50 minutes each, at a flow rate of 0.2 mL/minute. These were then made up to 50.0 mL and analysed for gold by AAS.

The results are displayed in Figure 4.26 as the concentration of gold on each resin (mg/g) as a function of total eluate volume. The total percentage of gold eluted from each loaded resin in this test was also calculated (Table 4.16).

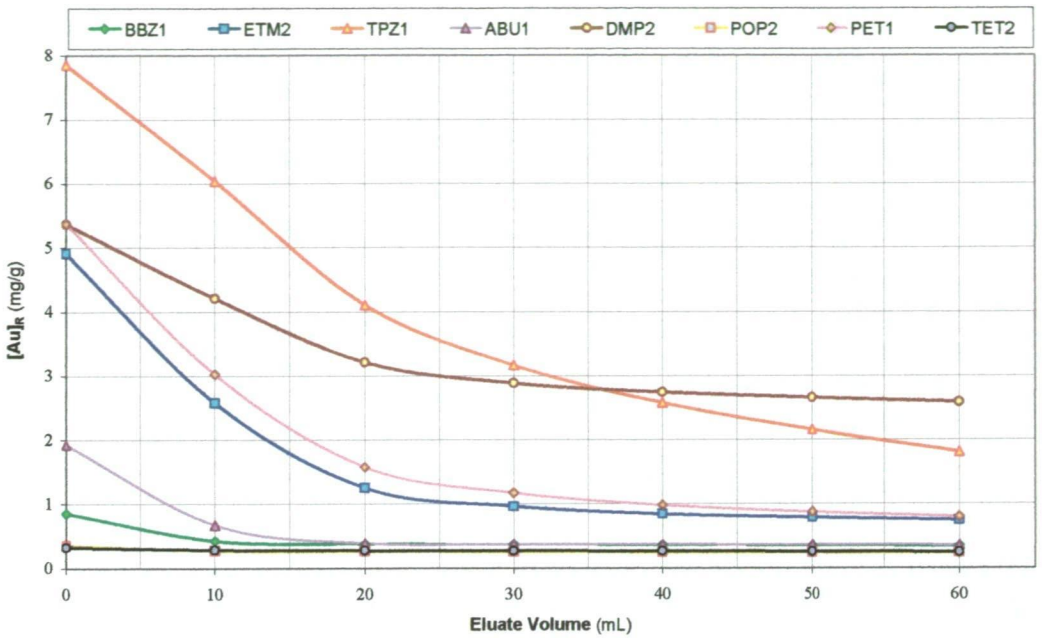

Figure 4.26 Elution using 2.0 M Nitrate + 50mM Thiosulfate (B/R #9)

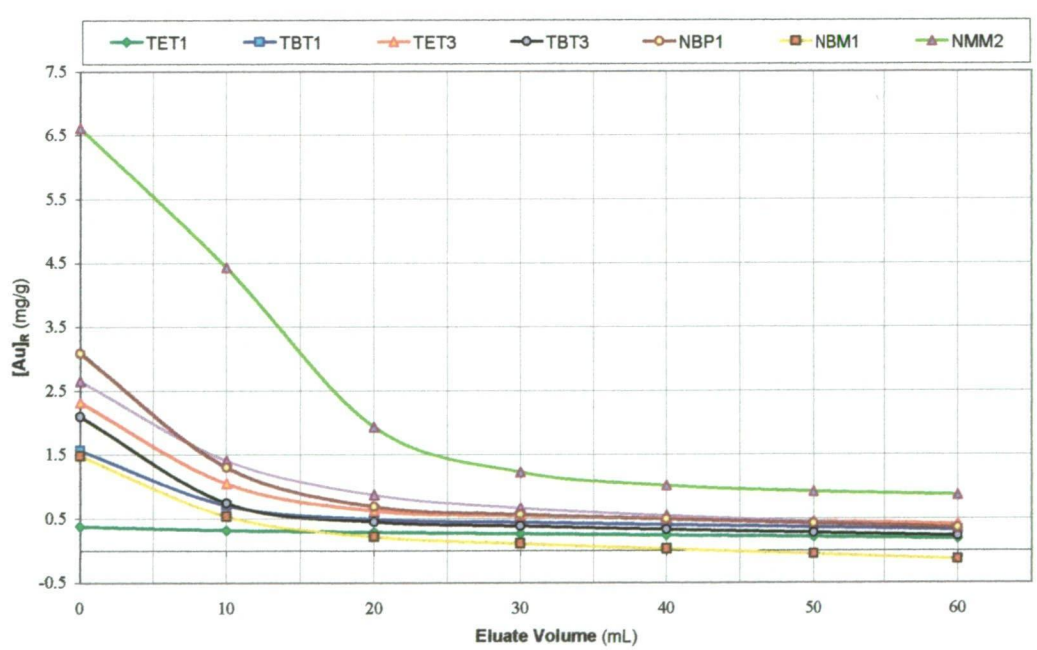

Figure 4.27 Elution using 2.0 M Nitrate + 200mM Thiosulfate (B/R #10)

Table 4.16 %Au Stripped using 2.0 M Nitrate Eluent (B/R #9)

Resin	**BBZ1**	**ETM2**	**TPZ1**	**TET2**
Au %	59.3	84.7	76.9	23.3
Resin	**ABU1**	**DMP2**	**POP2**	**PET1**
Au %	81.3	51.8	32.4	85.0

4.3.2.4 Elution of Gold from Polymers in B/R Test #10

Sodium nitrate (84.99 g, 1.000 mol) and sodium thiosulfate pentahydrate (24.82 g, 100 mmol) were dissolved in a minimum of water, and made to 500.0 mL. The resulting modified eluent solution, containing 2.0 M $NaNO_3$ and 200 mM $Na_2S_2O_3$, was used to elute gold from the resins that had been used in B/R test #10. Six eluate fractions of 10 mL each were collected, at a rate of 0.2 mL/minute.

The results of this elution are presented in Figure 4.27, configured as the concentration of gold on the resin (mg/g). The overall percentage of gold that was eluted from each resin in this experiment is shown in Table 4.17. It is believed that the result for resin NBM1 (>100% elution) has been distorted by an anomalously high AAS result.

Table 4.17 %Au Stripped using 2.0 M Nitrate Eluent (B/R #10)

Resin	**TET1**	**TBT1**	**TET3**	**TBT3**
Au %	51.1	79.2	82.3	89.1
Resin	**NBP1**	**NBM1**	**NMM2**	
Au %	88.4	(108.9)	86.8	

4.4 *Evaluation of Resin Performance*

4.4.1 Discussion of AAS Results

Precipitation of metals is a known problem in thiosulfate solutions, but was observed only in a number of diluted leach or eluate liquors that had been allowed to stand overnight (see Section 4.3). The formation of a visible precipitate was always reversed by acidic sample digestion. All glass sample vials were cleaned with aqua regia prior to use, to strip any adsorbed gold, sulfides, and other undesirable and unwanted trace elements from the glass surface. These precautions were taken to prevent carryover of precipitated gold from previous experiments, to reduce the oxidation of thiosulfate by trace metals and ions, and consequently to minimise gold losses from samples during storage (generally < 24 hours).

4.4.1.1 Discussion of Gold AAS Results

Gold standard solutions were randomly interspersed amongst the sample analyses to give an ongoing assessment of the accuracy and variability of the gold concentrations that were observed. It was found that ammoniacal thiosulfate liquors gave considerably more variation than the standard acidic chloride matrix used for the gold standards (see Table 4.4). This may be related to the unusual AAS flame behaviour discussed below. The variation in the AAS-determined gold values in a leach liquor containing 200 ppm copper was of the order of ± 0.2 ppm at wavelength 242.8 nm, and ± 0.4 ppm at the less sensitive wavelength of 267.6 nm. When this threshold was exceeded in an AAS standard, the instrument was recalibrated with the full set of standard solutions.

Flame shape defects and an orange discolouration of the AAS flame developed progressively during analysis of leach liquors, indicative of contamination

of the AAS burner. The precipitation of unknown salts on the AAS burner has the effect of causing 'carryover' of gold and/or copper between samples, gradually raising the background levels of these elements. This competes with the blocking of the burner aperture by precipitates, which diverts the gas flow and hence lessens the AAS response, resulting in under-reporting of metal content. This problem cannot be overcome by dilution, which would significantly reduce the sensitivity of the gold readings. Blank solutions and controls were analysed periodically during AAS analyses to monitor this effect and allow for normalisation of the data where necessary.

Small subsets of the resins were studied in liquors containing 10 and 20 ppm Au (Section 4.2.1) and 20 ppm each of Au and Cu (Section 4.2.2), none of which showed serious problems with AAS precipitation. Subsequent experiments using ~200 ppm copper showed reasonable reproducibility, however AAS recalibration was required after every ~ 40 samples.

Liquors derived from elution studies were often significantly more concentrated than the B/R liquors, and the additional dynamic range of the second AAS wavelength for gold (276.7 nm, see Table 4.4) made it more practical for such liquors. The different aqueous matrices of the eluate liquors introduced some additional variability into the results, particularly where multiple dilutions were required to achieve a gold concentration within the linear range. These liquors were analysed as-is where possible, and compared to the standards of $[AuCl_4]^-$ in 5% aqueous HCl. A linear response for gold standards in dilute nitrate eluent was established in Section 4.1.4.2.

Analysis of the nitrate eluate solutions resulted in precipitation of salts on the AAS burner. It was necessary to dilute some eluate liquors to bring the gold concentration into the linear range. Dilution reduces the thiosulfate concentration,

thereby increasing the rate of thiosulfate oxidation (decomposition). Decreased levels of thiosulfate and/or the presence of trace sulfides may result in the precipitation of gold from the liquor, leading to diminished gold concentrations in solution. The precipitates formed in the liquors from the first nitrate elution (Section 4.3.2.1) were probably due to the lack of excess thiosulfate ions.

An approach taken by Feng and van Deventer to minimise precipitation of the metals from the liquors on standing was to digest the gold-bearing thiosulfate liquor in hydrochloric acid and peroxide. This converts the metastable thiosulfate complexes into stable chloride complexes, whilst converting thiosulfate into sulfate. However, this step was taken to minimise reproducibility problems in an ICP-MS system, where the thiosulfate liquor proved particularly problematic [3]. This procedure is undesirable due to the additional sample handling and dilutions involved.

Preconcentration of gold in MIBK (methyl isobutyl ketone) [4] is unlikely to improve resolution in these cases. This method was developed for the more common gold lixiviant systems (chloride and cyanide), and correlation studies have been performed for those systems. The corresponding partition constant(s) of the salts of the aurothiosulfate complex into the MIBK are entirely unknown, and hence any results from this method would require extensive calibration and validation. This method is also undesirable due to the time consuming nature of the test, and the significant the error margin when handling small samples (< 10 mL).

4.4.1.2 Discussion of Copper AAS Results

The leaching test using a copper concentration of ~2000 ppm {B/R test #2}served to highlight several inherent difficulties in handling ammoniacal thiosulfate leach liquors containing high levels of copper. The most serious of these

was the analysis of the liquor by AAS, where significant variations in the response of standard solutions (copper and gold, ± 20%) were observed. This variance increased as additional samples were analysed, rapidly forming flame defects and discolouration. Dilution of the liquor (1:100) was found to increase the variance in the diminished copper values (± 50%). Due to the low gold content, analysis of diluted liquors for gold was not practical. The accurate determination of gold and copper in this solution proved impossible due to precipitation of copper salts upon the tungsten AAS burner.

In a closed system such as a bottle-roll test, the rapid consumption of all available oxygen by copper-catalysed oxidation of thiosulfate may produce high levels of copper(I) thiosulfate complexes. The rapid consumption of free thiosulfate ions by oxidation with Cu(II) is also of concern in high-copper liquors, as the entire complement of free thiosulfate may be consumed (see Section 4.1.4.2).

After these initial examinations, and taking the difficulties encountered above into account, it was decided to use a liquor with 200 ppm copper (introduced as $CuSO_4$ or $Cu(OH)_2$; see Table 4.2). Although the copper concentration is lower than many reported studies, it permits more reliable analyses of the solution.

Some consideration was also given to the presence of unwanted ions in the leaching system. Copper was initially introduced to the leach liquor as a concentrated solution of $Cu(NO_3)_2$ {B/R #2}, however nitrate ions are not generally found in thiosulfate leach liquors, and are indeed considered undesirable. Several latter experiments were performed using liquors prepared from technical grade $Cu(OH)_2$ {B/R #4, 5}, which avoids any unwanted ions entirely. Dissolution of the solid was not always easily achieved, and it was decided to replace this low purity reagent with analytical grade $CuSO_4.5H_2O$, which was used in all experiments thereafter.

4.4.2 Analysis of Resin Gold Adsorption

Resins were studied in B/R liquors containing 10 or 20 ppm Au (Section 4.2.1), 20 ppm each of Au and Cu (Section 4.2.2), or in latter studies 20 ppm Au with 200 ppm Cu (Section 4.2.3). The results, shown in Figures 4.3 – 4.13, reveal similarly shaped gold sorption isotherms for all resins. From the data obtained in the B/R Tests containing 20 ppm Au and 200 ppm Cu, the following resin characteristics have been determined:

(1) The minimum time in which maximum gold adsorption is achieved;

(2) The %Au adsorbed from solution by one gram of each resin, and

(3) The mass of gold adsorbed from solution by one gram of each resin.

From this information, and the IEX capacities of the resins determined in Chapter 3, it was also possible to calculate the amount of gold adsorbed per mol of resin IEX capacity, yielding the functional group loading, $[Au]_R/C_M$. These four characteristics of each resin are summarised in Table 4.11 (Section 4.2).

The number of moles of gold in each B/R Test solution batch was generally very much less that the number of resin ligands available. In particular, B/R Tests #1 (10 ppm Au) and #3 (20 ppm Au) held 25 and 50 micromoles Au respectively. For example, consider resin NMM1 in Bottle Roll Test #3:

NMM1: 1.003 g x 2.70 meq/g = 2708 μmol >> 50.0 μmol (Au in 498 mL).

Note that the gold is in a trivalent state, so three resin groups are required per gold complex (ie. 903 μmol capacity vs. 50.0 μmol Au). In general, an excess of resin was present to adsorb the available gold in each B/R test, should the functional group prove to be selective.

An analysis of the kinetics and reproducibility of the gold loadings in these B/R tests follows in Sections 4.4.2.1 and 4.4.2.2. Functional group structural trends associated with improved gold loading are evaluated in Section 4.4.5.

4.4.2.1 Assessment of Solution Kinetics

In the idealised Cu-free leach solutions analysed in Section 4.2.1, it may be possible to fit the gold adsorption data to standard reaction kinetics equations and derive a reaction order with respect to gold. This cannot readily be performed for the polymer groups, due to two complications: the abundance of competing ions, and the phase distribution between the resin and solution.

The reaction is of the type: $A + 3B \rightarrow C$ (4.3)

where $A = [Au(S_2O_3)_2]^{3-}$ $B = R_3N^+CH_2\{Polymer\}$

and $C = [Au(S_2O_3)_2]^{3-}.(R_3N^+CH_2\{Polymer\})_3$.

If the reaction is first order in both components, then the reaction rate is given by:

$$v = \frac{k'.[A]_t.[B]_t}{3} \tag{4.4}$$

where $[X]_t$ denotes the concentration of component X in solution at time t.

Given a large excess of reagent B relative to A (B >> A) then we can approximate:

$$k = \frac{k'.[B]_0}{3} \tag{4.5}$$

The integrated rate law for a first order reaction is:

$$\ln\frac{[A]_t}{[A]_0} = -k.t \tag{4.6}$$

Thus, a plot of $\ln[Au]_t$ against time will have slope $-k$.

Alternatively, if the reaction is second order in A then the reaction rate is:

$$v = \frac{k'.[A]_t^2.[B]_t}{3} \tag{4.7}$$

As before, if B >> A then we can make the approximation that $k = (k'.[B]_0)/3$.

The integrated rate law for a second order reaction is therefore:

$$\frac{1}{[A]_t} - \frac{1}{[A]_0} = -k.t \tag{4.8}$$

Thus, a plot of $1/[Au]_t$ against time will have slope $-k$.

For each resin used in B/R tests #1 and #3 (Section 4.2.1), plots of $\ln[Au]_t$ and $1/[Au]_t$ versus t were constructed according to equations 4.6 and 4.8. Sample plots are presented in Figure 4.28 for resins PET1 and TPZ1. The data was observed to fit poorly with the first order approximation, but quite well with a second order rate equation (as evidenced by the least-squares fit, $R^2 > 0.95$). The weak base and control (A378) resins had negligible gold loading ($[Au]_R$), and hence were omitted from this analysis.

The interpretation of these plots are complicated by the presence of increasing quantities of competing anions (eg. trithionate). Competition between gold and trithionate for IEX groups causes non-linear deviation from ideal adsorption behaviour. This effect increases over time, as the trithionate concentrations in leach solutions slowly increases. The fit of B/R Tests #1 and #3 with the second order kinetic model was improved when the last two data points (8 and 24 hrs) were omitted (Table 4.18: 1/[Au] vs t (1 - 6 h)).

In the B/R Tests containing ~200 ppm copper, there was no significant correlation with either of the kinetic models above. Many resins achieved their optimal functional group loading before the end of the B/R Test, as indicated in Table 4.12. It is likely that this is caused by the competitive adsorption of trithionate, tetrathionate and possibly the Cu(I) thiosulfate complexes. The concentration of these oxidation products increases over time, and this imposes a downward trend in $[Au]_R$. This is especially significant for the low capacity resins.

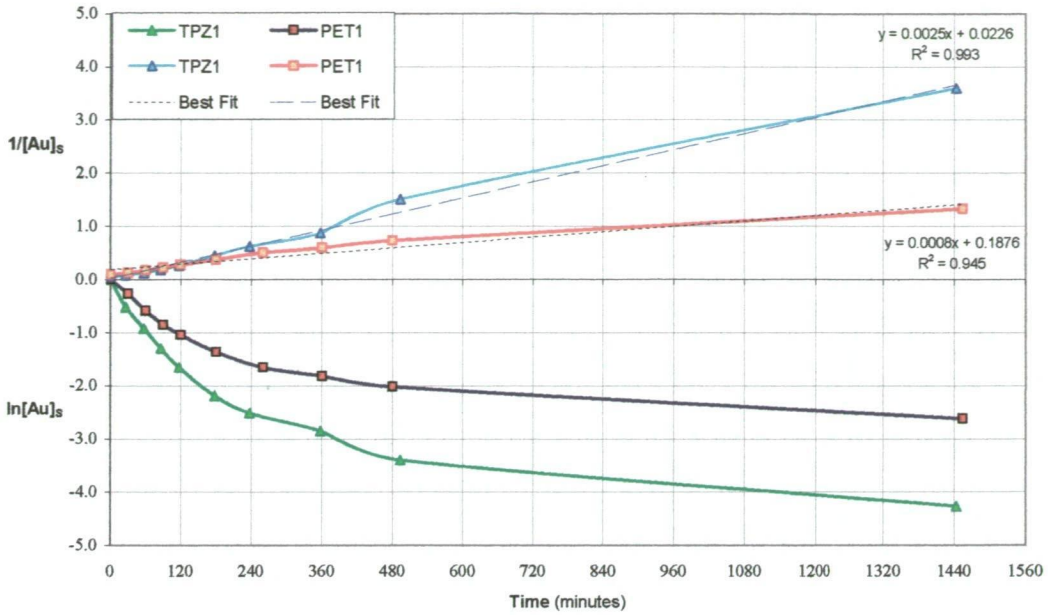

Figure 4.28 Kinetic Fitting Plots for Resins PET1 and TPZ1

Table 4.18 Kinetic Fitting of Data from B/R #1 and B/R #3

Resin	ln[Au] *vs* t (1 – 24 h)		1/[Au] *vs* t (1 - 24 h)		1/[Au] *vs* t (1 - 6 h)	
	R^2	$-k \times 10^3$	R^2	$-k \times 10^3$	R^2	$-k \times 10^3$
ABU1	0.7270	1.2	0.9374	0.4	0.9768	0.7
PET1	0.6794	1.6	0.9450	0.8	0.9902	1.5
NMM1	0.7895	2.5	0.9974	1.4	0.9739	1.2
NMP1	0.7519	3.3	0.9898	5.7	0.9608	3.6
TME1	0.8171	1.8	0.9935	0.5	0.9963	0.6
TBT1	0.8507	0.4	0.9184	0.05	0.9566	0.1
TBZ1	0.8229	2.4	0.9934	1.5	0.9804	1.1
TPZ1	0.7002	2.6	0.9930	2.5	0.9903	2.4

It can be inferred from Figure 4.13 that resins with larger average particle sizes tend to show slower kinetics than their smaller relatives. The commercial resin Dowex-1 achieved maximum gold loading after only one hour. The larger bead size of resin A26, with the same functional group as Dowex-1, took longer to achieve maximum gold loading (3 hours). The sized fraction 'A26 Big', was slower again, reaching peak loading only after 6 hours. The Type II resin, IRA-410, was somewhat slower to adsorb gold than the other commercial resins, possibly due to the less porous nature of the gel matrix. The fast kinetics shown by the resins with smaller particles is a function of the shorter diffusion barrier and higher surface area, permitting more rapid loading of aurothiosulfate.

This rapid diffusion effect is probably also responsible for what appears to be a more rapid elution by the ubiquitous polythionates. The gold loading of Dowex-1 fell constantly after the maximum at 1 hour, probably due to rapid fouling with polythionate anions. This is consistent with a low selectivity of the resin for gold. This effect was seen to a lesser degree on the other commercial resins examined. Despite the rapid sorption kinetics, fine adsorbent particles are not suitable for RIP schemes, as small resin beads are difficult to separate from the leach pulp.

4.4.2.2 Analysis of Replicate B/R Tests

In general, the performance of the resins was reproducible within 0.5 mg/g (see Figures 4.14 – 4.16). Significant variance (~ 1.0 mg/g) was seen in tests of resins MIM2 and QNU1, where gold sorption was higher in the later tests. The increase in the gold loading of these resins is probably due to lower porosity of the resins in the earlier tests, caused by to poor wetting and entrained residues. These problems were both eliminated during IEX conditioning prior to the latter tests.

The effect of 20 ppm Cu on the behaviour of a small set of resins was examined by comparison with the results of copper free liquors (Sections 4.2.1 and 4.2.2). The parameters compared in this analysis were gold recovery after 6 hours (%Au) and resin loading ($[Au]_R$; mg/g); these are summarised in Table 4.19. The gold loading of resin TBZ1 diminished over time, probably due to decomposition, whereas the loading of the other resins was virtually unchanged by the presence of 20 ppm copper in the liquor. This is because the copper present in solution consisted primarily of cationic Cu(II) ammine complexes. The resulting low concentration of anionic Cu(I) thiosulfate complexes is insufficient to significantly compete with gold for cationic IEX sites. Accelerated formation of polythionates by reduction of Cu(II) may have slightly diminished the maximum gold loading.

Table 4.19 The Effect of Cu (20 ppm) on Resin Performance

†: *Results from a Leach solution containing only 10 ppm Au*

Resin	**%Au (6 hrs)**		**$[Au]_R$ (mg/g)**	
Code	**B/R #1 + #3**	**B/R #6**	**B/R #1 + #3**	**B/R #6**
ABU1	72.2†	37.4	3.57†	3.66
TPZ1	94.2	89.6	8.81	8.77
TBZ1	88.8	57.3	8.39	5.58
PET1	83.7†	78.6	4.15†	7.44

4.4.3 Analysis of Resin Copper Adsorption

The copper concentrations in B/R Test #6 were followed by AAS (217.9 nm), revealing a near constant 20 ppm Cu (± 2 ppm) over the six hours of the experiment. These results indicate that the low level of copper present in this solution is unlikely to affect the adsorption of gold, and is thus consistent with the results in Table 4.19.

The AAS results for B/R Test #5 registered an initial copper concentration of ~184 ppm (4% higher than calculated). The AAS results for this batch were particularly unstable, and required frequent recalibration and burner maintenance. These problems may derive from the poor quality (technical grade) $Cu(OH)_2$ used to prepare the liquor.

In all the tests involving liquors containing ~200 ppm copper (Figures 4.17 – 4.20), only a few resins showed significant copper sorption (> 10 ppm), with the largest being for resin QNU1 (~30 ppm). Relatively high levels of copper were also adsorbed by BME1 (~22 ppm) and the commercial resins Dowex-1 (~16 ppm) and IRA-410 I (~13 ppm). Copper sorption was moderate with resins MIM2, NMP1 (~12 ppm), TPY1, NMM1 (~11 ppm), DTM2, PME2, TBT2 and TBZ1 (~10 ppm). Resins DTM2 and PME2 acquired a bluish hue during B/R Test #7, indicative of $[Cu(NH_3)_X]^{2+}$ adsorbed on amine sites by displacement of one or more ammonia ligands. The similar behaviour of these resins probably results from common structural features (1,2-diamine groups). The colour of the resins remained after nitrate elution, and was removed by washing with aqueous ammonia. Negligible loss of copper was observed in tests using the remaining resins.

The relatively high sorption of copper by these resins may be due to functional group selectivity for copper, or weak-base residues on the resin, such as 1,2-diamine, chelating Cu(II). However, the IEX capacity of QNU1 is slightly lower

than that of the commercial resins, and the resin is consistent with published data: there is little evidence of weak-base decomposition products. The resins expected to have some weak-base capacity (TME, TET, TBT) showed poor copper sorption, as did the incompletely alkylated resins BBZ1 and DAM1. Therefore, it appears likely that Cu(I) sorption from thiosulfate liquors is influenced by similar steric factors to Au(I) sorption. This is consistent with the similar structure and charge of the Au(I) and Cu(I) thiosulfate complexes (see Section 2.5).

In a number of resins (eg. MIM2, NMM1, Dowex-1 and IRA-410) , copper reaches a maximum concentration on the resin after a short time (1 - 3 hours), and diminishes over the remaining time. This is consistent with the displacement by a preferred anion, such as aurothiosulfate or trithionate.

The copper concentration was not followed in subsequent tests, since copper(I) thiosulfate complexes adsorbed onto resin IEX sites are likely to be displaced by the gold complex [5]. Additionally, the copper adsorbed from solution is of a similar order to that of gold, and not usually enough to saturate all resin IEX sites, even as the $[Cu(S_2O_3)_3]^{5-}$ complex.

Each of the test solutions used in the tests reported in Section 4.2.3 contained ~200 ppm of copper, which may form anionic thiosulfate complexes that compete with gold for IEX sites on a resin adsorbent. The copper concentration fell less than 30 ppm over the course of the B/R Tests studied (#4, #7 & #8). In most cases, less than half this amount of copper was lost from solution (see Figures 4.17 – 4.20). Maximum copper loading can be calculated as follows: 500 mL x 30 ppm = 15 mg Cu (0.24 mmol). This allows a maximum of ~1.2 meq of IEX groups occupied with the $[Cu(S_2O_3)_3]^{5-}$ complex. This was not generally sufficient to saturate the IEX resins, except in the cases of low-capacity resins (ie. < 1.2 meq/g).

This presumes that all the adsorbed copper must be as complexes of the form $[Cu(S_2O_3)_N]^{(1-2N)}$ (N = 1 – 3). However, sorption of Cu(II) by weak-base groups produced by degradation of functional sites may also contribute. The distribution of dissolved copper into Cu(I) and Cu(II), and the speciation of Cu(I) into complex anions is not known for these solutions. The relatively low sorption of copper in most cases may be a consequence of the skewed distribution of copper in favour of the +2 oxidation state, with only a small proportion of soluble copper present as Cu(I).

It should be noted that copper is present in ammoniacal thiosulfate solution as both Cu(I) and Cu(II), primarily as $[Cu(S_2O_3)_N]^{1-2N}$ (N = 1-3) and $[Cu(NH_3)_4]^{2+}$ respectively. The AAS system does not discriminate between these complexes, which both contribute to overall copper concentration. The contribution of each compound to the AAS response may be unequal, and hence the Cu(I)/Cu(II) ratio may influence the apparent distribution of copper between the adsorbent (IEX resin) and solution.

The ratio of Cu(I)/Cu(II) is controlled by the dissolved oxygen concentration [6], which is likely to change with each sampling step in an adsorption test. The metastable Cu(I) complexes are rapidly oxidised by Cu(II) in solution, possibly through a highly reactive oxygen-Cu(II) adduct. This is the basis of the selective copper-elution scheme outlined by O'Malley [1], wherein adsorbed anionic copper(I) thiosulfate complexes $[Cu(S_2O_3)_N]^{(1-2N)}$ (N = 1 - 3) are rapidly oxidised to the cationic $[Cu(NH_3)_4]^{2+}$ species by oxygenated ammonia. Following the copper distribution accurately requires controlled oxygenation of the leach solutions and therefore extremely careful sample handling, such as a recirculating flow-through cell to prevent exposure of the solution and/or the sample to the atmosphere. Such

preparations for bottle-roll testing are extremely time-consuming, and were considered beyond the scope of this project.

It is possible that the degree of copper adsorption onto IEX resins from ammoniacal thiosulfate solutions may be minimised by oxygenation, as the cupric species cannot adsorb onto anion-exchange resins. However, this has the disadvantage of enhancing thiosulfate oxidation and thus reducing leach solution stability.

4.4.4 Evaluation of Gold Elution Tests

4.4.4.1 Evaluation of the Efficacy of the Thiourea Eluent

For the first elution attempt (Section 4.3.1.1), the initial loading of gold was well characterised for the resins QNU1 (6.24 mg/g), TPY1 (1.16 mg/g) and BME1 (4.29 mg/g). From this data, the percentage of gold eluted was calculated for each resin to be: QNU1 (18.4 %); TPY1 (9.8 %); and BME1 (20.3 %). The final gold loading (after 48 hours) was not measured for the other resins in this set, hence they have been offset by 3 mg/g (Figure 4.22). The concentration of copper in the eluate was also followed by AAS (222.6 nm), but was always found to be within the level of experimental error (±10 ppm).

The rate of gold elution for each resin is shown by the slopes of the lines in Figure 4.22. These were found to be ordered by relative IEX capacity, with the high-capacity resin TPZ1 showing the most rapid gold elution profile of this batch of resins. This resin had turned rose pink at the end of the adsorption test (B/R #4), but was restored to the original off-white upon contact with the thiourea eluent. The cause of this behaviour is unknown, but appears related to solution pH.

None of the polymers eluted in section 4.3.1.1 were efficiently stripped of adsorbed gold, with resin TPY1 the most recalcitrant. This was possibly due to the

relatively low residence time of the eluent solution. The relatively rapid flow rate used (1.0 mL/minute) did not allow the eluent enough time to properly diffuse throughout the polymer matrix.

In subsequent tests (Sections 4.3.1.2 & 4.3.1.3), the eluent flow rate was reduced to 0.5 and 0.2 mL/minute respectively. Significant improvements in elution efficiency were observed (see Tables 4.15 and 4.16), although the slopes of the elution profiles generally remained proportional to the IEX capacity. It should be noted that the elution of gold from resins with less than ~1 mg/g Au was difficult to evaluate with accuracy. Complete elution of all adsorbed gold was not achieved with any resin, and this aspect was not pursued. Nonetheless, it can easily be seen which resins are amenable to efficient elution.

Resin DAM1 (a Type II resin) was the only resin to show a significantly more rapid elution profile (Figure 4.24). The elution profiles of resins NMM1, TME1 and BIM1 were relatively inefficient. Difficulty in eluting gold from these moieties may reflect their high affinity with aurothiosulfate relative to the HSO_4^- anion. In comparison to the loading of auricyanide from cyanide leach liquors, none of the novel resins were eluted as efficiently as the commercial resin Minix, which permits 95% elution in 4-10 bed volumes of acidic thiourea [7].

There are three principal difficulties associated with the use of acidic thiourea as an eluent for aurothiosulfate from the resins used in this work:

(i) The pH change caused by treatment with the thiourea eluent described above is quite large (pH 10.2 → pH < 2). The associated change in swelling of the resin can induce osmotic shock in the beads, causing them to shatter. In most instances, the eluted resins showed extensive fragmentation consistent with this effect.

(ii) The acidic eluent is not compatible with the leach liquor, which is both alkaline and contains anions that decompose in the presence of acid, ie. thiosulfate. Acid induced decomposition introduced undesirable compounds, such as polythionates, sulfide, and sulfur. Thiourea itself also decomposes over time, forming sulfinic compounds that may foul resin sites and induce the precipitation of gold [8].

(iii) Precipitation of metals from solution due to the presence of ligands such as sulfide which form insoluble complexes. This may also occur to the aurothiosulfate complex in the absence of free thiosulfate, as the metastable ligands decompose. This concern prompted the acidic digestion of precipitates from the decomposed eluate solutions in section 4.3.1.3.

4.4.4.2 Evaluation of the Efficacy of the Nitrate Eluent

It is clear from Figures 4.26 – 4.29 that the efficacy of this eluent was comparable to the thiourea eluent with most of the resins examined. A number of resins were eluted using both systems, allowing direct comparison. Gold was more efficiently eluted from resin BME1 with nitrate (80%) than thiourea (18%) under similar conditions (40 mL at 1.0 mL/minute). The efficacy of nitrate and thiourea eluents on resins DBP1 (57% vs. 53%) and BIM1 (12% vs. 14%) were similar, although the slower flow rate of the latter eluent (0.2 mL/minute) must be noted.

However, it was also noted that elution was less efficient with the imidazole-derived resins (BIM1 and MIM2) and the exhaustively methylated triazamacrocycle derivative DMP2 than the other resins. This may be associated with the delocalised imidazolium cation in BIM1 and MIM2. The polyammonium group of resin DMP2 has the capacity to encapsulate the gold to a greater degree than a simple ammonium group, and it may consequently be more difficult to effect elution.

Elution of adsorbed aurothiosulfate from a wide range of commercial IEX resins using nitrate solutions has been reported by Nicol & O'Malley [1, 5]. Elution of the majority of adsorbed gold from Amberjet-4200 resin was achieved within 10 bed-volumes, at a flow rate of 5 bed volumes (BV) per hour. However, the commercial resins used in this study (IRA-410 and Dowex-1) were eluted less efficiently (Section 4.3.2.2). Assuming the BV of one gram of hydrated resin to be ~2 mL, then 100 mL eluate equates to ~50 BV. The eluent flow rate used in Figure 4.25 approximates to 30 BV per hour (ie. 1.0 mL/minute x 60 minutes). It is clear that the gold has not been fully eluted (< 90%) from resins IRA-410 and Dowex-1, despite the large volume of eluate. More efficient elution was observed in subsequent elution tests by using lower eluent flow rates (0.2 mL/minute), as seen in Figures 4.26 and 4.27. This compares reasonably well with the elution profile of auricyanide from the commercial Aurix resin, where 95% elution may be achieved after ~40 bed volumes of 4% NaOH solution [9].

The principal problems associated with this eluent system appear to be fewer than found in the available alternatives. For example, nitrate salts such as $NaNO_3$ are hazardous solids, which act as oxidising agents and accelerants. The handling of large volumes of strong nitrate solutions in an industrial setting may be undesirable, but this risk must be weighed against the alternatives. Thiourea eluents are corrosive and a suspected carcinogen, whereas the polythionate-sulfide system is a two-step procedure with metastable components, requiring careful monitoring and process control to be effective.

One problem observed with nitrate eluents in this work is the precipitation of gold over time as the thiosulfate ligands decompose. The brown precipitate that formed in the eluate in Section 4.3.2.1 was most likely insoluble gold and/or copper sulfide(s) created by decomposition of thiosulfate. This necessitated treatment with

peroxide and HCl to redissolve the metal for analysis. The addition of thiosulfate to the eluent in later tests (Sections 4.3.2.3 & 4.3.2.4) minimised precipitation without compromising the efficiency of the eluent.

This effect is may not be a problem if the resins are eluted rapidly enough to prevent gold precipitate from forming amongst the adsorbent. In fact, the precipitation of gold in the eluate is desirable – it permits rapid and efficient recovery of gold values. The extent of this precipitation is unknown, but may be encouraged by the addition of sulfide ions. If the concentration of sulfide (and other contaminants) in the stripped eluent remains low, it may be recycled. In these circumstances, this eluent system is reasonably inexpensive and efficient.

In this work, it has not been possible to examine every possible combination of eluent system and resin to determine the optimum elution procedure for each resin structure. Of the two systems examined, the nitrate eluent appeared to yield superior outcomes to the more toxic thiourea eluent.

4.4.5 Selection of Optimal Resins

In the present circumstances, the ion exchange capacity of each resin has been evaluated in terms of the absolute number of cationic charges (+1) present per gram. The IEX capacities determined experimentally do not take the structure of the functional group into account. If it were desirable to normalise the gold loading ratio to whole functional groups, the IEX capacity can be divided by the number of amine/ammonium nitrogen atoms present in one functional group. This treatment assumes that only one kind of functional group is present – ie. that all derivatisation reactions have been 100% successful, and that no side reactions have occurred. This is not always the case with derivatisation of IEX resins, and hence the overall IEX capacity is more useful. This also permits more direct comparison of resins, as the apparently high selectivity of polyamine resins is often countered by low capacity.

The IEX procedure employed in this study used high pH solutions (pH = 10) and hence determines the total capacity of strong-base groups only. It may be possible to determine the total capacity of weak- and strong-base groups by IEX using low pH solutions (eg. pH = 2), and hence calculate the capacity of weak-base groups by difference. This would be useful as an evaluation of the efficacy of alkylation steps. This was not regarded as important in this project, as the resins were tested at an operational pH greater than 10 – where few weak base groups will be protonated. The experimentally determined IEX capacity results at pH 10 were taken as sufficient for use in the artificial leach liquors use in this project.

The important characteristics for each resin have already been summarised in Table 4.11, including a comparison of Au loading to capacity ($[Au]_R/C_M$). From comparison of these results, a number observations can be made:

- Little gold was adsorbed by the weak base resins (DET1, DIP1, NMZ1, TAA1) and the N-oxide resin (POP2). The behaviour of these resins is indistinguishable from that of the A378 substrate.
- Strong base resins APH1, TBA1, TOA1 & TOA2 show very little gold sorption. This is a consequence of their very low or negligible IEX capacity.
- Resins TET1 & TET2 show poor Au sorption. This is consistent with serious degradation of the functional group, leading to negligible capacity. Resin TET3 was less degraded, and had a higher selectivity for gold ($[Au]_R/C_M$).
- Resins TBT1 & TBT2 adsorbed gold quite poorly. The low selectivity ($[Au]_R/C_M$) may be due to due to decomposition of the functional sites. TBT3 was apparently less degraded, and had higher selectivity.
- A group of resins demonstrated relatively low gold sorption (< 1.5 mg/g) of a similar order to the control resin A2. This set comprised the following resins: BBZ1, DAB1, DBP1, ETB1, NBM1, TBB2, TBM2, TEB1, TEM1 and TPY1. Of this set, only the resin DAB1 showed significant selectivity ($[Au]_R/C_M$), and this may be an artefact of the high variance relative to the low capacity.

The remaining strong base resins were relatively effective in gold recovery. Functional group loadings ranged between 3.4 – 16.2 mmol Au per mol IEX capacity, ie. 1.0 – 4.9 % of all resin sites occupied by $[Au(S_2O_3)]^{3-}$. These relatively low loadings are not surprising, given the excess of IEX groups relative to the limited amount of gold present in the B/R tests, and the presence of the competing anions trithionate, tetrathionate and the Cu(I) thiosulfate complexes. The effects of the methyl and benzyl substituents may be evaluated by comparison of the gold loading of analogous structures, as summarised in Table 4.20.

Table 4.20 Steric Effects of Methyl and Benzyl Groups

†: resin with IEX capacity < 1.0 meq/g *: crosslinked diethylenetriamine

Backbone of ammonium group	Benzyl Derivative	$[Au]_R/[C]_M$ (mmol/mol)	Methyl Derivative	$[Au]_R/[C]_M$ (mmol/mol)
Piperidine	NBP1	7.0	NMP1	6.1
Morpholine	NBM1	4.5	NMM1	4.6
Ethanolamine	ETB1†	5.9	ETM2	9.4
Diethanolamine	DAB1†	10.7	DAM1	11.8
Imidazole	BIM1	16.2	MIM2	12.1
TMEDA	BME1	9.6	PME2	7.6
N-methylpiperazine	TBZ1	7.8	TPZ1	11.3
TET	TEB1	2.6	TEM1†	4.2
TBT	TBB2†	5.4	TBM2	3.9
DST *	DBP1	3.5	DMP2	10.1

Table 4.20 draws attention to certain structural trends. In particular, the gold loading is higher for the methyl analogues of N-methylpiperazine, ethanolamine, diethanolamine and TET, whereas the benzyl analogues were apparently superior for derivatives of piperidine, imidazole, 1,2-diaminoethane and TBT. However, the results for derivatives of TET, TBT, and TMEDA resins may be influenced by side-reactions resulting from degradation of the functional group.

The gold sorption ($[Au]_R/[C]_M$) of resins TET1 and TET2 was negligible (0.6 mmol/mol), whereas that of TBT1 and TBT2 (2.5 - 3.8 mmol/mol) was similar to the alkylated derivatives. A third preparation of both resins (TET3 and TBT3) yielded the highest gold loading of the triazine resins (6.7 - 6.8 mmol/mol), but it is unlikely that any of these will remain stable when used. Similarly, the preparations

of TMEDA resins showed quite different selectivity (TME1: 13.0 mmol/mol; TME2: 3.4 mmol/mol). This is clearly due to degradation processes, and therefore casts doubt upon the condition of the functional groups of the derivatives (BME1 and PME2).

There does not appear to be any significant influence of the piperidine or morpholine rings on gold affinity. The N-oxide resin POP2 was a poor adsorbent for gold in these conditions ($[Au]_R/[C]_M$ = 1.2 mmol/mol). However, the resin NMM2 was prepared from the D2780 substrate and performed significantly better than the first preparation (11.6 vs. 4.6 mmol/mol). The influence of the substrate is not clear, as the first preparation may have degraded.

The Type II (2-hydroxyethylammonium) resins prepared in this work also showed promising results. The gold loading of the N-(2-hydroxyethyl)piperidine derivative PET1 (11.9 mmol/mol) was much improved over the methyl- and benzyl piperidine derivatives (see Table 4.20). The derivatives of ethanolamine and diethanolamine were also quite effective adsorbents for gold, particularly the methylated versions. These are comparable with the commercial Type II resin IRA-410, which is believed to have the same functional group as resin ETM1.

Considering these caveats, most of the benzyl derivatives are not significantly more selective than their methyl analogues. The sole exception to this trend is the resin BIM1 (N'-benzylimidazole), where the alkyl group scarcely hinders the cationic site. The apparent trend of methyl derivatives having higher selectivity is supported by comparison of the optimal loading ($[Au]_R/[C]_M$) of the piperazine (PAZ) derivatives: NMZ1 (N-methyl-PAZ: 0.5 mg/g) < BBZ1 (N,N,N'-tribenzyl-PAZ: 3.7 mg/g) < TBZ1 (N,N'-dibenzyl-N-methyl-PAZ: 7.8 mg/g) < TPZ1 (N,N,N'-trimethyl-PAZ: 11.3 mg/g).

The commercial resins examined also had relatively high affinity for gold. These resins bear small alkylammonium groups: trimethylammonium (Dowex-1 and A26) and dimethyl(2-hydroxyethy)ammonium (IRA-410). The optimum loading of gold for these resins ($[Au]_R/[C]_M$ = ~11-12 mg/g) was of a similar order to the best performing of the novel resins prepared in this work.

The more rapid kinetics of the commercial resins (relative to those prepared in this work) may also enhance their maximum loading of gold, as there is less time for the competing species (polythionates and cuprothiosulfate anions) to form in the liquor. However, similar gold loadings resulted using the small bead resin Dowex-1 (~100 μm) and the large bead resin A26 (~800 μm). Resin A26 and the large fraction 'A26 Big' also had similar gold sorption (11.8 and 11.5 mmol/mol).

The quinuclidine resin QNU1 ($[Au]_R/[C]_M$ = 10.8 mmol/mol) is hindered by strictly confined alkyl groups, yet adsorbs gold as efficiently as tributylammonium resin ABU1 (9.5 mmol/mol). The loading of aurothiosulfate appears to be relatively insensitive to steric hindrance.

In summary, the structural features associated with gold affinity are:

- Quaternary ammonium group ($-N^+R_3$)
- Linear alkyl substituents (methyl – butyl)
- One or more 2-hydroxyethyl arm(s) ($-CH_2CH_2OH$)
- 1,2-Bis-quaternary ammonium group ($-N^+R_3CH_2CH_2N^+R_3$
- Imidazolium group (delocalised ring cation)
- Morpholinium group (localised ring cation)

A set of optimal functional groups has been selected for further development and testing (Table 4.21). These are denoted by the corresponding resin code, as new

batches of resin may be required in some cases. These will be examined in Chapter 5, with a view to examining selectivity over trithionate anions in leach liquors. A number of interesting resins were excluded from further development due to project time constraints. This includes the benzylimidazole resin (BIM1), which loaded well but eluted poorly. Development of a wider range of imidazole moieties may be justified, given the promising results of the two employed in this work.

Table 4.21 List of Optimal Resin Structures for Development

*: highest reported value for all preparations (mmol/mol)

Resin	**$[Au]_R/[C]_M$***	**Resin**	**$[Au]_R/[C]_M$***	**Resin**	**$[Au]_R/[C]_M$***
DAM	11.8	PET	11.9	A26	11.8
MIM	12.1	QNU	10.8	Dowex-1	11.4
NMM	11.6	TME	13.0	IRA-410	12.1
		TPZ	11.3		

Although it may be desirable to prepare high capacity versions of the novel resins in Table 4.21, such optimisation was not pursued in this project. The accurate determination of structural trends requires resins with relatively high IEX capacities of well-characterised functional groups. Many of the evaluations in this chapter were relatively crude, due to the low IEX capacities and side-reactions of some resins. The development of the low-capacity resins was generally not pursued. This parallels the development of industrial polymeric adsorbents, in which inexpensive, simple and robust syntheses are preferred. Functional groups which are unstable, expensive, or obtained in low yields are undesirable in a commercial context.

References:

1. O'Malley, G.P., "The elution of gold from anion exchange resins"; Murdoch University, Perth, WA., World Patent (WO 01/23626 A1), 2001.
2. Fleming, C.A., McMullen, J., Thomas, K.G., Wells, J.A., "Recent advances in the development of an alternative to the cyanidation process - based on thiosulfate leaching and resin in pulp"; *SME Annual Meeting (2001)*, Denver, Colorado. SME, 2001. 11 pp.
3. Feng, D., *Personal correspondence*; Monash University, Melbourne, 2002.
4. *AAS Analytical Methods Manual*; Publication No. 05-100009-00; Varian Australia Pty. Ltd., Mulgrave, Victoria, Australia, 1989.
5. O'Malley, G.P. and Nicol, M.J. "Recovery of gold from thiosulfate solutions and pulps with ion-exchange resin", in *Cyanide: Social, Industrial and Economic Aspects. Proceedings of a Symposium at the TMS Annual Meeting,* New Orleans, Louisiana. TMS, Warrendale, PA, USA, 2001. pp. 469-483.
6. Jeffrey, M.I. and Breuer, P.L., "Copper catalysed oxidation of thiosulfate by oxygen in gold leach solutions."; *Minerals Engineering*, **16**: 21-30; 2003.
7. Dicinoski, G.W., "Novel Resins for the Selective Extraction of Gold from Copper Rich Ores."; *S. Afr. J. Chem.*, **53**(1): 33-43; 2000.
8. Wan, R.Y., Le Vier, M., and Miller, J.D. *Chapter 27:* "Research and development activities for the recovery of gold from non-cyanide solutions", in *Proceedings of the Milton E. Wadsworth (IV) International Symposium on Hydrometallurgy. Hydrometallurgy : fundamentals, technology, and innovations*; Salt Lake City, Utah, USA. SME, 1993. pp. 415-436.
9. MacKenzie, J.M.W., Virnig, M.J., and Johns, M.W. "Henkel Aurix(R) resin - an update", in *Randol Gold Forum '95*; Perth, West Australia, 1995. pp. 425-431.

5. Selection and Testing of Optimal Resins

The set of functionalised resins utilised in this chapter comprises those with functional groups associated with the highest selectivity for gold from previous analysis {DAM1, MIM2, NMM1, NMM2, PET2, QNU1, TME3, TPZ2, and the commercial resins Dowex-1, IRA-410, and A26} (see Table 4.21, Section 4.4.5). These resins were further evaluated and the most promising ones selected. To this end, this chapter contains three sections: a study of the effect of trithionate on gold sorption by the resins (Section 5.1); a study of the effect of an adsorption-elution cycle on the resins (Section 5.2); and the cyclic adsorption-elution testing of the resin QNU1 (Section 5.3). The effects of copper on gold sorption were discussed in Chapter 4, and further examination is beyond the scope of this work.

Note that resin batches PET2 and TME3 were not previously examined using the B/R testing regime described in Section 4.1. These resins were prepared specifically for this evaluation, as the previous batches (PET1, TME1 and TME2) were insufficient in quantity.

5.1 Testing of the Optimal Resins against Trithionate

It would be desirable to have a resin with improved selectivity for gold over the polythionate anions. This selectivity may be examined by introducing trithionate into the leach liquor of a B/R Test, and comparing the gold uptake to a control without additional trithionate. Other polythionate anions, such as tetrathionate and pentathionate, were not found in significant concentrations in the leach liquors prepared

in this work. The high pH of the solution (~10) diminishes the stability of the higher polythionates.

A method developed recently by O'Reilly et al [1] using ion chromatography (IC) was employed for the direct determination of trithionate (T3), tetrathionate (T4) and pentathionate (T5) in dilute (1:5) leach liquor.

5.1.1 Ion Chromatography of Polythionates

This was implemented using a DX-600 IC system (Dionex Inc., Sunnyvale, California, USA) controlled by a PC running *Chromeleon* (PeakNet version 6.31 SP1) data collection software. The IC system consisted of an IC25 pump, an LC30 column oven at 35°C, an IonPac NS-1 (5 μm) analytical column and NG-1 guard column, an ASRS-1 eluent suppressor using 5 mM H_2SO_4 as external regenerant, and a CD25 Conductivity Detector. Samples were manually injected, and eluted with a degassed solution of tetrabutylammonium hydroxide (3.0 mM) and Na_2CO_3 (2.5 mM) in 28% acetonitrile, at a flow rate of 1.0 mL/minute with subsequent eluent suppression and conductivity detection. Two UV detection wavelengths were also examined briefly, using a Dionex PDA-100 (Photodiode Array) UV Detector Array at wavelengths of 214 and 205 nanometres. These were found to be as specific and sensitive as the conductivity detector, but were later omitted to simplify instrument operation. An evaluation of the UV detector response was made using the PET2 resin, with sampling of the liquor periodically over four hours (Section 5.1.4.2).

Purified samples of potassium trithionate ($K_2S_3O_6$), sodium tetrathionate dihydrate ($Na_2S_4O_6.2H_2O$), and potassium pentathionate hydrate ($K_2S_5O_6.1½H_2O$) were prepared and analysed using this IC method. These were then used to prepare standard

solutions (0.5-10 mM) for comparison with liquor samples (diluted 1:5 with water) using the IC method of O'Reilly et al [1]. The least-squares fit of the 3-point linear polythionate calibrations always had an r^2 better than 0.998.

5.1.2 Preparation of Sodium Trithionate

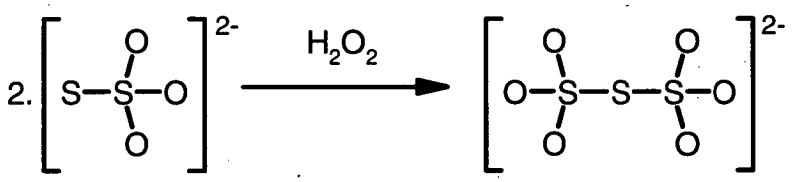

Figure 5.1 Oxidation of Thiosulfate to Trithionate

The method of Schlessinger [2] was followed in this procedure. A solution of $Na_2S_2O_3.5H_2O$ (62.00 g, 250 mmol) in water (50 mL) was stirred vigorously in a beaker at 0°C in an ice bath, whilst aqueous H_2O_2 (30%, 52.00 mL, 504 mmol) was added dropwise over one hour. The reaction temperature was carefully monitored, and briefly peaked at 42°C, resulting in a decrease in the rate of H_2O_2 addition in order to keep the temperature below 40°C. The solution was left to stir at room temperature for another hour, then chilled to ~ 4°C.

The cooled reaction mixture was filtered with a porosity 3 glass frit filter funnel, collecting a voluminous white precipitate (Crop 1). The filtrate was reduced to a syrupy consistency by a rotary evaporation (water bath temperature < 40°C) and then chilled in an ice bath. The resulting crystals (Crop 2) were filtered off with a porosity 3 glass frit filter funnel and washed with ethanol (2 x 30 mL). The addition of this ethanol to the filtrate produced a large amount of precipitate, which was also recovered (Crop 3) and rinsed with more ethanol (50 mL). The first crop of material was dried in a vacuum

oven at 30°C, while the other crops were air-dried by suction for ~20 minutes. All three crops were stored at -20°C in sealed glass vessels. A sample of each was taken for analysis by IC as described in Section 5.1.1, with the results presented in Table 5.1.

Table 5.1 Analysis of Sodium Trithionate Preparations

Crop	Mass (g)	$[Na_2S_3O_6]$	$[Na_2S_4O_6]$
1	22.3522	5.1%;	0.1%
2	23.6775	73.6%;	0.3%
3	8.8902	75.7%	0.3%

The first crop was found to consist primarily of sodium sulfate decahydrate, and was discarded. The 2nd and 3rd crops yielded mainly sodium trithionate in an unknown hydration state. The remainder (~25%) was principally sodium sulfate, sodium thiosulfate, and water. Small quantities of these substances are unlikely to disturb a leaching test, hence further purification was not required. These remaining two crops were stored in sealed vials in a freezer (–20°C). The overall yield was ~85%.

5.1.3 Preparation and Analysis of Artificial Leach Liquors

The liquor concentrations and B/R conditions used in this test are the same as those used in the majority of the B/R testing in Chapter 4 (Table 4.2). The liquor was composed of: ammonia (1.00 M), ammonium chloride (0.100 M), ammonium thiosulfate (0.100 M), cupric sulfate (3.149 mM; 200 ppm) and sodium aurothiosulfate (0.504 mM; 100 ppm). One litre of leach liquor was prepared for each resin, and

divided into 2 x 500 mL portions. Sodium trithionate (crop 2 or 3, ~1.617g, 5.00 millimoles) was dissolved in one 500 mL portion (over ~ 5 minutes), then time zero samples were taken. Batches of resin (1.00 g) were added immediately, the bottles sealed, and rolling commenced. Liquors were agitated for 24 hours at room temperature, and sampled periodically (5 – 10 mL) for analysis. Samples were analysed for gold at t_0, and after 30, 60, 90, 120, 180, 240, 360, 480, 720 and 1440 minutes. Polythionates levels were also recorded at t_0, and after approximately 30, 360, 720, and 1440 minutes, with sampling times recorded to the nearest minute.

Samples selected for polythionate determinations were analysed immediately to minimise degradation of the sample, using the method detailed in Section 5.1.1. Samples for gold analyses were analysed by AAS in one batch at the end of the test, using the method detailed in Section 4.1.4.

5.1.4 B/R Tests using Liquor containing 10 mM Trithionate

5.1.4.1 Results of B/R Tests with 10 mM Trithionate

Figures 5.2 – 5.13 show the gold concentration of the resins with and without the presence of 10 mM trithionate, overlaid with the polythionate concentrations in solution. For comparison, the composition of control solutions (no resin contact) are shown in Figure 5.14. The retention times of the polythionates on the IC column ranged from 5.28 – 6.98 minutes (trithionate) and 6.85 – 8.44 minutes (tetrathionate). This variation was caused by differences in the acetonitrile content of the eluent, arising from evaporation during degassing. IC polythionate calibration was performed at the beginning and end of the B/R Test to correct for this drift.

These results are compared and discussed in Section 5.1.5.

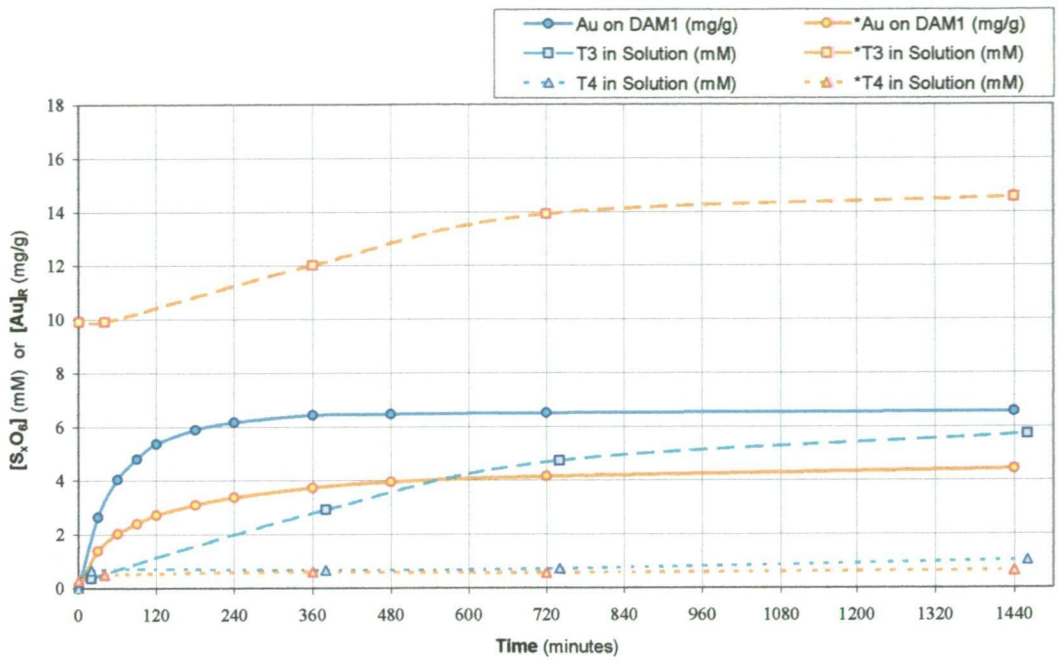

Figure 5.2 Effect of 10 mM Trithionate on B/R Test (Resin DAM1)

* denotes $[S_3O_6]_S$ = 10 mM at T_0

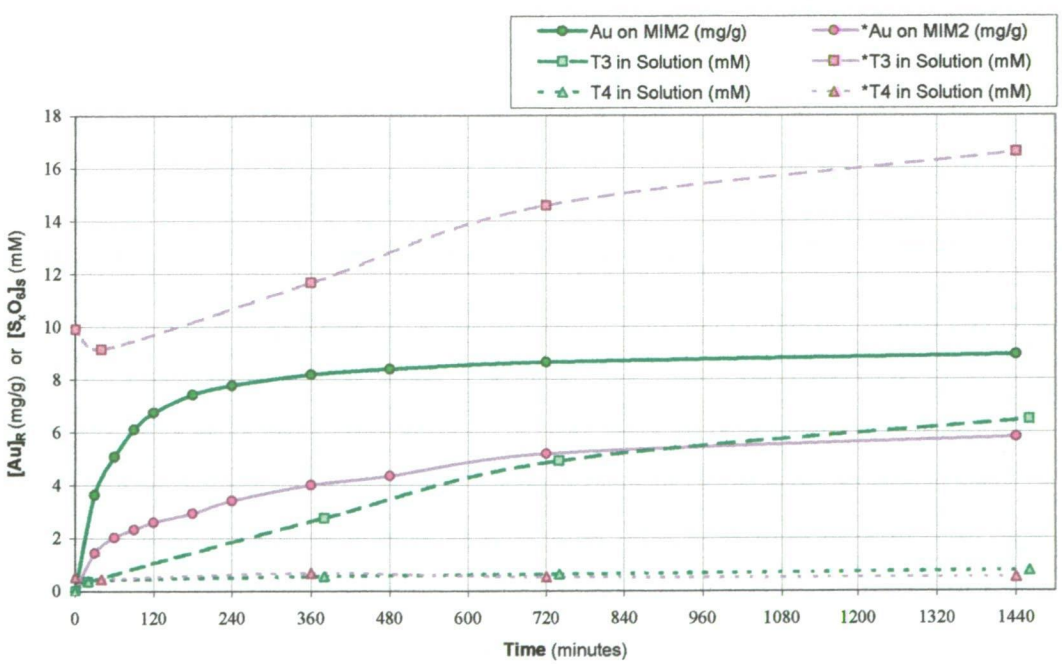

Figure 5.3 Effect of 10 mM Trithionate on B/R Test (Resin MIM2)

* denotes $[S_3O_6]_S$ = 10 mM at T_0

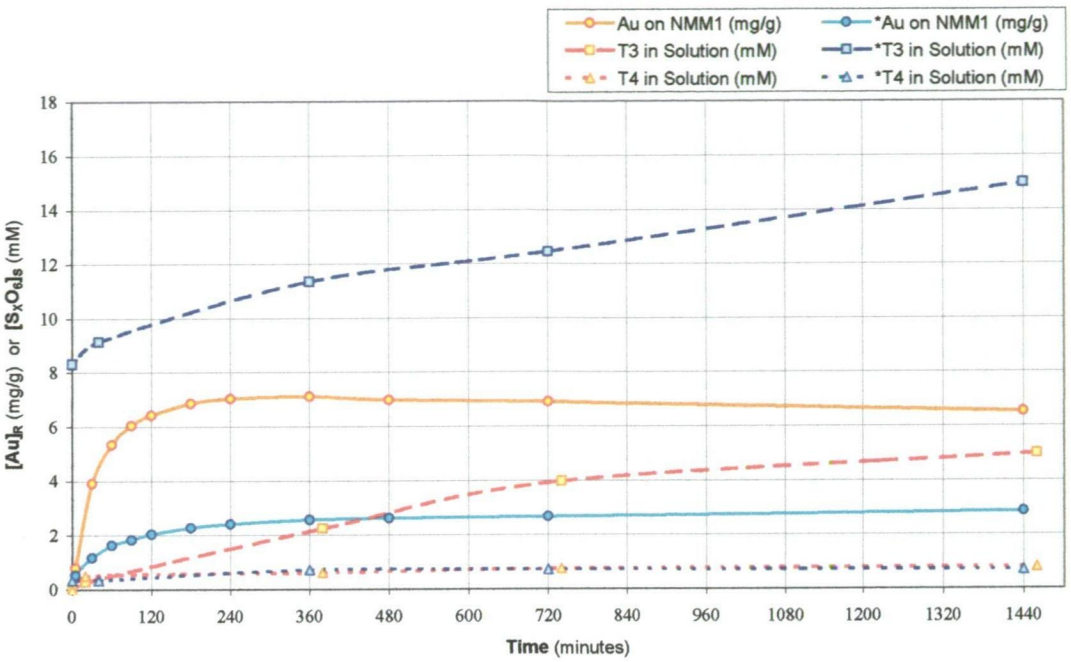

Figure 5.4 Effect of 10 mM Trithionate on B/R Test (Resin NMM1)

* denotes $[S_3O_6]_S$ = 10 mM at T_0

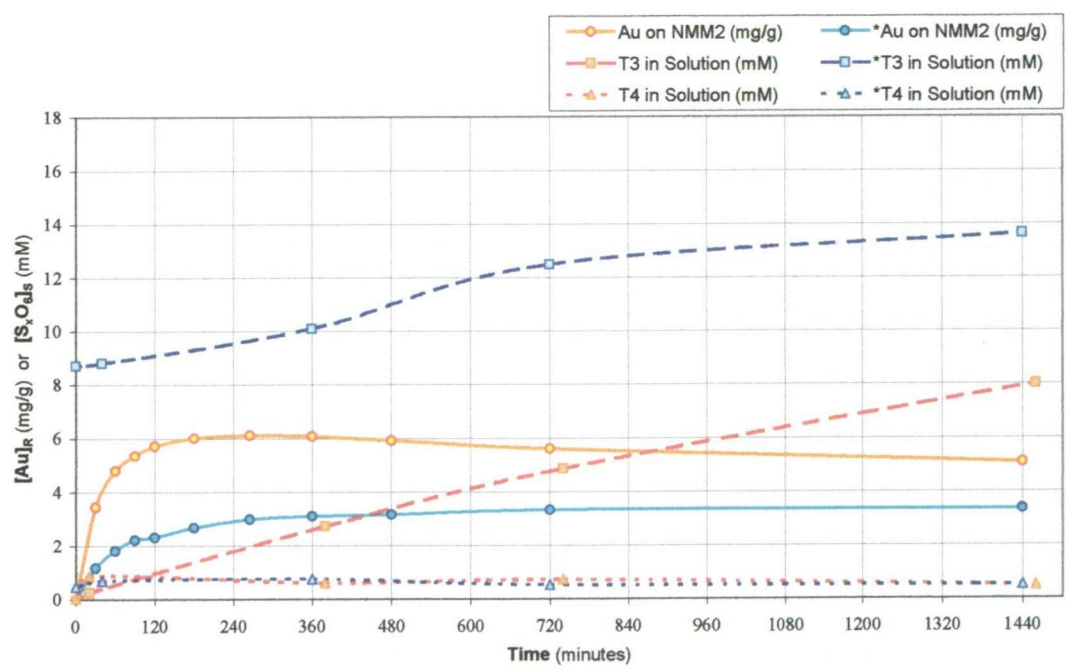

Figure 5.5 Effect of 10 mM Trithionate on B/R Test (Resin NMM2)

* denotes $[S_3O_6]_S$ = 10 mM at T_0

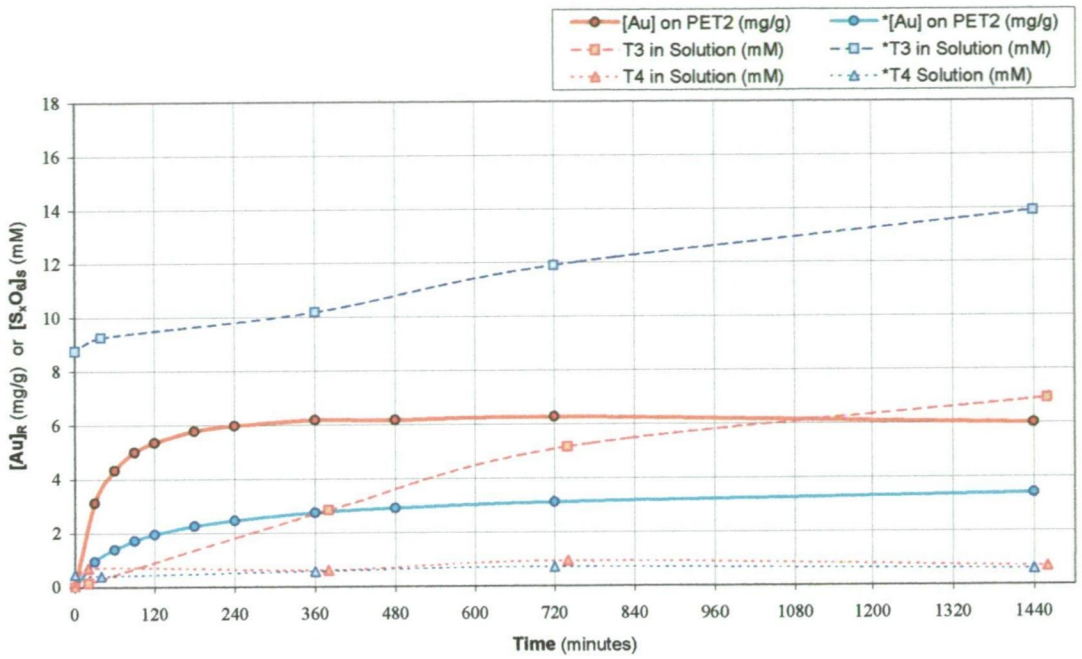

Figure 5.6 Effect of 10 mM Trithionate on B/R Test (Resin PET2)

* denotes $[S_3O_6]_S = 10$ mM at T_0

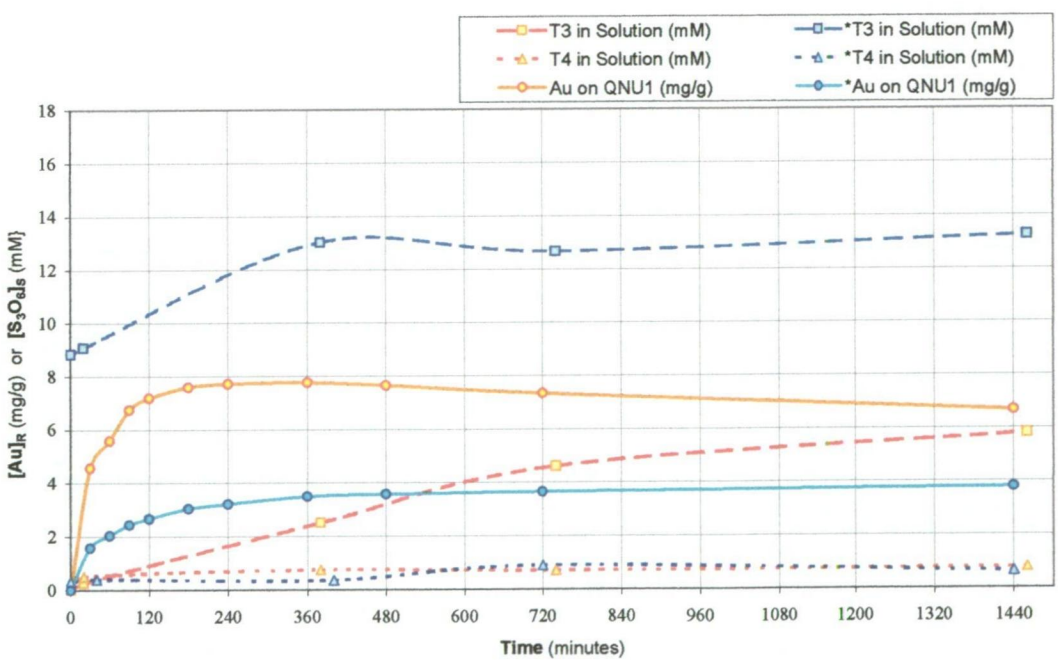

Figure 5.7 Effect of 10 mM Trithionate on B/R Test (Resin QNU1)

* denotes $[S_3O_6]_S = 10$ mM at T_0

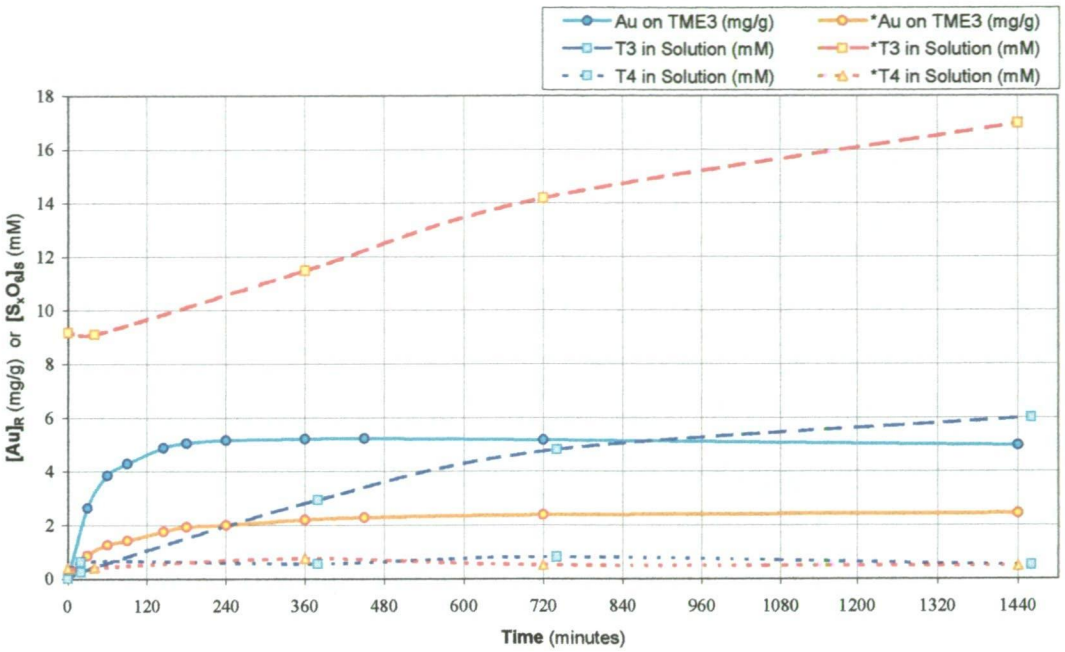

Figure 5.8 Effect of 10 mM Trithionate on B/R Test (Resin TME3)

* denotes $[S_3O_6]_S$ = 10 mM at T_0

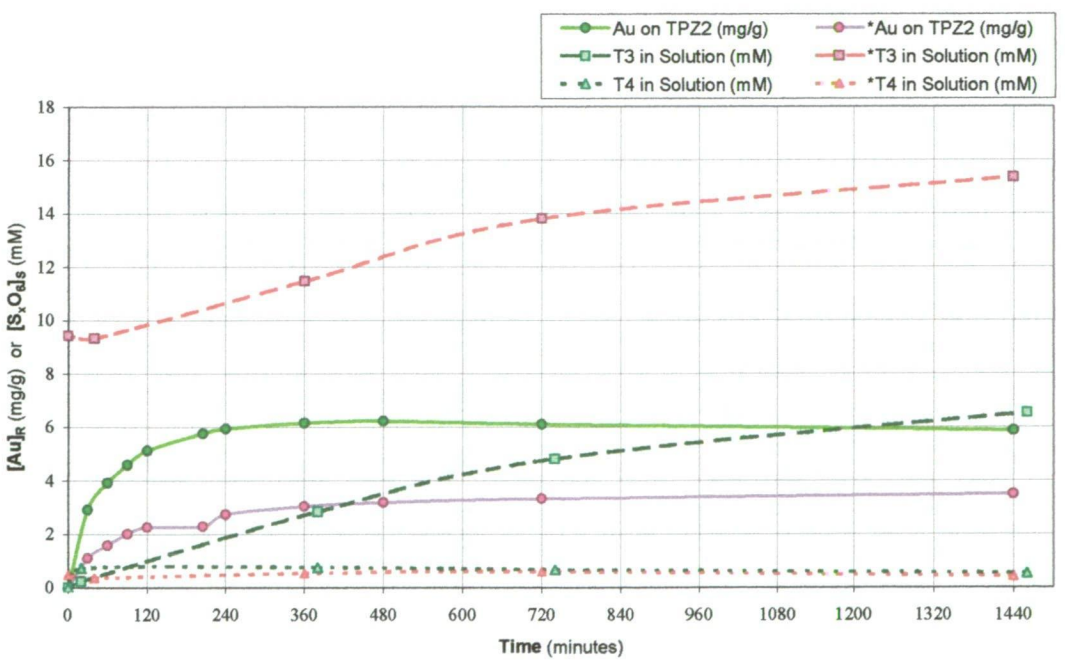

Figure 5.9 Effect of 10 mM Trithionate on B/R Test (Resin TPZ2)

* denotes $[S_3O_6]_S$ = 10 mM at T_0

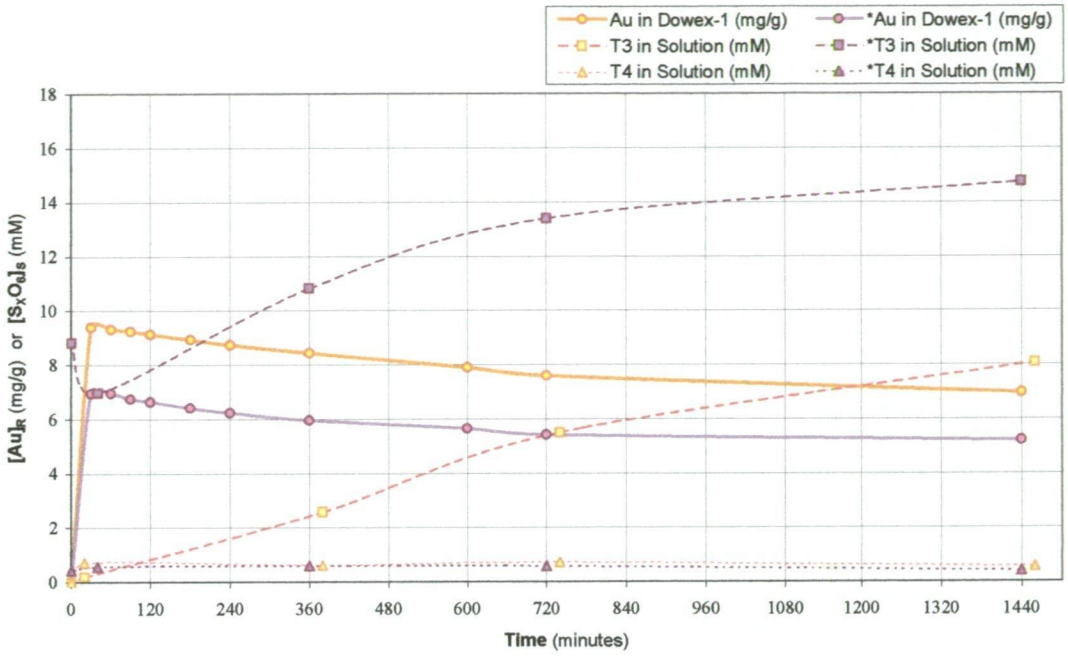

Figure 5.10 Effect of 10 mM Trithionate on B/R Test (Resin Dowex-1)

* denotes $[S_3O_6]_S$ = 10 mM at T_0

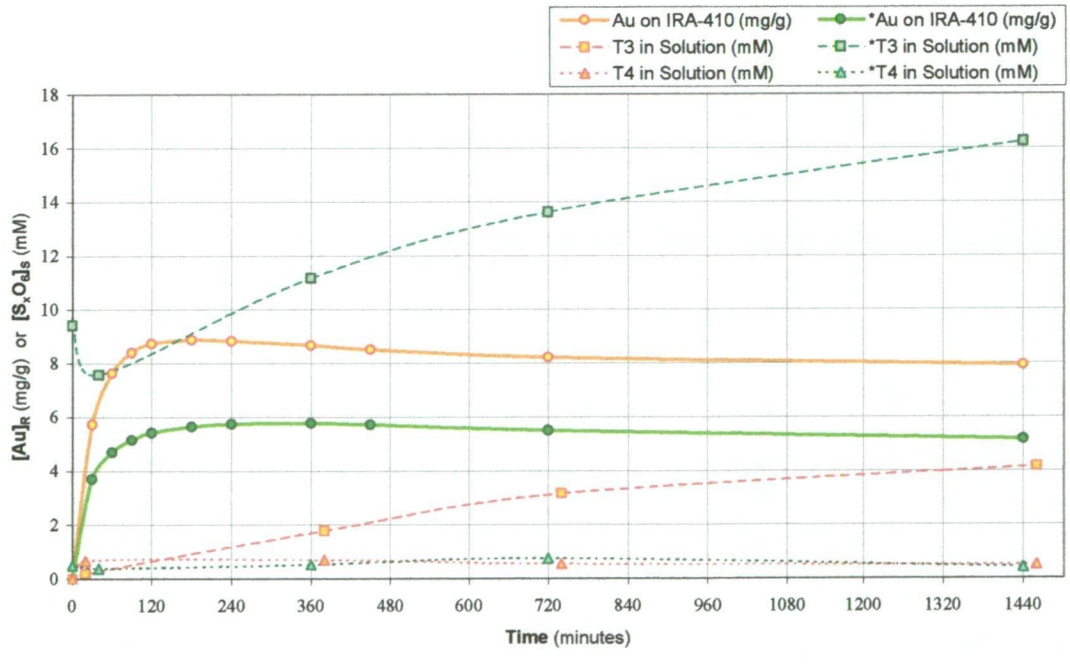

Figure 5.11 Effect of 10 mM Trithionate on B/R Test (Resin IRA-410)

* denotes $[S_3O_6]_S$ = 10 mM at T_0

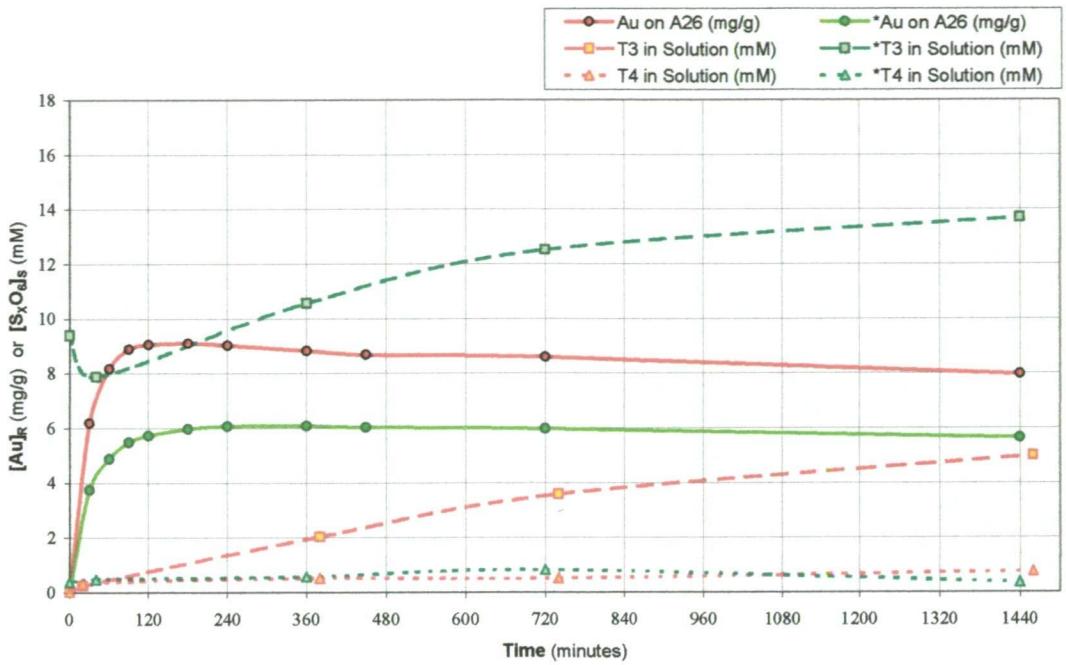

Figure 5.12 Effect of 10 mM Trithionate on B/R Test (Resin A26)

* denotes $[S_3O_6]_S$ = 10 mM at T_0

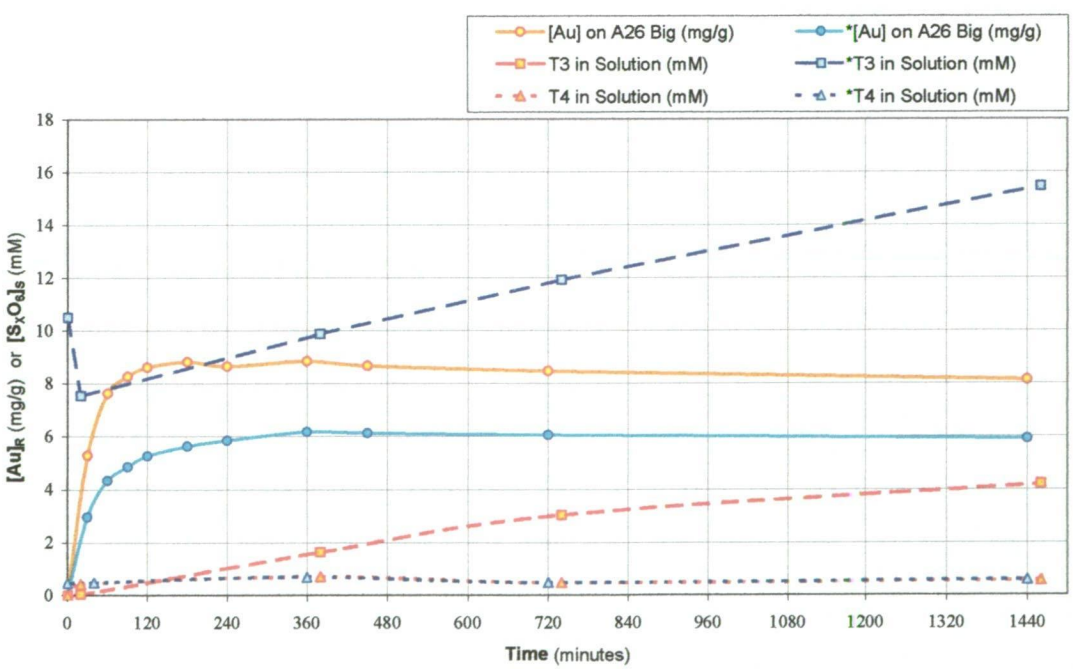

Figure 5.13 Effect of 10 mM Trithionate on B/R Test (Resin A26 Big)

* denotes $[S_3O_6]_S$ = 10 mM at T_0

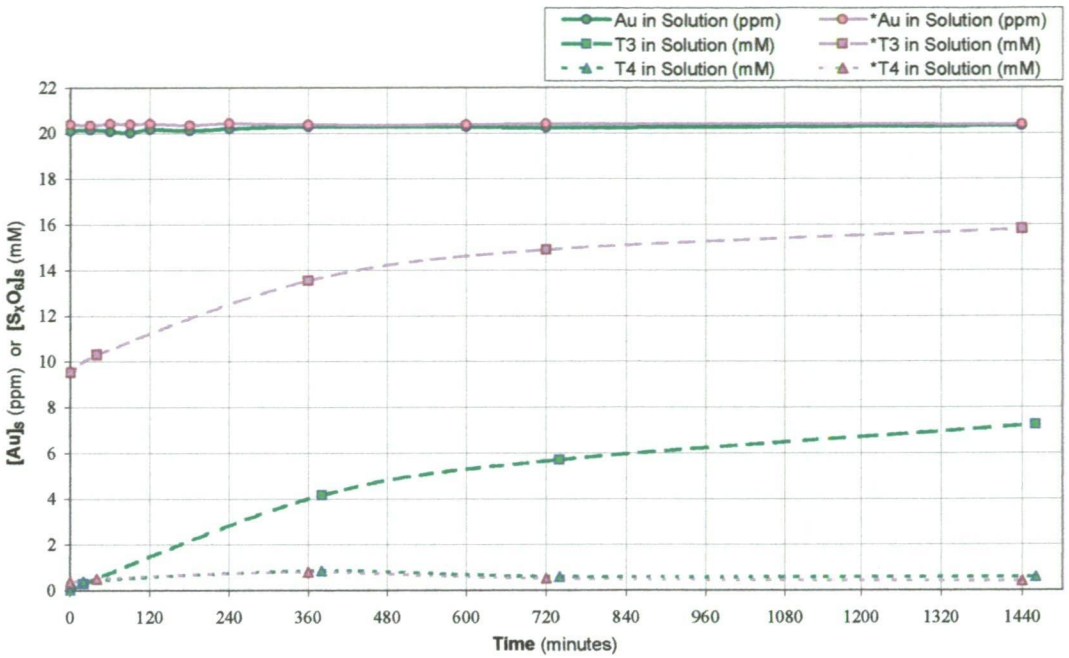

Figure 5.14 Control B/R Tests with & without 10 mM Trithionate

* denotes $[S_3O_6]_S$ = 10 mM at T_0

5.1.4.2 Simultaneous UV and Conductivity Detection

In one initial experiment, the polythionate concentrations were also followed by the response of a PDA-100 UV Detector Array at wavelengths of 214 nm (UV2) and 205 nm (UV3). The results from the first four hours of a B/R Test using resin PET2, with and without an initial 10 ppm trithionate, are shown in Figures 5.15 and 5.16. The scale of the latter plot has been expanded due to the low levels of tetrathionate observed. It is apparent that the polythionate levels reported by the three methods differ by up to 10% over the time interval examined. This perturbation may be due to a raised non-ionic UV background in the eluate over time, as the conductivity response (ECD) shows the lowest polythionate levels after the first hour. This effect was not investigated further, and the UV detector was not utilised in further testing.

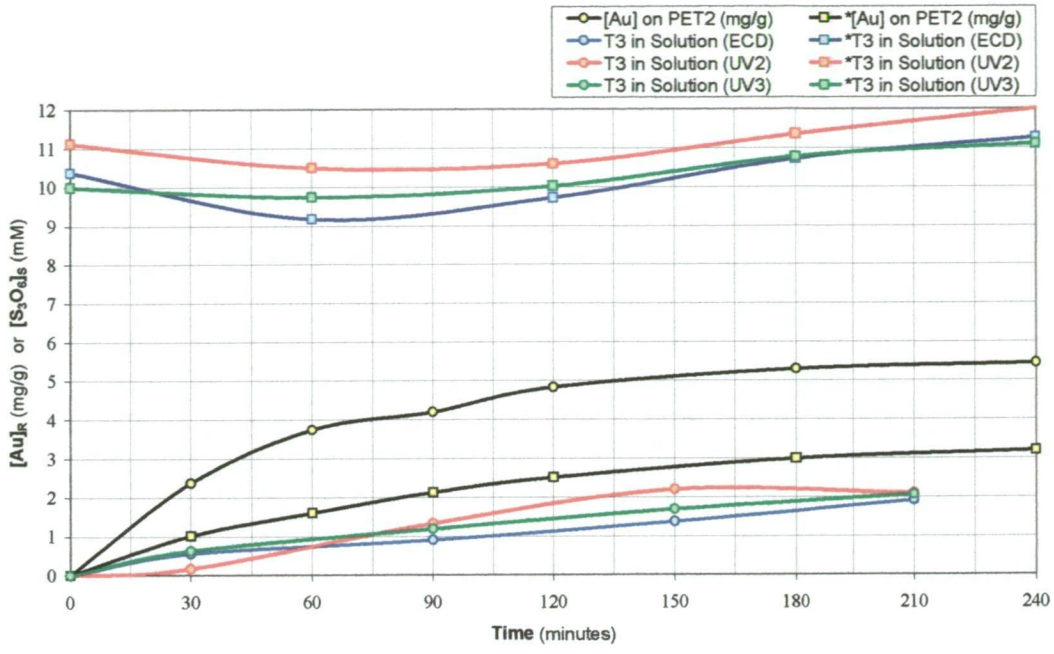

Figure 5.15 Comparison of Trithionate Analysis by UV and Conductivity

* denotes $[S_3O_6]_S = 10$ mM at T_0

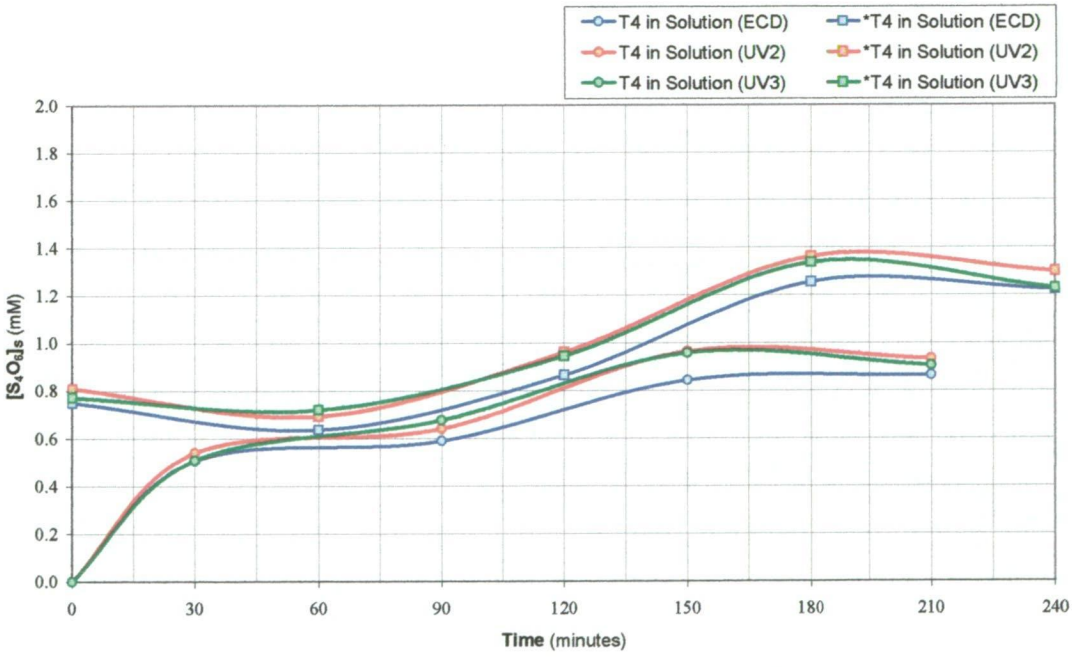

Figure 5.16 Comparison of Tetrathionate Analysis by UV and Conductivity

* denotes $[S_3O_6]_S = 10$ mM at T_0

5.1.5 The Effect of Trithionate on Gold Sorption by Resins

Some key results of these B/R tests have been summarised in Table 5.2. Resin performance is compared at various times, with ($*[Au]_R$) and without ($[Au]_R$) the presence of an initial 10 mM trithionate. The parameter ,$*[Au]_{\%}$, was derived by dividing $*[Au]_R$ by $[Au]_R$, and expressing as a percentage.

Table 5.2 Suppression of Gold Sorption by 10 mM Trithionate

Results in *italics* denote that maximum $[Au]_R$ has been reached.

	Capacity	***[Au]% at Time T =**			***[Au]R/CM**
Resin	**CM** (meq/g)	**1 hr**	**6 hrs**	**24 hrs**	(mmol/mol)
DAM1	3.01	50	58	68	7.5
MIM2	3.13	40	49	65	9.4
NMM1	2.70	31	36	*44*	5.4
NMM2	2.90	38	*51*	*66*	5.9
PET2	2.44	32	44	*57*	9.2
(replicate)		43	-	*59*	7.1
QNU1	3.07	36	45	*57*	6.3
TME3	2.15	33	42	*49*	5.8
TPZ2	2.27	41	49	*60*	8.6
(replicate)		52	-	*64*	7.8
Dowex-1	4.10	*75*	*71*	*75*	8.6
IRA-410	3.62	62	*67*	*65*	8.1
A26	3.90	60	*69*	*71*	7.9
A26 Big	3.90	57	*70*	*73*	8.0

Initial gold sorption rates for all resins are clearly enhanced in the absence of T3, diminishing as the concentration of the polythionate increases and competes with the gold complex for the resin IEX sites. Significant sorption of gold despite the presence of sufficient T3 to occupy all IEX sites, and a 100:1 ratio of T3 to gold in solution, demonstrates the relatively high selectivity of all the resins for gold. An initial drop or plateau in trithionate concentrations in the T3-spiked samples was observed for most resins (Figures 5.2 – 5.13), between time zero and the next sample at ~30 minutes. A significant fall in the T3 concentration from the initial calculated value was observed with novel resins MIM2, TME3 and TPZ2, and all the commercial resins (Dowex-1, IRA-410, A26 and A26 Big). This indicates rapid initial sorption of T3 by the resin, which occupies many of the free IEX sites. This effect was not evident with the remaining novel resins, although T3 formed during the preparation of the liquor was not assayed, hence initial T3 concentration may be slightly underestimated. After this point, each pair of solutions show similar rates of trithionate build-up, and consequently diminished gold sorption. Tetrathionate remained at very low levels of ~ 0.5 – 1.2 mM in all cases.

All the novel resins examined continued to adsorb gold from the trithionate (T3) spiked solutions over the course of the experiment, however at a diminishing rate. In the control solutions, these resins began to lose gold after ~6 hours, apart from DAM1, MIM2 and PET2. The larger commercial resins (IRA-410 and A26, with bead sizes > 150 μm) achieved peak loading rapidly in both solutions, and gold began to desorb after 3 hours (control) and 6 hours (T3 spike). The Dowex-1 resin achieved peak loading after only 1 hour in both solutions, due to the smaller diffusion path of the smaller resin beads (75 – 150 μm).

The results in Table 5.2 show that most of the novel resins performed similarly after 6 hours (*$[Au]_{\%} \approx$ 40-50 %). The commercial resins were somewhat less affected by the presence of trithionate (*$[Au]_{\%} \approx$ 65-70 %). Note that the data in Table 5.2 are biased by the shapes of the initial absorption curves, leading to a natural convergence of *$[Au]_{\%}$ as the polythionate concentrations become more similar. This is exacerbated by the formation of T3 in the control solutions, as gold is displaced from the resin after the point of peak loading. The *$[Au]_{\%}$ results obtained after gold displacement had commenced (*italics* in Table 5.1) are distorted due to this effect.

The *$[Au]_{\%}$ results for resins DAM1, MIM2, and NMM2 were relatively high after 24 hours. Resins PET2, QNU1 and TPZ2 were also promising, but no clear structural trends for selectivity (Au/T3) may be identified. The poor reproducibility of the replicate samples (PET2 and TPZ2, Table 5.1) indicates a significant error margin for *$[Au]_{\%}$ (ca. ± 6 %), and precludes any involved kinetic analysis of the process.

Using the suppression of Au sorption as an indicator of selectivity over trithionate, the best performance was found using the commercial resins Dowex-1 and IRA-410. These resins showed relatively high gold sorption in the presence of 10 mM trithionate, and *$[Au]_{\%}$ remained stable over 24 hours. Resin A26 and the large fraction A26 Big reached a similar level of efficacy only after 24 hours. There was no significant difference in the performance of the different sized A26 fractions.

In terms of absolute gold sorption, none of the novel resins performed as well as the commercial resins in the presence of T3 (~ 2 - 4 vs. ~ 6 mg/g Au, respectively). In the absence of accurate resin T3 loadings, a measure of resin selectivity may be made by comparing IEX capacity to gold loading (with and without 10 mM T3).

The *$[Au]_R/C_M$ results (mmol Au sorbed per mol of IEX groups, in the presence of 10 mmol T3 at t_0) indicated similar results across most resins. The commercial resins

still adsorbed 7.9 – 8.6 mmol/mol, but were surpassed by the experimental resins MIM2 (9.4 mmol/mol), PET2 (9.2 mmol/mol), and TPZ2 (8.6 mmol/mol).

The principal advantage of the novel resins over the commercial products is the continued sorption of gold in the presence of elevated trithionate concentrations (resins DAM1, MIM2 and PET2). This may be primarily due to the physical nature of the substrate employed (A378). The 2-hydroxyethyl structural feature present in DAM1 and PET2 may also be associated with improved selectivity over trithionate. There was no clear relationship between gold loading and other structural features.

The variation in performance of resins NMM1 and NMM2 (see Table 5.2 and Figures 5.4 and 5.5) may be due to the higher rigidity of the NMM2 backbone resin (see Section 3.1.10) altering exchange kinetics. It is suspected that pore structure of the commercial resins is wider than the novel resins, which may become occluded during functionalisation. Improved porosity enhances the kinetics of diffusion, permitting more rapid desorption of gold as T3 penetrates the resin. This may be examined in future work via direct resin porosity analysis.

5.2 *Cyclic Adsorption-Elution Test of Optimal Resins*

The optimal group of resins was further investigated by examining the robustness of these resins. This was performed by subjecting them to a complete cycle of adsorption, elution, and adsorption. Two B/R tests (17 & 18) were arranged using identical leach liquor, with composition detailed below, to permit simultaneous analysis of the efficiency of nitrate elution and recycling of the stripped resins. Only one commercial resin (A26) was represented in this procedure.

5.2.1 Experimental Conditions

The liquor concentrations used in this test were similar to those employed in the bulk of the B/R testing in Section 4.1.2 (Table 4.2). The liquor in this case comprised: ammonia (1.00 M), ammonium chloride (0.100 M), ammonium thiosulfate (0.100 M), cupric sulfate (3.149 mM; 200 ppm) and sodium aurothiosulfate (0.504 mM; 100 ppm). Note that an elevated gold concentration of 100 ppm was employed, and 2.0 mL of each wet resin was used throughout to achieve similar bed-volumes.

After loading in the B/R environment, the resins were isolated by vacuum filtration and wet-loaded into columns fitted with a porosity 3 glass frit at the base, followed by 2.0 mL of eluent solution. The eluent employed in this case was the nitrate solution used in Section 4.3.2, comprising $NaNO_3$ (2.0 M) and $Na_2S_2O_3$ (0.2 M). The columns were briefly agitated to dislodge air bubbles, and left to stand for 1 hour. The eluate was removed by suction through the glass frit and replaced by fresh eluent as above. This process was repeated 9 times (batches A-I), with batch F being left to stand overnight (12 hours), and batch G for 20 hours. The final two batches (H-I) were obtained after standing for 90 minutes each.

Resins were then rinsed with water (5 mL/minute for 20 minutes) and isolated by vacuum filtration. These were used without change (ie. in nitrate form) in a second and final B/R test with leach liquor containing 100 ppm Au. Elution was not performed on the resins after this second B/R test.

The B/R liquors were sampled after 24 hours, immediately prior to the isolation of the resin. A 1:4 dilution of these liquors was analysed for Au by AAS at 267.6 nm (see Section 4.1.4.1). The eluate liquors were diluted to 100 mL (1:50) and analysed in the same fashion. Further dilutions were performed as appropriate to keep $[Au]_S$ values in the linear range, particularly for the earlier eluate fractions of resins NMM1, TME3, PET2 and QNU1. Control analyses of several samples over the course of the AAS determinations yielded a mean Au variance of 0.9 ppm.

5.2.2 Results of Cyclic Testing

The results in Table 5.3 detail the percentage of gold removed from solution (%Au) in successive tests after 24 hours, along with the associated resin selectivity as expressed by $[Au]_R/C_M$ (mmol gold absorbed per mol IEX capacity). The efficacy of the intermediate elution step was also evaluated, based on the initial calculated loading, and the results of this batch elution process are presented in detail in Figure 5.17. An analysis of these results is presented in Section 5.2.3.

Table 5.3 Results of Cyclic Testing using Optimal Resins

† denotes % Au adsorbed by resin in B/R test (100 ppm Au) after 24 hours

	1st B/R Test		% Elution	2nd B/R Test	
Resin	**% Au †**	**$[Au]_R/C_M$**	(2M $NaNO_3$)	**% Au†**	**$[Au]_R/C_M$**
DAM1	61.0	62.6	57.3	50.3	51.5
NMM1	58.1	69.8	86.3	59.4	71.3
MIM2	89.9	92.6	21.7	54.1	55.7
PET2	64.0	78.6	76.7	70.3	86.4
QNU1	73.6	91.4	77.9	66.3	97.0
TME3	58.3	72.6	78.7	47.4	59.0
TPZ2	74.1	73.6	54.7	69.2	68.7
A26	84.2	92.3	63.4	54.7	59.9

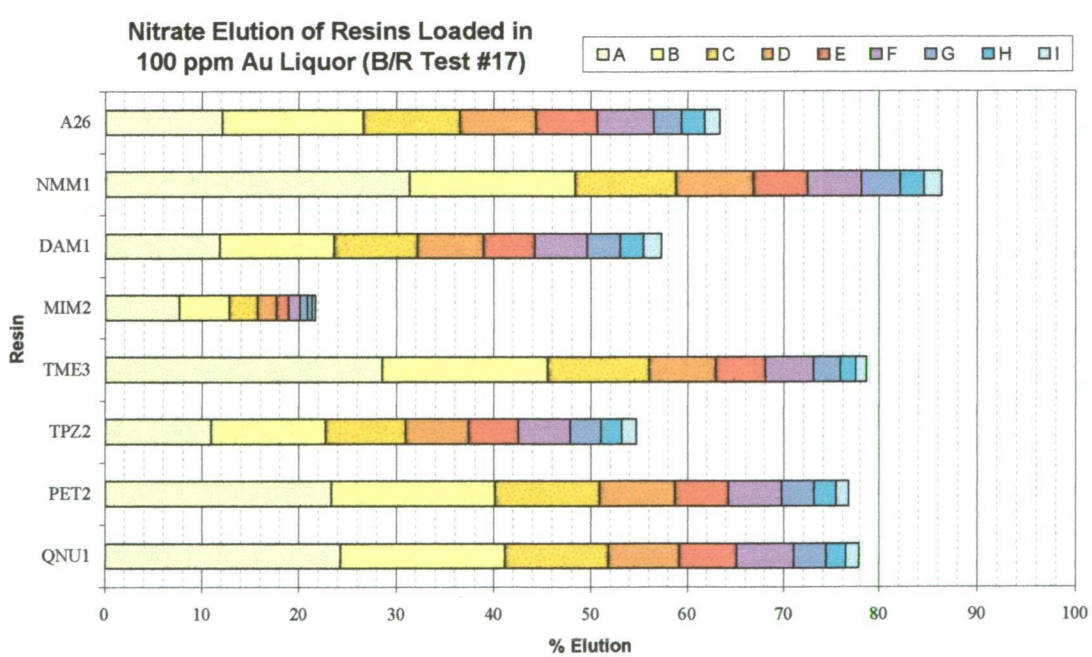

Figure 5.17 Efficiency of Nitrate Elution after B/R Test using 100 ppm Au

5.2.2.1 Acid Digestion of QNU1 after Elution

A sample of the QNU1 resin was taken after the final elution step, and dried in a vacuum oven for 2 hours at 40°C. The anhydrous resin (0.1003 g) was heated to 100°C in H_2SO_4 (AR, 98%, 5 mL) for 30 minutes with stirring, then HNO_3 (AR, 70%, 8 mL), was added in small portions over 3 hours with refluxing. The mixture was cooled, and beads were crushed with a glass rod before adding H_2O_2 (AR, 30%, 2 mL). The mixture was refluxed for a further 2 hours, adding portions of HNO_3 (7 mL) and HCl (AR, 32%, 6 mL) until solids were no longer visible in the solution. A control sample was prepared by applying the same procedure to a sample of the precursor resin A378 (0.1007 g). Both digest solutions were made to 250 mL and analysed for Au by AAS at 242.8 nm.

The liquor was found to hold 2.13 ppm Au, whilst the control sample (A378) held only 0.14 ppm. This corresponds to 5.31 mg/g Au on resin QNU1 after elution, which is less than half the 12.2 mg/g calculated by subtracting the gold in the eluate fractions from that in the loaded resin.

5.2.3 Evaluation of Cyclic Tests

Differences in resin behaviour have been made more evident by employing a liquor with a higher initial gold concentration (100 ppm). The solution pH was measured after each test, and was always found to be 10.2 - 10.3.

Gold loading of the resins after 24 hours ($[Au]_R/C_M$) ranged from 63 – 93 mmol/mol. The highest gold loadings in this test ($[Au]_R/C_M > 75$ mmol/mol) were found in resins MIM2, PET2, QNU1, along with the commercial resin, A26. The loading of resin PET2 improved in the second test, probably due to the eluent flushing synthesis residues from the pores and IEX sites. A similar enhancement may also have

influenced resin QNU1. Better than 75% of the adsorbed gold was eluted from resins TME3, NMM1, PET2 and QNU1 (Table 5.3). The loading of the latter three resins was not diminished after elution, while TPZ2 also performed well on the second B/R test. Poor elution (< 75%) may be associated with a loss of capacity, such as in resins DAM1, MIM2, TPZ2, and the commercial resin A26.

It is apparent from Figure 5.17 that complete elution may not be achieved for all resins in this regime, and was not pursued in this thesis. The last two eluate batches (H - I) were obtained over 1.5 hours each, when it became apparent that elution was not complete. The diminishing efficacy of the eluent is apparent, and the long eluent contact times of batches F and G show only slight improvement. Degradation of the gold complex may stifle any improvement due to longer leach times. The nature of the gold remaining on the resins in the second adsorption cycle has not been evaluated. Some may be "locked up" as a precipitate within the matrix, resulting in diminished resin porosity and hence a loss of sorption capacity.

Resin QNU1 performed particularly well in both B/R tests. A portion of the resin was consumed for gold analysis after the elution step. Less gold was adsorbed from solution due to the lower mass of resin, but the resin loading ($[Au]_R/C_M$) slightly improved. Digestion of the eluted resin showed less than half the calculated gold residue (Section 5.2.2.1). It is likely that the difference is due to systematic underestimation of Au values in leach, eluate and digest liquors by AAS, and the significant variance of the AAS instrument at low $[Au]_S$ values (~ 10 % of 2 ppm).

Any further development of this process requires further restriction of the optimal resin set. Of the promising resins discussed above, MIM2 eluted poorly and TME3 showed poor reproducibility. Resins PET2, TPZ2 and NMM1 are reasonable candidates, but QNU1 had the highest $[Au]_R/C_M$, and was chosen for further study.

5.3 *Cyclic Adsorption-Elution Testing of Resin QNU1*

5.3.1 Experimental Conditions

One batch of QNU1 resin (1.0011 g, 3.07 meq/g) was used throughout for 4 cycles of testing. The liquors and regime used in this test were the same as those employed in the majority of the B/R testing outlined in Section 4.1 (Table 4.2). The liquor was composed of ammonia (1.00 M), ammonium chloride (0.100 M), ammonium thiosulfate (0.100 M), cupric sulfate (3.149 mM; 200 ppm) and sodium aurothiosulfate (0.101 mM; 20 ppm).

The B/R liquors were sampled at time zero (t_0; without resin) and after 16 hours of agitation (175 rpm) at room temperature, immediately prior to the isolation of the resin by vacuum filtration (as detailed in Section 5.2.1). The resin was rinsed with water (100 mL) to remove entrained liquor, loaded into an IEX column, and immersed in a batch of eluent (2.0 M $NaNO_3$ + 0.2 M $Na_2S_2O_3$, 2.0 mL). The column was briefly agitated to dislodge air bubbles, and left to stand for approximately 30 minutes. The eluent was then drained from the column, and the process repeated to collect twenty batches of eluate (denoted A - T). The eluate liquors were diluted to 50.0 mL (1:25) and stored in polystyrene vials prior to analysis (within 24 hours).

The liquor and eluate solutions were analysed for gold by AAS, at 242.8 and 267.6 nm respectively (as per Section 4.1.4.1). Analysis of 'blank' (unused) eluate samples showed no significant gold present. Control standards gave a mean variance of ~0.4 ppm (~5% of response), while a lower variance (~0.2 ppm) was observed in the B/R liquors at 242.8 nm.

5.3.2 Results from Cyclic Sorption-Elution Tests

The results are detailed in Table 5.4 as the percentage of gold recovered from the leach solution after 16 hours contact with resin QNU1 (% Au). The corresponding loading of gold relative to the IEX capacity ($[Au]_R/C_M$) was calculated from this.

Table 5.4 Results of Successive B/R Tests (QNU1, 20 ppm Au)

† : % Au adsorbed after 16 hours ¿ : Gold sorption relative to resin capacity

B/R Test	$[Au]_S$ at t_0 (ppm)	% Au † (16 hours)	$[Au]_R/C_M$ ¿ (mmol/mol)	% Elution
1st	19.99	93.4	15.3	94.1
2nd	19.99	88.8	14.5	99.3
3rd	20.06	84.2	13.8	103.4
4th	20.21	82.9	13.7	102.2

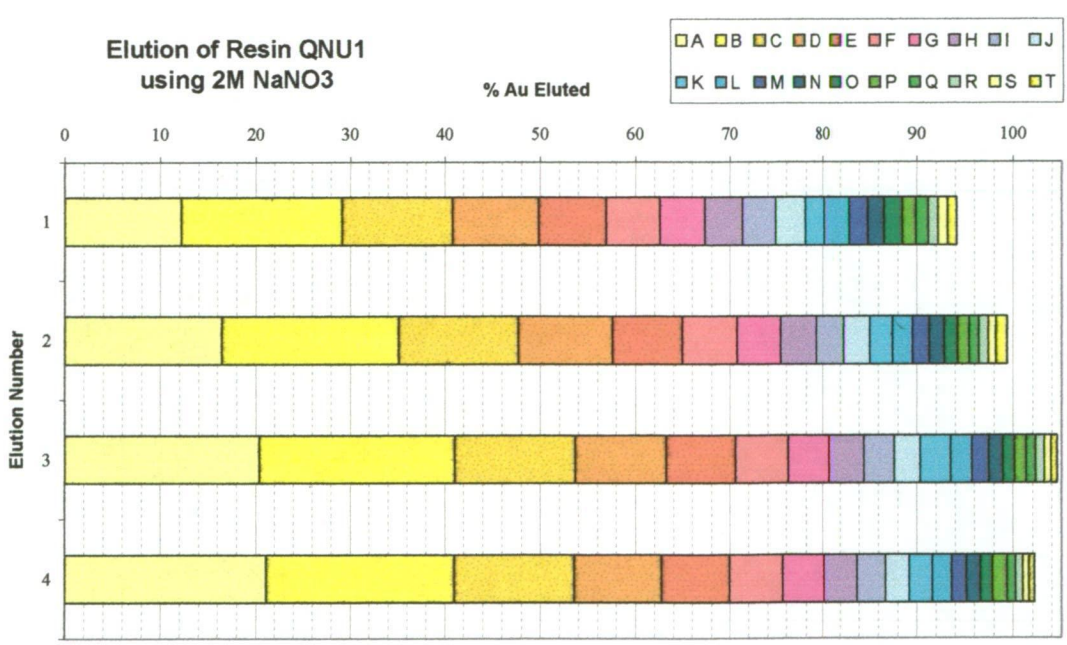

Figure 5.18 Successive Cycles of Batch Elution of Resin QNU1

The elution efficiency (% Elution) for each cycle was also calculated from the eluent concentrations and final resin loading. The rows in Figure 5.18 represent the stepwise progress of the elution of resin QNU1, through the four successive cycles.

5.3.3 Evaluation of Cyclic Testing of Resin QNU1

Resin QNU1 efficiently adsorbed ~90 % of the gold from the leach liquor, with a slightly diminished capacity in each successive cycle (Table 5.4). This fall in resin loading (% Au) is believed to be caused primarily by the resin becoming increasingly loaded with trithionate anions. Some restoration of the original resin capacity may be possible using sodium hydrosulfide (NaSH) to remove residual trithionate from IEX sites [3], however this was not pursued in this work.

The calculated $[Au]_R/C_M$ values for QNU1 in these tests were surprisingly high, and greater than those observed in Chapter 4 (10.8 mmol/mol). This batch was subjected to an IEX analysis prior to use (see Section 3.1.7), and this conditioning may have enhanced the diffusion of the liquor into the resin.

Elution efficiency was also very high, and reproducible over the four cycles. Some variations in the contact time of the eluent occurred, detailed as follows:

Elution 1: Fraction L (80 minutes), O (16 hours), S & T (1 hour)

Elution 2: Fraction T (16 hours);

Elution 3: Fraction K (21 hours)

Elution 4: Fraction N (45 minutes), P (18 hours).

Most of these were due to due to overnight standing during elution. The additional gold leached from the resin in this time causes obvious deviations from the elution trend (Figure 5.18). Fraction L from the first elution is similarly affected, with a

contact time well over the normal 30 minutes. The other eluent fractions with abnormal contact times do not appear to be outliers.

The additional gold recovered by these slightly longer contact times contributes to the elution efficiency, but does not in itself explain the abnormal elution efficiency of the later tests. Overestimation of Au values by AAS may introduce a systematic bias in the calculation of resin loadings, as the resin Au loadings were calculated by difference from leach liquor concentrations. However, a variance of ± 5% overall for the combined result of 20 AAS analyses is reasonable. Destructive analysis of the resin was not pursued in this case.

It is apparent that resin QNU1 can be successfully applied to the recovery of gold from ammoniacal thiosulfate leach liquor, along with being stripped of loaded gold and regenerated in an efficient manner. However, many more assessments must be conducted to evaluate the commercial viability of this resin. It remains to be seen if the resin can be fully regenerated after fouling with trithionate. Additionally, there are other economic aspects such as production and process costs. Finally, the constitution of a real leach liquor is likely to be far more complex than the simplified solution used in this work. Performance may be affected by the use of different liquor concentrations, and by the presence of competing species other than copper, thiosulfate, and trithionate.

References:

1. O'Reilly, J.W., "Chromatographic and electromigrative determination of sulfur-oxygen anions in gold thiosulfate leach solutions", PhD Thesis, 191 pp.; School of Chemistry; University of Tasmania, 2003.
2. Schlessinger, G.G., *Inorganic Laboratory Preparations*; Chemical Publishing Company (New York), 1962. p. 70.
3. Fleming, C.A., Wells, J., and Thomas, K.G., "Gold recovery from thiosulfate leach solutions and slurries using ion-exchange resin eluted with polythionate." US Patent 6344068; Barrick Gold Corporation, 2002.

6. Conclusions

This Chapter summarises the work conducted in this project, with a critical analysis of the final results and recommendations for further research.

6.1 Synthesis of Resins for Gold Recovery

A common approach was used for the synthesis procedures utilised in Chapter 3. The use of the solvent DMF at 100°C for 7 days gave a common control on the side-reactions and effects of this treatment on the resin. However, the side-reactions and degradation processes of the individual functional groups could not be controlled in such a fashion. Optimisation of each individual reaction was beyond the scope of this project, so a summary of the pertinent results is warranted.

6.1.1 Viable Resin Preparations

Most preparations resulted in resins with IEX capacities greater than 1.0 meq/g (Table 4.11), and their gold sorption profiles (Figures 4.3 – 4.13) were of similar shape, indicating similar kinetics. Many of the preparations yielded resins with reasonably high effective IEX capacities (~3.0 meq/g: eg. QNU1), and in a range similar to commercial products, such as Dowex-1, IRA-410 and Amberlite A26.

Characterisation of the functional groups was difficult due to the natural broadening of polymeric ^{13}C-NMR resonances, and the shortage of definitive IR bands for quaternary ammonium salts in general. Elemental analysis and determination of the effective IEX capacity of the product were required to support the proposed reaction scheme in many cases.

Most of the functionalised resins prepared in this work have not been reported in the literature, although it is likely that resins bearing similar structures have been examined in proprietary commercial research. The functionalisation schemes applied in Chapter 3 should apply to comparable chloromethylated polystyrene substrates, subject to the caveats mentioned in Section 6.1.3. The resins prepared herein have properties that are influenced by the common substrate (A378) employed in synthesis. The use of the alternative chloromethylated polystyrene substrate D2780 showed an improvement in the performance of the N-methylmorphilinium functionality (NMM1 vs. NMM2).

6.1.2 Problematic Resin Preparations

The difficulty in titration (Section 3.6.1.7), and the relatively slow sorption kinetics of all the novel resins observed in Chapter 4, is reasonable evidence of lower porosity relative to commercial products. Resin ETM2 was intended to bear the same moiety as the gel-resin IRA-410 [$R(CH_3)_2N^+CH_2CH_2OH$], and performed less efficiently: the maximum $[Au]_R/C_M$ (mmol/mol) was 9.4 at 6 hours (ETM2), versus 12.1 at 3 hours (IRA-410). An analogous resin to Dowex-1 or A26 [$R(CH_3)_3N^+$] was not prepared with the A378 substrate in this work, but may be a useful reference in future investigations due to the relatively high gold loading of the commercial resins.

The simplified reaction schemes for most resins (S_N2-alkylation in most cases) leaves few side-reactions available to complicate characterisation. The extent of an alkylation reaction was assessed by the discrepancy between the results of IEX and nitrogen content by elemental analysis (IEX/EA %). This was most apparent for the benzylated ammonium resins {ETB1 (21%); DAB1 (26%); BBZ1 (37%); DBP1 (38%);

TBZ1 (47%); BIM1 (49%); BME1 (63%) and NBM1 (84%)}. The presence of weak-base groups complicated the IR spectra of most of these resins.

Methylated derivatives did not follow this trend, although several resins {DMP2 (73%); TPZ1 (73%) and ETM2 (90%)} showed lower IEX capacities than calculated. Some loss of effective IEX capacity may also derive from sites inaccessible to the bulk solution, due to limitations of the swollen resin matrix. Several high-capacity, single-step resin preparations also showed a low IEX/EA ratio {ABU1 (68%); TME1 (73%); PET1 (79%) and NMM1 (89%)}, consistent with this effect.

Some of the functional groups attempted were chemically unstable. Hexahydro-1,3,5-triazine resins (TET and TBT) showed evidence of rapid degradation, with fragmentation of the triazine ring resulting in a low IEX capacity relative to the nitrogen content {TET1 (35%); TBT1 (53%); TBT2 (53%)}. This trend translated to their alkylated derivatives{TEM1 (28%); TEB1 (67%); TBB2 (36%) and TBM2 (75%)}. Several of these resins lost IEX capacity on storage, and it is possible that the triazine ring may even decompose in the leach solution (pH ~10).

A few resins showed an IEX capacity greater than elemental analysis results would suggest. In the case of resins PME2 (117%) and TME2 (151%), this appears to be caused by some bridging of chloromethyl sites by the diamine reagent (TMEDA). The surprisingly high IEX capacity of resins POP2 (117%), MIM2 (115%), and DAM1 (136%) can only be ascribed to degradation of the functional groups, via elimination of alkyl fragments and/or rearrangement resulting in low-mass quaternary ammonium groups. These degradation products were not readily characterised, due to their minor presence relative to the intended functional group.

Some resins were poorly characterised due to significant oxidative degradation of the resin during synthesis or work-up. Lower levels of carbon than expected were

found in many products, consistent with elevated levels of oxygen in the products. The carbonyl peaks noted in the IR spectra of the control resin A2 ($\bar{\nu}$ = 1665, 1718 cm^{-1}) apparently originated from uncharacterised oxidative degradation, and appeared to some degree in most products. Chloromethylated sites may be oxidised to carbonyl groups (aldehyde or carboxylic acid) at elevated temperatures in the presence of amine oxides [1]. A proposed reaction sequence for this oxidation is shown below (Eqn. 6.1).

$$(\text{Polymer})CH_2Cl \rightarrow (\text{Polymer})CHO \rightarrow (\text{Polymer})CO_2H \qquad (6.1)$$

Some degree of hydrolysis of the chloromethyl groups of the precursor resin A378 is evident (see Section 3.6.1.2, Equation 3.1) in all products. This may have been compounded by subsequent treatments (Equations 3.2 – 3.3). The elimination of chlorine was sometimes identified by elemental analysis, such as in resins A2, NMZ1, ETA1, and NBM1. Most perturbations of the elemental analysis results appears to be derived from oxidation, or the presence of residual counter-ions (eg. I^- on DAM1).

Alkyl fragments may be eliminated from quaternary ammonium groups as alkyl halides (Cl^- form, Eqn. 3.2) or alkenes (OH^- form, Eqn. 3.2). The latter give rise to alkene vibrations occasionally observed in the IR spectra ($\bar{\nu}$ = 1640 – 1675 cm^{-1}). Storage of resins in the hydroxide form also complicated characterisation due to the broad O-H vibrations in the IR spectrum, and some loss of IEX capacity by alkene elimination. Fragmentation of quaternary ammonium functional groups by the elimination of tertiary amines, alkenes, alkyl halides, or by oxidation, leads to moieties with little or no IEX character at high pH (ie. NR_3, $R_2C{=}CR_2$, RCHO and RCOOH groups). The degradation of the resins in this fashion led to relatively poor correlations

between EA results and functional capacity. However, commercial resins require durability to be viable, and fragile resins are unlikely to see practical application. Improvements to resin preparations are discussed in the following section.

6.1.3 Refinement of Resin Synthesis

Some of the synthesis procedures and storage conditions should be amended in any further work to minimise the degradation of the resin products. This includes the resin drying process, which may make charged functional groups more susceptible to degradation. Resins should be stored wet, and only dried immediately prior to analysis. Resin porosity may also be deleteriously affected by drying if the high temperature during synthesis allowed chloromethyl groups to form methylene bridging units between the aromatic groups of the substrate (Eqn. 6.2). This also results in the loss of chlorine, as was observed in a number of the resin products.

$$\text{(Polymer)}CH_2Cl + \text{(Polymer)} \rightarrow \text{(Polymer)}CH_2\text{(Polymer)} \qquad (6.2)$$

The presence of hydroxyl groups complicated the characterisation of the resins, a factor that may be minimised in future work by more careful storage and use of the chloromethylated substrate resin. The oxidative reactions responsible should be diminished by storage of the resin in a dark, cold, oxygen-free vessel. Lower reaction temperatures (below 80°C, preferably < 60°C) would also lessen the influence of amine elimination. The final resin porosity may also be improved by a lower temperature, as the consistently poor diffusion is consistent with diminished porosity. Drying should be eliminated for all but a representative sample to be analysed immediately.

Similar adjustments in resin work-up procedures should also improve the stability of the products and reduce degradation. A slower washing procedure, with gradual replacement of the solution when washing the products with successive organic solvents, and then aqueous solutions, will reduce osmotic shock and improve extraction of reaction residues. This is particularly relevant to the aqueous washes, where the slow kinetics require long contact times for effective ion exchange and deprotonation of weak base resins with NaOH. The latter treatment should be entirely eliminated for strong base resins, as the IEX affinity of hydroxide is generally poor [2] and the resins degrade more readily in hydroxide form. (eg. TBT1, TET1). Finally, the resins may have improved by more rigorous conditioning with aqueous solutions (pH 2-10) prior to use to improve porosity and flush ionic residues from IEX sites.

It is likely that the yield of many of the resin preparations performed in this work may be improved, and side-reactions and degradation minimised. The changes suggested above would be a starting point for such an investigation, but each individual functionalisation scheme may require different conditions for optimum yield. This applies particularly to the low-yielding or failed syntheses of resins, such as those bearing the triphenyl (APH), tribenzyl (TBA) and trioctyl (TOA) quaternary ammonium moieties. The fragility of hexahydro-1,3,5-triazine resins indicates that further investigation of these moieties is unlikely to yield a durable product.

Industrial synthesis of resins is generally geared toward high yield reactions using relatively simple methods and low costs, limiting the commercial viability of many of the preparations in this work. The principal benefit of a novel resin in this process must be improved selectivity for gold, with structural novelty facilitating potential patent protection.

6.2 *Structure and Selectivity*

6.2.1 Correlation of Structure with Selectivity

Although a great many of the intended preparations were successful, it was not possible to prepare all of the range of structures initially proposed in Chapter 2. The structures of the hexahydro-1,3,5-triazine resins (TET and TBT), the macrocyclic resin DTP1), and their derivatives were not as intended, due to side reactions or instability of the functional sites. Preparations of severely sterically hindered ammonium resins such as tribenzyl-, trioctyl- and triphenylamine were also unsuccessful. The majority of the remaining resin functional group characterisations were deemed sufficient to permit structural features to be associated with gold sorption (as measured by $[Au]_R/C_M$).

The effect of incomplete alkylation and reaction by-products is unlikely to impact on gold loading, and therefore $[Au]_R/C_M$, due to their uncharged nature in leach liquors. The gold loading of all the weak base resins examined was very low (< 1 mmol/mol), and their performance indistinguishable from the unfunctionalised precursor resin (A378). The degree of variance shown in the calculated gold loadings was found to be of a similar order (Section 4.4.2.2).

Resin groups with benzyl substituents were found to be less selective for gold than their methylated analogues in most cases (see Section 4.4.5), in accordance with the expectation that interaction of the bulky aurothiosulfate complex with the ammonium group will be hindered by bulky nitrogen substituents. This was not a major effect, as the high selectivity of the quinuclidine resin (QNU1) indicates. The gold affinity of the piperidine derivatives was improved by a 2-hydroxyethyl substituent (PET1), while the bis(ammonium) groups derived from piperazine and TMEDA were also promising.

Generally, quaternary ammonium resins were found to be highly selective for gold over trithionate, with significant percentages of gold being recovered in the presence of a 100-fold excess of trithionate. In standard leach liquors, with no initial trithionate, gold recoveries of a select group of resins ranged from 52 to 89 % after 6 hours, whereas in the presence of an initial 10 mM trithionate, the same resins still recovered 22 – 61 % over this time (Section 5.1.4). A factor in this selectivity is the higher charge of the metal complex, resulting in stronger interaction with the cationic site. The highest gold recoveries were achieved using the commercial resins (Dowex-1, A26 and IRA-410), which were also less perturbed by the presence of trithionate.

Corresponding loading of functional sites with gold ($[Au]_R/C_M$) ranged from 10.4 – 13.7 mmol/mol in standard liquors, with the best of the novel resins in a similar range. In the presence of 10 mM trithionate, novel resins TPZ2, MIM2 and PET2 retained high gold loading relative to commercial resins. All the novel resins continued to adsorb gold from this liquor over 24 hours, whereas the gold loading of the commercial resins peaked and began to fall in less than 6 hours.

The N-N distance of resins with bis(ammonium) moieties did not show any effect on selectivity, with the shortest (TPZ) and longest (PME) separations giving the two highest results in this class ($[Au]_R/C_M$ = 11.3 and 9.6 mmol/mol, respectively). This separation remained smaller than the mean S-M-S distance for both the important bis(thiosulfate) metal complexes (M = Au^+, Cu^+), where the charge resides primarily on the ligands. These ligands are free to rotate to better accommodate charge interaction.

In the B/R test using a gold-rich liquor (100 ppm Au, Section 5.2), the order of resin selectivity was similar to the standard B/R tests. However, resins NMM1 and TPZ2 performed somewhat less well than expected, while resins A26 and QNU1 showed higher loading than expected (ca. 92 mmol/mol each). The latter result justified

further study, and cyclic testing of resin QNU1 (Section 5.3) showed very high recoveries over four cycles of sorption (93 - 83 %) and elution (94 - 100 %). The N-methylimidazole resin MIM2 was found to be as efficient a sorbent for Au as QNU1 and A26, but was not studied further due to poor elution results (Section 4.4.4.2).

Finally, significant sorption of copper by several of the resins examined in Section 4.4.3 (QNU1, BME1, Dowex-1, IRA-410) may be associated with weak-base sites, ie. absorption of the cationic complex $[Cu(NH_3)_4]^{2+}$. This behaviour may permit concomitant stripping of copper and gold from leach solutions by successive treatments with weak- and strong-base resins. Absorption of copper(I) thiosulfate $[(Cu(S_2O_3)_n]^{(1-2n)}$ complexes is difficult to characterise relative to the functional group loading, due to the unknown ligand distribution (n).

6.2.2 Critical Comparison with Commercial Resins

The principal advantage of the novel resins over their commercial counterparts is the slower sorption kinetics, leading to less sensitivity to trithionate over time. For example, the gold loading of the commercial resins peaks after 30 minutes (Dowex-1) to 3 hours (A26), then begins to fall as trithionate is formed in solution and displaces gold from the IEX sites. The large size fraction 'A26 Big' and the gel-resin IRA-410 were only marginally affected by trithionate elution, due to the slower kinetics inherent to these substrates. This behaviour is minimal or non-existent in the novel resins, where gold loading generally increases at a diminishing rate over 24 hours.

In addition, slightly higher $[Au]_R/C_M$ values were found for a subset of the novel resins (BIM1, MIM2, NMM1, PET2, QNU1 and TPZ2), indicating improved selectivity of the functional group for gold in the standard leach liquor. The difference

was not very large, ca. 1-2 mmol/mol in these liquors (20 ppm Au). A subset of these resins (MIM2, PET2 and TPZ2) was also found to have $[Au]_R/C_M$ values competitive with commercial resins in the presence of an initial 10 mM trithionate (Table 5.2). In a subsequent test using an elevated gold concentration (100 ppm Au), the commercial resin A26 was as efficient as the best performing novel resins (MIM2 and QNU1).

More stringent testing of the novel resins would be required to accurately determine selectivity ratios for gold over trithionate, but a general trend toward small IEX moieties was apparent (Section 5.1.5). All the commercial resins examined were of this type, lending some bias to their comparison. The novel resins suffer from some of disadvantages relative to the commercial resins studied. These include lower IEX capacities, and slower diffusion (resulting in less rapid loading). The Au loading of the novel resins also diminished more sharply than the commercial resins in the presence of an initial 10 mM trithionate in the liquor.

These novel resins are also likely to be more expensive to produce in the short-term, and their long-term stability has not been examined. Many of these issues may be overcome by optimisation of the synthesis, although some properties, such as the perturbation by trithionate, may be more affected by a change of substrate than by the choice of ion-exchange group.

6.2.3 Further Development of Selective Resins

The favourable behaviour of the commercial resins in these studies indicates that small ammonium groups (such as NMe_3 and NEt_3) should be added to the set of IEX functional groups examined. To fully assess the behaviour of these moieties, these should also be prepared on the A378 substrate for comparison with A26 and Dowex-1.

Preparation of high-yield resins with very bulky ligands (akin to TOA, TBA) may also be explored to better assess the effects of strong steric hindrance.

There is reasonable confidence in the configuration of the MM+ optimised structures of the resin groups, despite the low level of theory applied, as the parameters are well tested on small organic molecules. The DFT models agree well with the empirical data (where available), but also provide charge distributions. The latter cannot be directly correlated to their degree of interaction with the MM+ optimised IEX groups. In future work, it would be desirable to perform semi-empirical modelling (eg. MINDO, ZINDO) of the ammonium groups to show the effects of charge delocalisation onto local alkyl groups (depending on structure). This may significantly alter the effective steric hindrance provided by the ammonium group substituents. Semi-empirical theory may also result in improved structure optimisation, particularly for the ring-delocalised imidazolium groups (BIM and MIM). Incorporating a number of surrounding water molecules into the calculation may also refine the model.

Development of a set of semi-empirical parameters for gold to be used in molecular modelling (eg. *Spartan*) would allow more direct comparison of structures. Further refinement of optimal IEX groups requires a protocol for measurement and optimisation of the strength of charge interaction between the important anions and each moiety. This is likely to be a prohibitively computationally intensive process, particularly if water molecules are included in the models.

6.3 *Prospects for Further Development*

6.3.1 Testing Procedures

The application of the resins in this work to simulated leach liquors has limited the scope of resin testing. More rigorous IEX conditioning of the resins prior to use may also improve resin performance, as discussed in Section 6.1.3. More refined data regarding the absolute IEX selectivity of the functional groups may be obtained from by more rigorously controlled test conditions.

This applies particularly to the effect of dissolved oxygen on the ratio of Cu(I) to Cu(II) and the concentration of polythionates in the liquor. The control and monitoring of dissolved oxygen concentrations ($[O_2]_S$) in the liquors should prevent deviations in oxidative behaviour. Cu(II) could be followed by UV/Vis spectroscopy in a sealed circulating cell, and hence the Cu(I)/Cu(II) ratio determined. Cu(I) may be determined by difference, but not the complex distribution (ie. $[Cu(S_2O_3)_N]$, where N = 1-3).

It would also be useful to investigate the use of other AAS wavelengths for more accurate copper determination in liquor samples.

The relative selectivity of the functional groups may be more directly comparable by the use of molar-equivalent quantities of resin in each B/R test, to fix the ratio of IEX groups to gold in solution. This has the disadvantage of altering the volume of resin required, thus altering the rate of diffusion of the solution into the resin.

In any event, trithionate will build up in solution at a rate related to the concentration of oxidants present in solution (ie. Cu(II) and O_2). A more rigorous analysis must include an examination of the IEX selectivity of trithionate in less complex solutions of known concentration (and pH). This includes solutions containing

trithionate and $[Cu(S_2O_3)_2]^{3-}$, $[Au(S_2O_3)_2]^{3-}$, or thiosulfate only. This would be better facilitated by resins with relatively fast kinetics, as the trithionate concentration can change significantly with time – increasing, as in leach liquors, or diminishing, in neat solution. The slow sorption kinetics of the novel resins in this work have prevented a more detailed analysis of trithionate selectivity due to this factor.

6.3.2 Prospective Functional Groups

As a result of the B/R testing conducted in Chapter 4, the initial group of 46 prospective functional groups were refined to seven candidates (DAM, MIM, NMM, PET, QNU, TME and TPZ). In many respects, these resins perform as well as the commercial resins examined, despite their relatively crude preparation. Comparison with analogous small trialkylammonium analogues on the same substrate would be useful for comparison with these moieties. There appears to be little prospect for significant improvement in selectivity for gold over trithionate anions beyond the 100-fold margin found for all the simple strong-base IEX groups examined. Elution schemes were of similar efficacy for most resins other than the imidazole-derived products (MIM and BIM). Further examination of their elution may be warranted, due to their relatively high performance in the B/R testing procedures.

A set of structural features associated with gold affinity were identified in Section 4.4.5. These tentative assignments are based on comparison of similar structural features within the limited set of functional groups prepared. Within this set, the preferred functional groups for the aurothiosulfate anion were quaternary ammonium groups with short linear alkyl or 2-hydroxyethyl substituents, 1,2-bis-quaternary

ammonium groups, or imidazolium group. Alkylated morpholinium groups and the sterically restricted quinuclidinium group also showed promising results.

Prospects for more selective functional groups for gold may be developed from this basis. This set of features stands to be refined, expanded or corrected by subsequent development and testing of new IEX resins. Development of new prospective IEX groups was aided by the modelling procedures applied in Chapter 2, and this process may be refined by the suggestions proposed in Section 6.2.3. The preparation of prospective groups may be improved by the changes in synthesis and handling procedures suggested in Section 6.1.3. Alternative substrates should also be considered, as the effect of resin substrate on selectivity may also be optimised.

6.3.3 Concluding Remarks

Changes in thiosulfate leaching processes in recent years include the elimination of ammonia and copper from the solution [3], permitting recovery of gold by precipitation. The application of this is limited to low copper ores, hence ammoniacal processes are still preferable for other feed materials, and resin-based recovery processes may be essential to the recovery of gold. The commercial viability of ammoniacal thiosulfate leaching is still questionable, and no major plant developments have been reported. It appears that the technology and process are viable, but not significantly improved over the existing (and dominant) cyanide processes in technical and economic terms. Development of a selective resin would improve commercial prospects for such technology. The novel resins developed in this work show a number of functional groups with relatively high selectivity for gold, but the resins require significant further development to compete with their commercial rivals.

References:

1. March, J., *Advanced Organic Chemistry*, 4th edition; John Wiley & Sons (New York), 1992.

2. Breadmore, M.C., Macka, M., Avdalovic, N., Haddad, P.R., "On-capillary ion-exchange preconcentration of inorganic anions in open-tubular capillary electrochromatography with elution using transient-isotachophoretic gradients. 2. Characterisation of the isotachophoretic gradient." *Anal. Chem.*, **73**, p. 820-828; 2001.

3. Ji, J., Fleming, C.A., West-Sells, P.G., Hackl, R.P., "Method for thiosulfate leaching of precious-metal containing materials."; World Intellectual Patent WO 01/88212 A2; Placer Dome Technical Services Ltd., 2001.

A378	ABU	APH	BBZ	BIM	BME
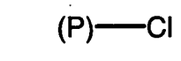	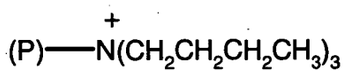	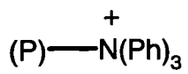	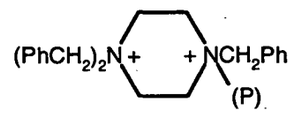		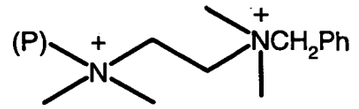
DAB	**DAM**	**DBP**	**DEA**	**DET**	**DIP**
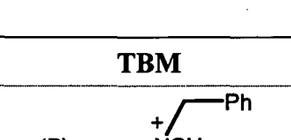	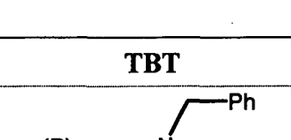	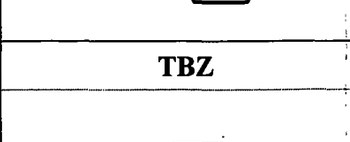		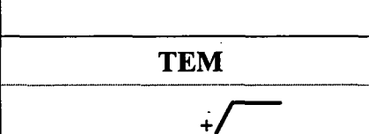	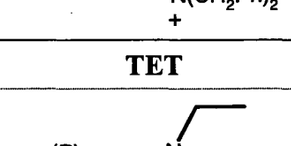
DMP	**DST**	**DTM**	**DTP**	**ETA**	**ETB**
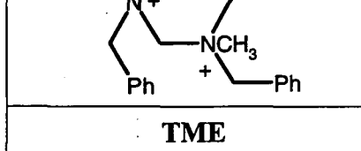	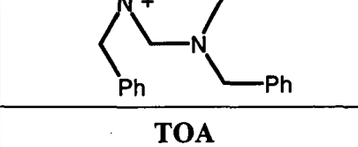	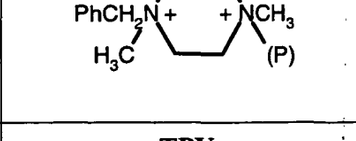	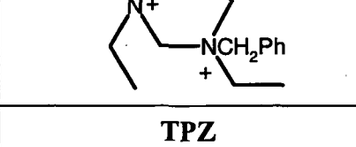	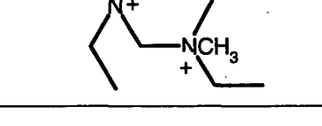	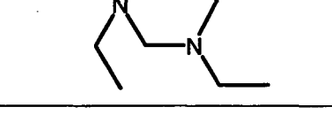
ETM	**IMZ**	**MIM**	**MOR**	**NBM**	**NBP**
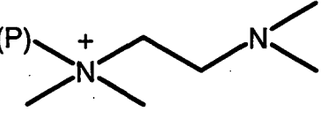	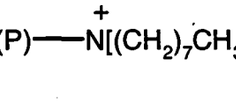	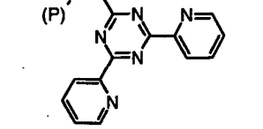	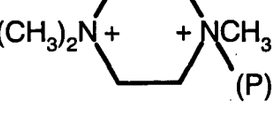	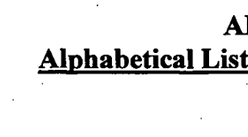	
NMM	**NMP**	**NMZ**	**PAZ**	**PET**	**PIP**
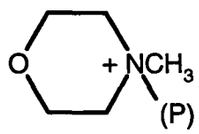	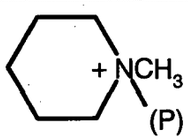	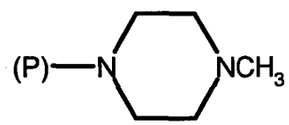	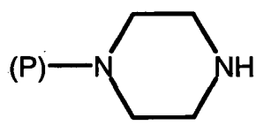	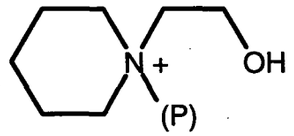	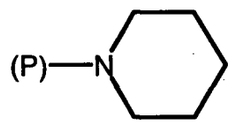
PME	**POP**	**QNU**	**TAA**	**TBA**	**TBB**
TBM	**TBT**	**TBZ**	**TEB**	**TEM**	**TET**
TME	**TOA**	**TPY**	**TPZ**		

APPENDIX A:
Alphabetical List of Resin Functional Groups